Mechanisms of otoacoustic emissions

A thesis submitted for the degree of

Doctor of Philosophy
of the
University of London

Richard David Knight

Institute of Laryngology and Otology,

University College London

2001

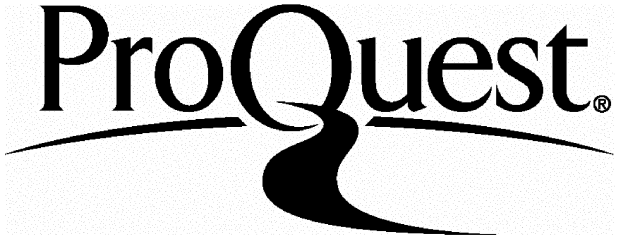

Abstract

Otoacoustic emissions (OAE) are sounds which are emitted by the ear in response to acoustic stimulation as a byproduct of normal mammalian auditory function. Published research into OAEs leaves many of their detailed characteristics unreported or of uncertain explanation. For example, the mechanisms by which the emissions occur and how many emission mechanisms or categories there are have not yet been clearly established.

The purpose of this study was to obtain comprehensive OAE data in a format which would permit specific questions regarding the mechanism of their generation and emission to be answered.

Both distortion and transient evoked OAEs responses (DPOAE and TEOAE) were obtained from healthy human ears. It was found these two responses can have similar characteristics but only if a restricted set of DPOAE stimulus parameters are employed, implying that under these conditions the underlying emission mechanisms are closely related. Another significant finding is that lower sideband DPOAE (e.g. $2f_1$-f_2) obtained with stimuli $f_2/f_1>1.1$ has fundamentally different phase characteristics (and hence origins) to all other DPOAEs.

A new frequency/area representation of detailed DPOAE intensity and phase data has been developed. This revealed that lower and upper DPOAE sidebands are a continuation of each other for $f_1 \sim = f_2$, implying a continuity of emission mechanism. This and the transition of behaviour pattern in lower sideband DPOAE for $f_2/f_1>1.1$ supports a one source/ two emission routes model for DPOAE.

DPOAEs arriving in the ear canal by these two routes have been successfully separated and analysed and inferences are drawn regarding the location of DP generation. Amplitude fine structure was demonstrated to be partly due to interference between the two components but also an additional mechanism is involved, perhaps interference within emission generation regions or internal reflections. A simple transmission line model demonstrated that the hypothesis can explain the results seen to a good approximation.

Contents

List of figures

List of tables

A. Introduction

I Overview of the human ear

The function of the external auditory system is to collect sound and convert it to a neural signal containing coding for sound frequency and level. It comprises three main stages. (1) The external ear collects the ambient sound, (2) the middle ear provides an impedance transformation from air in the external ear to fluid in the cochlea, (3) in the cochlea the sound vibration encodes a neural signal.

Vibrational energy, which is generated in the healthy cochlea in response to sound applied to the ear canal, can be emitted back to and measured in the ear canal. The cochlear mechanisms behind this process are the subject of this project. Nevertheless it is appropriate to consider the structure and function of the peripheral auditory system first as this affects the emitted sound that is measured in the ear canal.

a. Structure and function of the external ear

Figure 1 shows a section through the human ear. The external part of the ear includes the pinna and the external auditory meatus. In humans, the pinna has a limited effect of collecting sound energy which would otherwise have missed the ear canal.

The external auditory meatus transfers the sound collected by the pinna to the eardrum, and is approximately 3 cm long. It is open at one end and closed at the other by the eardrum. If the eardrum is assumed to be approximately rigid its first resonance occurs when the length of the auditory meatus = 1/4 λ. This corresponds to a frequency of approximately 3 kHz, and therefore the external auditory meatus resonates at around this frequency, increasing the sound transmission to the middle ear in this frequency region. The gain obtained by the external ear as a whole is direction-dependent and can be up to 20 dB (Shaw, 1974) (figure 2). The directional dependence of the external ear allows limited localisation with just one ear, especially if the head is turned during sound presentation or if the frequency content of the sound source is known. However most localisation is based on timing and intensity differences between two ears with the effect of the pinna helping to resolve up/down and front/back ambiguities.

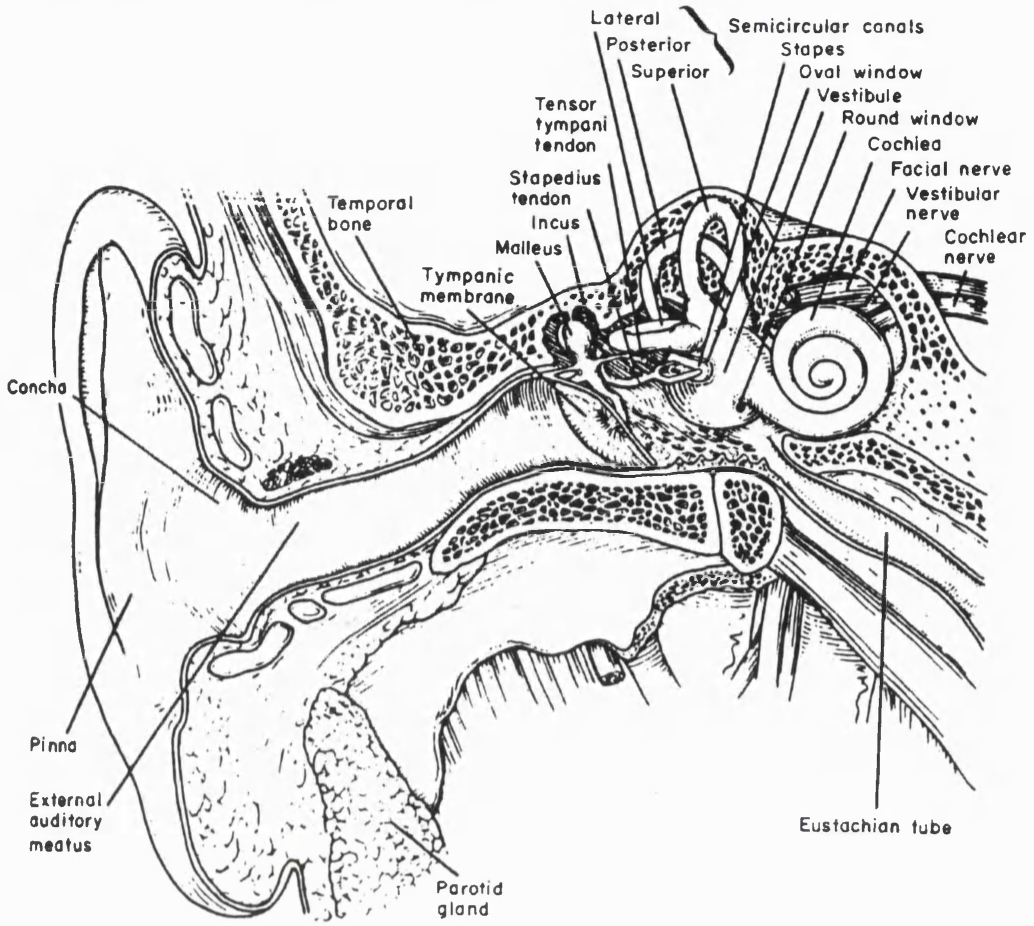

Figure 1. A section through the external, middle and inner ears in man, from Pickles, 1988. (Originally from Kessel and Kardon, 1979)

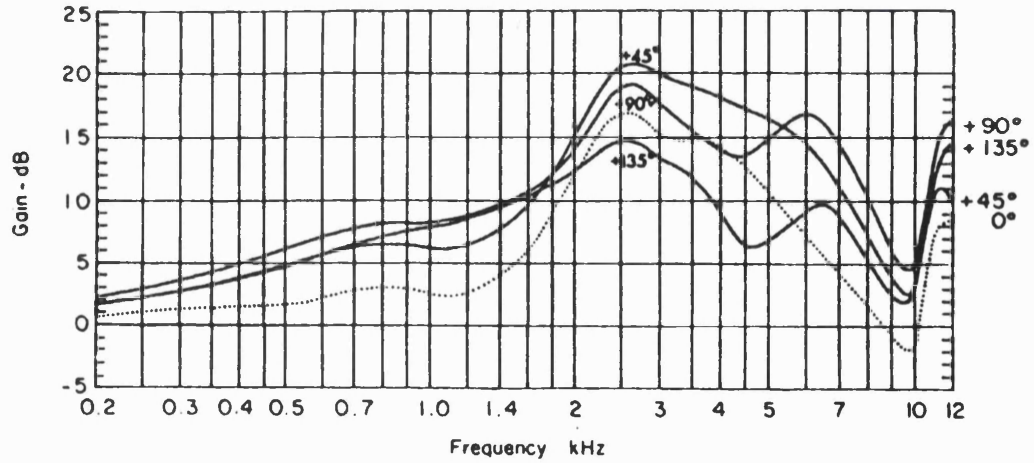

Figure 2. The average pressure gain of the external ear in man relative to the free field. Angles are horizontal degrees from straight ahead. (From Pickles, 1988, originally from Shaw, 1974.)

b. Structure and function of the middle ear

Transmission of sound energy from air in the outer ear (which is low impedance) to water-based fluid in the inner ear (which is high impedance) requires an impedance matching device in order to prevent loss of energy due to reflections at the boundary between the two media. This is the function performed by the middle ear.

There are three facets to the way in which the middle ear provides the necessary impedance transformation between the outer and inner ear (after Pickles, 1988, pp17-19)

1. The main factor is the difference between the area of the tympanic membrane and the area of the foot of the stapes. The area of the tympanic membrane is larger (by a factor of about 35 times in the cat), so the force applied to the tympanic membrane is focused onto a smaller area, increasing the pressure by this ratio.

2. The length of the malleus is about 1.15 times that of the incus, therefore the lever action increases the force and reduces the velocity by this factor. The impedance (which is the ratio of pressure/velocity) is increased by 1.15^2, i.e. 1.32. This is therefore a small factor.

3. Khanna and Tonndorf (1972), from observations made by time-averaged holography, showed that the tympanic membrane buckles as it moves in and out in response to an incident sound wave and that this buckling results in the arm of the malleus moving less than the tympanic membrane as a whole. The effect was seen at all frequencies studied (600 Hz to 6 kHz), the pattern of vibration becoming more complex above 3 kHz with higher modes of vibration being excited. This buckling motion could result in an increase in force with a reduction in velocity, potentially increasing the impedance perhaps by up to a factor of 4. It is arguable to what extent this is an efficient impedance change or how much it results in loss of energy through reflection.

The input impedance of the cochlea has been measured in human temporal bones by Aibara et al, 2001, whose measurements suggest an acoustic impedance of approximately 21 GΩ for the stapes and cochlea at 1-4 kHz. This was consistent with the earlier estimate of Puria et al, 1997 but lower than the estimate of Merchant et al, 1996, who obtained their estimate by measuring the impedance of the stapes/cochlea input impedance before and after draining the cochlea.

The question arises whether the impedance transformation of the middle ear is enough to perfectly match the impedances of air and the fluid filled cochlea. An estimate can be obtained from the figures presented here. If the three impedance transformation

mechanisms described above are multiplied (assuming that the third one is valid), the total transformer ratio is found to be 35×1.32×4=185.

The acoustic impedance of the stapes and cochlea measured by Aibara et al. (2001) was approximately 21 GΩ (Acoustic ohms) in the frequency region 1-4 kHz. Multiplying this by the area of the stapes footplate (3.2 mm^2) gives a value of 67×10^3 Ns/m^3 with the same units as specific acoustic impedance. Dividing this impedance by the estimated transformer ratio of the middle ear gives 67×10^3 $Ns/m^3/185 = 363$ N s/m^3, which is close to the specific acoustic impedance of air (430 N s/m^3).

Deriving the middle ear transformer ratio is, however, subject to some uncertainty. von Bekesy (1960) suggested that the human tympanic membrane has an element of a hinging action. Force applied near the hinge will result in less movement than force applied further from the hinge. It may therefore be appropriate to use a smaller 'effective' area for the tympanic membrane, but on the other hand, this tympanic membrane motion may result in a larger effective ratio for the lever action of the ossicles by effectively adding to the length of the malleus. It should also be remembered that estimates of the cochlear input impedance vary.

Bray, 1989 indicates, by considering Zwislocki's 1962 model of the middle ear, that the impedance presented by the middle ear from the ear canal would also be modified if the ear canal was occluded.

c. Transfer function of the middle ear

The sound pressure gain of the human middle ear has been measured by Aibara et al. (2001) (figure 3).

The gain peaks at 1.2 kHz, at which the gain is about 23.5 dB, rolling off at both higher and lower frequencies.

The low frequency part of the transfer function will be reduced by elastic stiffness provided by various elements in the middle ear, for example the elasticity of the tympanic membrane, ossicle ligaments and compression and expansion of the air in the middle ear cavity. These factors become more significant at low frequencies because, for constant sound pressure level, displacement is inversely proportional to frequency. Therefore low frequencies result in greater displacements of the middle ear structures and therefore a greater significance of the elastic stiffnesses.

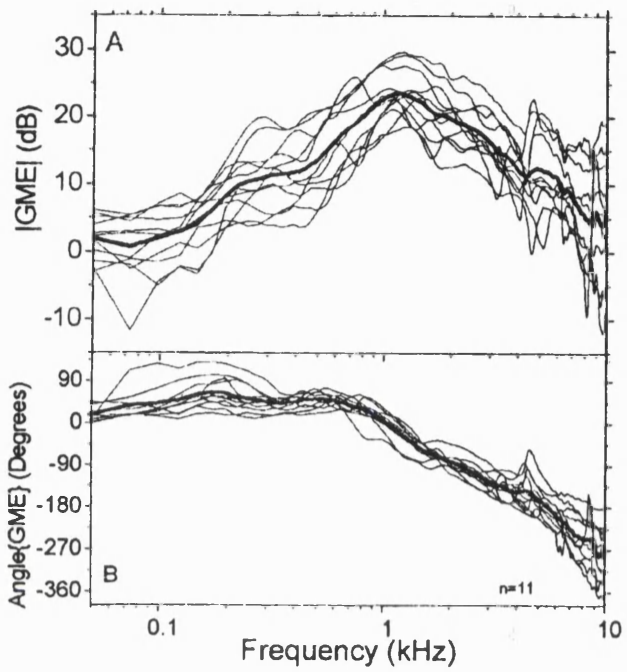

Figure 3. Human middle ear sound pressure gain (Aibara et al, 2001).

At high frequencies, the response will be limited because of more complex vibration patterns of the tympanic membrane reducing the effective area and the mass of the ossicles becoming significant – the greater accelerations required at higher frequencies requiring more force to be applied (Pickles, 1988, p22).

Resonances of the middle ear cavity become significant at high frequencies and are the likely cause of the irregularities above 4 kHz.

Reverse transmission through the middle ear is estimated to be less efficient than forward transmission by 12 dB (Kemp, 1980), based on calculations from Zwislocki's middle ear model (Zwislocki, 1962). Evoked otoacoustic emissions require both forward transmission of the stimulus through the middle ear and reverse transmission of the otoacoustic emission through the middle ear. The impedance changes from the occlusion of the ear canal mean that the middle ear impedance transformation may not perfectly match the cochlear and ear canal impedances. The source impedance of the reverse travelling wave is not accurately known. Reflections of the reverse travelling wave back into the cochlea will occur if there is an impedance mismatch at the stapes.

Zhang and Abbas (1997) have shown that impairing middle ear transmission by changing the middle ear pressure alters forward and reverse transmission equally.

d. Middle ear muscles

There are two middle ear muscles, the tensor tympani is attached to the malleus near the tympanic membrane and is innervated by nerve V. The stapedius muscle is attached to the stapes and is innervated by the facial nerve (VII). Contraction of these muscles increases the stiffness of the ossicular chain and therefore reduces transmission in the stiffness-controlled frequency region (Pickles, 1988, p23), which is below approximately 1 kHz (Borg, 1968). The stapedius muscle can be caused to contract by loud sound (e.g. above 75 dBA SPL), talking, tactile stimulation of the head, or general bodily movement (Carmel and Starr, 1963). In some cases, the middle ear muscles can be contracted voluntarily.

There are many possible reasons why the action of the muscles may be desirable (after Pickles, 1988, p24).

- The contractions result in attenuation which may protect the cochlea from noise damage. It has been shown that, in cases of unilateral Bell's palsy (which paralyses the facial nerve), greater temporary threshold shifts occurred as a result of low frequency noise exposure in the ear with Bell's palsy than in the other ear (Zakrisson and Borg, 1974). However the reflex takes around 100 ms to activate fully (Dallos, 1964; Clemis and Sarno, 1980) and is therefore too slow to save the cochlea from damage by impulsive noise.
- For low frequency stimuli, the middle ear muscles can act as an automatic gain control for a 20 dB range above the reflex threshold (Wever and Vernon, 1955, measured in cats). The intensity of input to the cochlea can be kept relatively constant when the level of the stimulus varies.
- The middle ear muscles may be able to reduce the depth and move the frequency of the dips in the transfer function in the region of 4 kHz attributed to the resonance of the middle ear cavity (Simmons, 1964).
- Attenuation of low frequencies in the cochlea can improve the perception of middle and high frequencies by reducing unwanted masking of high frequency hearing by lower frequencies.

Although all 4 factors are likely to be true, the first and the last are the most likely to be useful.

e. Structure and function of the cochlea

The cochlea is a coiled, fluid-filled structure which, in humans, has about 2 ½ turns. Figure 4 shows a cross section through the cochlear duct.

The scala vestibuli, scala media and scala tympani are all fluid filled spaces which travel the length of the cochlea. The scala vestibuli and scala tympani are joined at the apex of the cochlea and contain perilymph, whereas the scala media does not join the other two and is filled with endolymph. Perilymph is like extracellular fluid, with high Na+ and low K+ concentrations and in the cochlea is at the potential of the surrounding bone. Endolymph however is similar to intracellular fluid and has high K+ and low Na+ concentrations. In the scala media, endolymph is held at a high electrical potential of around +80 mV (Pickles, 1988, p26).

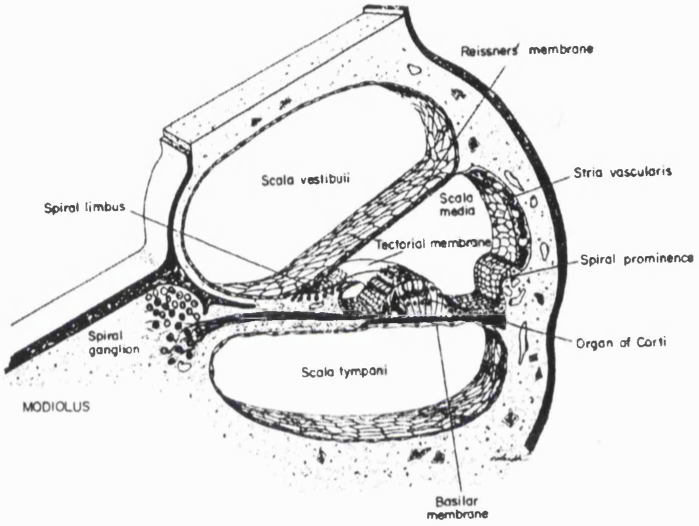

Figure 4. A cross section of the cochlear duct. (From Fawcett, 1986)

The endolymph potential, and the endolymph itself, is generally accepted as being produced by the stria vascularis (Dallos, 1992) as the cells of the stria have the properties of secretor cells. The function of the stria vascularis appears to include an active ion-pumping process adding K+ ions and hence positive charge to the endolymph.

The scala vestibuli is separated from the scala media by the Reissners' membrane, which is a thin membrane of only one or two cells thickness, but which is an effective barrier to prevent mixing of the perilymph and endolymph. The scala media is separated from the scala tympani by the basilar membrane, upon which sits the organ of Corti (Pickles, 1988, p26).

A detailed cross section of the organ of Corti is shown in figure 5.

The hair cells are arranged in rows which run lengthways along the organ of Corti. There are usually three rows of outer hair cells but in humans there are intermittently 4 or even 5 rows, especially towards the apex. There is one row of inner hair cells. It is

believed that the inner hair cells are the site at which the process of transduction of the acoustic signal to a neural signal occurs. The outer hair cells seem to enhance the transmission of the acoustic signal to the inner hair cells, probably involving active amplification. This will be discussed in more detail later.

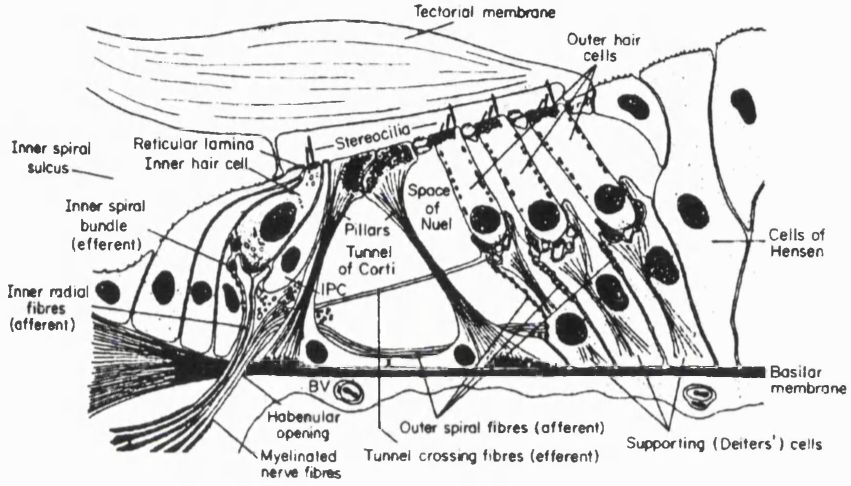

Figure 5. Cross section through the basal cochlea (modiolus to the left). Copied from Pickles, 1988, originally from Ryan and Dallos, 1984).

Figure 6 shows a detailed cross section of an inner hair cell and an outer hair cell (from Lim, 1986a). The outer hair cell is cylinder-shaped and has lateral cisternae running concentrically around the side walls (Dallos, 1992). These side wall structures mean that the cells are capable of changing shape in response to electrical stimulation (Ashmore, 1987) and appear to be designed to do so. The inner hair cell is flask shaped and lacks the thick lateral walls of an outer hair cell.

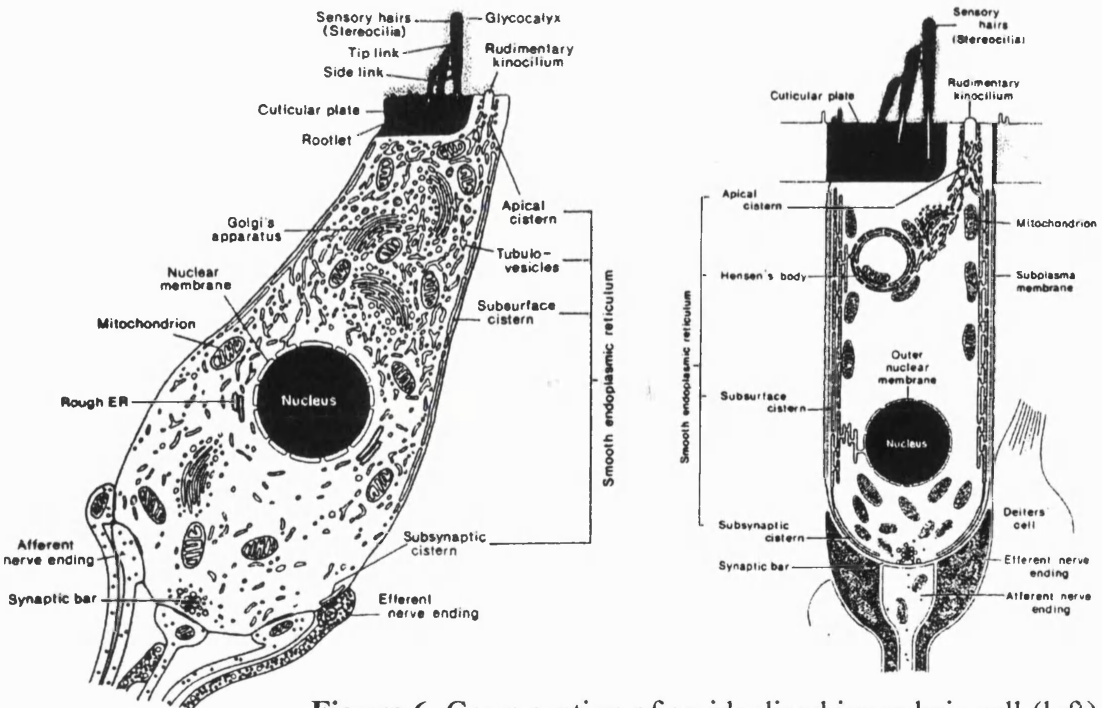

Figure 6. Cross section of an idealised inner hair cell (left) and an outer hair cell (right). (from Lim, 1986a)

The stereocilia are arranged in a V or W shape (outer hair cell) or an approximately straight line (inner hair cell) and are connected by tip links, which run from the top of each stereocilia to the side of the larger adjacent stereocilia. It is believed that these tip links may open and close an ion gate when the stereocilia are moved by movement of the basilar membrane relative to the endolymph (Pickles et al, 1984; Hudspeth, 1989; Preyer et al, 1995).

Outer hair cells have predominantly efferent innervation and the terminals enclose the base of the cell, but outer hair cells also have some type II unmylenated afferent fibres. Inner hair cells have predominantly type I mylenated afferent innervation. Efferent fibres also travel to the inner hair cells, but these tend to synapse to the afferent terminal rather than the cell body itself.

In all, around 90-95% of afferent fibres synapse with inner hair cells, with about 20 fibres going to each cell. The remaining fibres synapse with outer hair cells, each fibre synapsing with perhaps 10 hair cells (Pickles, 1988, p36).

So the OHC's mainly efferent innervation suggests that they are mainly 'under control' whilst the IHC's extensive afferent innervation suggests that they primarily have a 'detection' role.

The way the structure appears to function is that the transverse movement in the basilar membrane, enhanced by the outer hair cells, results in a lateral movement of endolymph between the hair cells and the tectorial membrane. The inner hair cells sit on a part of the basilar membrane which contains a shelf of bone and therefore is rigid, but the movement of the endolymph relative to the cells of the organ of Corti results in the deflection of the stereocilia of the inner hair cells, which causes ion gates in the stereocilia to open (Hudspeth, 1989; Dallos, 1992). The ions entering the outer hair cell change the cell potential, resulting in the nerve firing at the base of the cell. Nerve impulses produced in this way travel up the auditory pathway, ultimately providing a sensation of hearing.

f. The cochlear travelling wave

As the footplate of the stapes moves in response to sound, it applies force to the oval window of the cochlea. The cochlea is a rigid-walled structure and the only mobile part is the round window. Therefore as the oval window is moved in by the stapes, the round window moves out. The oval window is above the basilar membrane and the round window is below it, so the movement of the two windows causes a transverse displacement of the basilar membrane. Interaction between the basilar membrane and

the motion of the surrounding fluid initiates a travelling wave which progresses along the basilar membrane towards the apex of the cochlea.

There are gradual changes in cross-sectional geometry along the length of the cochlea. Towards the apex, the mass of the cochlear partition increases and the stiffness decreases, the width of the basilar membrane increases, the angle of the reticula lamina also becomes steeper and some of the features of the hair cells change, such as stereocilia length and cell geometry (Wever, 1938; Lim, 1980, 1986b; Fernández, 1952; Wright, 1984).

The effect of these changes is that a travelling wave set up by a single frequency sound at the base of the cochlea will move progressively more slowly as it travels apically because it encounters a basilar membrane with a progressively lower resonant frequency. Therefore the wavelength reduces and the energy density increases, resulting in an increase in the travelling wave amplitude. However as the wave moves more slowly, the energy losses due to the flow of fluid in the confined spaces of the cochlea increase (Mammano and Nobili, 1993) and the wave eventually reaches a point where the damping results in a rapid reduction in travelling wave amplitude. The distance into the cochlea which the wave travels depends on its frequency – low frequencies travel further towards the apex than high frequencies on an approximately logarithmic frequency-place scale.

i) Observations of the travelling wave

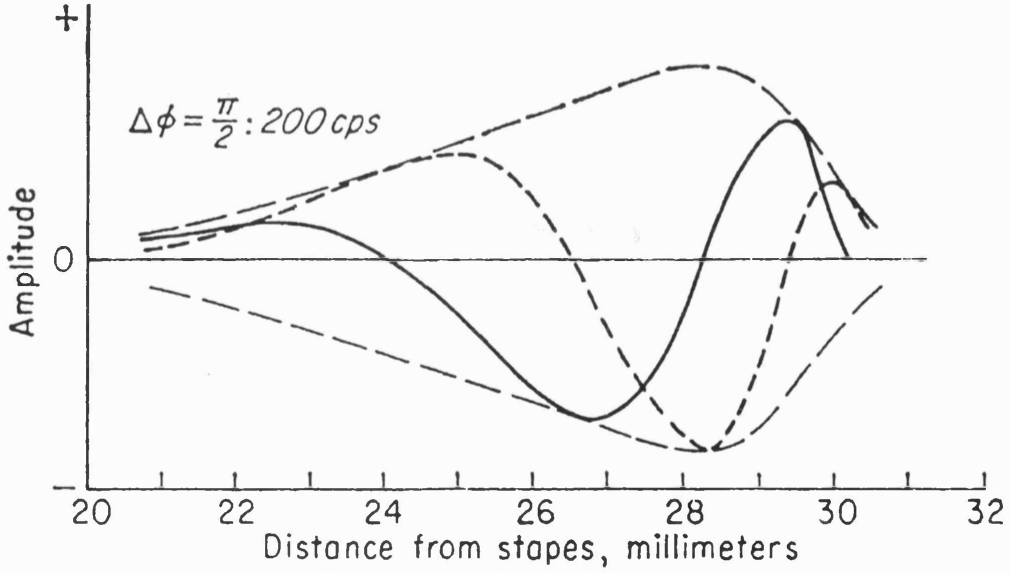

Figure 7. travelling wave, drawn by Bekesy from observations of the movement of the Reissners' membrane in cadaver cochleas. (From Bekesy, 1960)

The resulting envelope pattern of a gradual increase in amplitude followed by a precipitous decrease was first demonstrated by Bekesy (1960), who studied dead ears

and observed movement on the Reissners' Membrane and presumed that this was similar to the movement of the Basilar Membrane below it. An example of his data is shown in Fig 7. The broad tuning shown was not sharp enough to account for the fine frequency selectivity of human hearing, so it was presumed that this frequency selectivity was somehow achieved by processing at a more central stage of the auditory pathway.

However, Bekesy's results were achieved at high intensities (130 dB SPL), a level necessary in order to produce motion which could be observed in light under a microscope. Therefore the results are not a demonstration of the cochlea under normal working conditions. Also the cochleas that were used were dead (and therefore metabolically inactive) and were also very thoroughly opened up in order to allow good observation.

More recently, the Mossbauer technique (see Yates and Johnstone, 1979 for a description of the method) has allowed greater resolution in observation of the basilar membrane movement, meaning that measurements can be obtained at physiological sound levels. Adoption of less destructive surgical techniques means that measurements can be obtained from cochleae that are still metabolically active. Essentially, the method is based on the effect of Doppler shifting on the absorption of gamma photons by a radioactive isotope.

Measurements of cochlear motion using the Mossbauer technique to observe healthy cochleae have shown much sharper tuning of the travelling wave envelope and non-linear growth around the travelling wave peak (e.g. Rhode, 1971 (in Squirrel Monkeys); Sellick et al, 1982 (in Guinea Pigs); Robles et al., 1986 (chinchilla)). These data typically show about 2-3 cycles of phase delay to the travelling wave peak, and this does not change much with frequency. Therefore low frequencies take longer to reach their frequency place in proportion with their longer oscillation time period.

More recently, laser velocimetry has offered an alternative method, based on measuring velocity by detecting the doppler shift of light reflected from the basilar membrane (e.g. Recio et al., 1998 (in Chinchilla)). Usually a small glass bead is placed on the basilar membrane to allow a strong reflection to be obtained. It has been shown that this sharp tuning and compressive growth is not present in deaf ears and disappears rapidly after death and so could not have been measured by Bekesy using dead ears. The compressive growth characteristic means that even if Bekesy had used live ears, the high stimulus level would have still resulted in a broadly tuned characteristic being observed.

An illustration of the travelling wave is shown in figure 8, the peak is shown sharper than Bekesy's data to reflect the sharper tuning which has been discovered in healthy cochleae. Figure 9 shows travelling wave velocity, gain and phase from near the base of a chinchilla cochlea (Ruggero et al, 2000). The measurements were recorded at a single point and the stimulus frequency varied, hence the frequency scale on the x axis.

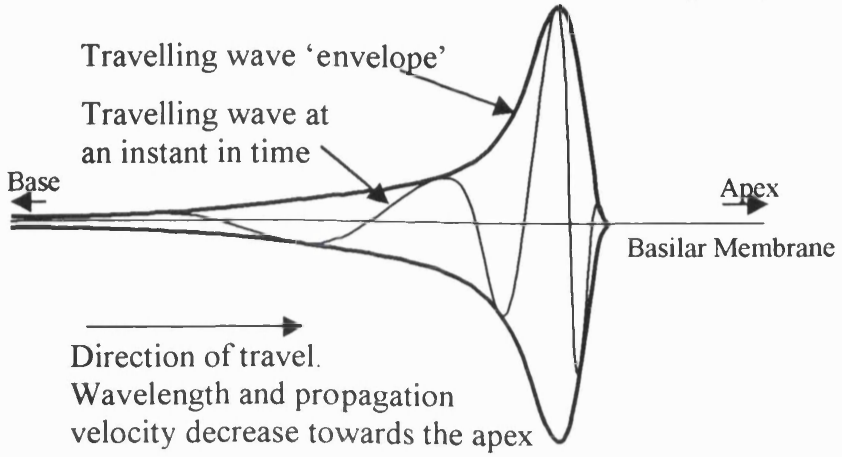

Figure 8. An illustration of the travelling wave from a single frequency stimulus. Note the reduction in wavelength with distance travelled into the cochlea and the rapid growth in the displacement amplitude near to the travelling wave peak. The travelling wave amplitude reduces rapidly on the apical side of the peak due to an increase in energy loss through damping.

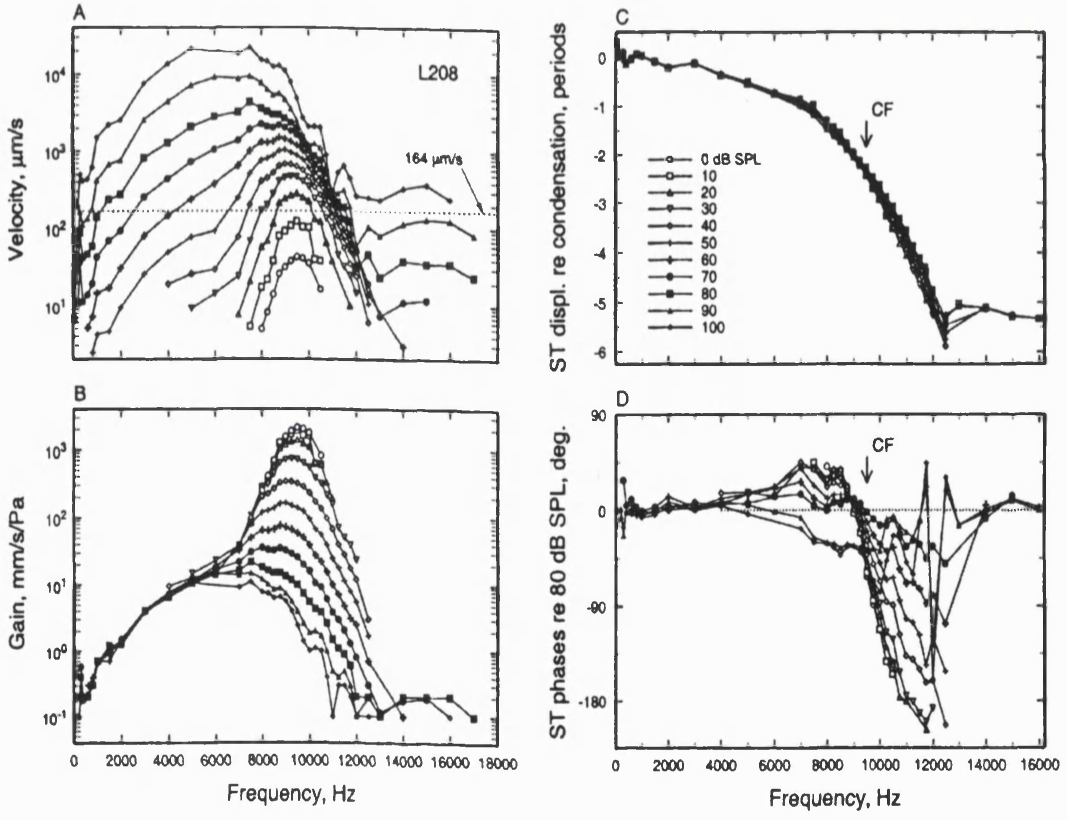

Figure 9. Measurements 3.5mm from the base of the cochlear travelling wave in chinchilla (Ruggero et al, 2000). (A) Velocity magnitude (B) Same as A but normalised to stimulus pressure. (C) Phase of basilar membrane movement relative to stimulus (D) Same as C but relative to 80 dB stimulus. Key in (C) relates to all parts (A-D).

ii) Controlling the travelling wave shape – damping and amplification

The sharpness of the travelling wave envelope is essentially controlled by the damping of the system. The more damping, the more energy is lost from the travelling wave as it progresses. The travelling wave envelope therefore becomes flatter and reaches a peak earlier. It is widely believed that removing all damping would not be sufficient to explain the amplitude growth along the basilar membrane and that amplification (or 'negative damping') is required (Gold, 1948; Brass and Kemp, 1993b; de Boer, 1983a,b; Davis, 1983; Kim 1980).

Although the presence of an active amplification process acting on the cochlear travelling wave is now generally assumed (e.g. Kemp, 1979a; Davis, 1983) it remains possible that a passive, saturating, physiologically vulnerable mechanism exists which provides the sharp tuning seen in basilar membrane measurements (Allen and Neely, 1992; Allen and Fahey, 1993; Allen, 1997; Allen, 1980). This will be revisited later, in the context of otoacoustic emissions.

The identity of the amplifying structure is presumed to be the outer hair cells. The structure of their lateral walls is such that they can and do change length with a change in cell electrical potential (Ashmore, 1987; Brownell, 1990). The compressive growth of the peak of the travelling wave envelope on the basilar membrane (Johnstone et al, 1986) is believed to be a result of saturating outer hair cell activity. In cases of cochlear hearing loss (due to a loss of outer hair cells), the low-level phon contours (see figure 10 for phon contours for normal hearing) are raised but the high level contours are little changed, reflecting a reduction in dynamic range and much more rapid loudness growth (Steinberg and Gardner, 1937).

iii) The cochlear pressure wave

Fluid pressure waves in the cochlea, in contrast to the travelling wave of the basilar membrane, show little change in phase along the length of the cochlea. This demonstrates that sound travels throughout the cochlea almost instantaneously (Dancer and Franke, 1980; Magnan et al, 1997; Dancer et al, 1997; Dancer, 1992). The 'pressure wave' does not apply differential pressure to each side of the basilar membrane and so does not result in basilar membrane movement, stereocilia deflection or nerve firing.

g. The retrocochlear afferent and efferent auditory pathways

Although detection of sound occurs at the inner hair cells, the signal must travel through the auditory pathway which passes into the brainstem and eventually to the

cortex before conscious auditory perception can occur. In order to obtain a perception of hearing and to interpret what is heard, the whole pathway is required to be intact.

There is also a less well studied efferent pathway and contralateral nerve pathways which have a controlling effect on cochlear function (Mountain, 1980; Siegel and Kim, 1982; Gifford and Guinan, 1987).

h. The overall frequency response of hearing

The frequency response of hearing is ultimately a result of the frequency responses of each stage of the auditory system being overlaid. The typical human hearing frequency response is shown in figure 10 (data from Robinson and Dadson, 1956).

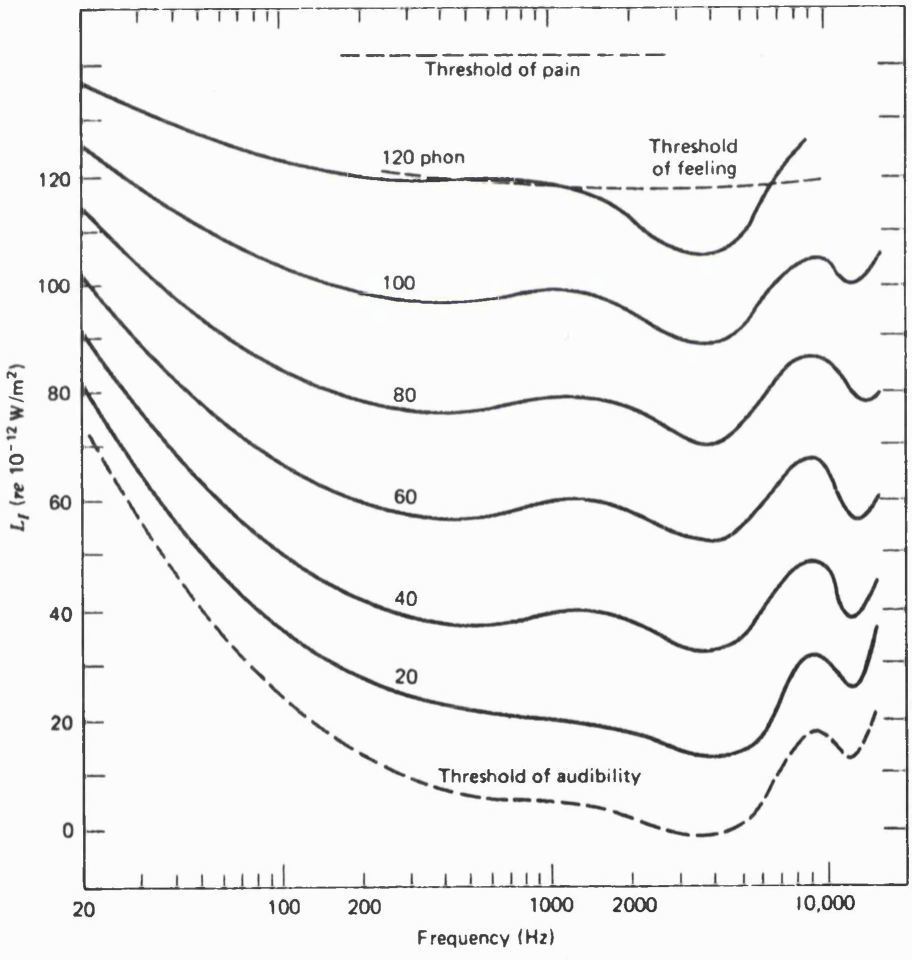

Figure 10. Thresholds and free field equal-loudness contours (Phons) for pure tones presented from directly in front of the subject. (Kinsler et al, 1982, data from Robinson and Dadson, 1956)

The pressure gain of the external ear is shown in figure 2 (Shaw, 1974). The maximum sensitivity of hearing, which is in the region of 3 kHz, coincides with the first resonant frequency of the ear canal.

The transfer function of the middle ear, measured by Aibara et al, 2001, is shown in figure 3. The function has a broad bandpass characteristic, peaking at 1.2 kHz.

Although the main frequency dependence of threshold of hearing can be related to the external and middle ear transfer functions, this doesn't fully explain the frequency response of hearing as it is level dependent, as indicated by the phon curves in figure 10. Ultimately there is a limited range of frequencies for which the basilar membrane is tuned, which Bekesy (1960) reported to approximately correspond to the typical 20-20000Hz frequency range of hearing in humans.

The quietest sound that the cochlea can detect is limited by the noise floor of the movement of the inner hair cell stereocilia. This sensitivity is enhanced by the activity of the outer hair cells, but these too have an effective noise floor based on the random noise movement of the basilar membrane in the absence of a travelling wave generated by an external acoustic stimulus. The maximum sound pressure level that the cochlea can respond to is commonly reported as approximately 120 dB SPL (threshold of feeling) or 140 dB SPL (threshold of pain), although damage to cochlear structures occurs when these sound levels are experienced.

II Introduction to otoacoustic emissions

The term 'otoacoustic emission' is applied to sound vibrations which are generated within the cochlea (either in the absence of acoustic stimulation or in response to acoustic stimulation), are transmitted through the middle ear and are measured as sound in the ear canal.

It is generally concluded that otoacoustic emissions arise specifically from the outer hair cells because (1) When OHCs are damaged by noise or other mechanisms such as ototoxic drugs, OAEs are not present (Brown et al, 1989) (2) Outer hair cells can be stimulated to move (Brownell, 1983; Ashmore, 1987; Brownell, 1990) and are therefore a good candidate as a source of sound vibration and (3) A saturating gain can explain the large dynamic range of hearing and this dynamic range is reduced when the outer hair cells are lost (Kiang et al, 1970).

Outer hair cell electro-motile activity is thought to be helpful for enhancing the sensitivity and frequency resolution of hearing. Otoacoustic emissions are assumed to be generated as a byproduct of this nonlinear motile response of the outer hair cells to basilar membrane motion, which sets up a reverse travelling wave. This proceeds to the base of the cochlea, is transmitted through the middle ear by the ossicles and can be measured as sound in the ear canal.

Measurement of an evoked otoacoustic emission is therefore dependent on both the forward and reverse transmission characteristics of the middle ear in addition to the mechanisms within the cochlea (Kemp, 1997).

Sound being emitted by the ear is contrary to intuition as, in the Bekesy (1960) travelling wave model of the cochlea, stimulus energy only travels from base to apex. In particular, emissions which occur in response to acoustic stimuli travel in the opposite direction to the travelling wave initiated by the stimulus and a mechanism for this 'turnaround' is required.

Kemp (1978) first measured otoacoustic emissions from human ears in response to click stimuli. The emissions were attributed to the cochlea because of the long time delay (responses earlier than 5 ms were excluded by time windowing), the emissions didn't adapt to changing stimulation rates and reversed polarity with the stimulus so were not of middle ear/muscular origin, and the emissions didn't occur in ears with cochlear deafness. In this regard, evidence of OAE frequency specificity continued to accumulate (Rutten, 1980; Kemp et al, 1990; Collet et al, 1991; Norton, 1993; Moulin et al, 1994).

Questions were initially raised regarding whether OAE are from the cochlea because of the difficulty in explaining waves travelling towards the base in the cochlea and also the time delay was longer even than that expected from electrophysiological estimates of cochlear travelling time. Even if OAE were of cochlear origin, it was debated whether the phenomenon was useful or only of curiosity value. However, the frequency dispersive nature of the response and the lack of an alternative reflection source implied that the source was in the cochlea. Gradually the doubts were satisfied by the detection of sharper tuning in the cochlea (including longer travel times) (Sellick et al, 1983; Johnstone et al, 1986; Robles et al, 1986) and increasing evidence of normal cochlear function being necessary for OAEs to be measured.

OAE's have since been put to extensive clinical use as an indicator of normal cochlear function and have also proved to be useful in research into cochlear mechanics.

a. Forms of OAE

Otoacoustic emissions occur in general in response to any acoustic stimulation. The question arises as to what stimuli would be interesting and useful to investigate. Stimuli can be designed in such a way as to yield responses which are of a convenient form for specific purposes.

i) Short duration stimulus

One example is a stimulus of short time duration, for example a click stimulus. Such a stimulus inherently has a wide frequency spectrum and evokes a response with a wide frequency spectrum. This form of measurement shows the transient response of the cochlea over a wide frequency range (typically 500 Hz to 5 kHz in humans). The otoacoustic emission returns to the ear canal several milliseconds (up to about 20ms) after the stimulus because of the travel-time delay associated with the cochlear travelling wave and therefore can be separated from the stimulus by time windowing. The first part of the time-domain response of a measurement obtained in this way is dominated by high frequencies, later parts of the response contain lower frequencies. This is because low frequencies take longer to travel to their frequency place in the cochlea and back than do high frequencies (section A I f (i)). At frequencies above about 5-6 kHz, the delay of the otoacoustic emission relative to the stimulus is short enough for it to be difficult to separate the cochlear emission from the ear canal ringing in response to the stimulus. This method is therefore not appropriate for high frequency measurements. Measurements of this form are commonly called Transient Evoked Otoacoustic Emissions (TEOAE). The TEOAE response is frequency specific in that the

response tends to be limited to frequency regions which were stimulated and at which hearing thresholds are close to normal (e.g. Kemp et al, 1990; Norton, 1993). However, Yates and Withnell (1999) have shown that TEOAE can also contain significant amounts of intermodulation distortion which would not need to be from the exact frequency place in the cochlea corresponding to the emission frequency. Also Avan et al (1997) have shown a possible correlation between high frequency hearing sensitivity and TEOAE level.

ii) Continuous stimulation by a single frequency

In the opposite extreme, a sound stimulus of a single continuous tone may be applied. The physiological response would be expected to show the suppressible or saturating characteristics of the cochlea, although at low levels (SL≤ 20 dB) emissions can exhibit linear growth with stimulus level (Zwicker and Schloth, 1984). The cochlear response to a single frequency stimulus is predominantly at the stimulus frequency, although otoacoustic emissions at harmonic frequencies are possible. Emissions which occur at the same frequency as a continuous stimulus tone cannot be separated from the stimulus in the ear canal by time windowing or frequency analysis and one of two other methods are employed. The presence of an otoacoustic emission can be demonstrated by suppressing it with a high level masking tone at a close frequency to the emission, the difference in level measured at the emission frequency with and without the masking tone indicates the presence of the emission (Kemp and Chum, 1980b; Brass and Kemp, 1991a).

Alternatively the emission can be demonstrated by showing that it saturates. The stimulus is applied at a low level and then at a higher level (presumed to swamp any otoacoustic emission). The difference between the measurement at low level and the measurement at high level scaled down indicates the presence of the emission (Zwicker and Schloth, 1984).

Emissions at the frequency of a pure tone stimulus (commonly called Stimulus frequency otoacoustic emissions, SFOAE) are not always found across a wide frequency range. Furst et al (1988) reported finding SFOAE in 4 ears out of 7, however Lonsbury-Martin et al (1990) found SFOAE in all 44 ears tested, although not across the full frequency range. The most common frequency for SFOAE to be successfully identified was between 700 Hz and 1.4 kHz.

SFOAE may be defined in terms of reflectance, being the ratio of forward and backward travelling waves, often defined at the stapes but measured from the ear canal (Shera and Zweig, 1993; Zweig and Shera, 1995).

iii) Continuous stimulation by a bi-tonal stimulus

In order to investigate nonlinear aspects of cochlear mechanisms with otoacoustic emissions, stimulation by two simultaneous tones can be employed, which results in the emission of a family of intermodulation distortion products at frequencies given by $f_2+N(f_2-f_1)$, where f_1 and f_2 are the stimulus frequencies and N is a small positive or negative integer (figure 11).

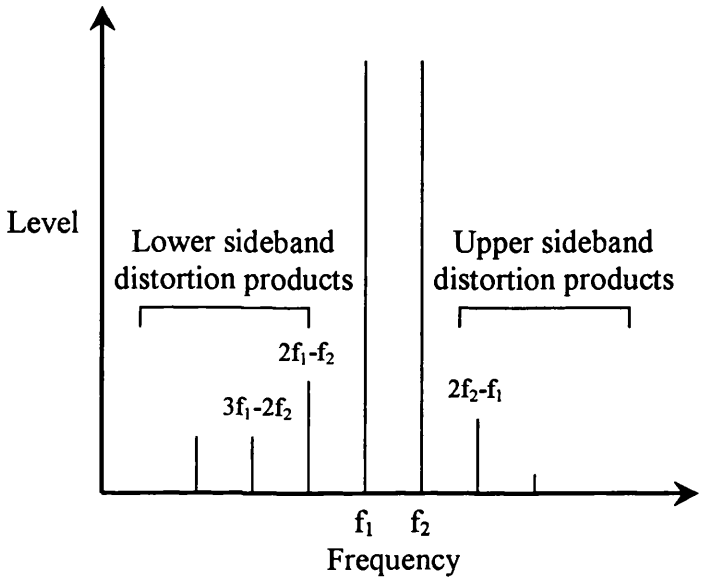

Figure 11. An illustration of a frequency spectrum of DP stimuli (at frequencies f_1 and f_2) with a family of distortion products. The spacings between each distortion product are equal, being f_2-f_1.

The presence of distortion products indicates that nonlinear behaviour is occuring at some location where f_1 and f_2 are present, although the mechanism by which the distortion product is emitted from the cochlea may be linear. These emissions are usually termed Distortion Product Otoacoustic emissions (DPOAE). They can conveniently be separated from the stimulus tones by analysis of the ear canal response in the frequency domain. The frequency resolution afforded by the Fourier transform from the time to the frequency needs to be adequate to separate the distortion products from each other and from the stimulus. The resolution in the frequency domain depends on the length of the time samples (frequency resolution is defined by 1/sample length). Higher frequency resolution than this reduces the amount of noise in each point in the frequency spectrum and therefore improves the signal to noise ratio if the noise is broadband.

The amount of each DP generated on the basilar membrane will depend on the shape of the input/output characteristic of the basilar membrane motion. Frank and Kossl (1996) demonstrated this by showing that if the working point of the cochlear partition

is shifted by applying a 5 Hz tone with f_1 and f_2, the levels of the $2f_1$-f_2 and f_2-f_1 DPOAEs can change by more than 10 dB.

The intensity of the distortion products also depends on the stimulus parameters. The $2f_1$-f_2 DP component is usually the largest and so has been most extensively studied, commonly with a frequency ratio f_2/f_1 between 1.2 and 1.3.

Even so, in humans the level of the $2f_1$-f_2 DP is typically at least 50 dB below that of the stimulus. In non-primate mammals, distortion products are easier to measure, with sometimes a forest of DPs being visible in the frequency domain and the $2f_1$-f_2 DP commonly being only 20 dB below the stimulus level in gerbils (Brown and Kemp, 1984; Brown, 1987).

iv) Otoacoustic emissions in the absence of a stimulus

Finally, otoacoustic emissions can occur in some ears in the absence of acoustic stimulation. They are characteristically pure tones which are emitted in the absence of acoustic stimulus (Kemp, 1979a; Zurek, 1981). Prevalence reported among humans varies depending on the measurement method, typically being between 30 and 70% per ear (e.g. Penner and Zhang, 1997; Moulin et al., 1993). Spontaneous otoacoustic emissions (SOAE) usually occur at frequencies between 1 and about 3 kHz although they can occur up to 8 kHz, and they are usually between –10 dB SPL and +20 dB SPL (Moulin et al, 1993) so the loudest are audible to others in quiet conditions. It was initially thought that these emissions may be a common cause for tinnitus, but it is now known that SOAE are rarely audible to the subject (review, Bright, 1997) with occasional exceptions (e.g. Penner, 1988). SOAE only occur in frequency regions of normal or near normal hearing (Moulin et al, 1991).

It is generally accepted that SOAE are a result of repeated reflections between the frequency place and the base of the cochlea resulting in 'feedback'. It has been shown that the level and frequency of SOAE are sensitive to postural changes, which can affect perilymph pressure in the cochlea (Wilson, 1980; Bell, 1992; de Kleine et al, 2000).

b. The significance of OAEs

OAEs have been shown to be of use mainly in 3 distinct areas: newborn baby hearing screening, diagnostic discrimination between peripheral and retrocochlear hearing loss, and research into the mechanical behaviour of the cochlea.

Otoacoustic emissions are utilised extensively in research as the detail of OAE responses is determined by characteristics of cochlear function, such as the travelling

wave phase characteristics, the non-linear gain and the tuning characteristics. OAEs therefore provide a noninvasive probe of cochlear function.

TEOAE and DPOAE have been shown to be highly effective for newborn baby hearing screening by several major clinical trials (White et al, 1993 – the Rhode Island project, Norton et al, 2000a,b), and in the UK the Wessex project (Kennedy et al, 1998). In the UK, ongoing screening has been running at Whipps Cross Hospital since 1991 (Watkin, 1996a,b). False positive rates (i.e. failure of a hearing ear to pass the screen) are typically below 5% (e.g. Watkin and Baldwin, 1999) and are almost always caused by middle ear fluid or a noisy baby. Use of an Automated Auditory Brainstem Response measurement on bilateral TEOAE fails in the Wessex project reduced false positive rates to below 0.6% (Kennedy et al, 2000). (Watkin and Baldwin (1999) preferred to retest bilateral TEOAE fails on a later date and then routinely use AABR only after a second bilateral fail). False negatives (i.e. a deaf baby passing the screen) are rare and are a result of either a retrocochlear hearing loss, an early onset progressive hearing loss history (e.g. Watkin, 1996b; Lutman et al, 1989; Stein et al, 1996) or are associated with risk factors such as time in a neonatal intensive care unit (Lutman et al, 1997).

As OAEs are of cochlear origin, the inner hair cells and retrocochlear pathway do not need to be functional for otoacoustic emissions to occur. Because of this, otoacoustic emissions are also used for diagnostic purposes in cases of known hearing loss (e.g. Bonfils and Uziel, 1989; Lutman et al, 1989; Robinette and Facer, 1991; Robinette, 1992; Kvaerner et al, 1996) as OAEs may still be measurable in cases of retrocochlear hearing loss but will be reduced or absent in a conductive or cochlear hearing loss. Otoacoustic emissions therefore provide a useful discrimination between retrocochlear and conductive/cochlear hearing losses although in some cases the cochlea can be damaged as a secondary effect by a retrocochlear pathology (review, Robinette and Durrant, 1997). Another clinical use for OAEs is that of monitoring cochlear function over time, particularly during the course of necessary ototoxic drug administration or a changing medical condition (Brown et al, 1989 (in guinea pigs); Yardley et al, 1998; Kusuki et al, 1998).

Which out of TEOAE and DPOAE is the better test depends on the specific application. TEOAE seems very suited to neonatal hearing screening as it is straightforward, is relatively stimulus parameter insensitive and has excellent artefact rejection (Bray and Kemp, 1987). There is also a vast database on which to base a pass/fail criteria. The TEOAE test is also continuous in the frequency domain, the resolution is only limited by the acquisition parameters. DPOAE, meanwhile, tests each

frequency sequentially and the frequency spacing between points is determined by the user, but a closer spacing means the test takes longer. The areas in which DPOAE is the preferable method are based on the fact that DPOAE can be measured at higher frequencies than TEOAE and can often be measured in moderate hearing loss. Therefore DPOAE is preferable in monitoring cochlear performance in known hearing loss and in assessment of high frequency cochlear function.

Otoacoustic emissions can be affected by noise entering the contralateral ear. Collet et al, (1990) report a reduction of up to 0.5-1 dB in OAE when contralateral noise was applied, while Brown (1988) found that in guinea pigs contralateral noise interfered with the recovery of the f_2-f_1 DP during a 'rest period' after a period of prolonged stimulation.

c. Can otoacoustic emissions provide proof of the cochlear amplifier?

Gold (1948) first proposed that active amplification may be taking place in the cochlea, as this would compensate for the excessive damping inherent in the fluid-filled cochlea and explain the sensitive thresholds and fine frequency selectivity of hearing. Gold proposed that the cochlea needed very high Q resonances to explain the frequency resolution of hearing. However his theoretical high Q values were heavily criticised and his theory was not accepted (reviewed by Kemp, 1998). It is now known that much lower Q values are consistent with the frequency resolution of the cochlea because the travelling wave envelope is asymmetrical and is only very sharp on the apical side of the peak. In 1958, Elliot reported sharp peaks and dips in the human pure tone audiogram which were about 50 Hz wide at 1-2 kHz, implying a Q of about 30. This was nowhere near as high as Gold required, but is nevertheless far higher than that implied by Bekesy's data.

The discovery of otoacoustic emissions reopened the possibility that amplification occurs in the cochlea. At first sight, the ability to get sound out from the cochlea, particularly when none was put in (Spontaneous otoacoustic emissions), would appear to prove that the cochlea contains a source of mechanical energy which is enhancing the travelling wave propagation (Kemp, 1979a). Certainly, the presence of spontaneous otoacoustic emissions is consistent with an active cochlea, but does not provide proof. Otoacoustic emissions are known to be related to a vulnerable cochlear mechanism that is necessary for good hearing function because otoacoustic emissions are not present in cases of cochlear deafness (Kemp, 1978) and fall rapidly if the cochlear blood flow is interrupted (Widick et al, 1994; Kim, 1980; Kemp and Brown, 1984).

However it is possible to explain stimulated otoacoustic emissions by a passive compressive non-linear mechanism which is important for sensitive hearing and decays rapidly after death. Spontaneous otoacoustic emissions could possibly arise from random 'Brownian-type' motion being reinforced at specific frequencies by in phase addition of multiple reflections, although this would imply a low-loss cochlea. The occasional very strong spontaneous emissions couldn't arise in this way but are not examples of normal cochlear function.

An alternative mechanism to provide the frequency specificity and nonlinear growth of the travelling wave without an active process invoked a 'second filter' mechanism to deliver energy to the basilar membrane motion around the travelling wave peak. Allen (1980) and Allen and Fahey (1993) proposed that the tectorial membrane may provide a tuned resonant mechanism which may result in the sharply tuned and compressive travelling wave. This arrangement would seem to require the tectorial membrane to be tuned over 10 octaves along the length of the basilar membrane in humans, for which there is no evidence. It should be borne in mind, however, that the tectorial membrane is usually in poor condition in histological preparations so there is little evidence regarding its exact role in cochlear function.

Part of the motivation behind the development of the second filter model was the discrepancy between the tuning of auditory nerve fibres and the tuning of basilar membrane motion. The basilar membrane seemed to be less well tuned, suggesting that an additional filtering mechanism was required (Evans, 1975). However, improvements in techniques for observing basilar membrane motion (e.g. Sellick et al, 1982) have now closed the gap between basilar membrane and neural tuning. The need for a second filter has therefore been largely removed (Ruggero et al, 2000).

Allen and Fahey (1992) attempted to measure the amplification of the cochlea by measuring the amplitude of a DPOAE at the ear canal and the neural activity at the DP place simultaneously whilst changing the frequency ratio of the stimuli and therefore sweeping the DP source location (which is around the f_2 frequency place) across the region of the cochlear amplifier. Their finding was that the amplifier was no more than 10 dB and may be nothing.

However this work does have some limitations. Changing the ratio changes the frequency of modulation and changes the spectral content of the distortion products (Kemp, 1987). They could get the f_2 frequency place no closer than within 2mm of the f_{DP} travelling wave peak so the amplifier could have been closer to the peak than this. More importantly, they assume that the directivity of the DP source does not depend on

the frequency ratio between the stimulus tones. It now seems that the phase gradient of the DP across the region at which it is generated around the f_2 place swaps from positive to negative as the ratio f_2/f_1 increases (Kemp and Knight, 1999). This results in preferential summation of the DP towards the apex when f_2/f_1 is small and towards the base when f_2/f_1 is large. In Allen and Fahey's study (1992), this effect would counteract the effect of a cochlear amplifier and result in a significant underestimate of the gain of the cochlear amplifier. The probable presence of a reflected DP component from the DP place would further complicate measurements of this type.

Brass and Kemp (1993b) have investigated previously published Mossbauer measurements of basilar membrane transverse velocity (from Robles et al, 1986) and concluded, by considering power flow, that the travelling wave gains up to 40 dB from somewhere as it travels to the peak at the characteristic frequency place. This figure is a net power gain – so the energy supplied is enough to counteract viscous damping and then another 40 dB in addition. Their discussion of the (many) assumptions shows that any errors are unlikely to account for such a large figure and indeed it may even be an underestimate.

In summary, the case for an active cochlea can currently be described as 'very likely but not directly proven'.

d. Neural tuning curves

The firing of a single fibre in the auditory nerve can be monitored by inserting a microelectrode into the nerve fibre. In this way a neural tuning curve can be recorded by presenting tone bursts to the ear canal and adjusting the intensity until a predetermined increase in the nerve firing rate has been achieved. If this is measured at a range of frequencies, the fibre will be found to have a low threshold at one frequency and the threshold increases rapidly at frequencies more distant than this optimal or 'characteristic' frequency. A v-shaped 'tuning curve' is therefore generated (Evans, 1972; Sellick et al, 1982; Ruggero, 1990; Robles et al, 1986). Examples are shown in figure 12 (from Liberman and Kiang, 1978). These neural tuning curves are closely related to the more recent measurements of basilar membrane motion using the Mossbauer technique or laser velocimetry discussed in section A I f (i) (Narayan et al, 1998; Ruggero et al, 2000).

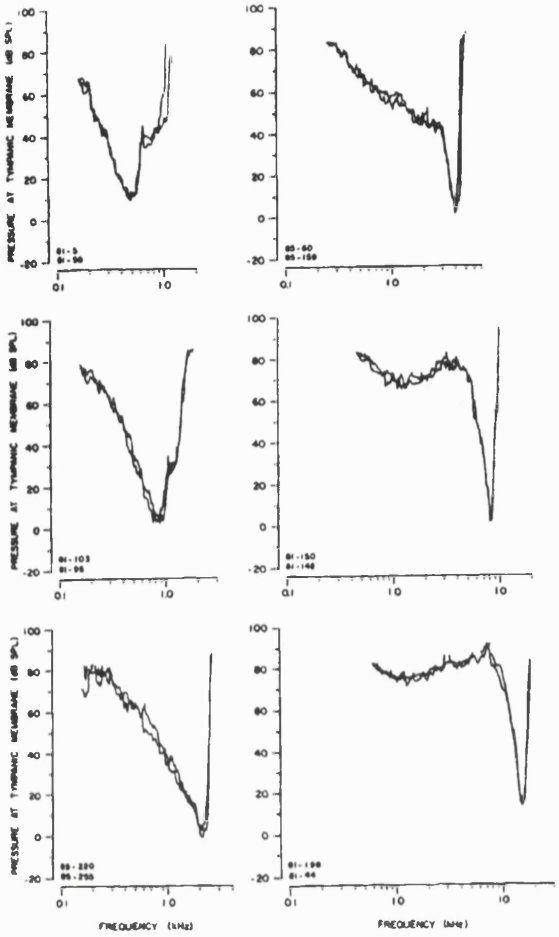

Figure 12. Neural tuning curves. (from Liberman and Kiang, 1978)

e) DPOAE suppression tuning curves

Tuning curves can also be generated for DPOAE. Two tones, f_1 and f_2 are fixed, and a third tone is added, the level of which is varied until the DPOAE is reduced in level by a predetermined criteria (commonly 1, 3 or 6 dB). If this is repeated using a range of frequencies for f_3, a 'DPOAE suppression tuning curve' is generated (e.g. Brown and Kemp, 1984; Kummer et al, 1995; Martin et al, 1987). OAE suppression tuning curves can also be obtained with TEOAE, if a pure tone is added to the click stimulus, the TEOAE response will reduce in the frequency region of the tone, giving a v-shaped 'suppression tuning curve' (Kemp and Chum, 1980a; Wilson, 1980; Tavartkiladze et al, 1994a, b).

By analogy with auditory nerve tuning curves, OAE suppression tuning curves are commonly used to imply the location(s) of DPOAE source(s) on the basilar membrane. This assumes by implication that the ease of suppression by a tone reflects the importance of the frequency place of that tone in making the emission (Brown and Kemp, 1984).

Suppression tuning curves obtained with OAEs are different to neural tuning curves in several ways.

1. With OAE the response is monitored back in the ear canal so the response is not inherently place specific. The response is in fact likely to be from an extended emitting region. The response may therefore be complicated by interference between contributions from different parts of the basilar membrane.
2. What is being measured is fundamentally different – a neural tuning curve finds an approximation of the 'hearing threshold' of the nerve fibre. A DPOAE suppression tuning curve finds the onset of suppression of DPOAE production with the whole system operating well above hearing threshold.
3. In the case of neural tuning curves, it is the increased firing rate of the nerve in response to the swept tone that is being measured, whereas with DPOAE suppression tuning curves the third tone suppresses the DPOAE which is being generated in response to two different stimulus tones. DPOAE suppression tuning curves are commonly used to determine the source on the basilar membrane of the DP that is measured in the ear canal, and the travelling wave envelope of the third tone is an inconvenient 'blurring' factor on the results.

DPOAE suppression tuning curves therefore differ fundamentally from neural tuning curves. Nevertheless they can be used to provide an indication of the primary location of the DPOAE source region on the basilar membrane, provided that the limitations are understood.

f. DPOAE suppression tuning curves and source location(s)

DPOAE suppression tuning curves have been widely used to imply the location of the cochlear source of DPOAE since the early work of Brown and Kemp (1984).

Nonlinear behaviour of the organ of Corti and the basilar membrane may be expected to cause distortion products at any point at which both stimulus tones are present (which in practice means within the f_2 travelling wave envelope), but in fact the dominant region for lower sideband DPOAE generation is believed to be in the region of the f_2 travelling wave peak (Brown and Kemp, 1984; Kummer et al, 1995). It has been argued that the source of lower sideband DPOAE is at the place of the 'geometric mean' of the primaries (Martin et al., 1987) and some studies have reported DPOAE results against the geometric mean frequency (e.g. Lonsbury-Martin et al, 1990). But at wide frequency ratios this can be outside the f_2 envelope and therefore not a possible initial source. The f_2 frequency place has been generally accepted as representing the source of lower

sideband DPOAE, although the actual source may be distributed over a region and its precise centre of gravity with respect to the f_2 place may vary depending on the stimulus parameters.

In the case of the lower sideband DP components, once the DP is generated it may travel along the basilar membrane in either direction - either straight back out or onwards to the DP frequency place. From the DP place it may be re-emitted back to the base as a 'stimulus frequency' emission. Sometimes tuning curves of $2f_1$-f_2 DPOAE have a small secondary dip in the DP frequency place, indicating that there could be a significant secondary source in this region (Kummer et al, 1995; Gaskill and Brown, 1996).

The situation is different for the upper sideband DPOAEs (that is, DPOAEs with frequencies higher than the stimulus frequencies, see figure 11). As frequencies fail to propagate apically to their characteristic place in the cochlea, upper sideband DPOAEs are emitted from a more basal region than the f_2 frequency place, corresponding to a frequency near to or a little above the DP frequency. This conclusion is supported by $2f_2$-f_1 DPOAE suppression tuning curves (Martin et al, 1987; Kemp, 1998; Martin et al, 1998).

Returning to the lower sideband, Sun et al (1994a,b) have presented a cochlear model capable of producing $2f_1$-f_2 DPOAE with fine structure with only a single source region centred around the frequency place of the higher frequency stimulus. He and Schmiedt (1993, 1997) argued that the fact that measured DPOAE fine structure moves in frequency when the stimulus level is changed supports this model. But in fact this behaviour would equally be predicted by a model with fine structure caused by a secondary DPOAE source at the DP frequency place. It is not known whether the model of Sun et al is capable of producing the divergent phase behaviour of DPOAE (Kemp, 1986), which will be discussed later.

Heitmann et al (1998) have shown that use of a third tone close to the DP frequency (first employed by Kemp and Brown (1983) to isolate a stimulus frequency reemission component of DPOAE) can reduce the amount of fine structure seen in lower sideband DPOAE. The simplest explanation of this is that the fine structure is caused by an emission from the DP frequency place interfering with an emission from the f_2 frequency region. Dreisbach and Siegel (1999) have used this 'suppression' technique to attempt to separate the two emission components and observe them individually. Two distinct phase patterns, as described by Kemp (1986), can be seen although total

separation is difficult to guarantee, especially when f_2/f_1 is close to 1 (Siegel et al, 2000).

In summary, the sources of generation and reflection are important for DPOAE observation.

g. DPOAE phase gradients and time delays

All evoked otoacoustic emissions exhibit delay relative to the stimulus and therefore OAE phase with respect to the stimulus is dependent on frequency. Phase versus frequency gradients have been shown, for example, with transient evoked otoacoustic emissions (TEOAE) (e.g. Kemp and Chum, 1980a; Wilson, 1980), distortion product otoacoustic emissions (DPOAE) (Kemp and Brown, 1983) and stimulus frequency otoacoustic emissions (SFOAE) (Kemp and Chum, 1980b). The group delay implied by these phase gradients (often referred to as 'OAE latency') is believed to contain information about the mechanism underlying otoacoustic emissions.

In the case of a single frequency acoustic wave travelling to a wall, reflecting and returning to where it started, the phase of the returning wave will be related to the phase of the wave sent. However, it is not possible to determine the time delay of the journey from this relationship because it is not known how many whole wavelengths the wave has travelled through. But if the frequency is changed slightly, the amount that the phase of the returning wave changes implies the path length by the following equation:

$$\text{Time delay (seconds)} = \frac{-\delta(\phi/2\pi)}{\delta(f)}$$

where ϕ is the DP phase in radians and f is the DP frequency in Hz.

Therefore it is the phase gradient versus frequency rather than the 'single point' phase that is of interest with otoacoustic emissions. With distortion products, as the frequency of the response differs from the frequency of the stimulus, the phase gradient is obtained by defining it relative to a notional DP generated without any delay.

Superficially it might seem that the phase gradient will definitively indicate the distance of the emission source along the cochlea. The implied assumption here would be that a longer delay implies that the OAE source is further into the cochlea. However, the 'latency' derived from OAE phase versus frequency gradients requires careful interpretation as an indicator of true time delay because of the dispersive nature of the cochlea (different frequencies travel at different speeds) and because the path length

varies with frequency. The phase gradient also doesn't directly indicate the relative source locations of the DPs along the basilar membrane as the DPs have different frequencies and would therefore travel at different speeds at the same location in the cochlea and also because different mechanisms may be involved in generating the reverse travelling waves.

For example, using an f_2 sweep paradigm the group delay of the $2f_2$-f_1 DP has been reported by Wable et al (1996) to be shorter than that of the $2f_1$-f_2 DP. This finding was used to support the generally accepted view that the generation region of the $2f_2$-f_1 DP is more basal than the $2f_1$-f_2 DP (Martin et al 1998). However this result is in fact dependent on the test paradigm - the opposite result could have been found using a sweep with a constant frequency ratio (Knight and Kemp, 1999b).

The onset delays measured by Whitehead et al (1996) are an alternative method of evaluating DP delay and the result is a more physically meaningful time delay, although the onset can be gradual resulting in uncertainty regarding the exact onset time. Despite the difficulties in interpretation, phase gradient-derived delays are useful as comparative probes of the mechanisms involved in cochlear function.

Usually, test strategies are adopted for obtaining DP phase gradients with either f_1 (e.g. Kimberley et al, 1993) or f_2 (e.g. O Mahoney and Kemp, 1995) being swept in frequency while the other is held constant. In the case of the 'f_1 sweep', the $2f_1$-f_2 DP generation region (which is related to the f_2 frequency place, (e.g. Brown and Kemp, 1984)) remains stationary, whereas with an 'f_2 sweep', the $2f_1$-f_2 DP generation region moves. It has been shown that in the case of the $2f_1$-f_2 DP, f_2 sweeps result in a higher value for group delay than f_1 sweeps (Kimberley et al, 1993; O Mahoney and Kemp, 1995). The $2f_2$-f_1 DP behaves differently. No significant difference between f_1 and f_2 sweep latencies is reported (Moulin and Kemp, 1996).

DPOAE phase gradients are not entirely smooth and monotonic. In addition to an overall gradual change in phase gradient from low to high frequency, there are also small scale irregularities. These irregularities are not only due to the effects of noise as they occur when the DPs are well above the noise floor. The irregularities are permanent and repeatable and are often associated with the fine structure of DPOAE amplitude (Moulin and Kemp, 1996). The irregularities could arise from interference caused by multiple reflections between the DP frequency place in the cochlea and the middle ear (Stover et al, 1996a), or by interference between either two DP sources (e.g. Brown et al., 1996; Talmadge et al, 1999) or between different parts of a distributed source region (e.g. Zweig and Shera, 1995; Sun et al, 1994a). It may be that more than

one of these effects can occur, either simultaneously or under different stimulus conditions.

h. OAE fine structure

All forms of evoked otoacoustic emissions tend to exhibit fine structure, that is, quasi-periodic fluctuations in level with respect to frequency. Kemp, 1979b and Zwicker and Schloth (1984) found close relationships between hearing threshold fine structure and TEOAE fine structure and frequencies of SOAE. This implies that the same mechanism may be responsible for the fine structure in each case. They propose that the fine structure is caused by interference between repeated reflections of OAEs within the cochlea. It remained possible, however, that it could just be luck that their fine structure coincided so well.

There is an alternative mechanism for the fine structure of TEOAE and SFOAE in which the fine structure results from interference between different elements within one OAE generating region.

DPOAE was not included in Zwicker and Schloth's (1984) study. He and Schmiedt (1993, 1997) demonstrated that $2f_1$-f_2 DPOAE fine structure shifts in frequency depending on the stimulus level, so any alignment of DPOAE fine structure with the fine structure of other OAEs would be controlled by stimulus level.

DPOAE fine structure may be fundamentally different from that of other OAE's as it may arise from interference between two sources (Kim, 1980, Kemp, 1986). If this were the case, it would explain why frequency alignment has not been reported between the fine structure of DPOAE and the other types of OAE.

i. Otoacoustic emission mechanisms

Gold (1948), in proposing that active amplification may be taking place in the cochlea, concluded that the cochlea needed very high Q resonances to explain the frequency resolution of hearing. He proposed that the active processes would require a self-regulation system in order to maintain an optimum operating point. Nevertheless he suggested that fading ringing of pure tones may occasionally be emitted from the ear in cases of disturbance of the self-regulation. Such tones would be due to the mechanical oscillations of a highly tuned and amplifying system. However he was unable to measure such acoustic emissions and his theories were not pursued.

When stimulated OAEs were first demonstrated, the immediate question arose as to how the sound came to turn around and come back out. It was initially felt that some

form of reflection mechanism was required (Kemp, 1978) and it was assumed that this mechanism would be associated with and induced by nonlinearity in the region of the peak of the travelling wave.

DPOAE are of particular interest for investigating the emission mechanism because of the involvement of different specific and known frequencies in the stimulus and emission processes which allows a wide variety of test paradigms to investigate phase behaviour. The possibility that there may be two sources for lower sideband DPOAE was suggested by Kim (1980). The initial generation site was the region of overlap of the stimulus tones on the basilar membrane but the DP may then travel on to the DP frequency place. Kemp and Brown (1983) proposed two mechanisms for DP emission.

Kemp (1986) introduced the terms 'wave fixed' and 'place fixed' to describe these mechanisms and demonstrated that $2f_1$-f_2 DPOAE phase behaviour changes depending on the ratio between the stimulus tones, f_2:f_1. When f_2/f_1 exceeds approximately 1.1, a frequency sweep with a constant frequency ratio yields an almost constant $2f_1$-f_2 DPOAE phase. With a smaller frequency ratio, a steep $2f_1$-f_2 DPOAE phase gradient results, the phase becoming more negative (i.e. greater phase delay) at higher frequencies. Therefore which mechanism of emission dominated was controlled by the ratio of the stimuli.

The classification of proposed DP emission mechanisms used in this study are summarised here:

Wave fixed The DP is emitted directly from the generating region by a mechanism which is inherently part of and moves smoothly with the stimulus envelope. Because of the approximately consistent logarithmic scaling of the cochlea, frequency shifts cause little change to the travelling wave phase profile, so that when a stimulus pattern is swept in frequency the phase at any point moving with the travelling wave envelope changes little. Therefore any OAE contribution from that point would have a very shallow phase gradient.

Place fixed The DP initially travels towards the apex, but encounters discrete irregularities in transmission characteristics with respect to position on the basilar membrane. These irregularities cause reflections or scattering of the travelling wave, which can travel towards the base. As a stimulus is swept in frequency and its excitation pattern moved along the basilar membrane, the stimulus phase at each reflector location will change, thus changing the DPOAE phase and causing a steep phase gradient to be obtained.

For convenience, the terms wave fixed and place fixed will be adopted here for DPOAE with shallow or steep phase-versus-frequency gradients respectively in a constant f_2/f_1 sweep. Nevertheless, the mechanisms are strictly unproven.

The important regions of 'reflection' in lower sideband DPOAE may be expected to lie in the DP frequency place region, as suggested by suppression studies using a third stimulus tone (e.g. Kummer et al, 1995; Gaskill and Brown, 1996; Heitmann et al, 1998) observation of DPOAE fine structure (Mauermann et al, 1999a, 1999b) and comparison of experimental data with mathematical models (Talmadge et al, 1999). If outer hair cell activity adequately compensates for the transmission losses in propagating back to the base and in reflection back a second time to the DP place, then the distortion product also could reflect repeatedly between the DP characteristic place and the base of the cochlea resulting in a feedback system causing interference effects, fine structure and occasionally resulting in spontaneous otoacoustic emissions (Kemp, 1980; Zweig and Shera, 1995; Talmadge et al, 2000).

The possible identity of these 'reflectors' has been the subject of some discussion, the difficulty being 'why don't these reflections tend to cancel each other out?'. Strube (1989) proposed that regularly spaced reflectors result in a place fixed emission by a process akin to 'Bragg scattering'. However, without descending to a single cellular scale, no suitable regular spacing has been found.

Zweig and Shera (1995) proposed that a mechanism, still based on Bragg scattering, could give rise to place fixed emissions even from randomly spaced reflectors. Their argument is that although the reflectors may be randomly spaced, only those with a specific spacial frequency (set by the travelling wave in the peak region) will have a phase change on reflection exactly counteracting the phase change of propagation to the reflection site and back and will dominate the net backward-travelling wave. The reflectors are described as needing to be 'densely spaced', although just how dense is not described. It is therefore not clear whether there is a good candidate for the source of randomly spaced reflectors. For example, the irregularities in the primate outer hair cell arrangements (Wright et al, 1987) are floated as a possible source of impedance irregularities, but Zweig and Shera's mechanism appears to require a close spacing of irregularities, and these outer hair cell irregularities may not be closely spaced enough.

It is possible that the detailed model described by Zweig and Shera is not necessary in order to get an emission from randomly spaced reflectors. If the reflectors were less densely spaced such that only 3 or 4 at a time were producing a significant reflection, the reflections would be unlikely to completely cancel out, so a resultant emission

would automatically arise. In this case, the outer hair cell irregularities would be a good candidate for the source of reflections.

With two emission mechanisms proposed (wave and place fixed) and two sources of lower sideband DP emission identified (the f_2 region and the DP frequency place), two emission routes can be proposed for lower sideband DPOAE, which are illustrated in figure 13.

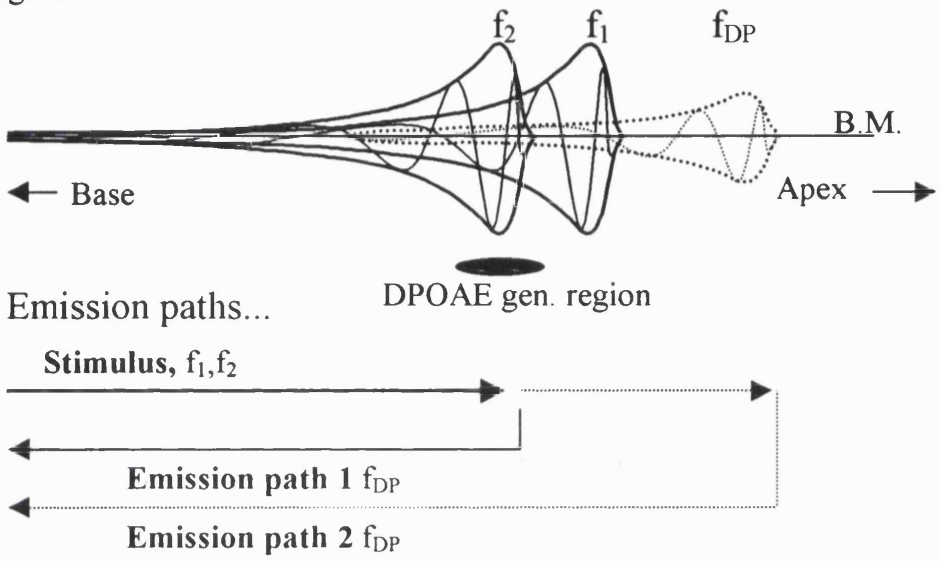

Figure 13. An illustration of the proposed emission paths for lower sideband DPOAE. Both paths begin with the forward propagation of the stimuli and generation of distortion products in the region of the f_2 peak. In path 1 the DP is propagated from here to the base of the cochlea by a reverse travelling wave along the basilar membrane. In path 2, the DP is propagated onwards to the region of the DP frequency place, where a reflection mechanism causes a proportion of the DP to reverse it's direction of travel and return to the base of the cochlea.

PATH 1: The DP travels directly to the base from the generation site

Kemp and Knight (1999) have suggested that the mechanism of DP generation may, for certain f_2/f_1, preferentially direct energy basally. This route may correspond to behaviour Kemp (1986) observed in the $2f_1$-f_2 DP with $f_2/f_1>1.1$. He termed it 'wave fixed' because its phase characteristics required the generator to move smoothly with the f_2 travelling wave in a frequency sweep.

Shera and Guinan, (1999) labelled the same phenomenon 'distortion emission' to emphasise that only non-linearity (not a reflection) is required for an ear canal DP to be produced. Path 1 results in 'low latency' DPOAEs.

PATH 2: The DP travels initially towards the apex, until it is reflected back towards the base.

This mode of DPOAE may correspond to behaviour seen in the $2f_1$-f_2 DPOAE for small f_2/f_1, which was separated by suppression by Kemp and Brown (1983). It was

described as 'place fixed' by Kemp (1986), because the phase characteristics required reflectors to be fixed in position on the basilar membrane.

Shera and Guinan (1999) described this mode of DPOAE as 'reflection DPs' to emphasise that the proposed 'turnaround' mechanism is a reflection. Path 2 would result in 'high latency' DPOAEs. TEOAEs have similar phase characteristics and have been said to require an impedance discontinuity (Kemp, 1978) or impedance irregularities along the basilar membrane to cause the reflection (Kemp, 1986; Lonsbury-Martin et al, 1988; Zweig and Shera, 1995).

The wave and place fixed mechanisms have recently been discussed by Shera and Guinan (1998, 1999), who emphasised fundamental differences between them. They showed that the 'wave fixed' mechanism was consistent with the shallow DPOAE phase gradient obtained with the most commonly used stimulus parameters in a constant frequency ratio sweep, but was incapable of generating the steep phase gradients obtained with stimulus frequency (SF)OAE and transiently evoked (TE)OAE. Therefore they argued OAEs fell into two entirely separate categories - a distortion emission class and a reflection emission class.

However these categories only refer to the 'turnaround mechanism' and not the generation mechanism as the steep and shallow phase gradient characteristics can both be observed in $2f_1$-f_2 DPOAEs obtained with constant stimulus frequency ratio sweeps. Kemp (1986) has shown that the $2f_1$-f_2 DPOAE has a shallow phase gradient consistent with the wave fixed model when stimulated using typical clinical stimulus parameters (f_2/f_1 is usually between 1.2 and 1.25 for clinical use), but has a steep phase gradient when stimulated using a small stimulus frequency ratio, e.g. f_2/f_1=1.05. Therefore, the $2f_1$-f_2 DP appears to change emission mode depending on whether a wide or small stimulus frequency ratio is used.

Kemp and Knight (1999) proposed that this changeover may be controlled by the phase gradient of the DP across the region in which it is generated, which causes the DP to sum constructively in one direction but to largely cancel out in the other direction. The phase gradient across the DP generating region is controlled by the stimulus frequency ratio, f_2/f_1.

As discussed in section A II (f), the situation is different for upper sideband DPOAE such as the $2f_2$-f_1 DP. The DPOAE must originate in the region of the f_2 envelope but also not more apically than the DP characteristic frequency place on the basilar membrane, since frequencies fail to propagate from positions apical to their characteristic place. The DP could be produced at the sites of the reflectors and

immediately travel basally, or it may be generated at a site removed from the reflectors and initially travel a short distance apically until a reflector is encountered.

Martin et al. (1999a, b), Martin et al. (2000) and Fahey et al. (2000) have shown that there may also be alternative basal sites for DP generation. These require more complex generation mechanisms, for example involving intermodulation distortion of harmonic distortion.

j. Methods to separate wave and place fixed DPOAE

In order to obtain the characteristics of the sources of DPOAE that are present in a recording, it is advantageous to first separate the wave and place fixed components of the response. This would remove a source of fine structure, allow greater certainty about the source of the DPOAE along the basilar membrane and may allow data trends to be seen which are otherwise confused by the mixing of the two DPOAE components.

One method which has been utilised is to suppress the activity in the region of the DP frequency place by adding a third stimulus tone close to the DP frequency. The emission is then only from the f_2 region. Vector subtraction between measurements obtained with and without the suppressing tone can provide an estimate of the DPOAE contribution from the DP frequency place. However it can be difficult to fully suppress the DP place without also affecting the f_2 region (Siegel et al, 2000). The method also requires two measurements, and the probe fitting conditions must not change between the two as changes in probe fittings would lead to incorrect inferences about contributions from the region of the DP frequency place.

An alternative method which could be employed for this purpose is inverse Fourier transformations of DPOAE frequency sweeps, which have been used to view complex DPOAE data obtained with f_1 stimulus frequency sweeps in the time domain. This has revealed coexisting DP components with different latencies whose relative strength varies depending on stimulus level (Fahey and Allen, 1997; Stover et al, 1996a). Stover et al also found that with low stimulus amplitudes a series of DPOAE amplitude peaks are sometimes seen in the time domain, which could be an indication of multiple reflections between the DP place and the stapes. If this method were applied to frequency sweeps with a constant frequency ratio, separate peaks could be expected for the wave and place fixed emissions because of their different phase gradients in such stimulus paradigms.

k. Relationships between TEOAE and DPOAE

Both the transient evoked OAE method (TEOAE) and the distortion product OAE method (DPOAE) must have similar mechanisms, but it is not clear how similar they are. The techniques are superficially very different so that it is reasonable to expect that the OAEs recovered by the techniques will also differ in their relation to hearing function.

With TEOAE recording, a wide-band click stimulus is repeatedly presented to the closed ear canal. The cochlea is therefore observed repeatedly 'returning' to its rest state following brief stimulation.

With the DPOAE method, stimulation can be continuous, consisting of two simultaneously applied tones with frequencies f_1 and f_2, with f_2/f_1 usually set to between 1.3:1 and 1.2:1 for maximum output.

Irrespective of differences in the signal recovery method, DPOAE production contrasts markedly with TEOAE production because a) with DPOAE, the portion of the cochlea stimulated is restricted to the excitation pattern of the two close tones f_1 and f_2 whereas a click applies all frequencies to the cochlea simultaneously, b) because TEOAEs and DPOAEs are different subsets of the total OAE response present, c) because the DPOAE response is produced in the 'steady stimulation' state whereas TEOAE is recorded after stimulation has ceased and d) TEOAE is obtained across frequencies simultaneously, whereas DPOAE is obtained sequentially. Point (c) is moderated by the fact that the combined DPOAE stimulus of f_1 and f_2 is amplitude modulated with a period of f_2-f_1.

TEOAE and DPOAE are the two most common methods used to study OAEs in research and in clinical practice. OAEs are accepted as an audiological tool, however it is not self evident which of these two convenient means of evoking and extracting an OAE yields a signal most closely linked to the functional status of the sensory mechanism.

It is not certain that the intensity of OAEs is the measure most likely to closely reflect the condition of the cochlea. Furthermore, DPOAE intensity depends not only on the stimulus intensity but it also varies very substantially with the particular stimulus frequency and amplitude ratios used. It is sometimes assumed that the frequency specific nature of DPOAE stimulation will logically lead to DPOAEs being more closely associated with function, but a close relationship to auditory threshold has yet to be found (e.g. Gorga et al, 1993; Moulin et al, 1994; Gorga et al, 1997; Dorn et al, 1998).

There are fundamental reasons for expecting a divergence between TEOAE or DPOAE intensity levels (even when averaged across frequency) and auditory threshold. Firstly, the otoacoustic re-emission mechanism itself is a by-product of cochlear function and is not directly part of the hearing process, and secondly the vital process of transduction at the inner hair cell which leads to audition does not participate in OAE production. The relationship between OAEs and hearing threshold is beyond the scope of the present study.

These considerations raise a question: which set of OAE stimulation and measurement parameters is least influenced by those intra and intersubject differences which do not alter hearing sensitivity? Such parameters would be most appropriate for the purpose of obtaining an index of cochlear status.

(i) Relationship between TEOAE and DPOAE level

As TEOAE and DPOAE both arise from cochlear sensory activity, a relationship between the levels of each may be expected. Moulin et al (1993) found that DPOAE and TEOAE had greater levels in ears with SOAEs than in ears without SOAEs and also found a correlation between TEOAE and DPOAE level, although the relationship was not close. Other studies into the relationship between TEOAE and $2f_1$-f_2 DPOAE amplitude have also only indicated weak correlations (Probst and Harris, 1993; Smurzinsky and Kim, 1992; Smurzinsky et al, 1993). However, these studies for the most part only covered the small range of DP stimulus parameters which are in clinical use. For example, f_2/f_1 ratios only ranged from 1.17-1.23. They also used little or no averaging across the OAE fine structure, which is prominent in both DPOAE and TEOAE. Moulin et al (1993) found a similar weak relationship between $2f_2$-f_1 DPOAE and TEOAE amplitude.

As noted above, most comparative work on OAEs has used limited ranges of parameters. This is because of the interest in clinical and screening applications that require the use of parameters which generate a large amplitude response and for which normative data is available. For DPOAE, the stimulus amplitude and frequency ratios giving maximum DP output levels have been preferred in order to optimise testing time and test specificity (e.g. Harris et al, 1989; Gaskill and Brown, 1990; Hauser and Probst, 1991) and to maximise differences between hearing and hearing impaired ears (e.g. Stover et al, 1996b; Moulin et al, 1994). Reductions in the absolute stimulus levels which give increased sensitivity to cochlear disorder are traded against increased testing time within the environment of a clinic. As a result, levels exceeding 60 dB SPL are

commonly used to achieve adequate specificity and speed. With TEOAE, sensitivity is generally maintained even with the highest click levels compatible with minimal transducer artefact levels (around 90 dB SPL peak) and these higher levels optimise the specificity (Prieve et al. 1993).

The stimulus parameters typically used for DPOAE and TEOAE in audiological investigation may not necessarily be optimal for describing the functional differences between two cochleae. The influence of spurious factors may or may not be minimised by the adoption of stimulus conditions yielding maximum DPOAE intensity. They may also not be optimal for deciding how closely the two OAE response modes (TEOAE and DPOAE) are physiologically related.

TEOAE and DPOAE arise from such different spatial and temporal excitation patterns of stimulation within the cochlea that relative differences between the levels of each is to be expected between individuals. Interference between elemental contributions distributed along the cochlea must effect the ear canal signal greatly and this may vary between individuals. One would therefore expect at least to have to average OAE activity over a range of stimulus parameters in order to arrive at a reliable indicator of cochlear status but this is not common practice. Also the very different stimuli used for TEOAE and DPOAE measurements must to some extent exercise different aspects of the sensory mechanism's input-output characteristic and this may also differ from ear to ear.

Clearly there are many unexplained sources of variance in OAEs, for example those between OAE detection modes, between parameter configurations, and between individuals which may not all be related to hearing function. If, by the selection of appropriate stimulation parameters, very closely correlated OAE characteristics were obtainable by two different and independent OAE measurement techniques across a subject population, it is likely that those particular OAE detection modes are influenced in a similar way by the intervening variables. More specifically, if for any stimulus configuration the DPOAE and TEOAE characteristics are found to agree across a population then it becomes more likely that, for that stimulus configuration, TEOAE and DPOAE generation relates to similar aspects of cochlear function.

(ii)Relationship between TEOAE and DPOAE phase

When a TEOAE response is observed in the frequency domain, its associated phase versus frequency gradient is steep (Wilson, 1980; Kemp and Chum, 1980a). The implied time delays from the TEOAE phase gradients are consistent with the 5-15 ms

delay seen in the time domain (Kemp, 1978). Measurements of SFOAE also generate a steep phase versus frequency gradient (Kemp and Chum, 1980b). However, the $2f_1$-f_2 DPOAE differs from this, because in a sweep with f_2/f_1 held constant it has a steep phase gradient if f_2/f_1 is below about 1.1, but a shallow phase gradient when f_2/f_1 is greater than 1.1. This shallow phase gradient implies that a different emission mechanism dominates under these stimulus conditions, so a close relationship between this emission and TEOAE or SFOAE should not necessarily be expected. The significance of OAE phase gradients will be discussed further in a later section.

The reason for the currently reported low correlation between TEOAE and DPOAE is yet to be determined. There are many technical reasons why the emissions may not be closely related, and the very different phase patterns imply that the underlying mechanisms may be different. Nevertheless the limited stimulus parameter ranges which have been investigated leave open the possibility that the stimulus parameters have not been adequately matched. Further work is therefore required in this area to determine whether there is a close relationship between TEOAE and DPOAE.

III Foundation to the present study

There are several interrelated issues which are currently unresolved, but if clarified they could provide information regarding emission mechanisms, emission sites and the stimulus parameter ranges for which they are effective.

It remains unknown how many distinct emission mechanisms there are involved in the production of OAE. Two distinct phase gradients have been identified in the $2f_1$-f_2 DPOAE, however it is not known whether either of these utilises the same underlying emission mechanism as TEOAE. Published data show only a poor relationship between TEOAE and DPOAE level. It may be that the lack of a close relationship is simply because the limited range of stimulus parameters which have been used are not the ones which will produce the closest relationship or perhaps the DPOAE data are being confused by fine structure arising from interference between two DP emitting regions of the cochlea. Alternatively, the two measurement methods may be eliciting fundamentally different mechanisms which are not closely related.

DPOAE have been studied predominantly within a restricted range of stimulus parameters and investigating DPOAE over a wider range of parameters may resolve the outstanding issues. For example a major change in DPOAE phase versus frequency gradient has been shown to occur, dependent on whether f_2/f_1 is greater or less than around 1.1. This may harbour clues as to the emission mechanisms involved in DPOAE and therefore requires further investigation. It is also not known what the connection is between the lower and upper sideband DPOAE, whether they are emitted by similar mechanisms and whether the phase delays involved are related.

DPOAE phase versus frequency gradients can be derived from different sweep paradigms, for example f_2 sweep, f_1 sweep, constant f_{DP} sweep. These sweeps give different results but the meaning of each or the differences between them are not clearly understood. A new unifying approach is needed, which can show how the different sweeps fit together.

Finally, as the lower sideband DPOAE has two discrete emission mechanisms, it would be beneficial to develop a method for separating the emissions and studying them separately. This would enable emission patterns to be studied without interference effects from different sources. Emissions could even be traced with stimulus parameters for which they have not previously been seen because they are obscured by a different larger emission. Patterns contained in such data could yield further clues regarding the cochlear mechanisms involved in DPOAE.

IV Aim

The aim of this study is to investigate the cochlear mechanisms involved in OAE production by obtaining OAE measurements in a format that will yield information regarding the generation of OAE and their emission routes.

It has been shown that DPOAE have two modes by which they are emitted. It has not been clarified whether either of these mechanisms corresponds to that involved in the production of TEOAE or alternatively whether there are at least 3 distinct emission classifications. The relationship between TEOAE and DPOAE will be studied over a wider range of DPOAE parameter configurations than is presently represented in the literature. This will determine whether there is evidence for similarities in the mechanisms involved in TEOAE and either of the DPOAE modes, despite the differences in method. To this end measurements of OAE phase gradients with frequency, and measurements of the less studied $2f_2$-f_1 DPOAE will also be investigated.

Kemp (1986) demonstrated that characteristics of the $2f_1$-f_2 DPOAE change at a stimulus frequency ratio of around 1.1. This work will be extended to find out whether there are other changes and to find the parameter areas of the different behaviour types. In order to delineate the potentially different emission modes, detailed DPOAE measurements will be obtained to trace a more complete picture of DPOAE characteristics over a wide range of stimulus parameters. This will allow a better understanding of the level and phase trends, determine the mechanisms involved and indicate areas of similarity and difference between the upper and lower sidebands.

Methods will be explored for separating the wave and place fixed parts of DPOAE so that they can be studied individually. This will eliminate the complications of interference, determine whether or not the emission modes are simultaneously active and enable the smaller of the two emissions to be studied under stimulus conditions in which the larger one dominates.

Based on these observations, a hypothesis of the mechanisms involved in DPOAE production will be developed and a simple mathematical model will be used to test whether the proposed mechanisms are able to produce the observed pattern of results.

B. OAE measurements

a. Instrumentation

Successful measurement of otoacoustic emissions requires (as well as a healthy ear) systems for sound waveform generation, sound delivery, sound collection and data acquisition and analysis.

Figure 14 shows a schematic outline of an OAE measurement system. For TEOAE, only one of the sound generation channels is required. For DPOAE, a separate channel with signal generation, amplification and loudspeaker is needed for each stimulus tone in order to avoid artifactual intermodulation distortion from the equipment, particularly the loudspeakers.

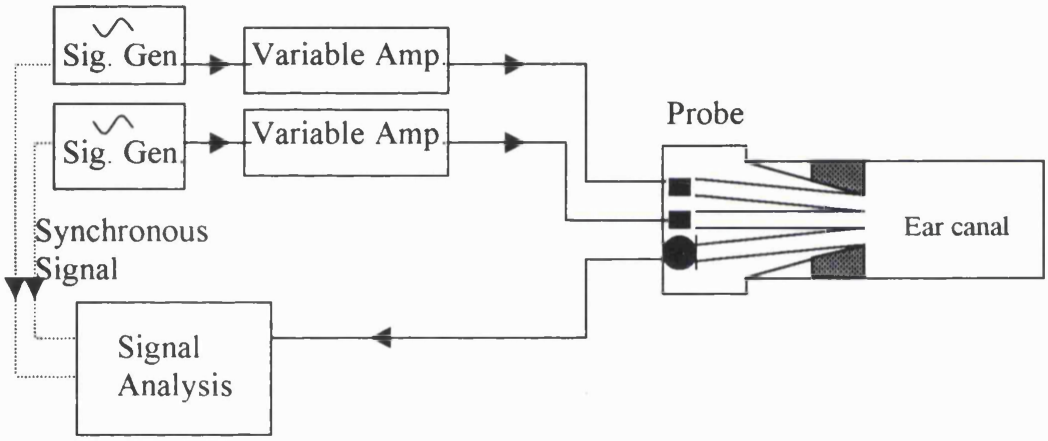

Figure 14. Schematic illustration of an OAE measurement system. (for TEOAE, only 1 of the signal generators is required, and is used to generate a click stimulus)

b. Probes

The probes used in this study comprise two loudspeakers (or three in the case of the 3-tone system) and one microphone (manufacturer: Knowles). For TEOAE measurements, only one loudspeaker is used. The probes are fitted into the ear canal by means of a foam tip or a plastic moulded tip. Probes used in this study were the Otodynamics BP-type probe (standard DPOAE probe for adults), a 3-tone BP-type probe and a CD-type (child) probe.

c. Analysis time windows and frequency resolution

For TEOAE measurement in this study, the 'ILO' nonlinear method was used. In this method, the stimulus is presented at 20.5 ms intervals. Each measurement is derived

from 260 nonlinear subaverages using a 2.5 - 20.5 ms time window with a 2.5 ms risetime. The subaverages are alternately added to one of two averaging 'bins'. Comparison of these two averaged waveforms provides an estimate of the signal (features common to both waveforms) and random noise (differences between the waveforms). A 512 point FFT is used at a sample interval of 40 μs (Bray, 1989; Bray and Kemp, 1987), which yields a time window of 20.5 ms and spectral harmonic values at 48.8 Hz intervals in the frequency domain. A click level of 0.3 pascals is employed.

DPOAE measurements use two simultaneous tones and apply a 2048 point FFT to 80 ms samples of ear canal measurements, yielding a frequency spectrum with a resolution of 12.5 Hz (Otodynamics Ltd., 1994).

d. Avoidance of artefacts in TEOAE

There are two main methods by which artefacts arising from passive responses to the stimulus are excluded from TEOAE measurements; time windowing and the non-linear click stimulus.

The TEOAE time window excludes the first 2.5ms after the stimulus in order to allow passive reflections from the ear canal and middle ear to die down. It is particularly important to exclude the period for which the detection system is saturated by the stimulus as this saturation would result in nonlinear growth which would get past the nonlinear stimulus paradigm described below. The security obtained by the time windowing is potentially at the expense of losing some high frequency TEOAE, which are emitted with low latency and so may be excluded by this time window

As additional assurance against passive reflections masquerading as TEOAE, a non-linear stimulus paradigm is used (Bray and Kemp, 1987; Kemp et al., 1986). 3 positive-going clicks are applied, followed by a click of the opposite polarity and 3 times the amplitude (figure 15). The responses to these clicks are then summed. Any response which grows proportionately with the stimulus (e.g. a long-ringing ear canal resonance) will cancel out exactly, leaving only the non-linear part of the response. This security is at the expense of a reduced S/N ratio, as any legitimate linear TEOAE and 50% of the saturated nonlinear TEOAE is also excluded. However, removal of the linear part of TEOAE makes it more likely to match DPOAE, which is also a nonlinear response. This therefore makes this TEOAE method particularly appropriate for the present study.

In order to reduce contamination by noise, a noise rejection threshold is set (in both TEOAE and DPOAE) which will automatically exclude data samples with a noise level

higher than a certain level which can be manually set. The aim is to set the rejection threshold above the OAE level, so samples which have a higher level than the rejection threshold (and are therefore excluded) will contain higher noise level. This method is inherently more suited to dealing with variable or intermittent noise than continuous steady noise.

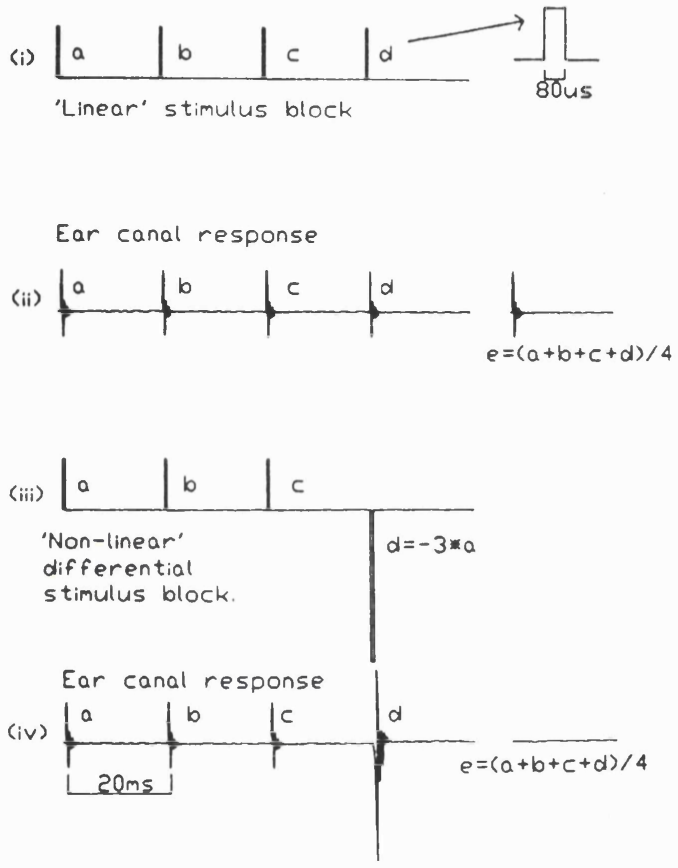

Figure 15. An illustration showing the non-linear stimulus method. Parts (i) and (ii) illustrate a 'linear' stimulus mode, in which 4 identical stimuli are presented and an average is taken of the 4 ear canal responses. Parts (iii) and (iv) illustrate the 'nonlinear' stimulus mode used in this study: 3 identical clicks (at 0.3 Pa) are followed by a 4^{th} click of 3 times the amplitude and opposite polarity. A subaverage of the 4 responses results in the cancellation of all linear elements in the responses, including the initial click and meatal response. The true OAE is also partially cancelled by this method, the method therefore reduces the signal to noise ratio. To compensate for the loss of level, the subaverage is divided by 2 instead of 4 to estimate the OAE level. From Kemp et al, (1990) (after Bray and Kemp, 1987).

e. Avoidance of artefacts in DPOAE

DPOAE artefacts can easily arise from a number of causes because of the low level of DPOAE relative to the stimulus. For example, even a very slight nonlinearity in the equipment input/output function (most commonly interaction in the transducers) would generate comparable distortion. In order to avoid this, a completely separate amplification chain is used for each stimulus tone so that intermodulation distortion can't arise in the equipment. To confirm that the equipment does not generate distortion, the test was run with the probe inserted into a 1cc test cavity - no distortion was seen above –15 dB SPL using $L_1=L_2=70$ dB SPL and $f_2/f_1=1.22$.

There is a possibility that, when stimulated at high levels, the cochlea or middle ear may generate 'passive distortion' which does not require the cochlea to be functional.

This possibility has been suggested in non-primate mammals but not in humans (Brown, 1987; Norton and Rubel, 1990; Whitehead et al, 1990). Nevertheless care is necessary when interpreting DPOAE measurements recorded with stimulus levels above 75 dB SPL as in any case the probe itself can begin to make significant distortion products when the stimulus level gets close to 80 dB SPL.

Two additional tests can be performed as a safeguard to check whether measured DPs are genuine cochlear DPOAEs. The growth rate can be investigated – a growth rate steeper than 1-2 dB/dB may be an indicator of a pathology or an artefact. However, true cochlear DPOAE can also occasionally incorporate a steep growth rate as well, arising from interference effects. Also, the phase gradient of the OAE can be assessed in an f_1 or f_2 sweep. Equipment artefacts would have virtually no time delay relative to the stimulus, so would have an almost flat phase gradient. Genuine cochlear responses typically have an inherent time delay of a few milliseconds, although occasionally a very low time delay or an undulating phase gradient arises over a frequency range of 100 Hz or so as a result of interference effects.

In order to reduce contamination by noise, a noise rejection threshold is set which operates in the same way as for TEOAE.

An estimate of the random noise level for DPOAE is obtained from the 10 closest harmonic frequencies either side of the DP frequency in the FFT. The mean noise level at these frequencies and the associated standard deviation provides an indication of whether the DP measurement is significantly greater than the background noise of the measurement. The software employed indicated the levels of 1 and 2 standard deviations above the noise. Criteria for accepting DP data in this study were based on the DPOAE level exceeding 1 standard deviation above the noise.

f. Calibration

i) Routine self test program

The manufacturers test program was run to ensure the internal electronic calibration was correct. The routine checked the connections, frequency response, attenuators and amplifiers of the internal system (excluding the probe) and also checked for system distortion and noise. The ongoing performance of the system, including the probe, was checked as follows:

ii) Otodynamics factory calibration

The probe loudspeakers are calibrated by driving them with a known voltage source and measuring the frequency response in a 1cc cavity (internal diameter 8 mm) with a calibrated Knowles microphone.

The microphone sensitivity was measured in free field conditions by comparing its response to an adjacent calibrated Bruel and Kjaer ½ inch microphone (type 4192). The calibration procedure covered frequencies up to 6 kHz.

The calibration of the probes used for this project was tested at the factory before and after the set of measurements was completed. Changes in microphone and loudspeaker sensitivities were less than 2 dB, and generally less than 1 dB. Differences between the probes used were less than 5 dB at all frequencies taken and generally less than 3 dB in the frequency range employed in the present study. Different probes were employed because of the requirement for 3 tones with some tests and the use of the CD (child) probe was necessary with one subject because the subject had very narrow ear canals. Different probes were not employed within a data set.

iii) Routine Probe testing

TEOAE

The probe was tested using a version of the TEOAE measurement program. This is essentially a self-test. The probe was fitted to a 1 cc acoustic calibration cavity and a test was conducted in which an artificial 'OAE' is sent through the probe, detected by the probe microphone, and recorded as three oscillatory tone bursts at 700 Hz, 2 kHz and 4 kHz. This test was compared to a previous probe test performed at the factory to confirm that the probe had not deteriorated.

As a further control, the probe was also checked on a day-by-day basis by measuring the OAE from my ear, as the initial OAE response was held as a reference. The total response level was found to not deviate by more than +/- 1 dB over the period in which recordings were made.

DPOAE

The probe is placed in a 1cc cavity and a frequency spectrum is measured for each loudspeaker by measuring the frequency response to clicks presented to each loudspeaker. This is similar to part of the in-ear calibration procedure described later.

This is essentially a 'loop test' and individual diagnostic testing of the probe components can be performed as described previously.

iv) Checking the probe fit in the ear.

TEOAE

In order to evaluate the probe fitting in the ear and to be able to set the stimulus level prior to recording, test clicks were presented and the time domain response was checked. A poor probe fitting is likely to affect the ear canal response (Kemp et al, 1990), for example by introducing ringing (which would indicate a possible leaky probe fit), a low frequency wave (partial probe blockage, e.g. against the ear canal wall), and a raised noise level. The stimulus level was adjusted if necessary to produce a peak close to 0.3 Pa at the probe in the ear canal (approximately 83 dB SPL peak equivalent).

In the frequency domain, the stimulus spectrum should be predominantly flat, preferably without any distinct peaks or dips which could be indicators of standing wave effects. Imperfections in the stimulus frequency spectrum were not corrected with TEOAE measurements, but the frequency spectrum of the stimulus clicks was stored as part of the data file.

DPOAE

Before each DP frequency sweep (in this case meaning a sequence of DPOAE measurements at a consistently incrementing frequency), a calibration procedure of the ear canal fit was undertaken. The responses to broadband clicks were recorded separately from each of the probe loudspeakers by the probe microphone. These responses were Fourier transformed and the two spectra were inspected to ensure that they were approximately equal and essentially flat in the frequency range 1-4 kHz (this is affected by a poor probe fitting, Kemp et al, 1990). Small differences between the loudspeaker spectra (approx 2-3 dB) were automatically compensated for, but larger differences imply that the probe is poorly fitted, so that accurate correction would be more difficult and that refitting was necessary.

After the fitting has been optimised and accepted, the broadband clicks are presented a further 16 times to obtain a reference spectrum of the accepted fit. This reference is used to balance and normalise the two stimuli at each of the test frequencies of the DP sweep except when an ear canal standing wave effect is suspected, as described below.

During the processing, the DPOAE phase is corrected for the measured phase changes induced in the stimuli by the probe loudspeakers and microphone (the system detects

the stimulus phase via the microphone and corrects automatically) but no phase correction is applied for acoustic delays along the ear canal.

These procedures and corrections are provided by the Otodynamics ILO 88DPi and ILO96 systems employed in this study.

g. Effect of ear canal standing waves on the in-ear calibration method

The limitation of this method of in-ear calibration is that the ear canal SPL measured at the probe is assumed to be the same as the SPL at the ear drum. Under most circumstances this is approximately true, however at frequencies above approximately 3 kHz the wavelength is such that the ear canal (as enclosed by the probe) can support a standing wave (Dirks and Kincaid, 1987; Siegel, 1994). In this case, the probe and the eardrum may not be at comparable positions in the standing wave pattern, resulting in very different sound pressure being occurring at the two locations. Under these conditions, using the probe SPL measurement to represent the eardrum SPL would lead to considerable error.

Therefore, when undertaking DPOAE measurements the ILO software normally corrects for the frequency response of the ear canal which it detects at the 'check fit' stage, but does not apply the correction around frequencies where the frequency response has a significant peak or dip. This is because although the frequency response at the eardrum may not be very flat at these frequencies, the frequency response correction which may appear to be appropriate may actually make the frequency response at the eardrum worse under these conditions.

The TEOAE method differs slightly because the ear canal frequency response is not normally corrected for, but ear canal standing wave effects can still be detected from peaks and dips in the frequency spectrum of the click stimulus measured in the ear canal.

A way to improve the in-ear calibration would be to attach the microphone to a fine probe tube and inset it deep into the ear canal close to the eardrum (Siegel and Hirohata, 1994). The sound pressure detected would then be more representative of the SPL that is being applied to the eardrum. However, this method is usually not considered to be necessary provided that the limitations of the standard measurement method are understood.

h. Significance of calibration in this study.

In this study, measurements of TEOAE will be compared to DPOAE obtained with the same probe. Patterns of behaviour will also be explored in extended sets if DPOAE data covering a large frequency range.

Absolute calibration and flat frequency responses are not vital in order for these relationships to be explored. Nevertheless, it is important that the correct level relationship between L_1 and L_2 is achieved as DPOAE response level is known to be sensitive to this. As the stimuli are typically less than ½ octave apart, undulations in the frequency responses do not affect L_1-L_2 much, provided that they are gradual.

C. An investigation into the relationship between TEOAE and DPOAE

This chapter is based on a re-examination of the findings and data of Knight (1997), which was work undertaken towards my masters degree prior to the commencement of my PhD studentship. Additional experimental work has been conducted specifically for the purposes of this thesis.

I Introduction

The relationship between TEOAE and DPOAE amplitude in individual human ears that has previously been reported has been weak (Probst and Harris, 1993; Smurzinsky and Kim, 1992; Smurzinsky et al, 1993). This is intriguing as both are believed to be a result of outer hair cell activity. However these studies have only explored a limited range of stimulus parameters. Whilst the TEOAE response is relatively insensitive to the stimulus parameters such as the stimulus click rate and level, the DPOAE response is very different depending on the absolute and relative levels of the two stimulus tones and the frequency ratio between them (e.g. Harris et al, 1989; He and Schmiedt, 1997). Also both DPOAE and TEOAE are subject to frequency dependent amplitude fine structure and this could weaken the apparent relationship between DPOAE and TEOAE amplitude if the fine structures are not fully resolved and single point values are taken without averaging across the fine structure. It is therefore concluded that the relationship between TEOAE and DPOAE has not been fully investigated.

In this study, TEOAE measurements will be compared to DPOAE measurements obtained using a wider range of stimulus parameters. The TEOAE and DPOAE responses will be averaged across a frequency region in order to reduce the confounding effect of fine structure.

The phase versus frequency gradients of the OAEs will also be analysed, similarities in the phase gradients of DPOAE and TEOAE would imply a similar emission mechanism may be involved whereas very different phase gradients would suggest that different emission mechanisms are involved.

II Method

The measurement procedure was designed to enable a detailed investigation of the relationships between DPOAE and TEOAE without demanding an excessive amount of time from each subject. As the phase and general waveform of TEOAE are not critically dependent on stimulus level, a single stimulus level was used for TEOAE measurements. DPOAE fine structure can be of the order of a peak to peak spacing of about $1/10^{th}$ of an octave (He and Schmiedt, 1993), so a frequency spacing of DPOAE measurements narrower than this was necessary to allow averaging across the OAE fine structure and derivation of phase gradients. Therefore to remain within the time

constraints the f_2 frequency of the DPOAE measurements was limited to approximately a ½ octave range centred on 2 kHz, within which a range of stimulus frequency ratios and stimulus levels were explored.

a. Subjects

9 left ears from subjects ranging in age from 22-41 years (mean 31.4 years) were given the OAE test battery (8 female and 1 male). All ears, when tested via standard audiometry, demonstrated normal hearing threshold sensitivity (≤20dB HL) from 125 Hz to 8 kHz with the exception of one ear, which gave a threshold of 25 dB HL at 4 kHz. All ears complied with normal tympanometry patterns.

b. Choice of OAE stimulus parameters

i) TEOAE

A stimulus peak level of 0.3 Pa was adopted as this gives a good level of OAE response whilst retaining test sensitivity and without triggering equipment artefacts. As TEOAE responses are not highly sensitive to the stimulus level (Kemp, 1978) or repetition frequency (a preceding masking click has little effect if the interval is greater than 5 ms, Tavartkiladze et al, 1996), other stimulus levels and repetition rates were not investigated. Before the TEOAE measurement, the probe fit and the stimulus level were checked as described previously.

ii) DPOAE

In view of the desire to obtain DPOAE frequency sweeps employing a small frequency step spacing but without taking too long, short DPOAE sweeps with f_2/f_1 fixed were constructed. The sweeps covered 16 f_2 frequencies in the frequency range 1660 - 2393 Hz, which was an adequate range to cover at least an auditory filter bandwidth (Holube et al, 1998; Kollmeier and Holube, 1992; Patterson, 1976). The frequencies of f_2 were chosen to coincide with each harmonic frequency in the Fourier transformation of the TEOAE response in this frequency range. (The TEOAE time window of 20.5 ms gives a frequency resolution of just under 50 Hz).

The parameters chosen for the DP sweeps (described below) were selected to cover as wide a range of conditions as possible within the time available. The DPOAE stimulus parameters are defined by L_1 (sound pressure level of lower stimulus tone of frequency f_1) and L_2 (sound pressure level of higher stimulus tone of frequency f_2).

L_1: Levels of 65, 70 and 75 dB SPL were used, which are similar to those used by Harris et al (1989). Gaskill and Brown (1990) used stimulus levels from 40 to 65 dB

SPL, but these lower levels were not included in this study as the lower amplitude responses which would have necessitated a longer averaging period for each measurement, reducing the range of conditions which could be studied within the time period.

L_1-L_2 (Level Difference): DPOAE measurements were made with L_2 reduced below L_1 by 0, 5 and 10 dB, so including the condition L_1=L_2 and also the conditions with L_2 reduced below L_1 which can result in larger amplitude $2f_1$-f_2 emissions because reducing L_2 below L_1 can match the basilar membrane displacement in the f_2 region caused by each stimulus tone, thus maximising DP generation. A test condition with L_1>L_2 has been preferred for clinical applications, e.g. by Whitehead et al., 1995, Stover et al., 1996b and Gorga et al., 1997.

f_2/f_1 (Frequency Ratio): Ratios of 1.05, 1.2, 1.27 and 1.32 were used, the latter 3 being clustered around the ratios 1.2-1.3 known to give maximum amplitude DPOAEs (Harris et al 1989; Gaskill and Brown, 1990), and the first ratio investigating a much smaller frequency ratio which has been shown to have different $2f_1$-f_2 DP phase properties (Kemp, 1986) and which may produce a larger amplitude $2f_2$-f_1 distortion product response (Erminy et al, 1996).

Measurements were made using the Otodynamics Ltd. ILO88 DPi, with software version 5.6Z. The macro programming facilities were utilised to run the test sequence semi-automatically.

Before each DP sweep, the probe fit in the ear canal was evaluated using the procedure described previously. Normally, if large changes in the spectrum with frequency are seen in the checkfit procedure, a standing wave effect within the ear canal is suspected and compensation for the frequency spectrum is not performed in the affected frequency range. However in this study, this condition was not accepted within the frequency range of interest at the calibration stage and so the level compensation always took place for the data presented here.

For each stimulus condition (stimulus level and frequency ratio), one complete sweep of the frequency range was completed and then individual points within the range were repeated at frequencies at which the signal to noise ratio was judged to too low. Each DP measurement was terminated manually, usually after all $2f_1$-f_2 responses exceeded twice the standard deviation of the noise.

The DPOAE test sequence typically lasted approximately 45 minutes, depending on the signal to noise ratio of the responses. The equipment was situated in a quiet office in which the ambient noise was typically 40 dBA SPL.

c. OAE Measurement Procedure

Following the audiometric tests, for each subject, the OAE probe was fitted with a foam tip and inserted into the ear canal and, after checking the probe fit, a TEOAE measurement was obtained. The same Otodynamics BP-type probe was used (with a different foam tip) for each subject.

Following this, the complete series of DP sweeps was collected. Generally the original probe position was retained throughout the session. The probe was only reinserted on occasions when the stimulus spectrum or level changed, or the measurement noise level rose significantly, indicating that the probe had moved during the test sequence. Where this occurred during a DP sweep, the probe fit was checked and the DP sweep measurement was re-run.

For each subject the DP measurements were obtained in the same order (illustrated in figure 16). Initially, with L_1=L_2=65dB SPL, four DP sweeps were obtained with frequency ratios of 1.05, 1.20, 1.27 and 1.32. L_2 was reduced by 5 dB and the DP sweeps with the four frequency ratios were repeated. L_2 was then reduced by a further 5 dB and the four DP sweeps were repeated again. This sequence was then repeated, beginning with L_1=L_2=70 dB SPL and then with L_1=L_2=75 dB SPL. In addition, at the start and end of the test sequence an additional DP measurement was obtained using the test parameters L_1=L_2=70 dB SPL and f_2/f_1=1.2. These two extra measurements were used to check the stability of the responses.

Figure 16. A flow diagram indicating the sequence in which the DP grams were obtained. Boxes with a thick border indicate when DPOAE measurements are being recorded, other boxes indicate changes in setting up stimulus levels for the next measurements.

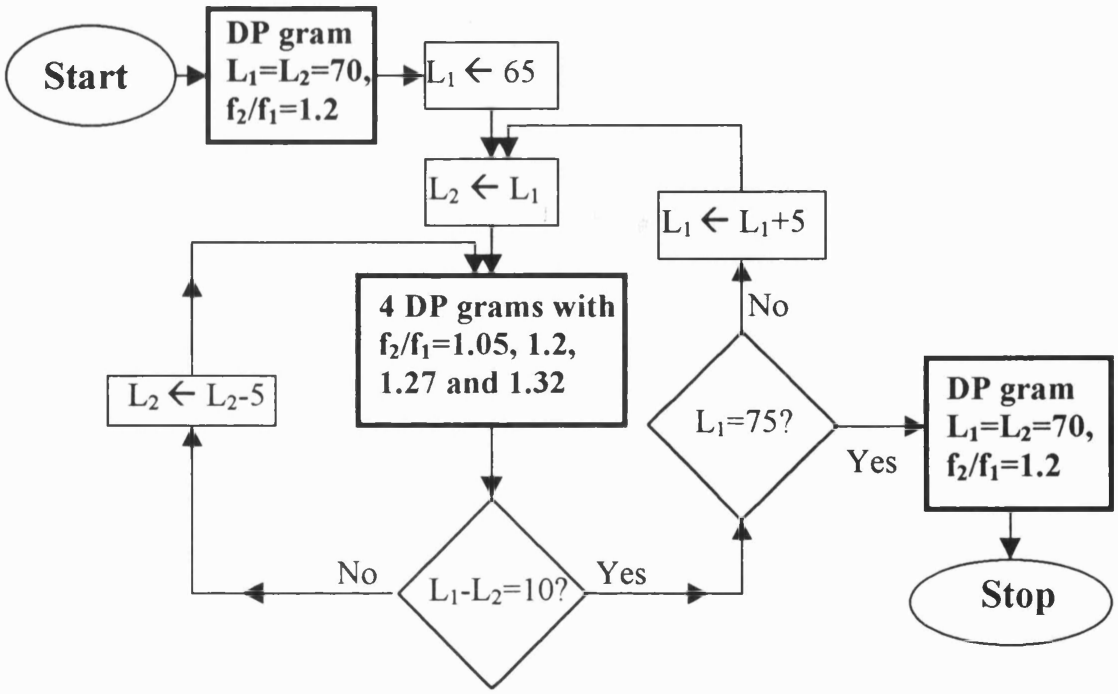

d. Analysis and calculations

Measurements obtained included the levels and phase-versus-frequency gradients of the $2f_1$-f_2 and $2f_2$-f_1 DPOAEs. These were compared with the corresponding level and phase-versus-frequency gradient of TEOAE.

i) Comparison of TEOAE and DPOAE amplitudes

In order to allow a straightforward comparison between TEOAE and DPOAE levels, a single figure was required which would represent the OAE power generated across the frequency range for each OAE stimulus configuration. In order to obtain this for TEOAE, the sum of the response over the frequency range was calculated. A different calculation method was adopted for DPOAE because the TEOAE measurement presents all frequencies to the cochlea simultaneously, whereas the DPOAE measurement tests each frequency sequentially. This means that for TEOAE the capacity for OAE generation is divided across frequency, whereas for DPOAE the full capacity of OAE generation is available for every frequency in the DP sweep. It is therefore appropriate to average DPOAE across frequency.

For this study, the sum of the 16 TEOAE spectral component levels from 1660 Hz to 2393 Hz was calculated and compared to the average level of each 16 point DP sweep:

$$DPOAE_{ave} = 10.\log((\sum_{i=1}^{16} 10^{DPOAE/10})/16)$$

$$TEOAE_{sum} = 10.\log(\sum_{i=1}^{16} 10^{TEOAE/10})$$

The different calculations make the reasonable assumption that the frequency range under investigation covers approximately one auditory filter. It increases the numerical value for TEOAE levels relative to DPOAE by 10.Log(16), i.e. 12 dB. The difference in calculation method has no effect on the subsequent data analysis of relationships between TEOAE and DPOAE.

ii) Interrelations between TEOAE and DPOAE level

In order to allow an assessment of the relationship between the TEOAE and DPOAE levels, a scattergraph was generated for each configuration of DPOAE stimulus parameters in which the frequency averaged DPOAE level was plotted against the band limited frequency averaged TEOAE level of each subject.

The $2f_1$-f_2 DPOAE level was plotted against the TEOAE level in the frequency band corresponding to the f_2 frequency range, whereas the $2f_2$-f_1 DPOAE was plotted against the TEOAE range corresponding to the $2f_2$-f_1 DP frequency. The reason for the $2f_2$-f_1 DPOAE being treated differently is that the generation site for lower sideband DPOAE (e.g. $2f_1$-f_2) has been demonstrated to be in the region of the f_2 place whereas the generation site for the upper sideband DPOAE (e.g. $2f_2$-f_1) is in the region of the emission frequency place (e.g. Martin et al, 1987, 1998; Kemp, 1998).

For each set of DPOAE stimulus parameters, a linear regression line was calculated from the paired DPOAE and TEOAE level data and the standard deviation of the data vertically from the regression line was calculated. This measure was used as the main descriptor of the relationship between the measurements in preference to a Pearson correlation as it indicates the uncertainty in dB associated with using the regression line to predict the DPOAE level from the TEOAE measurement.

The standard deviation calculated in this way will be referred to as the Prediction Standard Deviation (Prediction S.D.).

In order to investigate the influence of the across frequency averaging on the closeness of the relationship between TEOAE and DPOAE level, Prediction S.D. was also calculated using single point TEOAE and DPOAE data without cross-frequency averaging for two DPOAE stimulus configurations; with L_1=L_2=70 dB SPL and f_2/f_1=1.05 and 1.32. To ensure that the optimum frequency alignment of the TEOAE and DPOAE fine structure was achieved, the TEOAE data were shifted by successive frequency steps and a series of Prediction S.D. values were calculated. The lowest calculated value for Prediction S.D. was then compared to the corresponding figure for the averaged data. The difference indicated the extent to which the apparent relationship between TEOAE and DPOAE was weakened by the fine structure mismatch of the OAE's when unaveraged data was compared.

The gradient ($\Delta DP/\Delta TE$) of the best fit line was also obtained as an indicator of the relationship between TEOAE and DPOAE as a gradient close to 1 means that inter-subject factors affecting OAE level affect both OAE forms in equal proportion, implying similarities between the underlying mechanisms of TEOAE and DPOAE.

iii) Phase and Phase gradients

The phase of the OAE response relative to the stimulus is readily measurable and may help to characterise the origin of an emission. The phase versus frequency gradient associated with $2f_1$-f_2 DPOAE with stimulus sweeps of a constant frequency ratio is known to be fairly flat when f_2/f_1 exceeds approximately 1.1, but to develop a much

steeper gradient at smaller frequency ratios (Kemp, 1986). This is likely to indicate a difference in the means by which the $2f_1$-f_2 DPOAE is emitted at small and large f_2/f_1 ratios, probably a switch between the wave-fixed and place fixed behaviour first described by Kemp and Brown (1983).

The phase data obtained from the OAE recordings are only defined within the range +/- 180°. In the present study the data sequences were 'unwrapped' using the following procedure to yield the phase gradient.

Firstly, to deal with instances in which the data jumped up from -180° to +180°, 360° was subtracted if the phase of a data point differed from adjacent data points by more than twice the typical variance for a data series plus the maximum variation due to noise at each point (based on twice the S.D. above the noise mean). Secondly, to correct downward jumps from +180° to -180°, 360° was added if the phase gradient fell below the overall line gradient by more than 360° minus the maximum noise and twice the typical variance.

These criteria were chosen as they are logical and also appear to select the most appropriate phase correction without being triggered excessively by data points with a poor signal to noise ratio.

Subsequently, the phase gradient (relative to the change in emission frequency) was used to provide a calculation of the group delay. The full data series from each DPgram was utilised provided that all points exceeded the mean noise by at least 1 S.D.. Where this was not the case, the data sequence was shortened to include the longest continuous sequence of acceptable data. For a gradient to be recorded, a minimum of 3 consecutive data points were required.

The phase gradient of the $2f_1$-f_2 DP was compared to the TEOAE phase gradient across the frequency range of f_2 whereas the $2f_2$-f_1 DP was compared to the TEOAE phase across the frequency range corresponding to the emission frequency, reflecting the presumed sites of DPOAE generation.

III Results

a. DPOAE levels

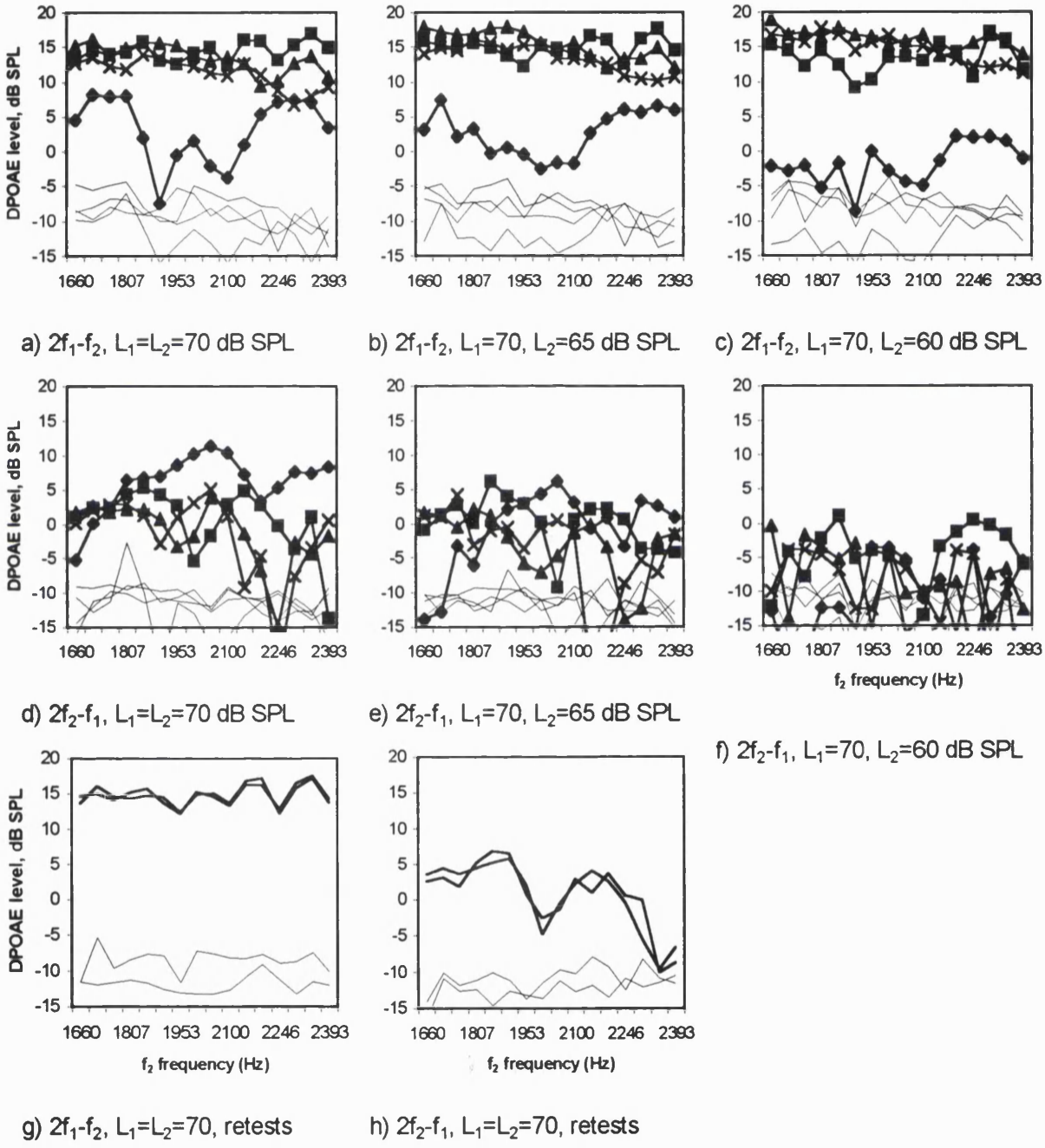

Figure 17. An example data set of DPOAE amplitude for subject D, with L_1=70 dB SPL. ♦= f_2/f_1=1.05, ■= f_2/f_1=1.2, ▲= f_2/f_1=1.27, ×= f_2/f_1=1.32. (a-c) shows the $2f_1$-f_2 DP, (d-f) the corresponding $2f_2$-f_1 DP and (g-h) two tests with L_1=L_2=70 dB SPL and f_2/f_1=1.2 from the beginning and end of the DPOAE test sequence, indicating the repeatability of the measurements. Thin lines show the mean noise estimates from the adjacent 10 spectral frequency bands to the DP. The standard deviation associated with each noise estimate was typically 2-3 dB.

The $2f_1$-f_2 distortion product exceeded the mean noise by 1 x the S.D. across the measured frequency range in all ears for all stimulus conditions with the exception of a few isolated points. The $2f_2$-f_1 distortion product was also measurable in all ears with some stimulus conditions, but some parameter configurations gave low amplitude responses containing a large number of points within the DP sweep which failed to meet the S/N criteria. As an example, figure 17 shows all DPOAE data obtained with L_1=70 dB SPL from one subject.

The levels of each DP to each stimulus condition, averaged across the frequency range and across the 9 subjects, are shown in the graph in figure 18.

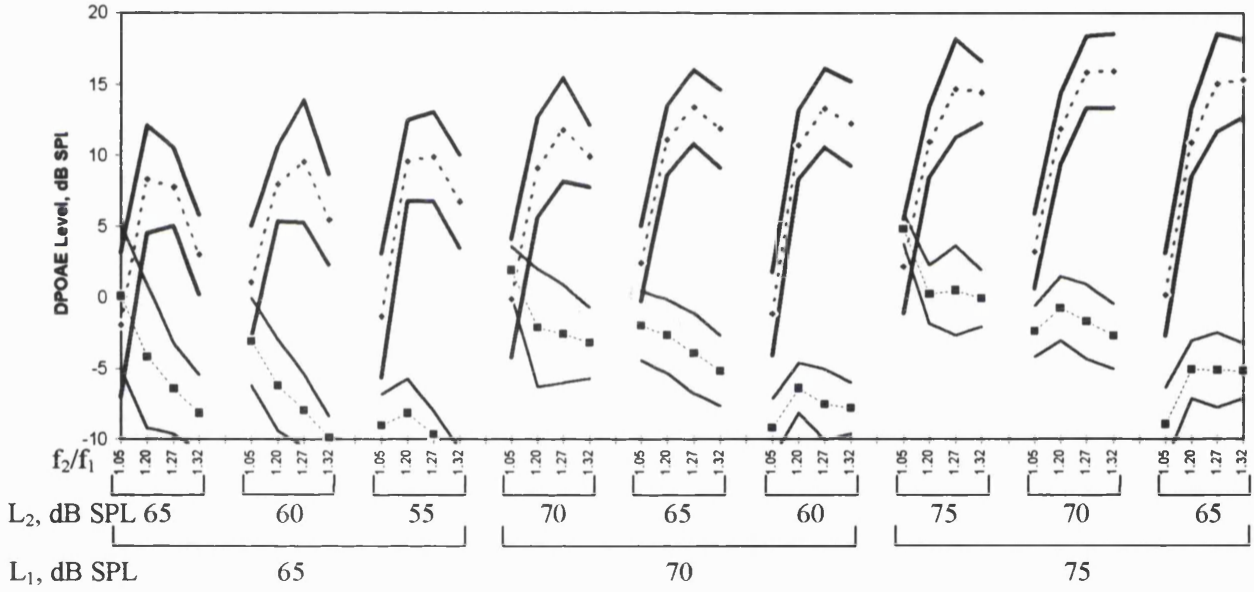

Figure 18. Average $2f_1$-f_2 and $2f_2$-f_1 DPOAE levels obtained with each combination of stimulus parameters in the frequency range 1660-2393 Hz. Errors shown are 2 × s.e. from the mean of nine ears. The average noise floor for each condition was always below -10 dB SPL. ♦=$2f_1$-f_2 DP, ■=$2f_2$-f_1 DP.

The overall trends seen in the amplitudes of the $2f_1$-f_2 distortion product responses with stimulus frequency ratio and stimulus level are consistent with those reported by Harris et al (1989).

The lowest amplitude $2f_1$-f_2 DP responses were obtained when f_2/f_1=1.05, whereas the frequency ratio to give the maximum amplitude response increased from 1.2 to 1.32 as L_1 increased and L_1-L_2 increased. The level difference resulting in the largest response level was 5 dB when f_2/f_1=1.05. However a level difference of 10 dB gave the largest response level when f_2/f_1=1.2-1.32, especially when L_1=65 or 70 dB SPL.

The greatest growth rate with increasing stimulus level seen in the $2f_1$-f_2 DPOAE was 1.4 dB/dB and can be seen by comparing the results with L_1=L_2=65,70 and 75 when f_2/f_1=1.32. The lowest growth rate was 0.1 dB/dB and occurred when f_2/f_1=1.05 and L_1=L_2+10 dB.

In contrast to the $2f_1$-f_2 DP, the highest level $2f_2$-f_1 DP responses were obtained when f_2/f_1=1.05 and L_1=L_2. Reducing L_2 below L_1 resulted in reductions in $2f_2$-f_1 DP response, the greatest being 1.4 dB per 1 dB change in L_2 when f_2/f_1=1.05 and L_1=75 dB SPL.

Increasing the frequency ratio above 1.05 also reduced the level of the $2f_2$-f_1 response, especially when L_1=65 dB SPL.

The greatest growth rates of the $2f_2$-f_1 DPOAE with increasing stimulus level occurred when f_2/f_1=1.32, although the response level generally remained lower than corresponding measurements with lower frequency ratios. As with the $2f_1$-f_2 DP, there was little growth in the $2f_2$-f_1 DP when f_2/f_1=1.05. This was particularly true especially with L_2<L_1, when virtually no response growth occurred.

The $2f_1$-f_2 DP level was always greater than the $2f_2$-f_1 DP level except when L_1=L_2 and f_2/f_1=1.05, in which case the $2f_2$-f_1 DP exceeded the $2f_1$-f_2 DP by 2-2.5 dB. The $2f_1$-f_2 DP, however, was up to 20 dB greater than the $2f_2$-f_1 DP with large stimulus frequency ratios and when L_2 was reduced below L_1.

b. Comparison of TEOAE and DPOAE levels

TEOAE responses exceeded the noise within the frequency region under investigation in all ears tested, with the exception of a few isolated points in some subjects. The summated TEOAE level within the frequency range varied from -2.0 dB SPL to 12.6 dB SPL between subjects, with the mean being 6.2 dB SPL. The TEOAE mean level was close to the mean for example of the averaged DPOAE sweeps with L_1=L_2=65 dB SPL and f_2/f_1=1.2 or 1.27. For each subject, the standard error in the mean TEOAE level was calculated from the set of individual TEOAE data points (this measure is likely to reflect the amount of fine structure, although it could also indicate an underlying smooth trend across the frequency range under test). The average of these was 1.3 dB, comparable with standard errors of all the $2f_2$-f_1 DPOAE measurements and $2f_1$-f_2 DPOAE measurements with f_2/f_1=1.05, which were typically in the range 1.2-1.6 dB. The mean $2f_1$-f_2 DPOAE measurements with larger f_2/f_1 had smaller standard errors mostly in the range 0.5-0.9 dB, indicating that these responses were flatter in the frequency range studied.

c. Relationships between TEOAE and DPOAE Amplitude

Examples of the scattergrams of bandlimited TEOAE level versus the average corresponding DPOAE level are shown in figure 19 with best fit lines calculated by linear regression.

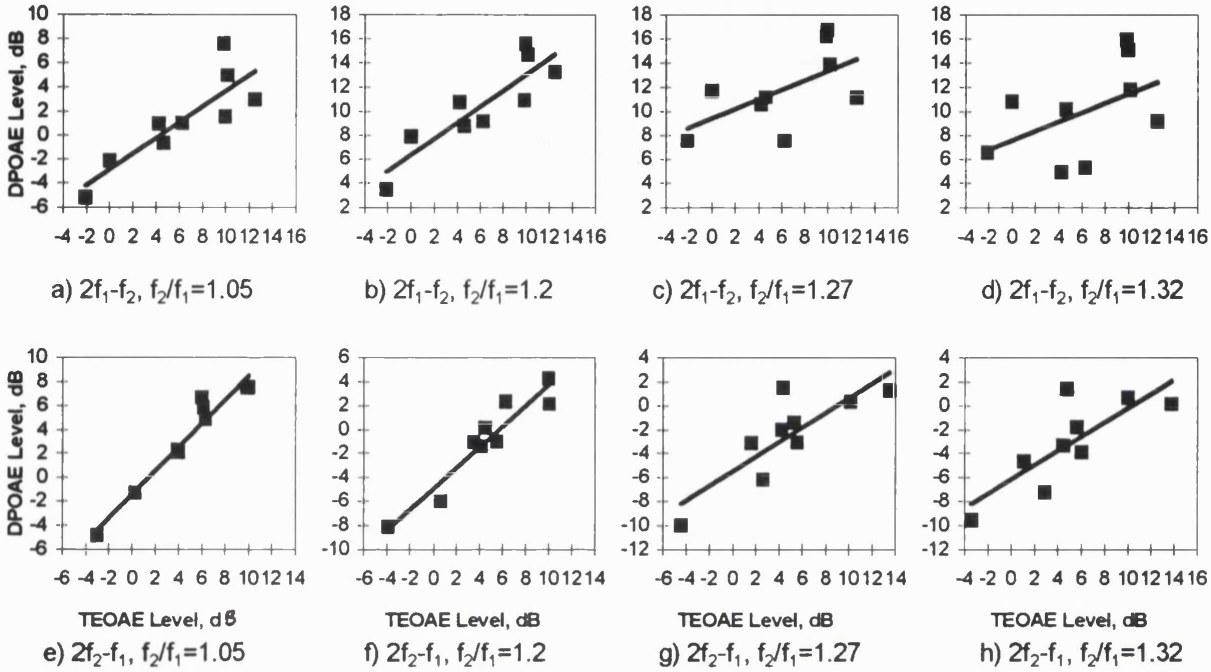

Figure 19. Example scatter charts showing a comparison of average DPOAE and total TEOAE level in the frequency range 1660-2392 Hz for 9 ears, with the best fit line calculated by linear regression. The TEOAE response is plotted against the DPOAE averaged across f_2 frequency range of the $2f_1$-f_2 distortion product and the emission frequency of the $2f_2$-f_1 distortion product. The examples shown were obtained with stimulus amplitudes L_1=L_2=70 dB SPL and frequency ratios: a) $2f_1$-f_2, f_2/f_1=1.05 b) $2f_1$-f_2, f_2/f_1=1.2 c) $2f_1$-f_2, f_2/f_1=1.27 d) $2f_1$-f_2, f_2/f_1=1.32 e) $2f_2$-f_1 f_2/f_1=1.05 f) $2f_2$-f_1, f_2/f_1=1.2 g) $2f_2$-f_1, f_2/f_1=1.27 h) $2f_2$-f_1, f_2/f_1=1.32. Both the $2f_1$-f_2 and the $2f_2$-f_1 DP's appear more closely related to TEOAE when the stimulus frequency ratio is smaller.

The standard deviation of the DPOAE level predicted from the TEOAE level with respect to the actual DPOAE level ('Prediction S.D.') was calculated for each of the 72 data sets. The calculated values are shown in Table I a) and b).

Considering the $2f_1$-f_2 DP, the general trend was for the closest relationships to TEOAE to be with smaller frequency ratios.

When f_2/f_1=1.05 or 1.2, there was also a trend for the Prediction S.D. values to be lower with lower stimulus levels. Therefore the closest amplitude relationship between the $2f_1$-f_2 DP and TEOAE occurred when L_1=65 dB SPL and f_2/f_1=1.05 or 1.2. The lowest single result (1.66 dB) was obtained with L_1=65 dB SPL, L_2=60 dB SPL and f_2/f_1=1.2.

Stim(dB SPL)		1.05	1.2	1.27	1.32
L1	L2	2f1-f2	2f1-f2	2f1-f2	2f1-f2
65	65	1.7	1.8	3.4	4.8
	60	1.8	1.7	3.5	5.1
	55	1.9	1.9	3.4	4.8
70	70	2.1	1.9	2.8	3.7
	65	2.0	1.9	3.3	4.0
	60	2.2	2.3	3.3	3.9
75	75	1.8	1.9	2.9	3.7
	70	2.3	2.4	3.1	3.8
	65	2.5	4.2	3.0	3.4

a) Prediction S.D., $2f_1$-f_2

Stim(dB SPL)		1.05	1.2	1.27	1.32
L1	L2	2f2-f1	2f2-f1	2f2-f1	2f2-f1
65	65	1.4	2.4	2.7	3.9
	60	1.2	2.3	2.1	2.7
	55	0.7	1.9	1.4	2.0
70	70	1.1	1.3	2.2	2.4
	65	1.2	2.1	2.6	1.9
	60	1.6	2.7	2.3	1.7
75	75	1.3	1.0	1.6	1.6
	70	2.1	1.9	2.4	2.8
	65	2.3	2.9	3.0	3.0

b) Prediction S.D., $2f_2$-f_1

Stim(dB SPL)		1.05	1.2	1.27	1.32
L1	L2	2f1-f2	2f1-f2	2f1-f2	2f1-f2
65	65	0.82	0.76	0.56	0.78
	60	0.72	0.81	0.70	0.90
	55	0.78	0.88	0.77	0.88
70	70	0.65	0.67	0.40	0.39
	65	0.63	0.71	0.54	0.48
	60	0.60	0.71	0.65	0.69
75	75	0.68	0.63	0.40	0.40
	70	0.63	0.62	0.51	0.51
	65	0.57	0.67	0.60	0.62

c) Gradient, $2f_1$-f_2

Stim(dB SPL)		1.05	1.2	1.27	1.32
L1	L2	2f2-f1	2f2-f1	2f2-f1	2f2-f1
65	65	1.25	1.04	0.84	0.94
	60	1.12	0.66	0.37	0.64
	55	0.85	0.38	0.06	0.48
70	70	0.99	0.91	0.84	0.81
	65	0.89	0.89	0.75	0.69
	60	0.52	0.60	0.50	0.10
75	75	0.67	0.76	0.68	0.62
	70	0.66	0.84	0.69	0.77
	65	0.51	0.68	0.28	0.54

d) Gradient, $2f_2$-f_1

Stim(dB SPL)		1.05	1.2	1.27	1.32
L1	L2	2f1-f2	2f1-f2	2f1-f2	2f1-f2
65	65	0.12	0.13	0.24	0.34
	60	0.13	0.12	0.25	0.36
	55	0.14	0.13	0.24	0.34
70	70	0.15	0.13	0.20	0.26
	65	0.15	0.13	0.23	0.28
	60	0.16	0.17	0.24	0.28
75	75	0.13	0.14	0.20	0.26
	70	0.16	0.17	0.22	0.27
	65	0.18	0.30	0.21	0.24

e) Gradient standard error, $2f_1$-f_2

Stim(dB SPL)		1.05	1.2	1.27	1.32
L1	L2	2f2-f1	2f2-f1	2f2-f1	2f2-f1
65	65	0.12	0.20	0.19	0.28
	60	0.10	0.19	0.14	0.20
	55	0.06	0.15	0.10	0.14
70	70	0.09	0.11	0.15	0.17
	65	0.10	0.17	0.18	0.13
	60	0.13	0.22	0.16	0.12
75	75	0.11	0.08	0.11	0.11
	70	0.18	0.15	0.17	0.20
	65	0.19	0.23	0.21	0.22

f) Gradient standard error, $2f_2$-f_1

Table I. Relationship between DPOAE and TEOAE amplitude shown by the standard deviation and the gradient of the best fit line for each set of DPOAE parameters.
(a and b) - Standard Deviations of a) $2f_1$-f_2 and b) $2f_2$-f_1 DPOAE amplitude (dB SPL) predicted from best fit line relationship with TEOAE (defined as Prediction S.D.). Heavy shading indicates Prediction S.D.>3.0 dB, light shading indicates 1.5<Prediction S.D.<3.0 dB, no shading indicates Prediction S.D. below 1.5 dB. **(c and d)** - Gradients ($\Delta DP/\Delta TE$) of best fit lines between TEOAE and c) $2f_1$-f_2 and d) $2f_2$-f_1 DPOAE amplitudes. Heavy shading indicates gradient < 0.6, light shading indicates 0.6<gradient<0.8, no shading indicates gradient above 0.8. **(e and f)** – Standard Errors of gradients between TEOAE and e) $2f_1$-f_2 and f) $2f_2$-f_1 DPOAE levels.

The $2f_2$-f_1 DP also showed an overall trend to have closest relationships to TEOAE level with lower stimulus frequency ratios. When L_1=65 dB SPL, the Prediction S.D. values were also lower with L_2 reduced below L_1, although with a very small response level. However, when L_1=70 or 75 dB SPL, L_1=L_2 produced lower values of Prediction S.D..

When L_1 and L_2 were equal, higher stimulus levels gave closer relationships between the $2f_2$-f_1 DP and TEOAE except when f_2/f_1=1.05, in which case there was no clear trend as the relationship was always close. Meanwhile when L_1=L_2+10, a lower stimulus level produced lower Prediction S.D. values but with very low level DPOAEs. Comparing rows of data in Table I b), the stimulus level combination which gave the highest values for Prediction S.D. was L_1=75 dB SPL and L_2=65 dB SPL.

$2f_2$-f_1 Prediction S.D. values close to 1 dB were obtained with L_1=L_2=70 dB SPL and f_2/f_1=1.05 and with L_1=L_2=75 dB SPL and f_2/f_1=1.2. The lowest single value (0.69 dB) was obtained with L_1=65 dB SPL, L_2=55 dB SPL and f_2/f_1=1.05, but this is a parameter combination which may not be very useful to pursue as it gives a very low level $2f_2$-f_1 DPOAE.

Each $2f_2$-f_1 Prediction S.D. was lower than the corresponding $2f_1$-f_2 value for the same stimulus conditions except some stimulus levels when f_2/f_1=1.2.

The overall magnitude of the Prediction S.D. values obtained for both the $2f_1$-f_2 and $2f_2$-f_1 distortion products has been confirmed by an additional study in which 5 of the DP sweeps were investigated for a further 10 subjects and Prediction S.D. values of a similar magnitude were obtained (Table II).

Stimulus, dB SPL			Distortion Product	
L_1	L_2	f_2/f_1	$2f_1$-f_2	$2f_2$-f_1
65	65	1.05	**2.1**	**1.5**
65	60	1.2	**2.2**	**2.7**
70	70	1.05	**2.3**	**1.3**
70	70	1.2	**2.4**	**1.3**
75	75	1.2	**2.6**	**2.8**

Table II. Repeat Prediction SD from a shorter series of DPgrams over the same frequency range (1660-2393 Hz) with 10 new subjects. These subjects did not undergo pure tone audiometry or middle ear testing but did not have any known audiological problems. These values of Prediction S.D. are generally slightly higher than the corresponding data from Table I but are of a similar magnitude.

P values

Paired t tests from whole columns of data in Table I a) indicate that the $2f_1$-f_2 Prediction S.D. values with stimulus frequency ratios of 1.27 or 1.32 were significantly higher ($p<0.05$) than with any smaller ratios.

Paired t tests from whole columns of data in Table I b) indicate that the $2f_2$-f_1 Prediction S.D. values obtained with $f_2/f_1=1.05$ were significantly lower ($p<0.05$) than values obtained with any higher frequency ratio.

Comparing rows of data from Table I b), $L_1=L_2=75$ dB SPL gave $2f_2$-f_1 Prediction S.D. values significantly lower ($p<0.005$) than with L_2 reduced by 5 or 10 dB.

Stimulus levels of $L_1=L_2=65$ dB SPL gave significantly higher values of $2f_2$-f_1 Prediction S.D. than $L_1=L_2=70$ or 75 dB SPL ($p<0.05$).

Comparing rows of data in Table I b), the stimulus level combination which gave the highest values for $2f_2$-f_1 Prediction S.D. was $L_1=75$ dB SPL and $L_2=65$ dB SPL. T tests indicate a high statistical significance ($p<0.05$) to the difference between this and all other stimulus level combinations except $L_1=L_2=65$ dB SPL.

d. Comparison of $2f_1$-f_2 and $2f_2$-f_1 Prediction S.D. values

A comparison of the average $2f_1$-f_2 and $2f_2$-f_1 Prediction S.D.'s in Table I a) and b) at each frequency ratio is shown in Table III.

	Stimulus frequency ratio			
DPOAE	1.05	1.2	1.27	1.32
$2f_1$-f_2	2.04	2.21	3.18	4.12
$2f_2$-f_1	1.42	2.05	2.25	2.44
Difference	0.62	0.16	0.93	1.68
p value	<0.001	≈0.25	<0.001	<0.001

Table III. A comparison of the average Prediction S.D. of the $2f_1$-f_2 and $2f_2$-f_1 distortion products for each frequency ratio from Table 1 a) and b). A positive difference indicates that the $2f_1$-f_2 Prediction S.D. values were larger than the corresponding $2f_2$-f_1 values. P values are derived via a paired t test.

The data confirm the apparent trend seen in Table I a) and b) that the $2f_2$-f_1 distortion product measurements were more closely related to the TEOAE level than the $2f_1$-f_2 distortion product. The differences were statistically highly significant with frequency ratios of 1.05, 1.27 and 1.32.

e. Averaging across frequency and the relationship between TEOAE and DPOAE

Prediction S.D. was also calculated using single point TEOAE and DPOAE data without cross-frequency averaging for three DPOAE stimulus configurations; with $L_1=L_2=70$ dB SPL and $f_2/f_1=1.05$, 1.2 and 1.32. The calculation was repeated with successive steps in the frequency alignment between DPOAE and TEOAE, and the minimum Prediction S.D. was recorded. The results are shown in Table IV.

f_2/f_1	D.P.	Single Point	Average
1.05	$2f_1-f_2$	5.21	2.08
	$2f_2-f_1$	4.65	1.09
1.2	$2f_1-f_2$	4.22	1.87
	$2f_2-f_1$	6.24	1.30
1.32	$2f_1-f_2$	4.00	3.71
	$2f_2-f_1$	5.45	2.39

Table IV. A comparison of Prediction S.D. calculated from single frequency points and the average Prediction S.D. values drawn from table I (a and b). Stimulus levels are $L_1=L_2=70$ dB SPL.

In general a much closer relationship was found between TEOAE and DPOAE when the data were averaged across frequency, with the exception of the $2f_1-f_2$ DP with $f_2/f_1=1.32$ in which case the averaging only resulted in a small reduction in Prediction S.D.. This implies that when the $2f_1-f_2$ DPOAE was stimulated by a wide frequency ratio, the poor correlation of the OAE fine structures was not the main limiting factor in the Prediction S.D. calculated without averaging.

With a frequency ratio of 1.05, the Prediction S.D. was lowest with both the $2f_1-f_2$ and $2f_2-f_1$ DPs when the TEOAE frequency was matched the DP frequency. However with a frequency ratio of 1.32 the exact frequency alignment was much less critical, suggesting that the fine structure pattern of the wide ratio DPOAE responses differed more from that of the TEOAE responses so that frequency misalignment was less significant. With $f_2/f_1=1.2$, the frequency alignment of the $2f_1-f_2$ DP was of little significance (suggesting that the DPOAE fine structure was not correlated with that of TEOAE), but with the $2f_2-f_1$ DP the Prediction S.D. was lowest when the TEOAE frequency was aligned with the DP frequency.

f. Comparison of mapping the $2f_2$-f_1 DPOAE to the TEOAE band corresponding to the frequency of the DP or to f_2

The Prediction S.D. associated with the $2f_2$-f_1 distortion product was also calculated using the TEOAE component corresponding to the DPOAE f_2 stimulus frequency and compared to the Prediction S.D. values shown in Table I b), which were calculated using the TEOAE component corresponding to the DPOAE $2f_2$-f_1 emission frequency.

When f_2/f_1=1.05, the Prediction S.D. values were significantly lower ($p<0.005$) when based on matching the emission frequencies of TEOAE and DPOAE, consistent with the $2f_2$-f_1 DPOAE level being defined in the region of the emission frequency place on the basilar membrane. However when f_2/f_1=1.27 or 1.32 ($p<0.005$), the Prediction S.D. was lower when the TEOAE band was matched to the DPOAE f_2 frequency. With a frequency ratio of 1.2, the Prediction S.D. values showed a non-significant tendency to be lower at the f_2 frequency. It is surprising that the upper sideband DPOAE with f_2/f_1=1.27 or 1.32 may be related to the f_2 region on the basilar membrane, as the DP is not expected to be able to propagate efficiently along the basilar membrane in this region. It may be that the relevant frequencies of the TEOAE come from a basilar membrane region more basal than their frequency place, and so the $2f_2$-f_1 DPOAE also corresponds to a region more basal than f_2.

g. Amplitude best fit line gradients

The gradients of the best fit lines can also be considered to be indicators of the similarities between the DPOAE and TEOAE mechanisms, a gradient of 1 being indicative of a close agreement. This is distinct from a comparison of OAE growth rates, as it is an inter-subject measure and each gradient is derived from only one stimulus level for DPOAE and TEOAE. Instead it is a measure of whether inter-subject factors causing a difference in TEOAE amplitude result in the same proportional difference in DPOAE amplitude. (In the stimulus parameter ranges used in this study, TEOAE growth rate is normally lower than that of DPOAE). The gradients of the best fit lines derived from the TEOAE vs. DPOAE scattergrams are shown in Table I c) and d). The standard errors associated with these gradients are shown in Table I e) and f).

The best fit line gradients of the level relationship between $2f_1$-f_2 DPOAE and TEOAE ranged from 0.39 to 0.90 (the gradient of the amplitude relationship is defined as ΔDPOAE/ΔTEOAE), but were generally closer to 1 at lower stimulus levels and smaller

stimulus frequency ratios. With larger stimulus frequency ratios, the gradients were closer to 1 if L_2 was 10 dB below L_1.

At higher stimulus levels, the gradients were greater with smaller stimulus frequency ratios.

All gradients over 0.8 associated with the $2f_1$-f_2 DP occurred with L_1=65 dB SPL, but were spread across the frequency ratios and the highest single figure with the $2f_1$-f_2 DP (0.90) occurred with f_2/f_1=1.32.

With the $2f_2$-f_1 DP, the best fit line gradients were closest to 1 with L_1=L_2 (Table I d)) and with smaller stimulus frequency ratios. When f_2/f_1=1.05, the gradient was also closer to 1 at low stimulus levels, but at higher frequency ratios this only remained true when L_1=L_2.

Although the gradients closest to 1 with the $2f_2$-f_1 DPOAE occurred with lower stimulus levels and f_2/f_1=1.05, there were also some gradients over 0.9 with L_1=L_2=65 or 70 dB SPL at the larger stimulus frequency ratios.

P values

Paired t tests of whole rows of data from Table I c) indicate a strong significance ($p<0.05$) for the tendency of the gradients with stimulus levels of L_1=65 dB SPL and L_2=60 or 55 dB SPL (rows 2 and 3) to be higher than with any combination with L_1=70 or 75 dB SPL (rows 4-9).

At higher stimulus levels the gradients were higher with smaller stimulus frequency ratios, and comparing whole columns of data, the best fit line gradients with f_2/f_1=1.05 or 1.2 were significantly higher ($p<0.05$) than with f_2/f_1=1.27 and the gradients with f_2/f_1=1.2 were also significantly higher than with f_2/f_1=1.32.

With the $2f_2$-f_1 DPOAE, stimuli at 65 or 70 dB SPL (rows 1 and 4) had significantly higher best fit line gradients than any combination with a 10 dB stimulus level difference (rows 3, 6 and 9).

$2f_2$-f_1 gradients with f_2/f_1=1.05 or 1.2 (columns 1 and 2) were higher than with f_2/f_1=1.27 or 1.32 (columns 3 and 4, $p<0.005$).

h. Comparison of repeat DPOAE measurements

Verification that the response level was consistent throughout the test sequence was achieved by repeating one DP sweep at the start and end of the DPOAE test series as well as in sequence halfway through the series. The repeated test used the following stimulus parameters: L_1=L_2=70 dB SPL and f_2/f_1=1.2. For each subject the levels of

DPOAE were determined for the first and last tests and the differences between the two measurement levels were calculated. The standard deviation of the differences for the $2f_1$-f_2 DPOAE was 0.9 dB, whereas for the $2f_2$-f_1 DPOAE it was 1.4 dB.

The higher variations seen in the $2f_2$-f_1 distortion product are likely to result from a greater influence of noise on a weaker $2f_2$-f_1 signal, as the two distortion products were measured simultaneously and the greatest retest differences for the $2f_2$-f_1 distortion product were seen in subjects with the lowest amplitude responses. There was no significant trend for the DPOAE's to increase or decrease during the test sequence, although the $2f_2$-f_1 distortion product showed a slight tendency to have a higher level in the later test (mean difference 0.4 dB).

i. Phase gradients and group delays

The phase gradient-derived latencies, averaged across all subjects, are shown in fig. 20a ($2f_1$-f_2 DP) and fig. 20b ($2f_2$-f_1 DP). The results for all subjects fell into two distinct categories, with the $2f_1$-f_2 DP at wide frequency ratios producing very shallow phase gradients and hence a small group delay whilst the $2f_1$-f_2 DP with f_2/f_1=1.05 and all $2f_2$-f_1 DP measurements produced steep phase gradients, similar to the TEOAE phase.

The TEOAE group delays in figure 20 b) are calculated in the frequency band corresponding to the DPOAE f_2 frequency range and also at the frequencies corresponding to the $2f_2$-f_1 emission frequency for each of the stimulus frequency ratios. The TEOAE group delays corresponding to the $2f_2$-f_1 DP frequency with wider stimulus frequency ratios are slightly shorter as they are derived from slightly higher frequency bands.

The $2f_2$-f_1 results with L_1=65, L_2=55 and f_2/f_1=1.27 and 1.32 are based on 1 subject because of low level responses resulting in a failure to meet the signal to noise ratio criteria in at least three consecutive frequencies in most subjects. All other data are based on at least 5 subjects.

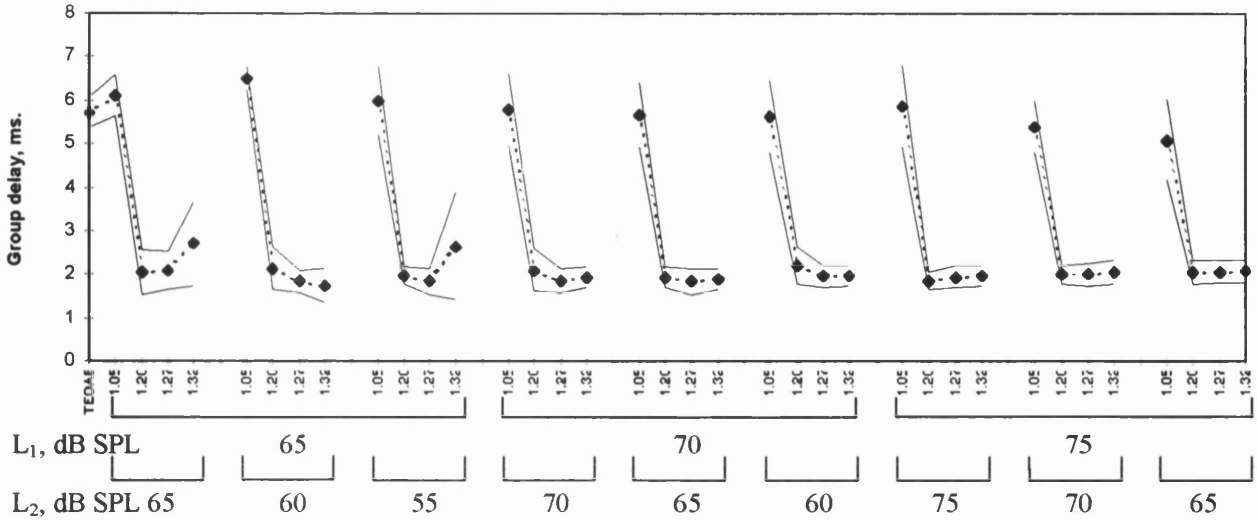

a) Group delay, $2f_1$-f_2 DPOAE

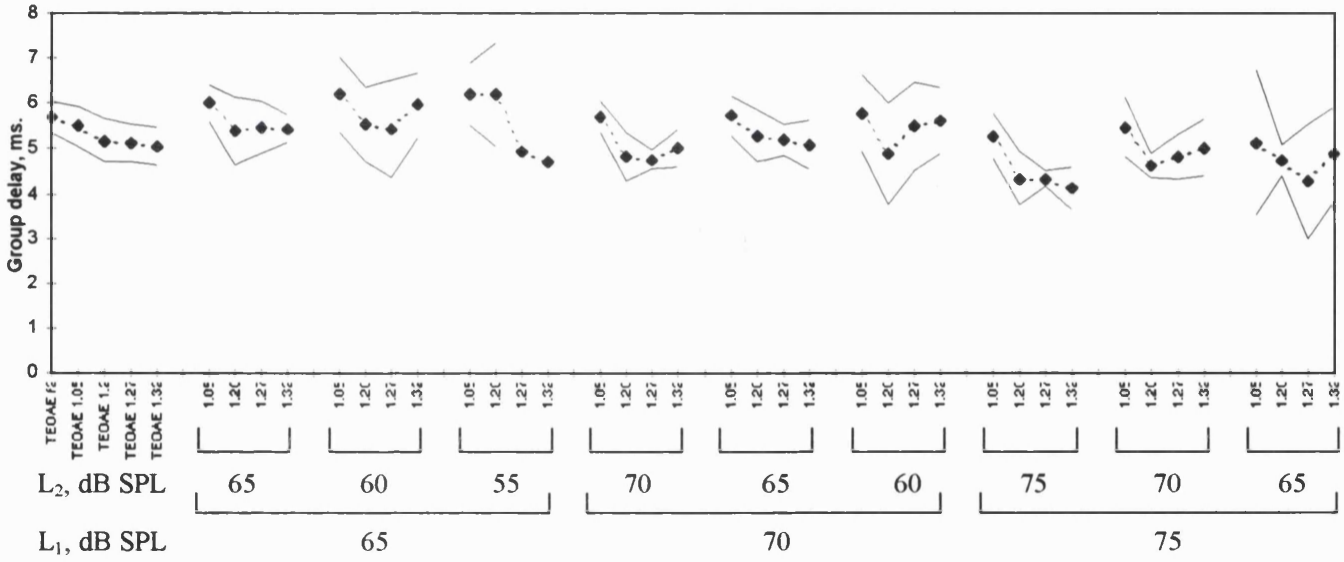

b) Group delay, $2f_2$-f_1 DPOAE

Figure 20. Group delay, derived from the DPOAE phase gradients obtained from sweeps with constant f_2/f_1. Results are an average from 9 subjects. Errors shown are 2 x s.e. from the mean. The corresponding TEOAE data is shown for comparison. a) $2f_1$-f_2 DP, b) $2f_2$-f_1 DP. In b), the TEOAE data are shown corresponding to the f_2 frequency of the DP measurements and also the frequency of the $2f_2$-f_1 DP at each frequency ratio. Group delay is considerably lower for the $2f_1$-f_2 DP with f_2/f_1=1.2-1.32 than with the $2f_1$-f_2 DP with f_2/f_1=1.05 or the $2f_2$-f_1 DP or TEOAE.

The phase of the DPOAE and TEOAE data from one subject is shown in figure 21 a-d). The phase gradient of the $2f_1$-f_2 DP at stimulus frequency ratios of 1.2 and greater was considerably less than that of all other DPOAE and the TEOAE measurements.

The behaviour of the $2f_1$-f_2 DP phase confirms the earlier findings of Kemp, 1986. In the case of the $2f_2$-f_1 DP meanwhile, the steep phase gradient which is seen only at small frequency ratios in the $2f_1$-f_2 DP is retained out to ratios of at least f_2/f_1=1.32.

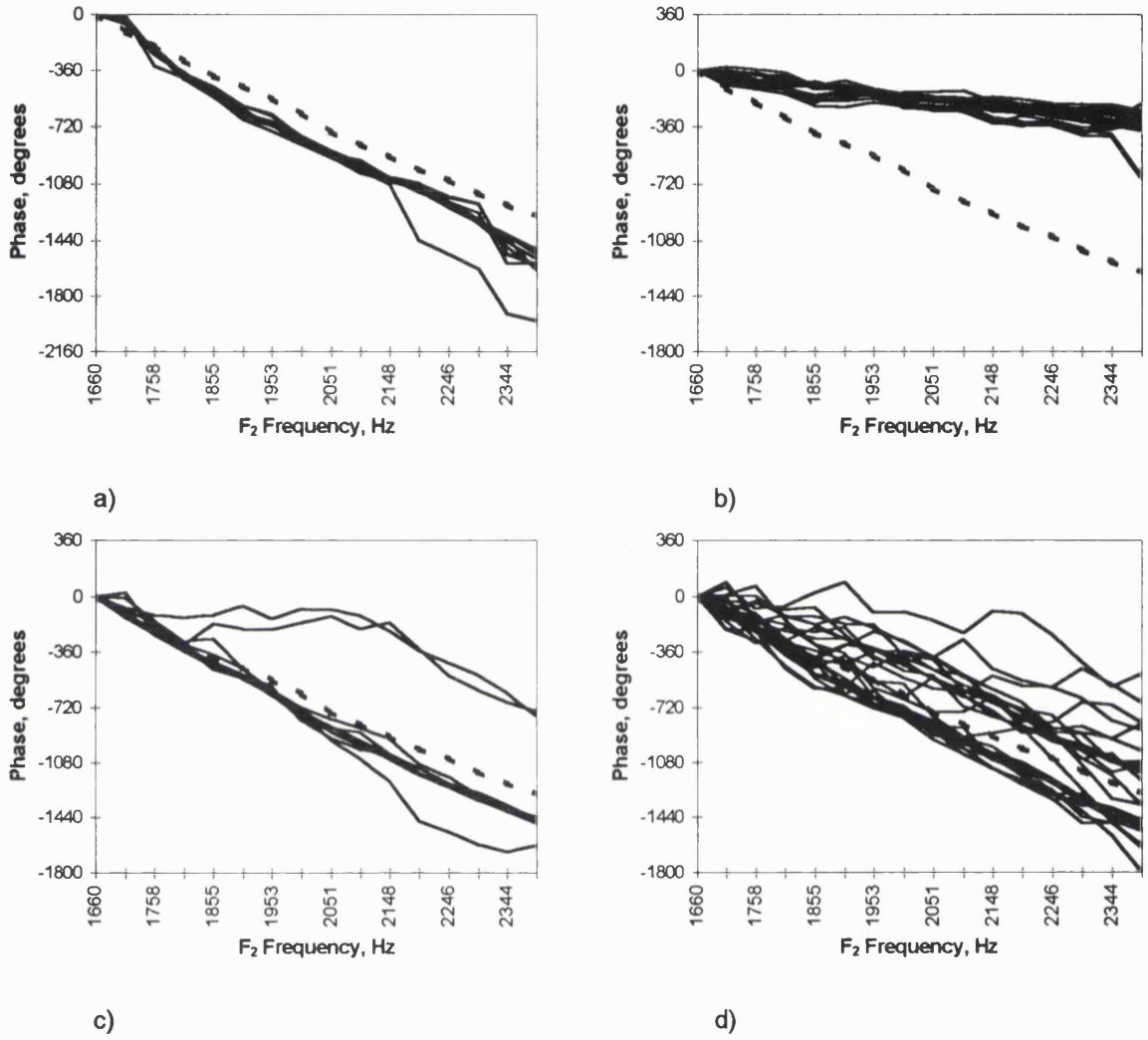

Figure 21. DPOAE phase (solid lines) plotted with TEOAE phase (broken lines) corresponding to the f_2 frequency of the DPOAE measurements for subject A. a) $2f_1$-f_2 DP, f_2/f_1=1.05. b) $2f_1$-f_2 DP, f_2/f_1=1.2, 1.27 and 1.32. c) $2f_2$-f_1 DP, f_2/f_1=1.05. d) $2f_2$-f_1 DP, f_2/f_1=1.2, 1.27 and 1.32. The gradient of the $2f_1$-f_2 DP phase in b) is considerably shallower than all other DP data and the TEOAE. Scattering seen in d) occurs in data with a poor signal to noise ratio.

IV Discussion of Results

a. DPOAE amplitudes

i) $2f_1$-f_2

The amplitudes of the $2f_1$-f_2 DPOAE measurements passed through a maximum at a stimulus frequency ratio which increased from 1.2 to 1.32 as the stimulus level

increased from 65 to 75 dB SPL (figure 18). This finding is in agreement with results presented by Harris et al (1989) and Gaskill and Brown, (1990).

All stimulus configurations used in the test sequence gave responses which exceeded the mean noise by at least 1 x the S.D. with the exception of a few isolated points. However measurements with ratios of stimulus frequency 1.2, 1.27 and 1.32 gave larger amplitude responses than the 1.05 ratio and were therefore quicker and easier to measure.

The lower growth rates with stimulus level seen in the DPOAE measurements with a stimulus frequency ratio of 1.05 imply that the generation or emission mechanisms may be more saturated than it is with a wider frequency ratio. It is likely that when f_2/f_1 is small, the site of $2f_1$-f_2 DPOAE generation is closer to the peak of the f_1 travelling wave where the f_1 travelling wave envelope growth is highly compressive, so this may be the reason for the saturated DPOAE growth. The relatively low level of response indicates that under these stimulus conditions either the distortion product does not easily escape back to the ear canal or the response induced in the basilar membrane produces less energy at that DP frequency.

Conversely, the high growth rates seen with a frequency ratio of 1.32 (of up to 1.4 dB/dB) suggest that the DP generation or emission mechanisms for wider spaced tones are not so easily saturated, leading to the higher DP level.

ii) $2f_2$-f_1

The levels of the $2f_2$-f_1 DPOAE's (figure 18) are sensitive to changes in frequency ratio and differences between L_1 and L_2, particularly at lower stimulus levels, with the highest level responses being obtained with smaller frequency ratios and equal stimulus levels. This is the opposite of the $2f_1$-f_2 DP behaviour, for which a larger frequency ratio and $L_1>L_2$ increased the OAE level. The trend shown by Erminy et al (1996) for a larger $2f_2$-f_1 DP level to be obtained with f_2/f_1=1.12 than with f_2/f_1=1.22 has been shown to continue at both higher and lower ratios.

As with the $2f_1$-f_2 distortion product, the $2f_2$-f_1 DP growth rates were smallest when f_2/f_1=1.05 implying a more saturated generation or emission mechanism, and greatest when f_2/f_1=1.32 implying a less saturated response. In the case of the upper sideband, this can be explained in terms of the location of the DP frequency place as the DP is presumed to originate from here. When f_2/f_1 is small, the $2f_2$-f_1 DP frequency place is close to the f_1 and f_2 travelling wave peaks where the growth with stimulus level is compressive. But when f_2/f_1 is large, the $2f_2$-f_1 DP frequency place is displaced basally away from the peaks of the primary tones to a region where the travelling wave

envelopes of f_1 and f_2 grow linearly with stimulus level. Therefore the increase in $2f_2$-f_1 DPOAE generation would increase more rapidly with increasing stimulus level when f_2/f_1 is large.

b. Relationships between TEOAE and DPOAE amplitude

i) $2f_1$-f_2

A close relationship was found between the frequency averaged levels of the $2f_1$-f_2 DPOAE and TEOAE, particularly when the frequency ratio was small (Table I (a)). With larger stimulus ratios, there was a tendency for the Prediction S.D. to be smaller with higher stimulus levels, a condition which coincided with shallower DPOAE vs. TEOAE level gradients (Table I c). A smaller DPOAE vs. TEOAE level gradient would reduce the values obtained for Prediction S.D. and so the lower Prediction S.D. values obtained with higher stimulus levels may not in this case indicate a closer relationship between DPOAE and TEOAE.

The relationships found in the present study are closer than expected from the literature. Calculations from data presented by Smurzinsky and Kim (1992) and Smurzinsky et al (1993) produced approximate $2f_1$-f_2 Prediction S.D. values at 2 kHz of 3.7 dB (Preterm infants), 3.6 dB (Fullterm infants) and 2.7 dB (Adults) using DPOAE stimulus parameters of L_1=L_2=65 dB SPL, f_2/f_1=1.18-1.23 with 1/4 octave steps between points (1/2 octave averaging in analysis). It is likely that a closer agreement was seen here between TEOAE and DPOAE with adult subjects than with infants because of easier measurement conditions. A difference remains between the Prediction S.D. from their adult data (2.7 dB) and the corresponding result using a comparable stimulus frequency ratio and level from the present study (1.8 dB). This is likely to be because of the finer frequency interval within the DP sweeps of the present study and hence the greater degree of across frequency averaging and also the use of the same probe fitting for both DPOAE and TEOAE measurements in the present study resulting in the removal of possible variance arising from variations in probe fitting.

The corresponding calculated Prediction S.D. associated with the work of Moulin et al (1993) and Probst and Harris (1993) are 4.1 dB and 3.9 dB respectively, which correspond to Prediction S.D. values of 1.8 dB and 1.7 dB obtained with comparable stimulus parameters in the present study. Moulin et al used DPOAE stimulus parameters of L_1=L_2=60 dB SPL and f_2/f_1=1.17 and compared unaveraged single DPOAE points to 200Hz averaged TEOAE bands. The larger Prediction S.D. obtained from the data by Moulin et al presumably arises from the reduced averaging in both the TEOAE and

DPOAE data. Probst and Harris used a frequency ratio of 1.22 and a stimulus level difference of 6 dB SPL and compared the TEOAE and DPOAE levels across the full frequency range and so the TEOAE and DPOAE mean responses may have been dominated by different frequency regions.

Therefore it appears that there are two main reasons why closer relationships have been observed between the levels of TEOAE and DPOAE in the present study than had been previously shown:

a) the averaging process across a frequency range removes to a large extent the effect of the OAE fine structure, and

b) the DPOAE configurations which give the closest agreements are not those which have the largest amplitude and so have not previously been investigated so extensively.

ii) Relationships between TEOAE and DPOAE amplitude, $2f_2$-f_1

As with the $2f_1$-f_2 DP, the $2f_2$-f_1 DP was also most closely related to TEOAE when evoked by smaller frequency ratios and stimulus levels (Table I (b)), although the relationship did not deteriorate at wider DP stimulus frequency ratios to as great an extent as was the case with the $2f_1$-f_2 distortion product. Interestingly, although when L_1=70 or 75 dB SPL it was preferable for the stimuli to be of equal level, when L_1=65 dB SPL the values of Prediction S.D. were lower when L_1>L_2. However these produced very low level $2f_2$-f_1 DPs and are associated with very shallow amplitude gradient relationships and therefore in this case the association with TEOAE may not be as close as it may appear.

c. Gradient of DPOAE/TEOAE amplitude relationship

Gradients close to 1 imply that intersubject differences affecting OAE level (for example middle ear conductive differences) act in equal proportion on both DPOAE and TEOAE, thus suggesting similarities in generation and/or emission process. There are various factors which could effect the amplitudes of TEOAE and DPOAE. Variation in the efficiency of sound conduction through the middle ear would maintain a 1:1 relationship between TEOAE and DPOAE and would probably affect TEOAE and DPOAE level equally. Changing the DP parameters may change the DPOAE level, but would not necessarily of itself alter the 1:1 gradient unless the change led to unequal saturation of TEOAE and DPOAE. However, if DPOAE and TEOAE were of unequal sensitivity to the condition of the outer hair cells or if they arose from different emission mechanisms the 1:1 gradient would probably be lost. As both DPOAE and TEOAE

(measured with the nonlinear stimulus method) are both a result of non-linear cochlear processes, their amplitudes might be expected to behave similarly.

i) Gradient of DPOAE/TEOAE amplitude relationship, $2f_1-f_2$

The DPOAE/TEOAE amplitude gradients associated with the $2f_1-f_2$ DP results were generally closer to 1 with lower stimulus levels and when $L_1>L_2$ (Table I c)). This indicates that inter-subject factors affecting OAE level have a proportionate effect on DPOAE and TEOAE with these stimulus conditions, implying that the mechanisms involved in generating or emitting the two OAE types are related. At higher stimulus levels there was also a tendency for the gradients to be higher with smaller frequency ratios, in spite of the lower DP growth rates associated with these stimulus parameters. These findings generally agree with the Prediction S.D. data with the exception of the level difference, L_1-L_2: Reducing L_2 tended to increase the best fit line gradient (implying closer agreement), but also increased the Prediction S.D. (implying worse agreement) when f_2/f_1 was small.

ii) Gradient of DPOAE/TEOAE amplitude relationship, $2f_2-f_1$

The $2f_2-f_1$ gradients were near to 1 with low stimulus levels, small frequency ratios and $L_1=L_2$ and were lower with other DPOAE stimulus parameters (Table I (d)). The pattern of results is therefore consistent with the Prediction S.D. data. The tendency for the gradients obtained with a low stimulus level to be high may be a result of avoidance of a saturated DP response, whereas higher gradients obtained with small frequency ratios and $L_1=L_2$ are associated with higher DPOAE levels and may therefore arise from the avoidance of the influence of noise.

Comparing the average DPOAE/TEOAE amplitude gradients of the two distortion products at each frequency ratio, the gradients associated with the $2f_2-f_1$ DP were closer to 1 than those of the $2f_1-f_2$ DP when $L_1=L_2$, but the $2f_1-f_2$ DP gradients were closer to 1 when $L_1=L_2+10$.

Considering the Prediction S.D. and amplitude gradients together, both the $2f_1-f_2$ DP and the $2f_2-f_1$ DP levels appear to be generally most closely related to TEOAE with smaller frequency ratios and lower stimulus levels. Additionally, the $2f_2-f_1$ DP is also more closely related to TEOAE when $L_1=L_2$.

d. Retest Error

The mean test-retest difference for the $2f_1$-f_2 distortion product was found to be 0.9 dB, so the values of Prediction S.D. would not reliably fall below this even if there is no difference at all in the mechanisms involved in the TEOAE and DPOAE. Additionally if a similar test-retest error is present in the TEOAE measurements (TEOAE test-retest variation of approximately 1 dB has been reported by Harris et al, 1991) the combined effect would result in a Prediction S.D. floor of 1.25 dB. Several of the $2f_2$-f_1 DP test configurations have produced Prediction S.D. values which are of this order and so there may not be any significant difference between the TEOAE measurement form and some configurations of DPOAE.

Possible additional random error arises from the possibility that the fine structure ripple may not be completely eliminated by the frequency averaging over only approximately ½ of an octave and may not match perfectly between the frequency regions adopted from the TEOAE and DPOAE responses.

e. Phase Gradients and delays

$2f_2$-f_1 DPOAE phase data from a fixed f_2/f_1 paradigm have not been presented in the literature. There is limited data in the literature regarding the phase behaviour of the $2f_2$-f_1 DP and it tends to be measured using an f_1 or f_2 sweep. Wable et al (1996) used an f_2 sweep test and found that the $2f_2$-f_1 DP group delay was less than that of the $2f_1$-f_2 DP if the emission frequencies were matched, and Moulin and Kemp (1996) found no difference between $2f_2$-f_1 DPOAE group delays obtained with f_1 or f_2 sweeps. This is in contrast to the $2f_1$-f_2 DP, for which group delays obtained with f_2 sweeps are usually greater than those obtained using f_1 sweeps.

Derivation of the group delay from the phase data associated with the TEOAE and DPOAE measurements (figure 20) has indicated that $2f_1$-f_2 measurements with f_2/f_1=1.05 and all $2f_2$-f_1 measurements have phase gradients close to that of the corresponding TEOAE measurements, implying that the mechanisms by which the two forms of OAE are emitted are related. Stimulus frequency otoacoustic emissions (SFOAE) are also known to have similar steep phase versus frequency gradients (e.g. Shera and Guinan, 1999; Zwicker and Schloth, 1984; Kemp and Chum, 1980b). However the phase gradients of the $2f_1$-f_2 distortion product with larger frequency ratios were considerably shallower (consistent with Kemp, 1986), suggesting that these emissions differ considerably from TEOAE.

f. Extension to a wider frequency range

In order to investigate the relationship of DPOAE to TEOAE across a wide frequency range with a small DPOAE frequency ratio, an extended fine structure DP sweep was obtained with stimulus parameters f_2/f_1=1.05 and L_1=L_2=70 dB SPL for one subject covering the frequency range 500-7000 Hz. The $2f_1$-f_2 and $2f_2$-f_1 DPOAEs are shown in figure 22 with a corresponding standard TEOAE, with each response plotted against the frequency of the emitted response on a logarithmic scale. The level of the TEOAE response in figure 22 was increased by 12 dB to correspond with the summation method used in the averaging of the responses earlier in this study.

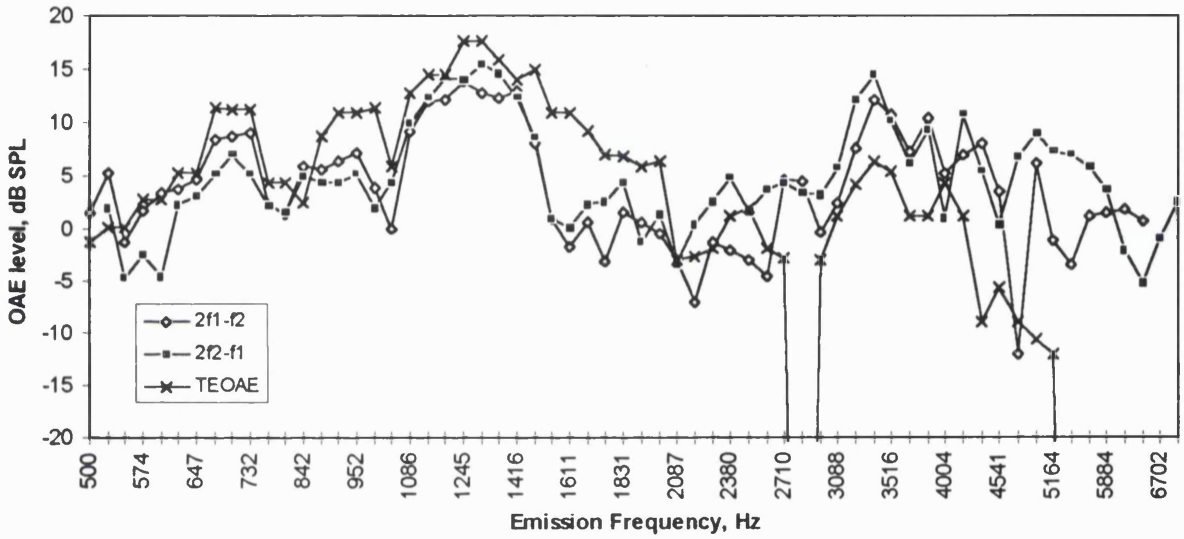

Figure 22. Extended fine structure DPgrams with corresponding TEOAE response on a logarithmic frequency scale. Each OAE is plotted against its emission frequency. The TEOAE amplitude is increased by 12 dB to correspond with the summation method used elsewhere in this study. DPOAE stimulus parameters are L_1=L_2=70 dB SPL, f_2/f_1=1.05. Close agreement is seen in the fine structure of the three OAE forms.

It can be seen that both of the distortion products shown were measurable across the complete frequency range, whereas as expected the TEOAE response level decreased sharply above 4 kHz at least partly as a result of the time windowing to remove low latency artifacts. The behaviour of the $2f_2$-f_1 distortion product with these parameters therefore differs from the wider frequency ratios used by Erminy et al (1996), who observed a reduction in $2f_2$-f_1 level towards higher frequencies. It can also be seen that the fine structures of the three responses show excellent agreement, indicating that with these stimulus parameters the fine structure of each OAE is determined by the emitted frequency rather than the stimulating frequency.

He and Schmiedt (1997) have shown that the fine structure of the $2f_1$-f_2 DPOAE shifts in frequency with changes in stimulus level at frequency ratios of f_2/f_1=1.11, 1.2 and 1.33. Therefore the finding presented here indicates that either the frequency shifting effect does not occur when f_2/f_1=1.05 or that the DPOAE parameters chosen coincidentally are subject to the same frequency shift as TEOAE, allowing the accurate relationship with TEOAE to occur.

V Origins of TEOAE and DPOAE

The frequency ratio which produced the maximum level of the $2f_1$-f_2 DPOAE was in the region of f_2/f_1=1.2-1.3 and it is largely for this reason that ratios between 1.2 and 1.3 have tended to be preferred for clinical use as the larger response results in a clearer differentiation between normal and hearing impaired ears.

In the case of the $2f_2$-f_1 DP, the largest levels were obtained with a small stimulus frequency ratio and with L_1=L_2. From a consideration of the cochlear travelling waves, this pattern could be expected. A small frequency ratio brings the $2f_2$-f_1 frequency closer to the stimulus frequencies where the transverse displacement on the basilar membrane due to the travelling wave is greater, whilst reducing L_2 below L_1 may reduce the travelling wave modulation depth in the $2f_2$-f_1 frequency region and so reduce the effect of non linear distortion associated with the basilar membrane movement. Indeed, it is a general property of compressive nonlinearities that upper sideband distortion product generation is enhanced if L_2 exceeds L_1 by a small amount (Kemp 1987).

The amplitude relationships between TEOAE and DPOAE in some stimulus configurations have been found to be unexpectedly close despite the many obvious differences in the manner in which each emission is stimulated and extracted, supporting the view that with these stimulus conditions the same information is provided by results obtained by either OAE method and that the same underlying mechanism is responsible for both.

Both the $2f_1$-f_2 and $2f_2$-f_1 DP levels were more closely related to TEOAE when stimulated with a frequency ratio of f_2/f_1=1.05 than with the wider ratios of 1.2-1.32. Therefore DPOAE is more like TEOAE when stimulated with a small frequency ratio in which the emission frequency is close to that of the stimuli than when stimulated with a wide frequency ratio in which the emission frequency differs more markedly from the stimulus frequencies.

The amplitude relationship between TEOAE and DPOAE was closer with the $2f_2$-f_1 DP than the $2f_1$-f_2 DP. There are fundamental differences between these two DPOAEs which may indicate why the $2f_2$-f_1 DP is more closely related to TEOAE: 1) The $2f_2$-f_1 DPOAE generation site must be linked to the emission frequency place on the basilar membrane rather than the region of the stimulus frequencies, 2) The $2f_2$-f_1 DPOAE has only one possible emission region whereas the $2f_1$-f_2 DPOAE has two and, 3) The phase behaviour of the $2f_1$-f_2 and $2f_2$-f_1 DPOAEs differs.

Close agreement between the TEOAE and the $2f_2$-f_1 DP and also the low ratio $2f_1$-f_2 DP was seen in the phase data. The shallower phase gradient seen in the $2f_1$-f_2 DP at wider stimulus frequency ratios suggests that the $2f_1$-f_2 DPOAE may have a different mechanism of generation and/or emission depending on the ratio f_2/f_1.

The two distinct phase gradient categories are consistent with the two emission creating modes described as 'place fixed' and 'wave fixed' (e.g. Kemp, 1986; O Mahoney and Kemp, 1995; Kemp and Knight, 1999) or 'reflection' and 'distortion' (Shera and Guinan, 1998, 1999). The wave fixed model, in which the emission source is locked to the travelling wave envelopes and so moves smoothly with frequency, would produce an almost flat phase gradient because the number of waves to the basilar membrane travelling wave peak is almost independent of frequency (demonstrated by measurements of basilar membrane motion, e.g. Rhode, 1971). This flat phase gradient is seen in the wide ratio $2f_1$-f_2 DP sweeps. The place fixed model, which requires a series of fixed impedance or activity irregularities on the basilar membrane to reflect or scatter OAE energy back towards the base of the cochlea, would result in a comparatively steep phase gradient in a constant frequency ratio sweep, formed by the travelling wave envelopes of the stimulus tones passing over the reflectors as the stimulus frequencies change. This steep phase gradient is seen with TEOAE, SFOAE, the $2f_2$-f_1 DP and the $2f_1$-f_2 DP behaviour when f_2/f_1 is small.

Yates and Withnell (1998) have suggested that TEOAE may consist mostly of intermodulation distortion components, but TEOAE nevertheless has the phase characteristic of the reflection-based place-fixed model and therefore is not dominated by wide stimulus ratio low phase gradient lower sideband components. If TEOAEs included a component like the $2f_1$-f_2 DP at wide ratios, this would primarily be emitted with a low phase versus frequency gradient. It remains possible that lower latency components of the TEOAE exist but because of the shorter time delay they are excluded by the time windowing employed to extract the OAE from the stimulus and middle ear response.

The results raise the question of whether it would be valuable to change the DPOAE parameters used in clinical applications in order for the response to fall within the place fixed category. However the issue of whether the wave fixed or place fixed category of OAE is more closely linked to auditory function remains unresolved and so currently the only reason to change DP parameters would be to allow reliable interchangeability between DPOAE and TEOAE measurements. This would be at the expense of a loss of DPOAE intensity, resulting in a less efficient DPOAE measurement.

VI Summary/Conclusions

A closer agreement has been observed between TEOAE and DPOAE amplitude than has previously been found.

This is thought to be because

a) averaging over a frequency range has been used to reduce the variance which arises from the fine structure in DPOAE and TEOAE, and

b) DPOAE parameters which are seldom used clinically have been found to produce the closest relationships.

When $f_2/f_1=1.05$, the level fine structure of TEOAE, $2f_1-f_2$ DPOAE and $2f_2-f_1$ DPOAE have been demonstrated to be related at the frequency of emission, indicating that the emission mechanisms involved may be very closely related.

The phase gradients of the TEOAE, $2f_2-f_1$ DPOAE and the $2f_1-f_2$ DPOAE with $f_2/f_1=1.05$ are similar and are consistent with a place fixed reflection based emission mechanism. SFOAE is also known to have a steep phase versus frequency characteristic consistent with this mechanism.

The phase of the $2f_1-f_2$ DP with a larger stimulus frequency ratio deviates markedly from this and instead is consistent with a wave fixed emission mechanism. It therefore seems that this form of DPOAE is emitted by a mechanism that is distinct from that of all other evoked OAE's.

The apparently common emission mechanism for TEOAE, $2f_2-f_1$ DPOAE and the $2f_1-f_2$ DPOAE with $f_2/f_1=1.05$ and separate behaviour pattern for the $2f_1-f_2$ DPOAE with a wide frequency ratio suggests that two main categories for evoked otoacoustic emissions can be identified, rather than a larger number of different mechanisms with a different one for each mode of stimulation.

D. A detailed study of DPOAE level and phase to investigate the emission mechanisms

I Introduction

In the previous chapter it was shown that the emission mechanism involved in TEOAE appears to be similar to a mechanism that is commonly involved in DPOAE. However, within DPOAE measurements there is divergence of phase behaviour and hence a divergence in emission mechanism depending on the stimulus parameters.

The transition between the two emission mechanisms and the relationship between the upper and lower DPOAE sidebands have not been explored in detail. DPOAE measurement sequences are usually obtained in one of 4 forms of frequency sweeps which may each reveal complementary information about the DPOAE:

1. fixed f_2/f_1. With this sweep, both f_1 and f_2 are incremented in frequency, with the ratio between them remaining constant. This paradigm has been used to demonstrate two distinct phase behaviours in DPOAE, proposed to arise from wave and place fixed emission mechanisms (Kemp, 1986).
2. f_1 sweep. f_1 is incremented and f_2 is kept constant. With lower sideband DPOAE, the value of this paradigm is that if the DPOAE generation is site linked to f_2, which is presumed to be the case with lower sideband DPOAE, the generation site doesn't move.
3. f_2 sweep. f_2 is incremented and f_1 is kept constant. The presumed DPOAE generation site will move during this sweep.
4. Fixed DP frequency sweep (e.g. Allen and Fahey, 1992). In this sweep, the f_1 and f_2 are swept at different rates in order to keep f_{DP} constant. In the case of the $2f_1$-f_2 DP, f_2 is swept at twice the rate of f_1. In the case of the $2f_2$-f_1 DP, it is the other way round.

Each measurement paradigm is appropriate for different research applications. For example, in order to use the phase gradient to confirm that a DP is not an artifact, a fixed f_2/f_1 sweep is not appropriate because this sweep can generate a very shallow phase gradient from cochlear DPs, which may not be distinguishable from the flat phase gradient of an artefact. The best sequence for this kind of validation is an f_2 sweep, as this usually has the steepest phase gradient (Moulin and Kemp, 1996).

However a fixed f_2/f_1 sweep is appropriate for clinical use, as the measurement sequence results in a comparable assessment of cochlear function across a frequency range which is more straightforward to interpret than the f_1 and f_2 sweeps in which the frequency ratio is different for each data point.

The use of fixed f_2/f_1, f_1 and f_2 sweeps to investigate DPOAE provides an incomplete picture of DP phase behaviour and the true significance of the 'partial' latencies obtained via these methods remains unclear. The aim of this study is therefore to reach a better understanding of what stimulus conditions result in DPOAE of the wave fixed and the place fixed type and to determine how the production of $2f_2$-f_1 DPOAE is similar to or different from the $2f_1$-f_2 DP in this respect.

Previous reports on DPOAE phase behaviour have been fragmentary and invariably presented as isolated sweeps of either f_1, f_2 or occasionally constant f_2/f_1 sweeps. In the present study, a new representation is adopted in which multiple sweeps are combined within two dimensional stimulus domains providing a more complete picture of DPOAE phase versus frequency behaviour.

Phase gradients over the stimulus frequency surfaces rather than over isolated linear sweeps will allow the delineation all of the conditions in which the DPOAE behaviour is consistent with the 'wave fixed' mechanism and when it matches the 'place fixed' emission mechanism. Also the transition region between the two domains will be clearly visualised, previously only known from single sweep data. Direct comparison of the $2f_1$-f_2 and $2f_2$-f_1 DP's will allow exploration of the links between them and identification of any common characteristics.

a. Phase differences expected from 'wave' and 'place' fixed emissions

i) Wave fixed DPOAE

As discussed in section A II (i), the near-geometric frequency scaling of the cochlea means that the phase of a 'wave fixed' DPOAE would be expected to be roughly constant through a frequency sweep maintaining a constant stimulus frequency ratio.

However, if the frequency ratio changes, the relative phases of f_1 and f_2 must change at each point over the whole excitation region and so the DP phase must also change. In the case of an f_1 change, even if the DP generator itself were fixed to the f_2 wave envelope the DP generator would still 'read' the changing phase of f_1 at the generator site. Similarly for an f_2 frequency change the generator site would be moved to a new location where the phase of f_1 would be different. Therefore for either an f_1 or f_2 sweep the wave fixed DPOAE phase would change smoothly with a changing frequency ratio.

ii) Place fixed DPOAE

In the case of a 'place fixed' lower sideband DPOAE, DP energy would be released from a region inside the f_2 excitation envelope basal to the DP frequency place and propagate apically towards the DP frequency place, from where it would then be re-

emitted. (Upper sideband DPOAE may also travel apically before being reflected basally in this way, or may be generated at fixed points already travelling in a basal direction). It seems reasonable to assume that much of the latency would be associated with the travelling wave behaviour at the DP place. In this case it is helpful to consider a constant DP frequency sweep as the DPOAE source region is believed to be associated with the DP frequency place and so would remain fairly stationary during such a sweep.

For the $2f_2$-f_1 DP at wide frequency ratios, the inward travel time of the stimulus tones to the DP place would be very short and almost constant with f_1 and f_2 frequency changes because the f_1 and f_2 peaks would be far removed apically from the DP place. The DPOAE phase would therefore depend primarily on the DP frequency and so the phase contours for the $2f_2$-f_1 DP would be expected to closely follow lines of equal DP frequency. In the case of a constant-DP-frequency sweep (for which, in the case of the $2f_2$-f_1 DP, f_1 is incremented at twice the rate of f_2) a flat phase characteristic would in this case be observed. With a smaller frequency ratio, the situation may be more complex, as some inward f_1 and f_2 delay could accumulate and so the DPOAE iso-phase contours may then deviate from following lines of equal DP frequency. However, the DP may be generated basal to the DP place and propagated apically before being reflected at the DP place. The amount of inward delay may depend on how close the DP generator is to the DP frequency place on the basilar membrane: the closer to the DP place, the more the inward travel time would increase.

For the $2f_1$-f_2 DP, in the case of a 'place fixed' emission, substantial phase delays for the primaries would be expected to accumulate by the DP generation site in the region of the f_2 frequency place, which would add to the phase delay contributed by the re-emission from the DP place. $2f_1$-f_2 DPOAE iso-phase contours would not necessarily therefore be expected to lie along lines of constant DP frequency.

b. f_1, f_2 area

Figure 23 (a) defines the first way in which the DPOAE data will be presented. The two axes are defined by the frequencies of the two stimulus tones. The predicted phase contour patterns are indicated in the figure. Constant ratio frequency sweeps are straight lines on this representation radiating from the 0, 0 Hz point. Iso-phase contours would also be expected to follow this pattern in the case of a pure 'wave fixed' emission mechanism.

Lines of constant DP frequency are a family of parallel lines and cross the chart with a gradient of 2 (because the stimulus frequency which is more distant to the DP frequency

must change at twice the amount of the closer stimulus frequency in order to maintain a constant DP frequency). Phase contours would be expected to follow this pattern in the case of a pure 'place fixed' emission mechanism.

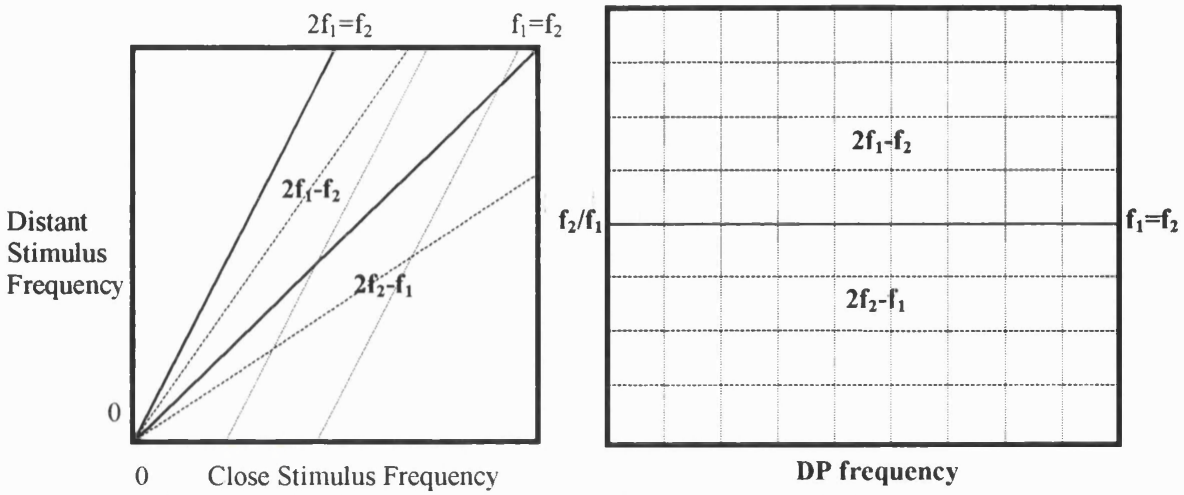

Figure 23. (a) The f_1, f_2 scheme for presenting DPOAE data. The frequency scales are linear and the x and y axes are the 'Close' and 'Distant' stimulus frequencies respectively. These terms refer to the stimulus frequencies which are closer to or further away from the DP frequency, i.e. the 'close' stimulus frequency to the $2f_1$-f_2 DP is f_1 and the 'close' stimulus frequency to the $2f_2$-f_1 DP is f_2. The reason for employing this definition for the axes rather than simply using f_1 and f_2 is that it allows both upper sideband and lower sideband DP data to be combined on one chart. The leading diagonal line on the chart is f_1=f_2, a condition at which DP measurements are not possible. Above this line is the $2f_1$-f_2 DP area, below the line is the $2f_2$-f_1 DP area. The line running from the origin with a gradient of 2 is f_2=$2f_1$. At this line, the $2f_1$-f_2 DP frequency falls to 0 Hz and therefore becomes mathematically impossible. In practice, the DP becomes unmeasurable well before this. No similar limitation exists with the $2f_2$-f_1 DP, although the DP also becomes unmeasurable if f_1 and f_2 are very widely separated. Dotted lines show the orientation of constant f_2/f_1 and constant DP frequency sweeps.
(b) The f_2/f_1 versus DP frequency scheme for presenting DPOAE data. f_1=f_2 is a horizontal line at the centre of the chart (i.e. f_2/f_1 =1). Above this is the $2f_1$-f_2 DP, below it is the $2f_2$-f_1 DP.

c. f_2/f_1 ratio, DP frequency area

Figure 23 (b) defines the second way in which the DPOAE data will be presented. The frequency of the DPOAE is plotted on the horizontal axis and the vertical axis is the frequency ratio between the stimulus tones. Moulin et al (1999) has shown amplitude data using a related presentation method, but with f_2/f_1 versus f_2 instead of DP frequency. In figure 23 (b), by definition, lines of constant frequency ratio are horizontal

and lines of constant DP frequency are vertical. Therefore phase contours which are horizontal on this chart are consistent with a 'wave fixed' emission mechanism and phase contours which are vertical are consistent with a 'place fixed' emission mechanism.

II Measurement Method

a. Subjects

Data presented in this study are drawn from an exhaustive study of DPOAE conducted using the left ears of two subjects: a male (RDK) aged 29, and a female (RN) aged 24 at the time of the measurements. Prior to commencing the DPOAE study, the ears were confirmed as having normal auditory thresholds and middle ear function. In addition, standard DPgrams (f_1/f_2=1.22, L_1=65, L_2=55 dB SPL) were obtained which were within normal limits (Gorga et al, 1997). RDK was one of the small normal-hearing group investigated for relationships between TEOAE and DPOAE phase characteristics and was typical of that group (Chapter C).

b. Experimental Method

For subject RDK, an ILO88 DPi instrument was used with an Otodynamics BP probe for f_1 versus f_2 charts, whilst for the data in the DP frequency versus f_2/f_1 ratio charts an ILO 96 instrument was employed with an Otodynamics BP probe (3 tone type, but the third tone was not used here). For subject RN, an ILO 96 instrument was used with an Otodynamics CD-type probe (this probe was used with this subject because it is small, and the subject had very narrow ear canals).

Custom stimulus 'sweeps' could be preprogrammed with either f_1, f_2 or f_1 and f_2 incrementing with time. f_1 or f_2 sweep sequences began with a small frequency ratio, with either f_2 being successively incremented or f_1 being decremented until several successive $2f_1$-f_2 and $2f_2$-f_1 DPOAEs were unobtainable or until the limits of the frequency range under investigation were reached. Constant frequency ratio sweeps began at low frequency and swept towards higher frequencies. The probe fitting in the ear canal was checked before each sweep, and where the frequency response was not substantially flat in the frequency region to be tested, the probe was removed and reinserted.

Each measured DP sweep data point was obtained from averaging of 64 (RDK) or 32 (RN) signal samples, each of the standard 80 ms duration. The noise rejection facility was set to between 2 and 4 mPa depending on the ear fitting and on the frequency range

to be tested. The equipment was situated in a quiet room with a typical background noise level of 40 dBA SPL.

For measurements with RDK with L_1=L_2=60 or 75 dB SPL, sequential measurements were mostly in the form of f_2 sweeps with 12 Hz steps. A series of these sweeps were obtained with f_1 incremented by approximately 48 Hz. Where required to clarify detail (for example where the data contained sharp notches), additional f_2 sweeps were added at intermediate f_1 frequencies which halved the frequency spacing between adjacent sweeps to 24 Hz. These data were crossed by f_1 sweeps and constant frequency ratio sweeps in order to clarify the phase relationship between the adjacent f_2 sweeps.

For RDK and RN with L_1=L_2=70 dB SPL, the data were obtained in constant f_2/f_1 sweeps, with the ratio incremented by 0.25 for adjacent sweeps.

The overall stimulus frequency range studied extended from 1300 Hz to approximately 3 kHz for the f_1, f_2 area representation, which was extended to a DP frequency range of 1-4.1 kHz for the f_2/f_1 versus DP frequency area representation.

For each area chart, up to approximately 3,500 data points were obtained per DP from up to approximately 70 f_1 and f_2 sweeps. On occasions single points were repeated at intersections of f_1 and f_2 sweeps and in these cases an average was taken. Typically, repeated points agreed to within 2 dB (level) and 20° (phase).

In order to be accepted, each DP sweep data measurement was required to exceed the mean measured noise level in the adjacent 10 harmonic frequencies of the 80ms data sample by at least 1 S.D. In order to be visible above the floor in the amplitude chart, the DP amplitude also needed to exceed -15 dB SPL. Constant frequency ratio sequences swept from low frequency towards higher frequencies.

A range of stimulus levels were employed. The 75 dB SPL level facilitated successful measurements at wider frequency ratios than could have been obtained using smaller amplitude stimuli and the DPs could be recorded with better signal-to-noise ratios. This level is higher than that typically employed for clinical assessment but did not lead to a significant risk of artefactual DP contamination and did not generate measureable DPs in a 1cc test cavity. A 60 dB stimulus level was also employed to see if the same pattern of results would be found. An intermediate stimulus level of 70 dB was also employed as it enabled DPOAE measurements to be obtained over a wide range of frequency ratios with a stimulus level close to those used widely by other workers.

At each frequency point, the data for the first pair of DPs was obtained simultaneously, i.e. the $2f_1$-f_2 and $2f_2$-f_1 DP data were obtained simultaneously for frequency points on the chart with the stimulus frequencies transposed.

c. Data Analysis

DP amplitude and phase data from every DP sweep were entered into 2 dimensional frequency planes in Excel spreadsheets. Linear interpolation was employed between unmeasured data points. However, no interpolation was allowed across data points which failed to meet the S/N criteria or at data points where adjacent measured data implied that a DPOAE would not have met the S/N criteria if attempted. This restriction was to prevent excessive 'filling in' of amplitude notches or smoothing of irregularities in the phase data.

The phase was unwrapped by adding or subtracting multiples of 360° in order to minimise adjacent phase steps. The absolute number of whole 360° cycles is unknown for each DP. With the $2f_1$-f_2 DP, a choice was necessary as to whether to optimise the smoothing of the phase at small or at large stimulus frequency ratios. This was because optimising the smoothing of the phase with small f_2/f_1 led to some large phase steps with large f_2/f_1, and vice versa. This curious feature of the phase data is described in more detail in results section c.

III Results

a. f_1, f_2 area representation

i) Subject RDK

1) L_1=L_2=75 dB SPL

Amplitude features

The amplitude data for the $2f_1$-f_2 and $2f_2$-f_1 DPs are shown in figure 24a. In general, the maximum amplitude tended to occur with the $2f_1$-f_2 DP using a frequency ratio of 1.3-1.35, consistent with the results of Harris et al, 1989. In addition for this ear, the DP amplitude was generally raised in 2 broad areas, one in the $2f_1$-f_2 DP below f_1=1.8 kHz and one in both DPs above approximately f_1=2.2 kHz.

Also in this ear two well defined valleys with a depth of 10-15 dB can be seen in the $2f_2$-f_1 DP data. The notches occur at constant DP frequencies and possibly continue into the $2f_1$-f_2 DP data. The $2f_2$-f_1 DP was measurable at very wide frequency ratios away from the centre line, extending up to f_2/f_1=1.9. This contrasts with the $2f_1$-f_2 DP, which was not measurable at frequency ratios greater than f_2/f_1=1.5. Notches are typically seen

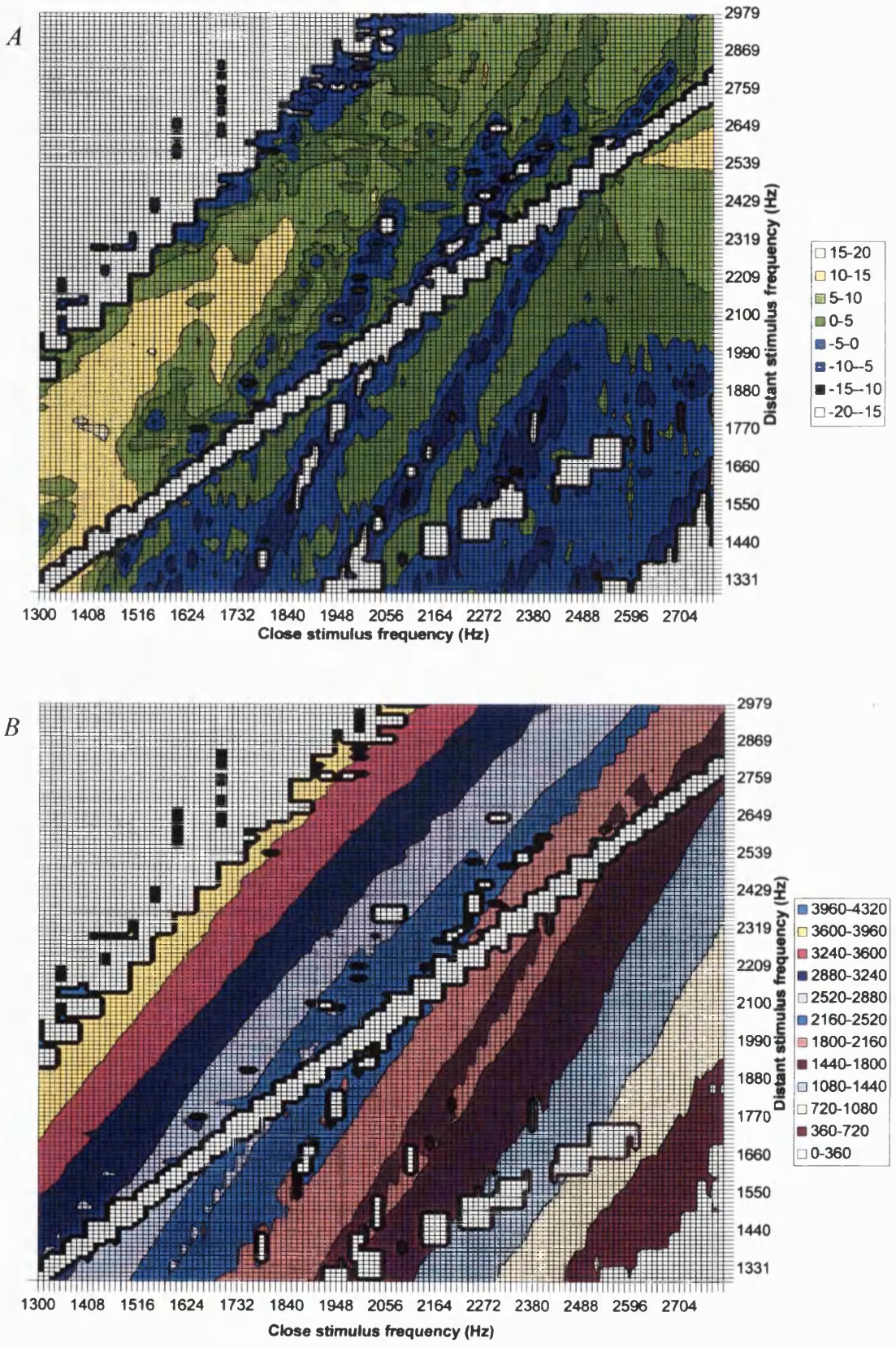

Figure 24. f_1, f_2 area format of (a) level, dB SPL and (b) phase, degrees of $2f_1$-f_2 and $2f_2$-f_1 DPOAE with L_1=L_2=75 dB SPL with subject RDK. In charts of this format, $2f_1$-f_2 DPOAE data are above the leading diagonal line and $2f_2$-f_1 DPOAE data are below the leading diagonal line. For figures of this format, the level scale is in 5 dB increments and the phase scale is in 360 degree increments.

in DP gram data and the 2D representation shows how these notches would shift position for DPgrams constructed with different primary ratios. The amplitude data of the $2f_1$-f_2 DP contain a smooth plateau along the maximum amplitude region of f_2/f_1=1.3-1.4, whereas at smaller frequency ratios a series of valleys occurred which followed lines of approximately constant DP frequency. There are missing data in both DPs at f_2/f_1=1.5, which was caused in the $2f_1$-f_2 DP by the fact that the difference tone was coincident and in the $2f_2$-f_1 DP by harmonic distortion at $2f_1$ (which may have been cochlear or from the transducers) appearing in the noise spectrum.

Phase

Overall the 2D representation shows lines of equal phase running from lower left to upper right bending to become less steep on the lower sideband side.

It is highly significant that the $2f_2$-f_1 DP phase contours (lower right region) all lie along constant DP frequencies (figure 24b) in contrast to the $2f_1$-f_2 DP region (upper left).

The $2f_2$-f_1 DP data also contained phase steps which occurred at constant DP frequencies and coincided with the amplitude notches seen in figure 24 (a).

With a small frequency ratio (close to the diagonal f_1=f_2 line), the $2f_1$-f_2 DP phase contours tend to be a continuation of the $2f_2$-f_1 DP phase contours with iso phase lines crossing directly between the two DP regions. At larger frequency ratios, the $2f_1$-f_2 DP phase contours turn to follow constant frequency ratios. The transition occurs at a frequency ratio of around f_2/f_1=1.1-1.15.

2. Reduced stimulus levels, L_1=L_2=60 dB SPL

The overall pattern of results obtained at L_1=L_2=75 dB SPL was not specific to that stimulus level although significant differences were found with stimulus level, mainly in the amplitude data.

Amplitude differences

The measurements were repeated with the stimulus reduced to L_1=L_2=60 dB SPL. The amplitude data obtained using a lower stimulus amplitude (figure 25a) is much more complex. The two pronounced valleys in the $2f_2$-f_1 DP data are no longer present, but have been replaced by another at approximately 3 kHz. The $2f_2$-f_1 DP amplitude is still strong at small frequency ratios, but at frequency ratios above f_2/f_1=1.2 there has been a larger reduction in amplitude, resulting in difficulty obtaining measurements. The $2f_1$-f_2

DP data also appear more complex, with valleys which are not always straight following approximately constant DP frequencies. The valleys in some cases appear to divide into two, for example when the close stimulus frequency (f_1) is 1700 and 1900 Hz. The amplitude features are not just noise as the data are well above the noise floor (except the very lowest amplitude points), are repeatable, and related patterns occur across adjacent data sweeps. No smooth plateau occurs in the $2f_1$-f_2 DP data and the maximum amplitude occurs at a smaller frequency ratio than was the case with the stimulus levels at 75 dB SPL (approximately f_2/f_1=1.2 instead of 1.3).

Phase

The phase data (figure 25b) essentially follows the same patterns as with the higher stimulus levels, where the data met the S/N criteria. In the case of the $2f_1$-f_2 DP, the transition at which the phase contours turn from following a constant DP frequency to following a constant frequency ratio occurs at a slightly larger frequency ratio of approximately f_2/f_1=1.15.

ii) L_1=L_2=70 dB SPL, subject RN

Amplitude

The amplitude data, shown in figure 26 (a), contain many of the features which were seen with subject RDK. Amplitude 'valleys' are seen in the $2f_2$-f_1 DP data, which follow constant DP frequencies and continue into the $2f_1$-f_2 DP. The $2f_1$-f_2 data become smoother at wider frequency ratios, rising to a peak at a ratio of approximately f_2/f_1= 1.2-1.25 before falling into the noise floor at approximately f_2/f_1= 1.4-1.45. The $2f_2$-f_1 DP, meanwhile, reduces in amplitude gradually towards wider frequency ratios, but remains above the noise floor up to frequency ratios of f_2/f_1= 1.7-1.8.

There are differences in the detail of the results from the two subjects. The results from RN are of higher amplitude and contain more valleys in the $2f_2$-f_1 DP data. The amplitude ridge and valley features do not occur at the same frequencies in the two subjects.

Phase

The phase data from RN (figure 26b) follow the same pattern as RDK, with $2f_2$-f_1 DP phase contours following constant DP frequencies and crossing to the $2f_1$-f_2 DP. The $2f_1$-f_2 DP phase contours also follow constant DP frequencies when f_2/f_1 is small, but switch to following constant frequency ratios when f_2/f_1 exceeds approximately 1.1-1.15.

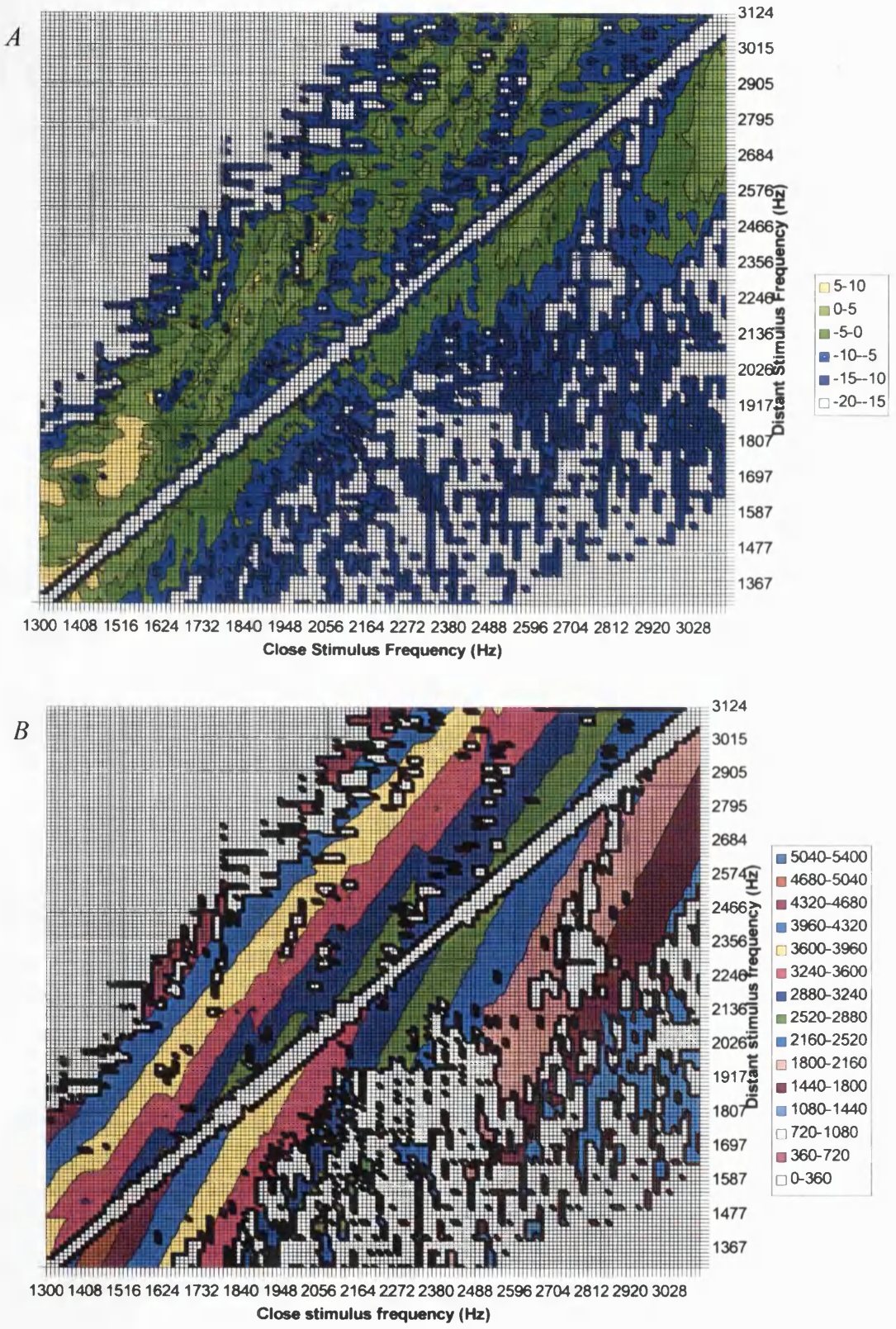

Figure 25. f_1, f_2 area format of (a) level, dB SPL and (b) phase, degrees of $2f_1$-f_2 and $2f_2$-f_1 DPOAE with L_1=L_2=60 dB SPL with subject RDK. Compared to figure 24, the amplitude profile of the $2f_1$-f_2 DPOAE is much more complex, with no smooth plateau seen with any ratio of f_2/f_1. Two pronounced amplitude valleys which were seen with $2f_2$-f_1 DPOAE in figure 24 are absent, but another has appeared at a higher frequency. The overall phase pattern is similar, except the 'transition' region in the $2f_1$-f_2 DP occurs at a slightly larger ratio of f_2/f_1.

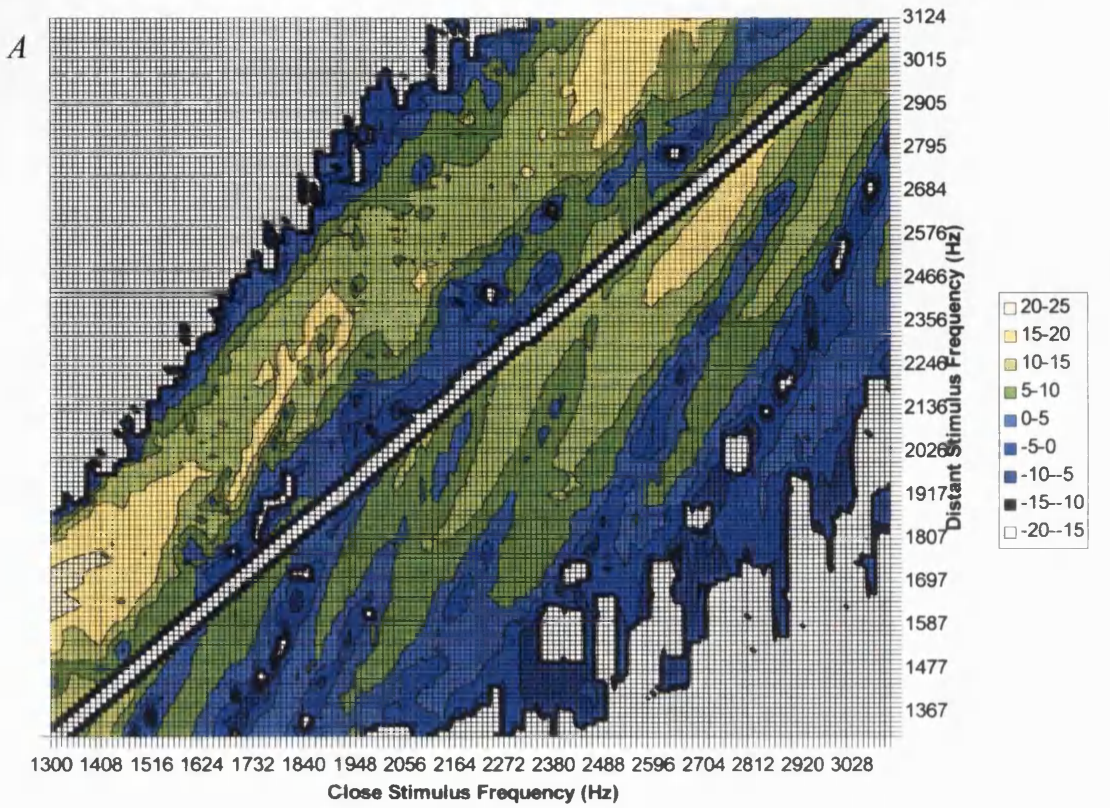

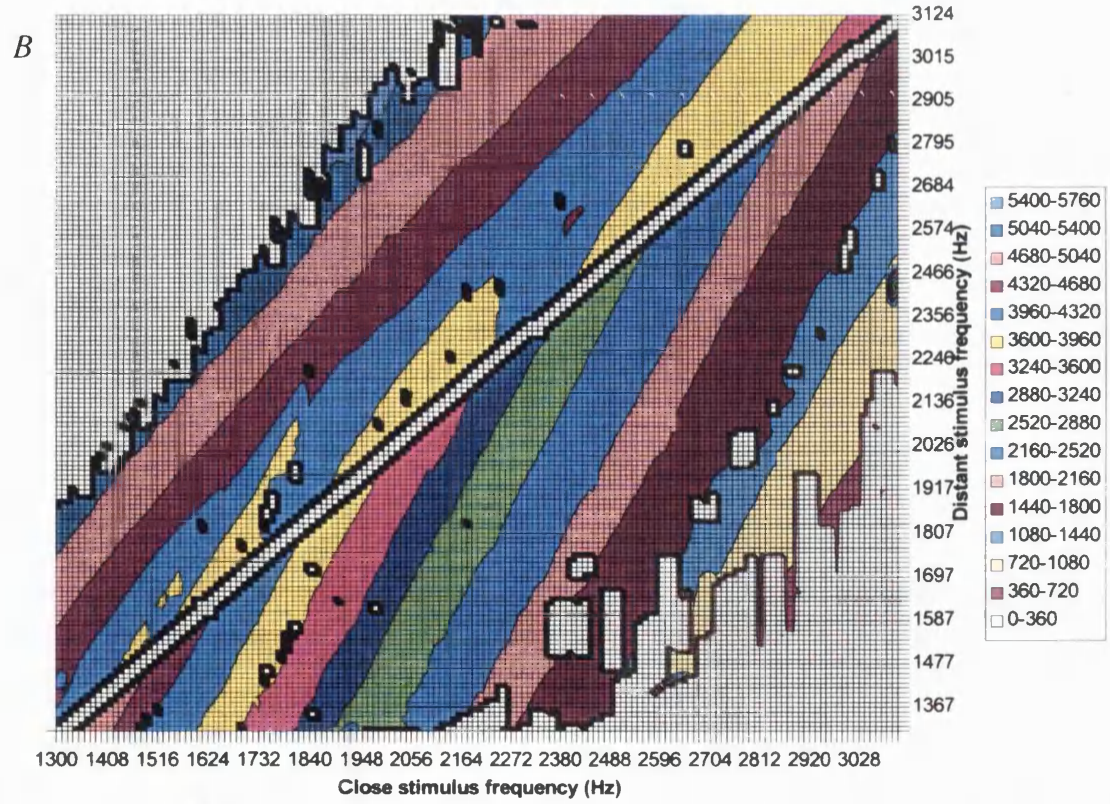

Figure 26. f_1, f_2 area format of (a) level, dB SPL and (b) phase, degrees of $2f_1$-f_2 and $2f_2$-f_1 DPOAE with L_1=L_2=70 dB SPL with subject RN. Compared to RDK, there is a greater amount of fine structure in the $2f_2$-f_1 DPOAE, with valleys and ridges occurring across the frequency range. The level of the DPs is a little higher generally, but otherwise the overall pattern of results is very similar.

b. f_2/f_1 versus DP frequency representation

i) $L_1=L_2=70$ dB SPL, RDK and RN

Figures 27 and 28 show data for each subject with $L_1=L_2=70$ dB SPL using the alternative presentation format, plotting stimulus frequency ratio f_2/f_1 against DP frequency.

Amplitude

With this format (figs. 27(a) and 28(a)) the amplitude valleys in the $2f_2-f_1$ DP are approximately vertical, indicating that they are defined by the DP frequency. The valleys cross to the $2f_1-f_2$ DP. The amplitude fine structure in the $2f_1-f_2$ DP at frequency ratios above 1.1 is not fixed to emission frequency, but instead drifts towards lower frequencies at larger frequency ratios. With subject RDK, the amplitude data becomes smoother when the DP frequency is above 3 kHz, whereas with RN the fine structure continues across the whole frequency range investigated.

Phase

The $2f_2-f_1$ phase contours (figures 27(b) and 28(b)) are almost vertical, with a slight drift towards lower DP frequency at small f_2/f_1 which is more marked above approximately 2 kHz. This is to be expected from figures 22, 23 and 24 and is consistent with a 'place fixed' emission mechanism. The slight deviation from vertical indicates a very small influence of the stimulating frequencies on the resulting phase of the DPOAE. This may result either from (i) greater inward delay in the cochlea to the DP place because of the smaller frequency ratio (and hence the DP place is closer to f_2), (ii) a small movement of the DP generating region, or (iii) it merely reflects greater inward phase change of the stimuli as they travel along the ear canal because of the higher frequency and therefore shorter wavelength of the primaries.

The phase contours clearly cross directly between the $2f_2-f_1$ and $2f_1-f_2$ DP's in both subjects suggesting a continuity of emission mechanism, but within the $2f_1-f_2$ DP the phase contours switch from vertical (phase determined by DP frequency) to horizontal (phase determined by f_2/f_1) at larger ratios. This is consistent with a change from the 'place fixed' to the 'wave fixed' emission mechanism.

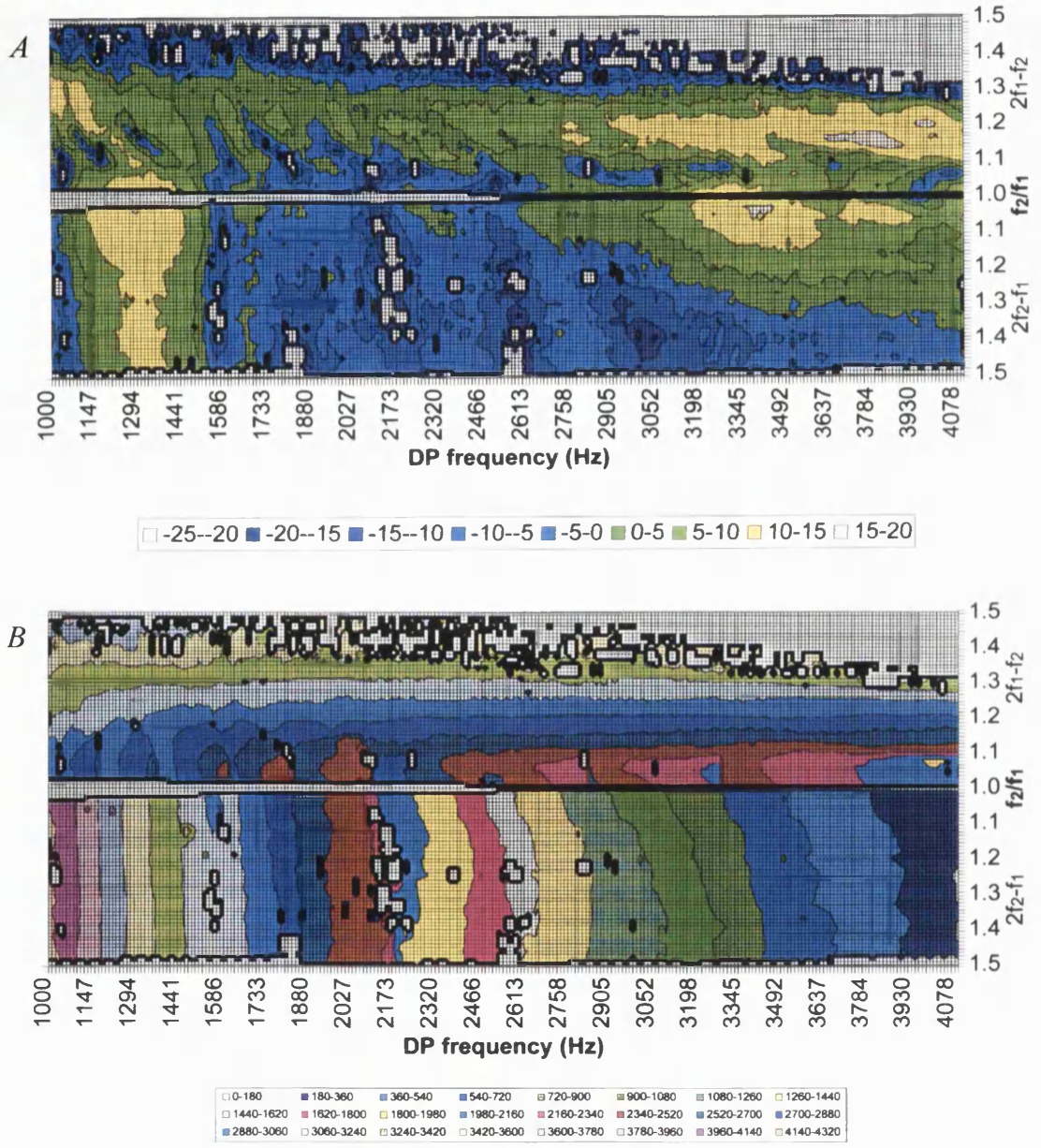

Figure 27. f_2/f_1 versus DP frequency representation of (a) level, dB SPL and (b) phase, degrees of $2f_1$-f_2 and $2f_2$-f_1 DPOAE with L_1=L_2=70 dB SPL with subject RDK. On this chart format, the $2f_1$-f_2 DPOAE is in the top half of the chart and the $2f_2$-f_1 DPOAE is in the lower half of the chart. For all figures of this format, the level scale is in 5 dB increments and the phase scale is in 180 degree increments. Using this format, the transition between wave-fixed and place-fixed behaviour can be clearly seen as the phase contours change from horizontal to vertical.

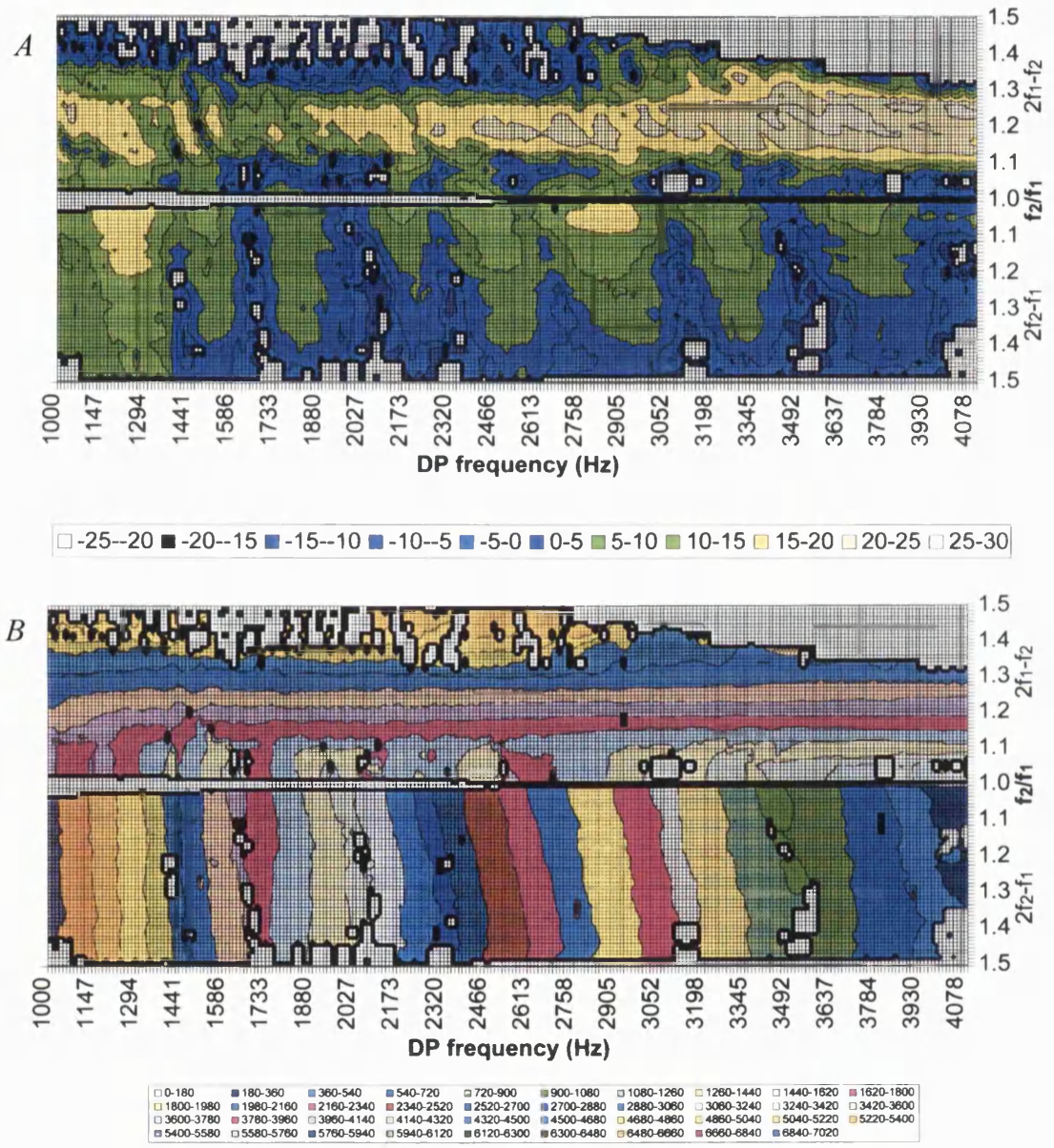

Figure 28. f_2/f_1 versus DP frequency representation of (a) level, dB SPL and (b) phase, degrees of $2f_1$-f_2 and $2f_2$-f_1 DPOAE with L_1=L_2=70 dB SPL with subject RN. The same general pattern is seen as for RDK, except the fine structure of the $2f_2$-f_1 DPOAE is more pronounced and extends along the full frequency range.

ii) The $3f_1$-$2f_2$ and $3f_2$-$2f_1$ DPs

The corresponding data for the $3f_1$-$2f_2$ and $3f_2$-$2f_1$ DPOAEs are shown in figure 29 (subject RDK). It can be seen that data follow similar patterns to the $2f_1$-f_2 and $2f_2$-f_1 DPs, except the change between being dominated by wave or place fixed modes happens at a smaller frequency ratio of around f_2/f_1=1.05. Both of the DPOAEs are mainly only measurable at small frequency ratios, however there is a region of strong emission in the $3f_2$-$2f_1$ DP at around 1300Hz which yields a measurable DP at all frequency ratios up to f_2/f_1=1.5.

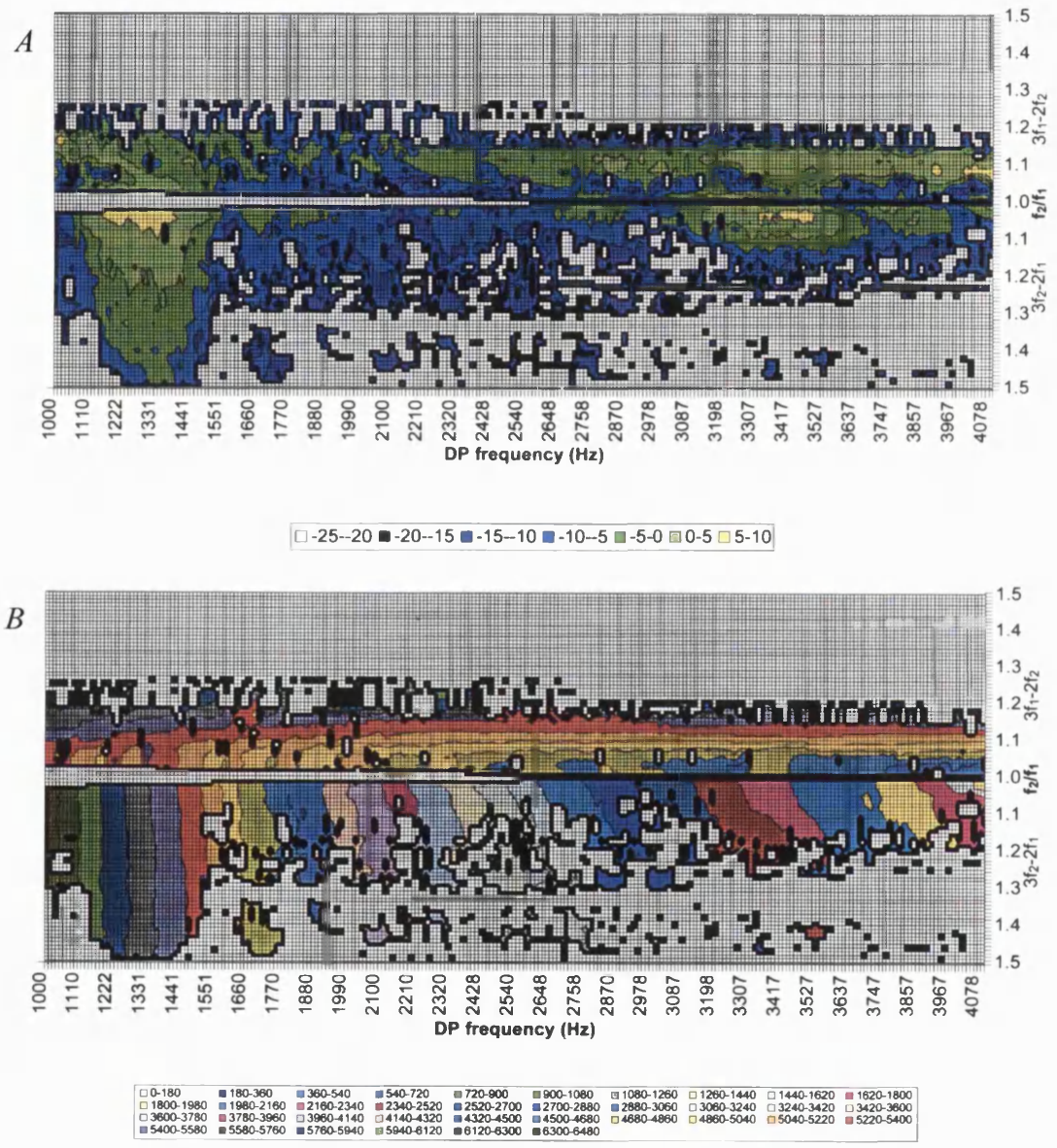

Figure 29. f_2/f_1 versus DP frequency representation of (a) level, dB SPL and (b) phase, degrees of $3f_1$-$2f_2$ and $3f_2$-$2f_1$ DPOAE with L_1=L_2=70 dB SPL with subject RDK. The data was acquired simultaneously with that of figure 27. The DPs are only measurable over a smaller range of frequency ratios, but the same transition between wave and place fixed behaviour is seen.

c. The $2f_1$-f_2 DP transition

In order to investigate the $2f_1$-f_2 DP transition between the 'wave' and 'place' fixed mechanisms, successive short constant frequency ratio sweeps were obtained with the frequency ratio incremented for each sweep. Each sweep covered the $2f_1$-f_2 DP frequency range 1490-1678 Hz. The stimulus level was L_1=L_2=70 dB SPL, and the frequency ratio was varied from f_2/f_1=1.08 up to 1.2 (figure 30).

When the frequency ratio was large, the DP sweeps had shallow phase gradients. As the frequency ratio reduced, the phase gradient became steeper with a compensatory upward step. When the frequency ratio reached 1.15, the upward step exceeded 180° and so the step was smaller if the phase was unwrapped with a downward step. Ultimately at the narrowest ratios ($f_2/f_1 \approx 1.1$) the step approached 360° and the phase resolved to a new steep gradient. The frequency at which the step occurred increased slightly with smaller stimulus frequency ratios. There was a corresponding amplitude notch which came and went during this transition.

This process by which 360° is 'lost' as the stimulating frequency ratio is increased explains the necessity in the area DP data for either downward 360° steps at low frequency ratios or upward 360° steps at high ratio when attempting to join the phase data up in a 2D frequency array.

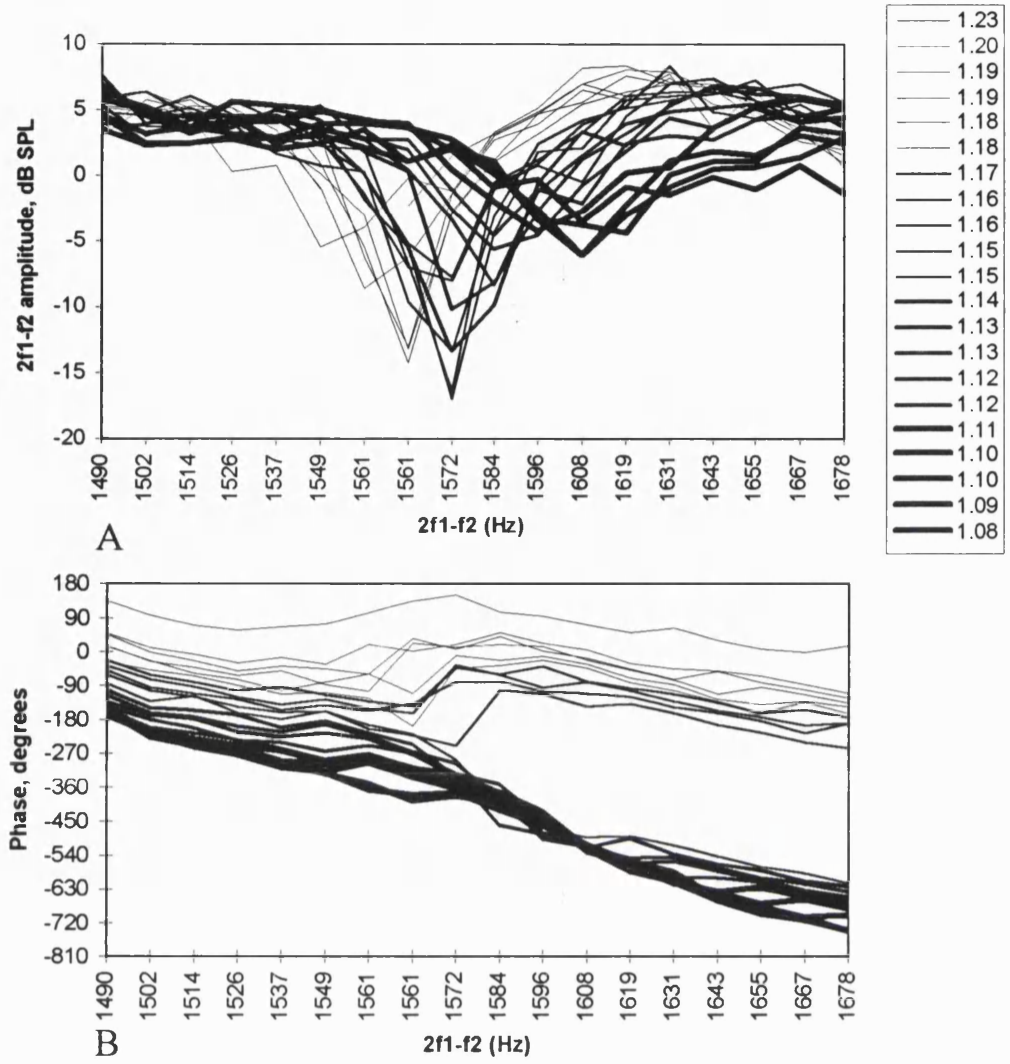

Figure 30. Detail of a $2f_1$-f_2 DPOAE phase discontinuity which occurred in the transition between wave and place fixed behaviour (subject RDK). Sweeps are constant f_2/f_1 and successive sweeps are at incremented f_2/f_1. Phase (B) is seen to switch between a steep or a shallow gradient by gaining or losing a 360° step. A corresponding level notch (A) comes and goes during this transition, moving slightly towards lower frequencies at larger f_2/f_1.

IV Discussion

a. Comparison of latency with literature

The DPOAE phase gradients contained in this study can be compared with those available in the literature by using the f_1 and f_2 sweep phase data obtained with $L_1=L_2=60$ dB SPL (figure 25) to calculate 'partial' latencies from the phase gradients as follows:

Latency = $-\delta(\phi/2\pi)/\delta(f)$

where ϕ is the DP phase in radians and f is the DP frequency in Hz.

The frequency ranges of the examples were selected to avoid discontinuous data or data containing large irregularities.

In the case of the $2f_2-f_1$ DP, the latencies calculated via the f_2 sweep method were only marginally greater than the f_1 sweep latencies (ratio of f_1 sweep/ f_2 sweep latency = 0.92-1.00). In this respect the results are consistent with those of Moulin and Kemp (1996), who used stimulus parameters of $L_1=65$, $L_2=60$ dB SPL, $f_2/f_1=1.2$-1.22, and reported no significant difference between f_1 and f_2 sweep latencies for the $2f_2-f_1$ DPOAE. Each individual latency found here is also consistent with those found by Moulin and Kemp (which in the frequency range 1-3 kHz ranged from 9.5 ms to 6 ms ($2f_1-f_2$, f_2 sweep), 7.7 ms to 4 ms ($2f_1-f_2$, f_1 sweep), 9 ms to 4.5 ms ($2f_2-f_1$, f_2 sweep) and 7 ms to 4.5 ms ($2f_2-f_1$, f_1 sweep)). For the $2f_1-f_2$ data in this study, the f_2 sweep derived latencies exceed the f_1 sweep latencies when measured using large frequency ratios (ratio of f_1 sweep/ f_2 sweep latency = 0.75-0.86). This was consistent with studies by Kimberley et al (1993) and O Mahoney and Kemp (1995), who found that f_1 sweep phase gradients were 20% lower than those of f_2 sweeps. However when f_2/f_1 was small, the latencies calculated from the present data for the f_2 sweep method were only marginally greater than the f_1 sweep latencies (ratio of f_1 sweep/ f_2 sweep latency = 0.89-1.02), as was the case with the $2f_2-f_1$ DP.

b. Emission modes

In the introduction to the DP frequency vs. f_2/f_1 ratio representation of DP data (section D I (c)) it was predicted that 'wave fixed' emission mechanisms would result in horizontal phase contours on this chart format. It can be seen from the results in figs 27 and 28 that the $2f_1-f_2$ DP does follow this trend when $f_2/f_1>1.1$-1.15. 'Place fixed' DPs

were predicted to result in vertical phase contours, following lines of constant DP frequency. The $2f_2$-f_1 DP and the $2f_1$-f_2 DP with f_2/f_1<1.1-1.15 tend to be of this form. The division is not simply between the upper and lower sideband distortion products (where f_2/f_1=1 on the charts), but instead the transition occurs within the $2f_1$-f_2 DP data at a frequency ratio of approximately 1.1, with a transition region in which both mechanisms coexist and give rise to interference effects.

To summarise, at large frequency ratios the $2f_1$-f_2 DP phase behaviour implies a wave fixed emission mode, whereas the $2f_1$-f_2 DP with a small frequency ratio and the $2f_2$-f_1 DP are consistent with a place fixed emission mode.

c. The origins of DPOAE fine structure

The issue of whether the fine structure associated with the $2f_1$-f_2 DP is caused by interference between two distinct regions of DP emission or a local effect of interactions within one source region remains controversial. Clearly, two sources of differing latency would give rise to fine structure by interference, but repeated reflections between the base and a single DP place fixed reflector could also produce a fine structure (as in SFOAE). Mechanisms have been proposed by which interference could also arise from within a single distributed source region (Zweig and Shera, 1995). Evidence that part of the $2f_1$-f_2 DPOAE may be from the DP place under some conditions has been provided by suppression tuning curves (Kummer et al, 1995) and suppression of the fine structure (Heitmann et al, 1998). The data presented here strongly support this model, that two distinct generating regions are present and can be expected to generate interference. However the upper sideband DPOAE shows no evidence of a low latency component and is believed to originate solely in the region of the DP frequency place (section A II (f)), so the fine structure seen in the upper sideband is likely to be a result of multiple reflections between the base and the DP frequency region or a result of interference between discrete reflectors in a single DP generating region.

d. Wave and place fixed emissions.

The results presented in the present study provide further evidence that the high latency 'place fixed' part of the $2f_1$-f_2 DP arises from the region of the DP frequency place. At small ratios, the continuation of the phase contours between the $2f_1$-f_2 and $2f_2$-f_1 DPs across the f_1=f_2 or f_2/f_1=1 line suggests a continuation of the same emission mechanism between the upper and lower sidebands. As the $2f_2$-f_1 DP must be primarily

emitted from the region of or basal to the DP frequency place, this result strongly suggests that the 'place fixed' $2f_1$-f_2 DP is also emitted largely from the region of its DP frequency place via a reflection mechanism. In the case of the $2f_1$-f_2 DP, this is a re-emission of a DP which must have been generated in the frequency region of the primary tones on the basilar membrane.

As TEOAE and SFOAE phase behaviour is also consistent with the place fixed model (Kemp and Chum, 1980a; Wilson, 1980; Kemp and Chum, 1980b), the clinical $2f_1$-f_2 DPOAE, for which the frequency ratio is normally approximately 1.2, is part of a subset of 'wave fixed' OAEs which only includes lower sideband DPOAEs stimulated with a wide frequency ratio. All other stimulated OAEs appear to be 'place fixed'.

e. Characteristics of DPOAE fine structure

The $2f_1$-f_2 DP showed a quite smooth amplitude function with wide frequency ratios when stimulated by L_1=L_2=75 dB SPL (figure 24), but when the stimulus tones were reduced to 60 dB SPL the amplitude function remained complex at all frequency ratios, up until the DP sank into the noise floor at approximately f_2/f_1=1.4 (figure 25). The uneven amplitude of the $2f_1$-f_2 DPOAE at wide ratios with lower stimulus levels could be a result of the 'wave fixed' emission failing to completely dominate the 'place fixed' emission, or an increase in interference between out-of-phase elements within a single DP-generating region, or multiple reflections between the base of the cochlea and the DP place becoming more significant.

The most striking feature of the $2f_2$-f_1 DP (upper sideband) amplitude data from RDK in figure 24 is the two valleys which approximately follow constant DP frequencies (2150 Hz and 2550 Hz). Similar features were also seen with RN across the whole frequency range under investigation. The possible causes would seem to be an interference effect or localised cochlear anatomical features, however the notches disappear at lower stimulus levels (RDK) (which is not a normal feature of SFOAE) and so localised anatomical irregularities are unlikely. With the $2f_2$-f_1 DP there is one obvious region on the basilar membrane from which this DP is emitted (unlike lower sideband DPs), i.e. the DP frequency place, so the remaining possible sources of interference are from different parts of a large region of generation or reflection, or from cancellation between multiple reflections between the DP place and the stapes. The latter is less likely as the reflections would be unlikely to become relatively more significant with higher stimulus levels. Another possibility is suggested by Martin et al (1999a, b), who have suggested that a source of the $2f_2$-f_1 DP exists basal to the DP

frequency place due to the interference of the harmonic $2f_2$ with f_1 to produce another source of the $2f_2$-f_1 DP, reintroducing the possibility of interference between two DP generating sites. The situation is potentially therefore quite complex.

f. Location of the $2f_2$-f_1 DP generator in this data

It is interesting that the $2f_2$-f_1 DP phase contours in the data presented here do not deviate much from following lines of equal DP frequency even with a very low frequency ratio, despite the expectation that under these conditions the DPOAE would gain delay from the increased travelling time of the stimuli to the DP place.

As the frequency ratio is reduced, the DP frequency place becomes closer to both the f_1 and f_2 frequency places. The DP phase is oppositely related to f_1 and f_2 (phase at generation site $=2\phi_2-\phi_1$) so the fact that DP phase remains closely related to DP frequency when f_2/f_1 is small implies that the influence of the increasing proximity to both the f_1 and f_2 travelling wave peaks is small because it is largely self-cancelling.

It may be that the $2f_2$-f_1 DP generation region is significantly basal to the DP frequency place (Martin et al, 1998, 1999b), therefore remaining far enough from the region of the stimulus frequencies so as to allow DPOAE phase to be closely related to the DP frequency even when the DP frequency is close to f_2.

g. Are these results typical?

The results presented in this study contain some features that have been previously shown, and others that are new. Both subjects had a change in phase behaviour in the $2f_1$-f_2 DP in constant f_2/f_1 frequency sweeps, with steep phase gradients recorded with f_2/f_1 below approximately 1.1 and shallow phase gradients at wider frequency ratios. This has been shown previously (Kemp, 1986 and present study, chapter C) and is undoubtedly a general feature of normal ears. The exact ratio at which the changeover occurs is known to be variable across subjects and also to be slightly frequency and stimulus level dependent. Both subjects also produced maximum levels of $2f_1$-f_2 DPOAE with frequency ratios of approximately 1.2-1.25 (figs. 21(a), 22(a)) and this is also known to be typical (Harris et al, 1989). The exact ratio at which the maximum level occurs is also known to vary between subjects and to be frequency and stimulus level dependent.

Where data are dominated by 'place fixed' behaviour, the phase is almost independent of the frequency ratio for a given DP frequency. As this occurs in both subjects it is likely to be typical of normal ears. The continuity of the amplitude and phase contours

between the lower and upper sideband DPOAEs also occurs in both subjects at all frequencies studied and appears to indicate a continuity of emission mechanism which would be true of all normal ears.

The presence of amplitude ridges and valleys in the $2f_2$-f_1 DP data appears to be less certain to be general, as in subject RDK they didn't occur across the whole frequency range or at all stimulus levels. This is therefore likely to be a common but not necessarily universal feature.

Data from both subjects with the $2f_1$-f_2 DP 'wave fixed' emission show evidence of amplitude valleys which drift towards lower emission frequencies at wider frequency ratios. However the exact location of specific amplitude features are not correlated between the two subjects.

The emission frequency range covered extended from 1 kHz to 4.1 kHz, it remains possible that different patterns of results may be seen outside this range.

h. Effect of ear canal standing waves

Standing wave positions are dependent on frequency and ear canal dimensions and so the frequency response detected by the probe becomes characteristically uneven when standing waves occur. In the ears studied in this project, this phenomenon was seen above about 4-5 kHz, therefore the accuracy of the stimulus level presented to the eardrum will have been reduced with stimulus frequencies above this. It should be remembered that for a lower sideband DP of a given frequency the stimulus frequencies are higher than the emission frequency. In this study stimulus frequencies up to 8 kHz were employed although only emission frequencies up to 4.1 kHz were included. Therefore, standing waves are likely to have been present in the higher frequency measurements of the lower sideband. The potential errors arising from standing waves were reduced by not applying a correction for the frequency response when the frequency spectrum varied sharply with frequency (this is a characteristic of standing waves and so when present it suggests that the proposed correction would have been misleading).

The significance of the uncertainties in the stimulus levels is minor for the central findings of the present study. The results demonstrate that the main patterns observed in DPOAE are not greatly changed by the stimulus level: DPOAE recorded with the stimulus as low as 60 dB SPL and up to 75 dB SPL show the same overall patterns with only differences in the details of the fine structure and the signal to noise ratio of recordings.

V Summary

For lower sideband DPOAEs, whether the 'wave' or 'place fixed' mechanism dominates depends on the stimulus frequency ratio, the DP order and the stimulus amplitude. Therefore the 'wave fixed' emission mode cannot be explained as the simple direct leakage of DP energy from the generation site. It may depend on a source region which has ratio dependent directivity.

Upper sideband DPOAEs are always dominated by the 'place fixed' emission mode.

The phase of corresponding 'place fixed' upper and lower sideband DPs appeared to be continuous between the DP components at small frequency ratios, suggesting continuity of mechanism.

Whilst the presence of two separate emission regions for the $2f_1$-f_2 DP is presumably the cause of much of the amplitude fine structure seen in this DP, the presence of amplitude notches in the $2f_2$-f_1 DP indicates that fine structure may also arise from either multiple reflections within the cochlea or from interference within a distributed DP generating or reflecting region.

The emission model suggested by these results can be summarised as follows.

1. For the 'wave fixed' emission, distortion in the basilar membrane motion is the generator and the DP is emitted directly, albeit in a frequency ratio dependent manner.
2. For the 'place fixed' emission, distortion occurring within the f_2 envelope is still the generator of the DP, but DP energy appears to be projected apically and is emitted only when a separate process such as a reflection in the region of the DP frequency place causes it to reverse.

E. Use of a third tone to investigate DPOAE generation

I Introduction

In the previous chapter, two distinct DPOAE emission mechanisms were shown, with a transition occurring in the lower sideband at a ratio of about f_2/f_1=1.1. It is believed that this change also relates to a change in the location of the emission source, with the wave fixed emission type being emitted directly from the f_2 region and the place fixed emission being emitted via a reflection in the region of the DP frequency place.

Clarification of the location of the sources of DPOAE on the basilar membrane is of interest because it determines the frequency specificity of OAE and because this would yield information regarding the emission mechanisms. Suppression is one method to explore the place responsible for an emission.

Published DPOAE suppression tuning curves suggest that the $2f_1$-f_2 DPOAE source is around the stimulus peaks or more specifically around f_2 on the basilar membrane. It is arguable whether there also may be a contribution from DP region (Brown and Kemp, 1984; Kummer et al, 1995). Conversely, tuning curves for the $2f_2$-f_1 DPOAE suggest that the emission source is exclusively in the region of the DP frequency place (Martin et al, 1987; Kemp, 1998; Martin et al, 1998).

Phase sweep data shows that there are two distinct emission mechanisms: a 'wave fixed' emission which dominates lower sideband DPOAE when f_2/f_1 is large, and a 'place fixed' emission which dominates the lower sideband when f_2/f_1 is small and always dominates the upper sideband. As discussed in section (A II i) these emissions may be from different sites, the 'wave fixed' emission being from the f_2 region and the 'place fixed' emission being from the region of the DP frequency place. However the place fixed emission source has only been shown in the literature to be at the DP place in the case of upper sideband DPOAE.

As discussed in section (A II e), the effect of suppression by a third tone on a distortion product derived from the other two stimulus tones can be used to imply where along the basilar membrane the DPOAE might be generated, on the grounds that the maximum suppression by f_3 occurs at the f_3 travelling wave peak. This method is intended to provide information regarding the site of the DPOAE emission but doesn't directly indicate the mechanism of emission. In other words, the method doesn't indicate whether the emission is wave or place fixed.

Previous workers exploring DPOAE suppression tuning have tended to avoid a close stimulus spacing because it is then harder to resolve which significant frequency the tuning curve is centred on. A wide frequency spacing spreads out the stimulus peaks and the DP frequency place, aiding resolution of the suppression tuning curve. However the wave fixed mechanism is known to dominate the $2f_1$-f_2 DPOAE at wide ratios so the published data are not representative of all stimulus conditions and may not be relevant to place fixed DPOAE.

Therefore, performing DPOAE suppression tuning curves with frequency ratios below f_2/f_1=1.2 may be of interest as the emission mechanisms may be different with smaller frequency ratios. However there are various factors which may complicate the results.

If there is more than one DP emitting region or a distributed source region, interference effects are likely as in general the various contributions will not summate in phase. Suppression of only a part of the total source will change the balance of the DP source contributions with unpredictable effects depending on the phase relationship between the suppressed part of the DP and the total summed DP. For example, suppressing an out of phase part of the source region can result in enhancement of the DPOAE amplitude.

Specifically, if there are sources of DP in the region of f_2 and the DP frequency place, the ear canal DP depends on the phase relationship between the two sources, particularly if the two contributions are of similar magnitude. Suppression of just one source will result in either suppression or enhancement of the ear canal DP depending on whether the two sources were summating in phase or out of phase.

If the DP frequency place contributes significantly to the DPOAE, it must be a reemission of DP generated in the region of f_2 because f_1 and f_2 don't reach the DP frequency place. Therefore the emission site is different to the generation site. In this case, a suppressor tone would suppress the emission whether it was added at a frequency corresponding to the generator site or the emission site.

The effects of suppression are in themselves quite complex – the third tone suppresses the DP, but also can suppress the primaries and the primaries can suppress the third tone. Therefore the travelling waves of each of the three stimulus tones can be altered by the presence of the other two tones. This can alter the shape of the DPOAE suppression tuning curve.

Suppression by third tone is a 'blunt instrument' in that the envelope of the third tone covers (and may have a significant effect over) an extended part of the basilar membrane, and not just at the peak of the travelling wave. Therefore there may be an

effect on both the DP frequency place and the primary tone region of the basilar membrane at the same time. The shape of the third tone travelling wave envelope will also change shape depending on its level – the frequency resolution that can be applied to the results deteriorates at higher levels of stimulus.

As indicated at the end of section (A II i), addition of a third tone also introduces other possible additional sources of DP generation. These are discussed by Martin et al. (1999b), Martin et al. (2000) and Fahey et al. (2000).

Nevertheless, in this study the effects of suppression by a third tone on DPOAE production will be investigated using intermediate and small frequency ratios, at which there should be a significant 'place fixed' emission. Such measurements may provide evidence for the location(s) of DPOAE source(s) under these stimulus conditions and specifically determine whether indications of a contribution from the DP place can be identified.

II Measurements

Otoacoustic emission measurements were made using an Otodynamics Ltd. ILO 96 system with an Otodynamics BP 3-tone adult probe using the left ear of subject RDK. Most of the measurements were obtained with quite low levels for L_1 and L_2 (down to 55 dB SPL). This allowed the suppression effects to be seen with similarly modest levels of L_3. This is advantageous because the travelling wave envelope is sharper at lower stimulus levels and so its suppression effect would be limited to a smaller area on the basilar membrane.

a. Suppression tuning curves

DPOAE suppression tuning curves were measured using equi-level (L_1=L_2) stimuli. With f_1, f_2, L_1 and L_2 fixed, a DPOAE reference measurement was recorded without the third tone, then at a range of frequencies for f_3, the third tone level required to reduce this by 3 and 6 dB were noted. A new reference DPOAE level was recorded before each new frequency for f_3 was investigated, use of a single reference measurement for the whole measurement sequence was not considered adequately accurate because of small changes in DP level over time and possible small changes in the probe placement during the measurement sequence.

This measurement was initially performed with f_1=1746 Hz and f_2=2002 Hz (f_2/f_1=1.14). Tuning curves were produced with 4 stimulus levels; L_1=L_2=55, 60, 65 and 70 dB SPL.

Two further frequency configurations were investigated using smaller frequency ratios: with f_1=1807 Hz and f_2=2002 Hz (f_2/f_1=1.11) and with f_1=1709 and f_2=1794 Hz (f_2/f_1=1.05).

Two alternative test protocols were used: increasing the level of a third tone of fixed frequency, and sweeping the frequency of a third tone of fixed level. These are described below in parts (b) and (c).

b. Increasing the level of the third tone

In order to see the onset of suppression and observe any phase change as the DP is progressively suppressed, the increase in suppression as the level of the third tone was incremented was investigated.

The bi-tonal DPOAE stimulus was fixed with L_1=L_2=55 dB SPL, f_1=1672 Hz, f_2=1758 Hz. A third tone was introduced and L_3 was increased in 1 dB steps from 40 dB SPL to 70 dB SPL, with an additional measurement at 75 dB SPL. $2f_1$-f_2 and $2f_2$-f_1 DPOAE level and phase were recorded. Four f_3 values were used, selected to be at appropriately above, below and inbetween f_1, f_2 and f_{DP}.

c. Third tone of constant level swept in frequency

As an alternative to the tuning curve test paradigm, the frequencies of f_1 and f_2 fixed as before and f_3 was swept past. The effects on the level and phase on the $2f_1$-f_2 DP were noted. These measurements were obtained using L_1=L_2=55. The third tone was swept at 50, 55 and 60 dB SPL. Each line therefore represents a constant level of L_3 instead of a constant amount of suppression.

III Results

a. Tuning curves

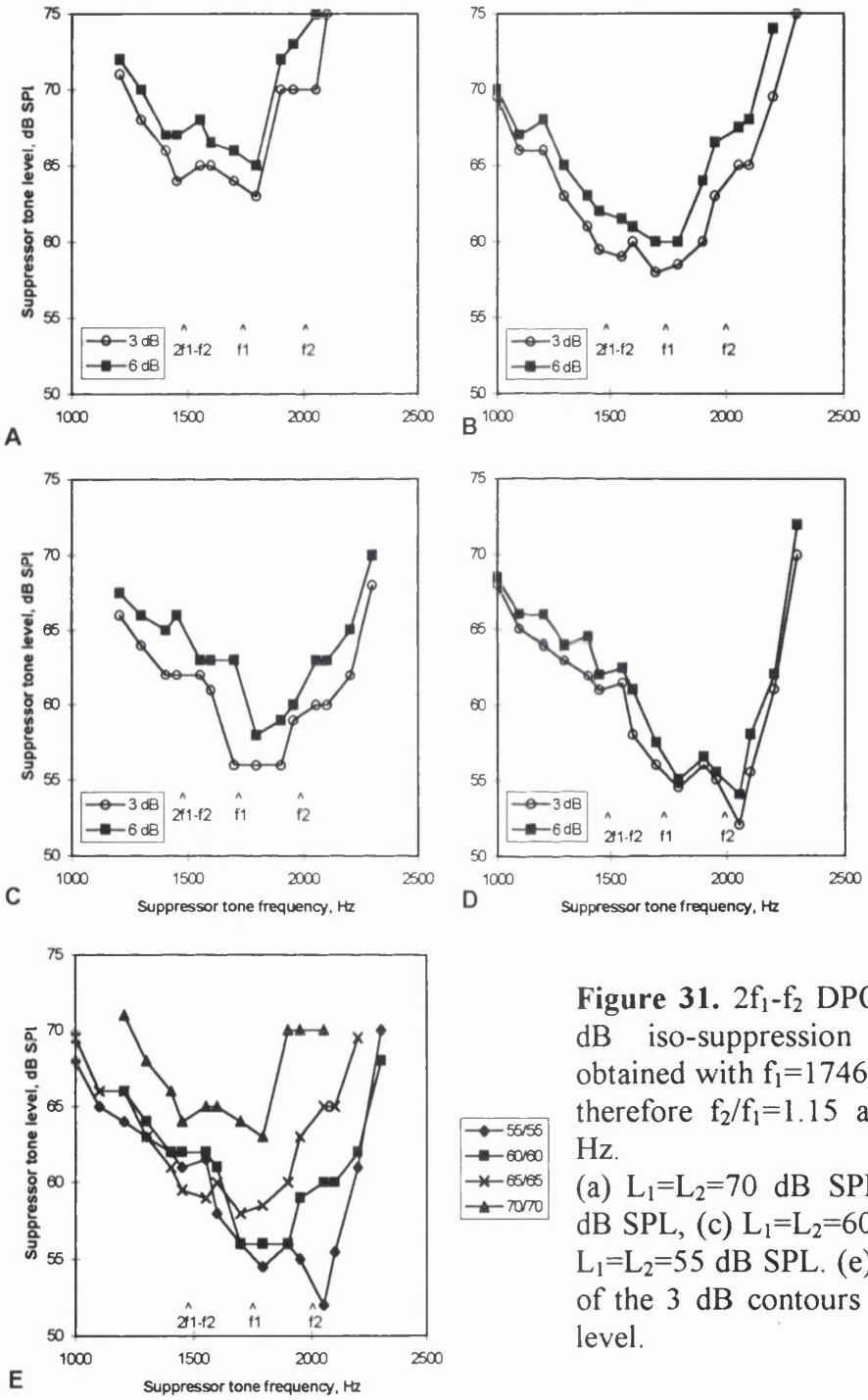

Figure 31. $2f_1$-f_2 DPOAE 3 dB and 6 dB iso-suppression tuning curves obtained with f_1=1746 Hz, f_2=2002 Hz, therefore f_2/f_1=1.15 and $2f_1$-f_2 =1490 Hz.
(a) L_1=L_2=70 dB SPL, (b) L_1=L_2=65 dB SPL, (c) L_1=L_2=60 dB SPL and (d) L_1=L_2=55 dB SPL. (e) is a compilation of the 3 dB contours at each stimulus level.

When f_2/f_1=1.15 (figure 31), the tuning curve dipped to a minimum at around f_2 when L_1=L_2=55 dB SPL. At higher levels of stimulus, the dip became broader and moved towards lower frequencies. This could arise from either a change in the location of the DPOAE source region or from the travelling wave envelope of the third tone itself

becoming broader and extending basally as the level increases, so the shift seen could reflect a change in the shape of the suppressor tone envelope.

The efficiency of the third tone in suppressing the DP when close to f_2 was reduced at higher stimulus levels (approx. 20 dB more level was required for f_3 when L_1 and L_2 are increased by 15 dB), but this was less marked at lower f_3 frequencies – an increase of only 5-6 dB in f_3 level was needed for a 15 dB change in stimulus level to achieve the same amount of suppression.

Some of the tuning curves possibly have slight steps or 'wiggles' at around the DP frequency, but these are not significant as such features also occurred at other frequencies.

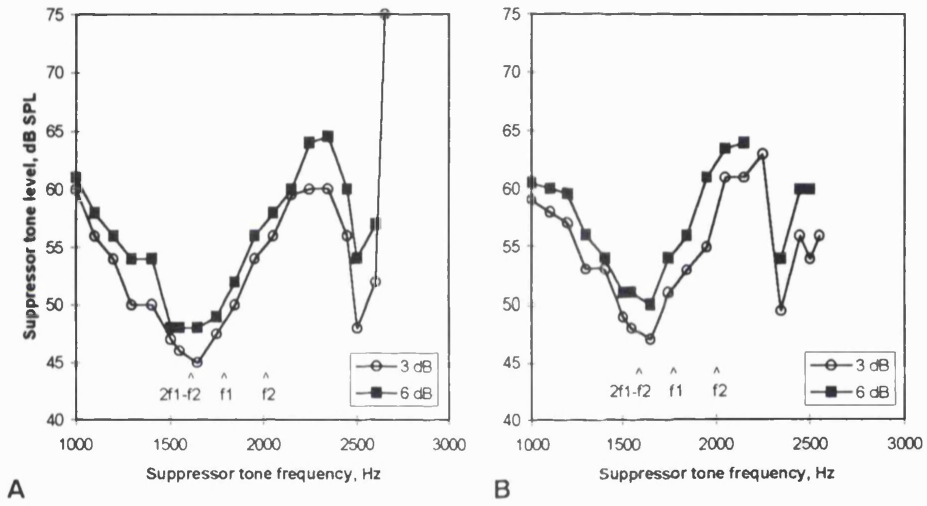

Figure 32. $2f_1$-f_2 DPOAE 3 dB and 6 dB suppression tuning curves obtained with f_1=1807 Hz, f_2=2002 Hz, therefore f_2/f_1=1.11 and $2f_1$-f_2 =1612 Hz.
(a) L_1=L_2=55 dB SPL, (b) L_1=L_2=60 dB SPL.

The tuning curve obtained with f_2/f_1=1.11 (figure 32) has a broad dip around the DP frequency but no noticeable feature in the region of the stimulus tones. There is also a very sharp second dip in the tuning curve at a higher frequency, at around 2.5 kHz when L_1=L_2=55 dB SPL. This frequency doesn't correspond to a whole-number multiple of either f_1, f_2 or f_{DP}, being approximately $1.38f_1$, $1.25f_2$ or $1.55\ f_{DP}$. The dip moves 150 Hz to 2.35 kHz when the stimulus level is increased to 60 dB SPL. This extra dip may be a result of the third tone altering the basal part of the main region of DP generation, or the third tone may be altering the phase gradients within the DP generating region and therefore disrupting the summation of a distributed DP source region. Alternatively, the dip could result from the $2f_2$-f_3 DP, generated within the cochlea, suppressing the $2f_1$-f_2 DP. The level of the $2f_2$-f_3 DP would have to be large to have such a large effect.

The tuning curve obtained with f_2/f_1=1.05 (fig 33) has a broad dip which may be centred on the DP frequency place. But this location is defined by only one data point and the general broadness of the dip and the closeness of the frequencies f_1, f_2 and f_{DP} makes it impossible to be certain that the dip is centred at the DP frequency rather than f_2.

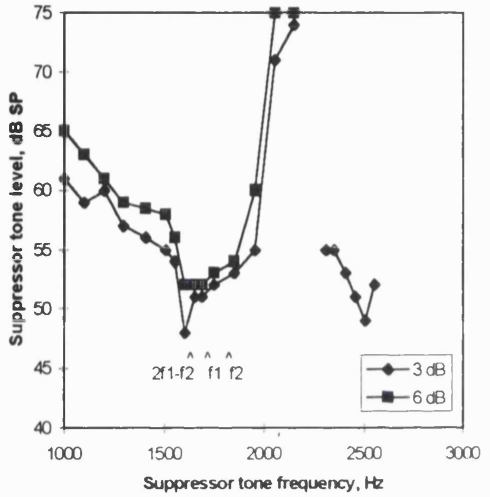

Figure 33. $2f_1$-f_2 DPOAE 3 dB and 6 dB suppression tuning curves obtained with f_1=1709 Hz, f_2=1794 Hz, therefore f_2/f_1=1.05 and $2f_1$-f_2 =1624 Hz. L_1=L_2=55 dB SPL.

b. Increasing the level of the third tone

The effect of incrementally increasing L_3 in an otherwise stationary stimulus condition is shown in figure 34.

In the case of the $2f_1$-f_2 DP, the greatest suppression occurred when f_3 was between f_2 and f_{DP}. There was no suppression (only enhancement) when f_3 was 350 Hz above f_2. Typically suppression began when L_3 was a few dB below L_1 and L_2, but the amount of suppression increased rapidly when L_3 was close to or slightly in excess of L_1 and L_2. In phase, a 180° shift was seen when a large amount of suppression occurred, but only when $f_3<f_2$.

With the $2f_2$-f_1 DP there was no enhancement of the DPOAE by the third tone. Suppression occurred at the lowest values of L_3 with the highest f_3. The $2f_2$-f_1 DPOAE was more sensitive to suppression by a third tone 268 Hz above the DP frequency than 37 Hz below. Several dB of suppression were seen at the highest frequency of f_3 even when L_3 was 10 dB below L_1 and L_2. These results could be a part of a tuning curve which dips to a minimum at a frequency above the emission frequency, but

unfortunately the range of frequencies adopted for f_3 doesn't extend high enough to show the other side of the curve.

In general small phase changes were recorded with the $2f_2$-f_1 DPOAE, but the biggest change was when L_3 was close to f_{DP}.

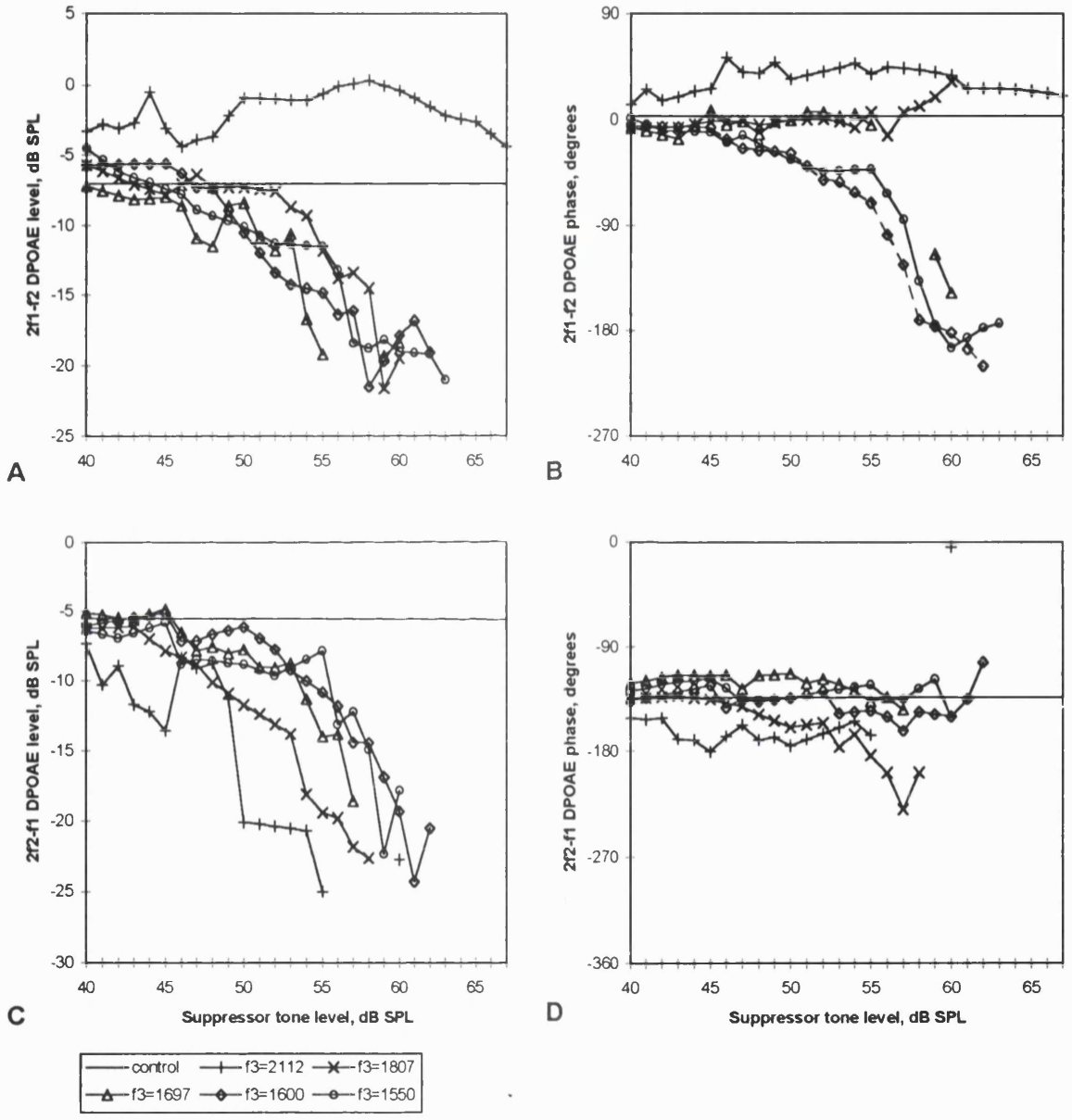

Figure 34. The effect on DPOAE of increasing the level of L_3 with an otherwise constant stimulus. f_1=1672 Hz, f_2=1758 Hz, L_1=L_2=55 dB SPL. (a) $2f_1$-f_2 DPOAE, level, (b) $2f_1$-f_2 DPOAE phase, (c) $2f_2$-f_1 DPOAE, level, (d) $2f_2$-f_1 DPOAE phase.

c. Third tone of constant level swept in frequency

The features seen in the level data are very complicated. Broad or irregular dips are seen, occurring at frequencies which were not always of any obvious significance.

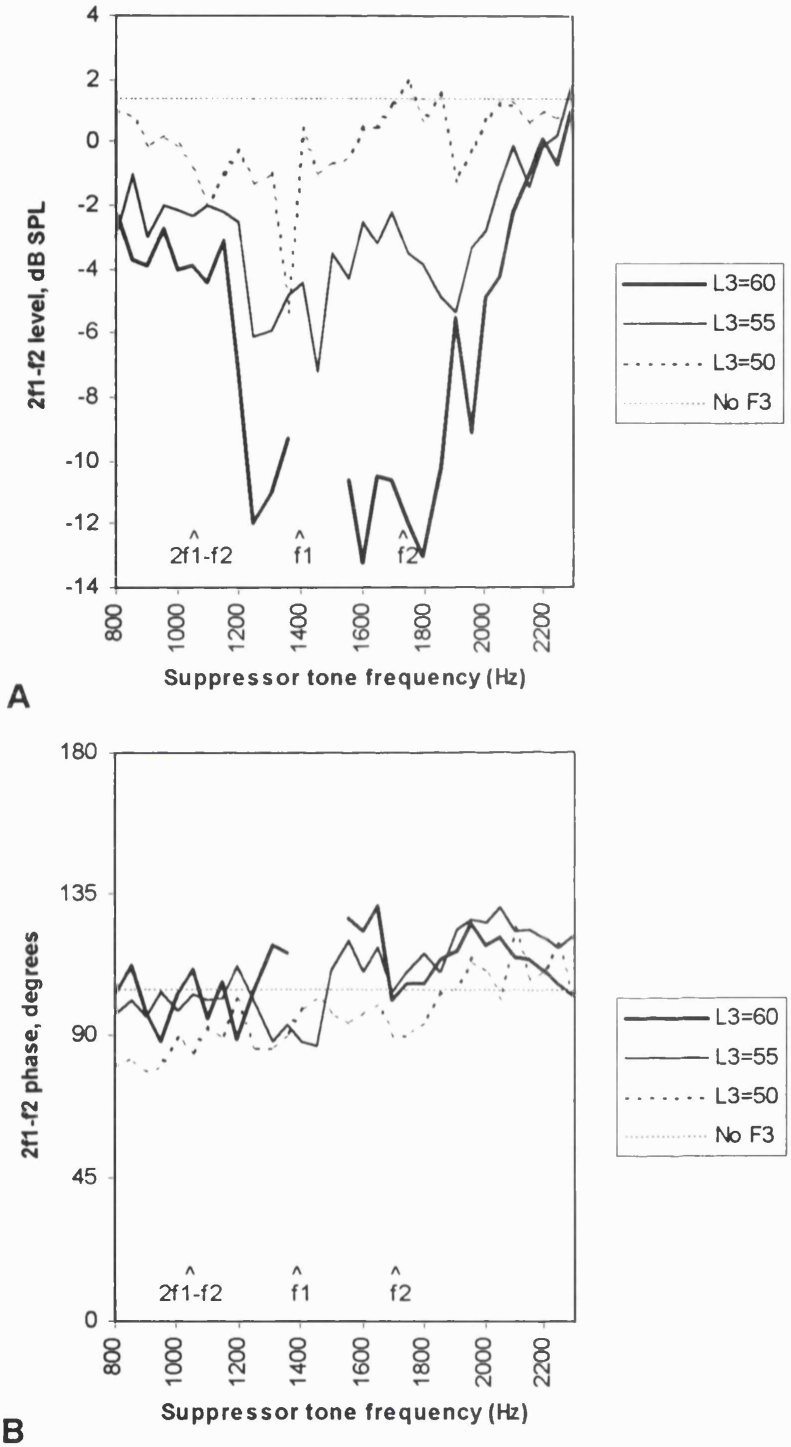

Figure 35. The effect on the $2f_1$-f_2 DPOAE of a third (suppressor) tone swept in frequency at a constant level. f_1= 1404Hz, f_2= 1758 Hz, so f_2/f_1=1.25 and $2f_1$-f_2 = 1050 Hz. L_1=L_2=55 dB SPL. (a) DPOAE level, (b) DPOAE phase.

With f_2/f_1=1.25, a broad, irregular dip is seen (fig 35) which extends from above f_2 to between f_1 and f_{DP}. With f_2/f_1=1.14, 3 different measurement sets 100 Hz apart gave totally different amplitude patterns with dips at different places (figures 36, 37, 38).

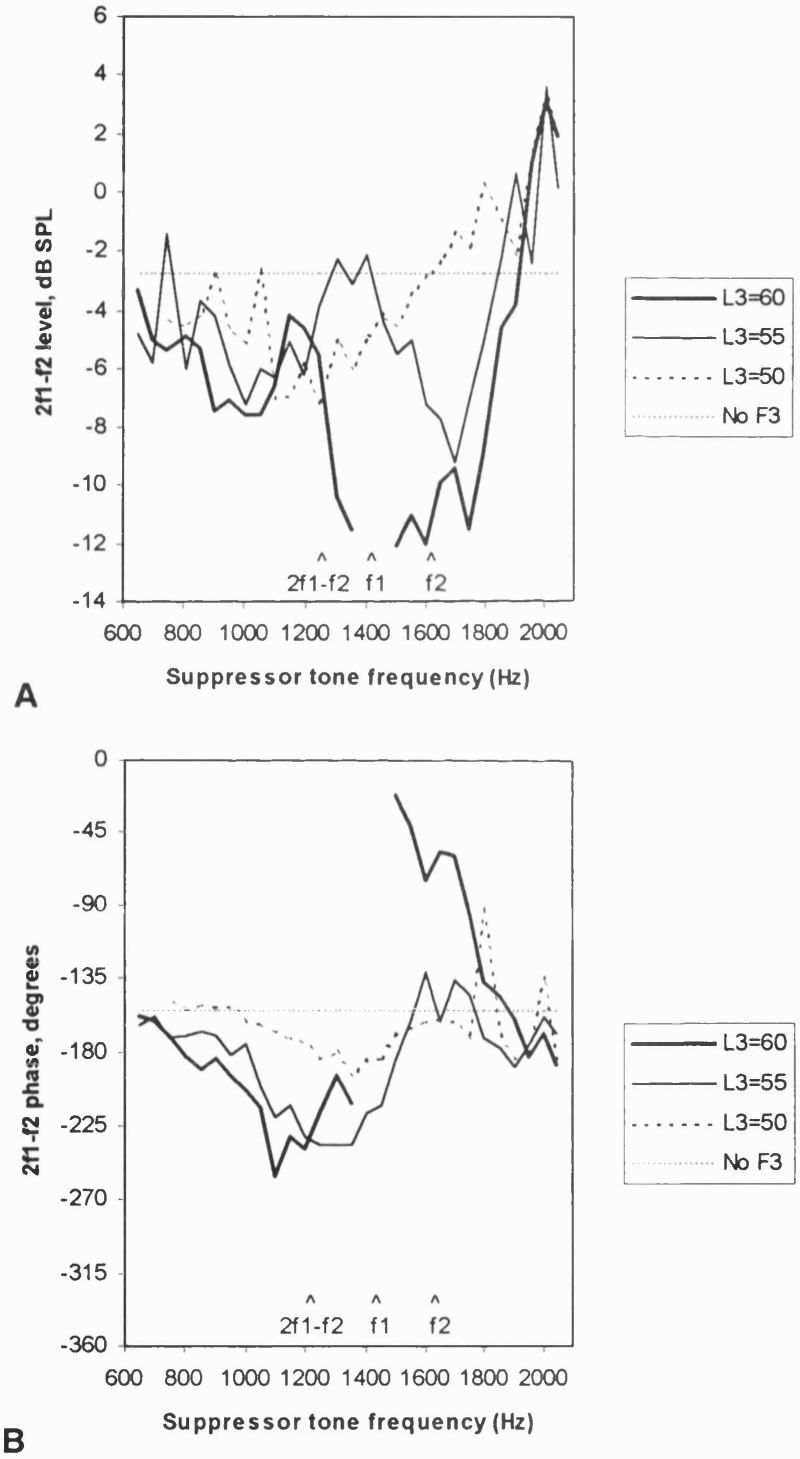

Figure 36. The effect on the $2f_1$-f_2 DPOAE of a third (suppressor) tone swept in frequency at a constant level. f_1= 1416 Hz, f_2= 1611 Hz, so f_2/f_1=1.14 and $2f_1$-f_2 = 1221 Hz. L_1=L_2=55 dB SPL. (a) DPOAE level, (b) DPOAE phase.

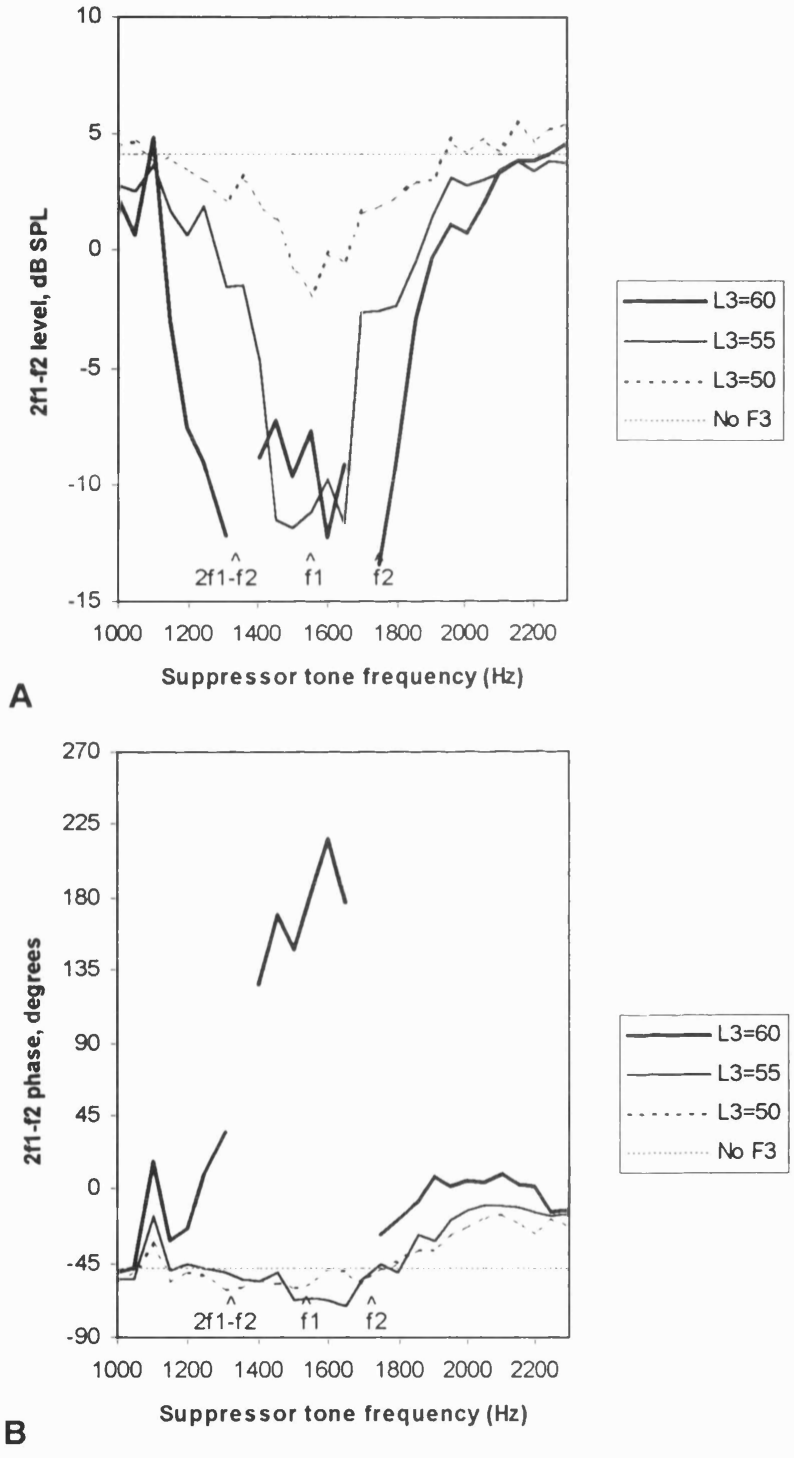

Figure 37. The effect on the $2f_1$-f_2 DPOAE of a third (suppressor) tone swept in frequency at a constant level. f_1= 1538 Hz, f_2= 1755 Hz, so f_2/f_1=1.14 and $2f_1$-f_2 = 1321 Hz. L_1=L_2=55 dB SPL. (a) DPOAE level, (b) DPOAE phase.

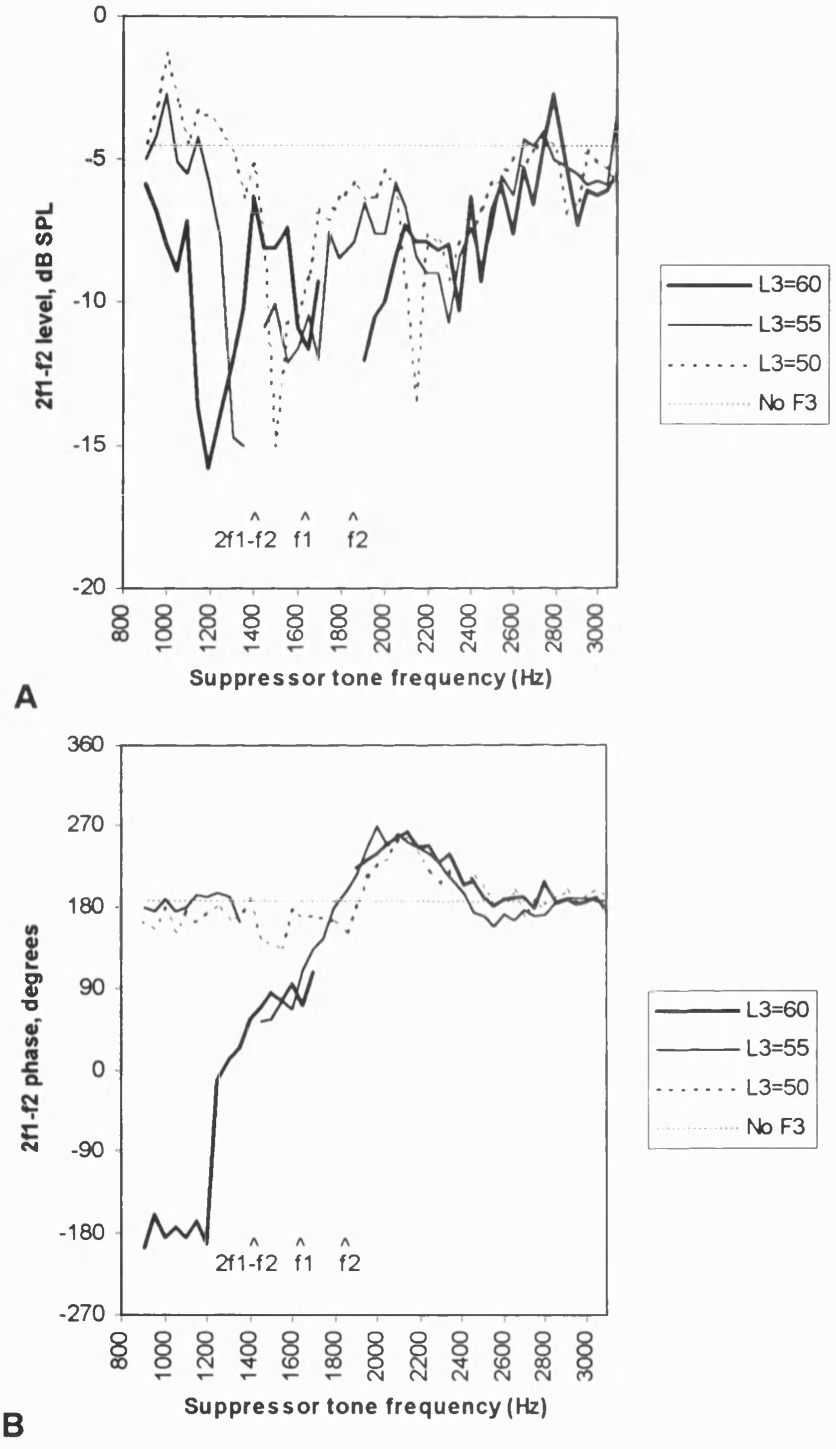

Figure 38 - The effect on the $2f_1$-f_2 DPOAE of a third (suppressor) tone swept in frequency at a constant level. f_1= 1624 Hz, f_2= 1855 Hz, so f_2/f_1=1.14 and $2f_1$-f_2 = 1393 Hz. L_1=L_2=55 dB SPL. (a) DPOAE level, (b) DPOAE phase.

This behaviour is consistent with interference effects arising from multiple emission sources or a distributed source and so the detailed features seen do not necessarily indicate locations of DP sources.

Enhancement of the DPOAE was seen with f_2/f_1=1.05 with a higher frequency tone (figure 39), but not under other stimulus conditions.

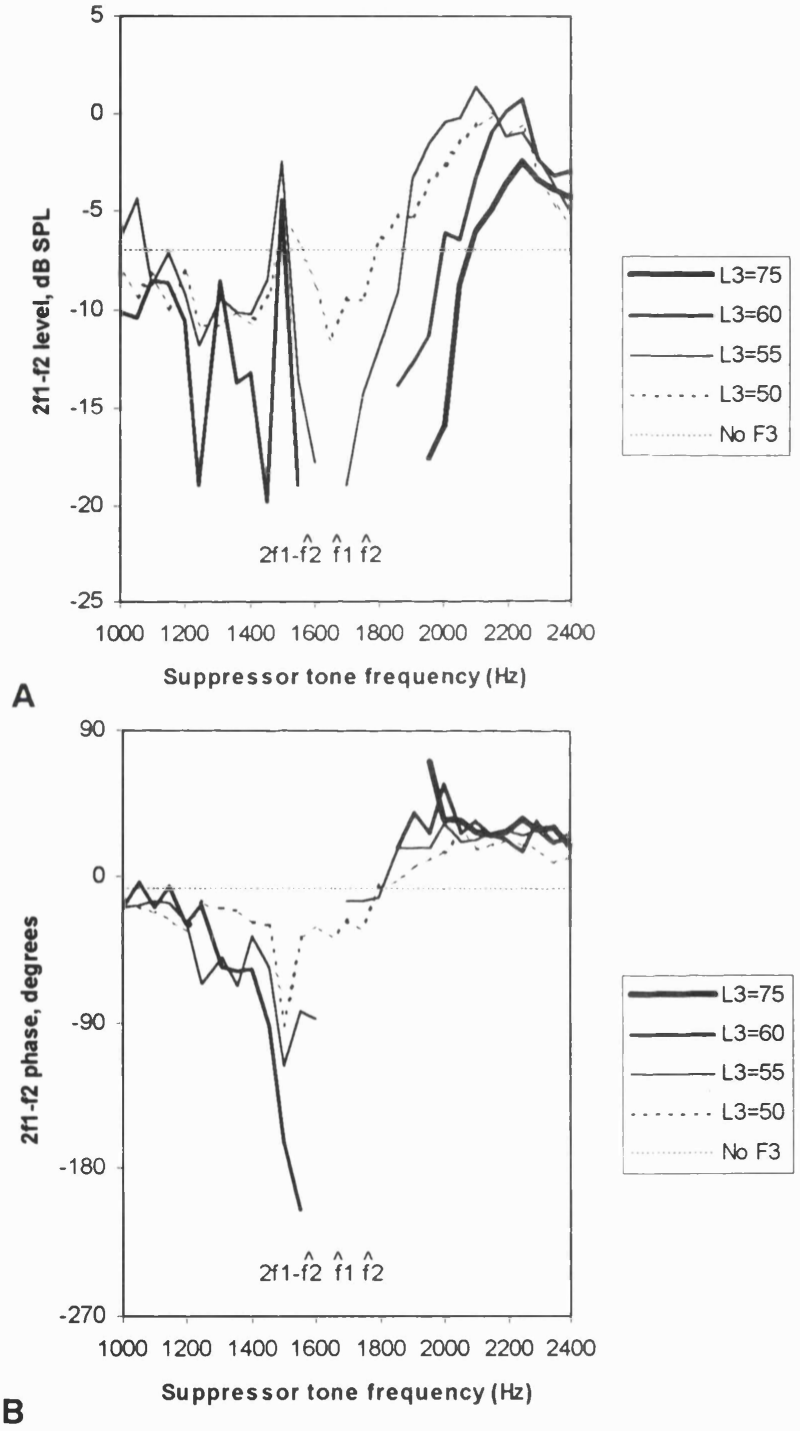

Figure 39. The effect on the $2f_1$-f_2 DPOAE of a third (suppressor) tone swept in frequency at a constant level. f_1= 1672 Hz, f_2= 1758 Hz, so f_2/f_1=1.05 and $2f_1$-f_2 = 1586 Hz. L_1=L_2=55 dB SPL. (a) DPOAE level, (b) DPOAE phase.

The associated phase was a little more consistent. Little phase change was seen when f_2/f_1=1.25 (figure 35), which may be understandable because there is thought to be only one main source of the $2f_1$-f_2 DP at this ratio - there may not be a great deal of interference effects occurring under these stimulus conditions.

When f_2/f_1=1.14 there was either a phase change one way then the other as f_3 is swept from higher to lower frequencies (figures 36, 38), or there was little phase change (figure 37 – except for a 180° switch seen at the highest level of L_3). This is consistent with the contributions from two sources being either in phase (hence no phase change when one is suppressed) or out of phase (leading to significant phase changes when one or other of the DP sources is suppressed).

When f_2/f_1=1.05 a phase change can still be seen (figure 39), a small change in one direction when f_3 was above the stimuli and a larger change in the opposite direction when f_3 was below the stimuli. This may be due perhaps to the lingering effect of a small direct (wave fixed) emission, or partial suppression of a distributed DP source which is not entirely in phase with itself, or mechanical loading altering the phase of travelling waves.

Figure 40 shows the $2f_2$-f_1 DP data measured at the same time as the $2f_1$-f_2 DPOAE in figure 38. The curves show a broad dip centred in the region of the DP frequency. Phase changes are small, being less than 70°, except a couple of outlying points.

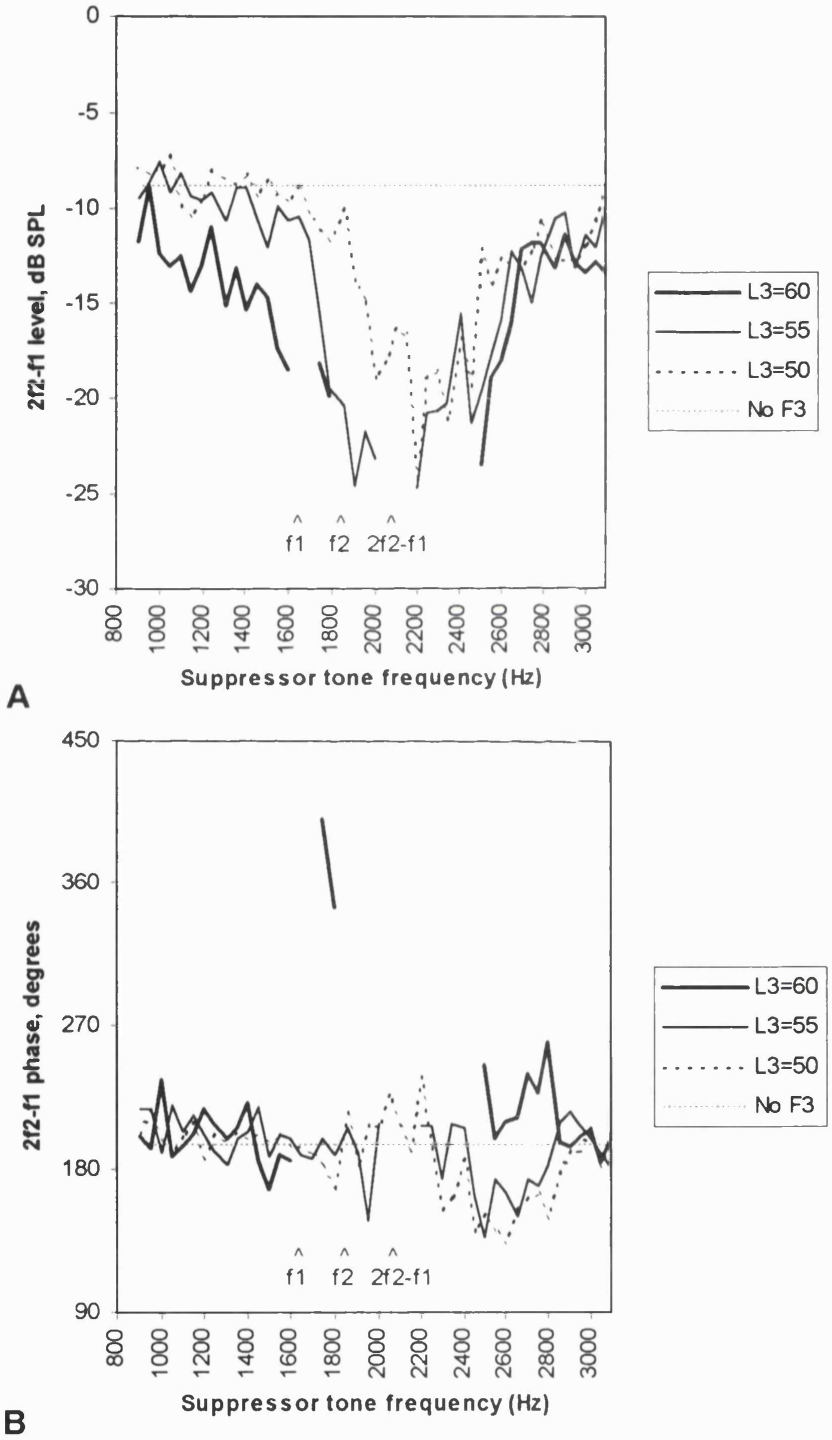

Figure 40. The effect on the $2f_2$-f_1 DPOAE of a third (suppressor) tone swept in frequency at a constant level. f_1= 1624 Hz, f_2= 1855 Hz, so f_2/f_1=1.14 and $2f_2$-f_1 = 2086 Hz. L_1=L_2=55 dB SPL. (a) DPOAE level, (b) DPOAE phase. Stimulus frequencies used here are the same as for figure 36, but a different distortion product is being observed.

IV Discussion

Although the stimulus levels are not directly comparable, the tuning curves presented here show features which are consistent with published data. The depth of the dip in the tuning curve (the suppressor level required to achieve a given amount of suppression) is comparable to that of Brown and Kemp (1984), who used a stimulus level of 60 dB SPL and measured in a comparable frequency range to the present study but with a frequency ratio of f_2/f_1=1.32. Kummer et al (1995) needed approximately 5 dB less level for the third tone to achieve the desired amount of suppression (i.e. the tuning curve dip was 5 dB lower). However their results are less directly comparable to the present study as they used a higher stimulus level (75 dB SPL), investigated a higher frequency region and used a larger frequency ratio. The depth of the tuning curve is therefore perhaps surprisingly similar to the present data.

Kummer et al also presented 'growth of suppression curves' similar to figure 34. Again the parameters used differ from the present study, but the main point of interest for comparison is that Kummer et al found no enhancement of DP production with a third tone of any frequency, whereas consistent enhancement was seen in the present study with a third tone at a higher frequency than f_2. It can only be assumed that this is a feature that happens in some subjects with some stimulus parameters, and Kummer et al happened not to find it. It is presumed that it occurs when either an out of phase DPOAE component is selectively suppressed, or the suppression tone may alter basilar membrane characteristics to either change the phase relationship between DPOAE emission components or to change the phase curves of the travelling waves an in some way encourage transmission of a DP in the basal direction.

Kummer et al (1995) did sometimes find tuning curves with dips both at f_2 and the DP frequency which was not seen in the present study. This is presumably also an intermittent feature, although it was surprising to not find such a curve in the present study given that the dip transferred from f_2 to f_{DP} with a ratio change from f_2/f_1 = 1.15 to f_2/f_1=1.11.

This finding in isolation would imply that there is an almost instant and complete switch from DPOAE being emitted from the f_2 region to being emitted by the DP frequency region, however a DPOAE frequency sweep in this frequency region shows considerable interference, suggesting that two sources may be simultaneously present. The tuning curves may therefore be being complicated by interference and interactions between out-of-phase emission sites.

When f_2/f_1=1.05, the tuning curve seems to dip around the DP frequency, however this is defined by only one data point and the curve is otherwise quite broad. Given the complicated patterns found in other tuning curves, this cannot be taken as proof of the DPOAE coming from the DP frequency place under these stimulus conditions.

The data based on sweeping f_3 have yielded complicated results, but the trend for the phase under some circumstances to change in one direction and then the other as f_3 was swept through is consistent with the DPOAE being emitted from two sources which can be out of phase. It may also be consistent with a single distributed DP source region with a phase gradient across it.

V Conclusion

The effect of a third tone on DPOAE at intermediate ratios of f_2/f_1 is very unpredictable and different patterns can be achieved with only slightly different stimulus parameters. It is not possible to determine the DP sources from the detailed patterns seen with such stimulus configurations.

Although it is difficult to make detailed conclusions, the effects on DPOAE phase are consistent with the existence of two sources of $2f_1$-f_2 DPOAE, which may be in or out of phase.

F. Separate wave and place fixed DPOAE maps of human ears

I Introduction

In chapter D, detailed DPOAE measurements were presented and discussed. It was observed that measured DPOAEs took one of two forms which, it is proposed, are a result of either a wave fixed or a place fixed emission mechanism. Emissions from both mechanisms may occur simultaneously, but whichever DP emission path results in the higher DP amplitude in the ear canal will dominate the phase behaviour of the measured DPOAE. The dominant emission mechanism for the $2f_1$-f_2 DP is primarily determined by the stimulating frequency ratio f_2/f_1. This dependence on the frequency ratio was first reported by Kemp (1986).

The results in section D also showed that the pattern of place fixed behaviour of the $2f_1$-f_2 DP when f_2/f_1 is small is contiguous with the pattern that is seen in the $2f_2$-f_1 DP for all f_2/f_1. However the ear canal $2f_1$-f_2 DPOAE was dominated by a wave fixed emission mode when f_2/f_1 exceeded approximately 1.1. A similar relationship was also seen between the $3f_1$-$2f_2$ and $3f_2$-$2f_1$ DP's, but with the transition between the wave fixed and place fixed emissions occurring at a smaller frequency ratio.

a) Reasons to separate the wave and place fixed emissions

Whilst the data in section D are interesting and informative, the full picture of the wave and place fixed emissions cannot not seen because the DPOAE behaviour that is observed is dominated by whichever mode is the stronger. Therefore it is not known whether the two DP paths both continue to be significant for all f_2/f_1 ratios or whether DP production tends to be bi-modal with only one mode usually present and just a small transition region at which both emissions can occur. If both modes were always present and could be separated then the phase behaviour of the 'residual' or 'minority' emissions could be studied in the context of the travelling wave excitation patterns. The systematic trends that have previously only been seen in restricted stimulus parameter conditions could be pursued over a wider range of frequency ratios.

Observation of the place fixed phase behaviour will be of particular interest, especially through the crossover between the lower and upper sidebands. The lower sideband f_2/f_1 ratio at which the phase pattern which continues from the upper sideband changes, and the phase behaviour in the lower sideband at moderately wide ratios would also be

interesting. These features will provide further clues regarding the locations of the initial DP generating region relative to the f_2 frequency place and the reflecting region relative to the f_{DP} place.

b) Methods to separate the wave and place fixed DPOAE components

Separating the wave and place fixed emissions is not a straightforward task. One approach is to add a third stimulus tone to suppress activity at the DP place, leaving only the DP emitted directly from the f_2 region. Dreisbach and Siegel (1999) have proposed a method in which vector subtraction of DPOAE measurements obtained with and without the third tone can yield the DP place contribution. However Siegel et al (2000) have shown that it can be difficult to ensure that the DP place is fully suppressed without the f_2 region, and hence DP generation, also being affected. This risk is greatest with small stimulus frequency ratios.

An alternative method is pursued here, in which the wave and place fixed DPOAE are separated by a phase gradient dependent post processing method. Shera and Zweig (1993) and Zweig and Shera (1995) have used Fourier transforms to investigate the frequency domain of SFOAE. Stover et al (1996a) and Fahey and Allen (1997) used Fourier transforms on DPOAE frequency sweeps to observe the phase gradient-derived latency.

This method has the advantage of avoiding the unpredictable nonlinear interaction effects of a third tone. For definite separation of emissions with different phase gradient behaviours to be achieved, a long frequency sweep is required in order for the Fourier transformations to be of sufficient resolution. This technique has the potential to allow the 'wave' and 'place' fixed DPOAEs to be observed separately, allowing behaviour which is usually masked to be uncovered.

There is a fundamental difference between the third tone (suppression) method and the Fourier transform method. The third tone selectively affects the emission modes on the basis of their place on the basilar membrane and it turns out that these emissions are different modes. The Fourier transform method separates the emission modes on the basis of their different phase gradients and their probable origin from different places in the cochlea is not relevant to the technique. The suppression and phase gradient methods are comparable if the 'place fixed' emission happens to be from the region of the DP frequency place and the 'wave fixed' emission is from elsewhere.

In the present study, inverse Fourier transforms are applied to constant f_2/f_1 DPOAE frequency sweeps. Wave and place fixed DPOAE have different phase gradients with

these frequency sweeps, so in the 'time' domain peaks are produced at different time delays. Low and high latency DPOAE components are then windowed in the quasi-time domain and then transformed back to the frequency domain separately so that new separate maps can be drawn.

II Measurements and Data Analysis

Data presented here have been obtained from an additional analysis of data from subjects RK and RN in figures 27 and 28. The DPOAE measurements which have been used for this analysis were obtained with $L_1=L_2=70$ dB SPL with DP frequencies ranging from 1 kHz to 4.1 kHz in 12 Hz steps. Stimulus frequency ratios from 1.01 to 1.5 were employed. From these data the two components of interest, which have differing latencies, were separated by the following post-processing method.

A 512 point frequency array was set up, ranging from 0-3100 Hz, thereby preserving the original 3100 Hz range. An exponential frequency transformation was adopted in order to linearise the underlying curve in the phase versus frequency relationship of the place fixed DPOAE and therefore produce clearer peaks in the time domain. The exponential frequency points were calculated as follows:

$$f_i=1000\times4.1^{((i-1)/511)}-1000$$

...where f_i=the frequency of the i th array point.

For convenience only, the measured data points, which span 1000 Hz –4100 Hz, were frequency shifted down 1000 Hz and inserted into this array with linear interpolation between data points where required. The level and phase data were converted to complex number format for the inverse Fourier transformation.

No frequency domain windowing was applied before the inverse Fourier transformation. Although there is a risk of artefacts, the artefacts are easily distinguishable from the signal in this case as the artefacts would be spread throughout the time window whereas the true signal would form peaks early in the time window. The time domain windowing which was subsequently employed would therefore largely remove any such artefacts. The positive advantage of this approach was that the data were not weighted in favour of data from the middle of the frequency range and the final separated data were more easily compared with the original unprocessed data.

As the frequency array had an exponential characteristic, the meaning of the time scale of the inverse Fourier transform was not straightforward. The timescale in the time domain which is indicated in figure 41 was calculated as follows:

Time increment per point (ms)= $\frac{1000}{\text{frequency range(Hz)}}$

This gives a time increment of approximately 0.32 ms per point.

This calculated time interval most accurately reflects true time for data from the middle of the frequency range (2-3 kHz). It is an underestimate for the lower frequencies and an overestimate for the higher frequencies because of the exponential frequency transformation used. The definition of this timescale is not relevant for the subsequent windowing and processing of the data. The transformation into the 'time' domain produced separate amplitude peaks representing the low and high latency components (figure 41).

The peaks were separated by time-windowing. The windowing was designed to separate the wave and place fixed DPOAE and the crossover point was set at the 'time' defined midway between the wave and place fixed peaks. The chosen crossover point for the 'early' and 'late' time windows was the 5th data point, which is about 1.6 ms. A flat topped window with a raised cosine edge was adopted. The cosine curve 'edge' extended from the 3rd to the 7th data points (approx. 1.00-2.25 ms). The 'late' window was rolled off more gradually between the 40th and 50th data points (12.9-16.1 ms), comfortably after the DPOAE peaks had died down to the noise floor.

Each windowed part of the time domain response was returned to the frequency domain by a forward Fourier transform. The data were returned to level and phase format and converted back to the original 256 point linear frequency array.

Separate area charts were then constructed for the low and high latency DPOAE.

III Results

a. Time domain view of constant f_2/f_1 DPOAE frequency sweeps

The magnitudes of the inverse Fourier transforms derived from 3 $2f_1$-f_2 DPOAE sweeps of 256 points are shown in figure 41(a), using stimulus frequency ratios of f_2/f_1=1.04, 1.1 and 1.2. Each peak has an implied group delay, derived from the rate of change of phase in the DP sweep. The group delay associated with the frequency ratio of f_2/f_1=1.04 is 3-4 ms, compared to 0.5-1 ms with a frequency ratio of 1.2. When the frequency ratio is 1.1, components with both group delays are seen, rather than a single peak with an intermediate time delay. Therefore, two components of DPs are identified, with two distinct group delays. As the sweeps had constant stimulus frequency ratios, the peak with a small group delay is consistent with the 'wave fixed' emission mechanism, whereas the later peak is consistent with the 'place fixed' emission mechanism. Which one dominates the measured DPOAE depends on the ratio f_2/f_1.

Similar data have been obtained for the $2f_2$-f_1 DP (figure 41(b)). In this case, there is no sign of the low latency peak that was seen with the $2f_1$-f_2 DP.

The windowing employed for subsequent separation of the low and high latency DPOAE components is indicated at the bottom of the figure.

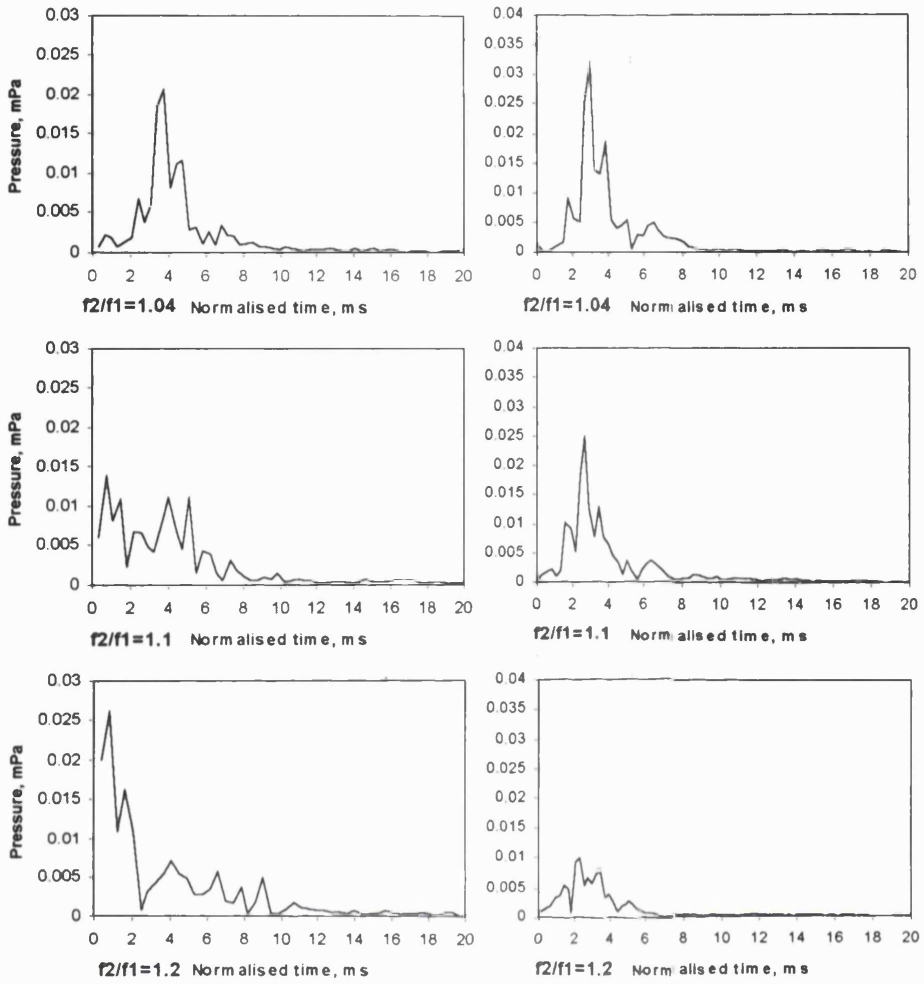

a) $2f_1$-f_2 DP b) $2f_2$-f_1 DP

c) Windowing employed to separate low and high latency DPOAE

Figure 41. Magnitudes of inverse Fourier transforms of 256 point constant frequency ratio DP sweeps with L_1=L_2=70 dB SPL (subject RDK). f_1 was incremented in 12 Hz steps, starting at 1 kHz. The frequency intervals were converted to a log scale prior to the fourier transform to remove an underlying gradual change in phase gradient. (a) $2f_1$-f_2 DP - A low 'latency' and a high 'latency' component can be identified. When f_2/f_1=1.04, there is almost no trace of the low latency component, when f_2/f_1=1.1, both components are present and approximately equal in amplitude, and when f_2/f_1=1.2, the low latency component dominates although higher latency elements are also present. (b) $2f_2$-f_1 DP – No low latency peak is seen, the level is lower with wider frequency ratios, but the 'latency' remains about the same. (c) indicates the windowing which was employed to separate the low and high latency DPOAE.

b. Frequency domain view of the low latency component (figures 42 and 43)

Following the windowing of each data set in the time domain, they were returned to the frequency domain by a forward Fourier transform. Separate frequency maps were then constructed for the low and high latency DPOAE components.

The low latency portion of the $2f_1$-f_2 DPOAE had a high level when f_2/f_1 was between 1.1 and 1.3. Outside this range the level fell rapidly. The DPOAE is likely to be restricted to a limited ratio range because the phases of the DP sources in the generating region of the basilar membrane can only sum positively in the basal direction with a limited range of ratios (Kemp and Knight, 1999). The phase contours were approximately horizontal, indicating that phase was dependent on the frequency ratio, but almost independent of DP frequency. There was good vertical agreement between successive constant f_2/f_1 sweeps, with phase being steadily more positive at larger stimulus frequency ratios. The low latency portion of the $2f_2$-f_1 DPOAE (figures 42 and 43 parts a and b) was of very small amplitude. In one subject (RDK, figure 42) it was mostly below –20 dB SPL, but the other subject (RN, figure 43) had a clear low latency peak in the inverse Fourier transform (figure 44) which was above –20 dB SPL in the frequency domain (the lower half of figure 43a) with most combinations of f_1 and f_2. In the frequency domain the associated phase, where measurable, had a tendency to gradually be more positive when f_2/f_1 was smaller, but the phase was less dependent on the DP frequency.

The absence after processing of the fine structure which had been seen in the unprocessed data of figures 27, 28 even when the wave fixed emission appeared to dominate, suggests that the fine structure was caused by interference between the low and high latency DPOAE components.

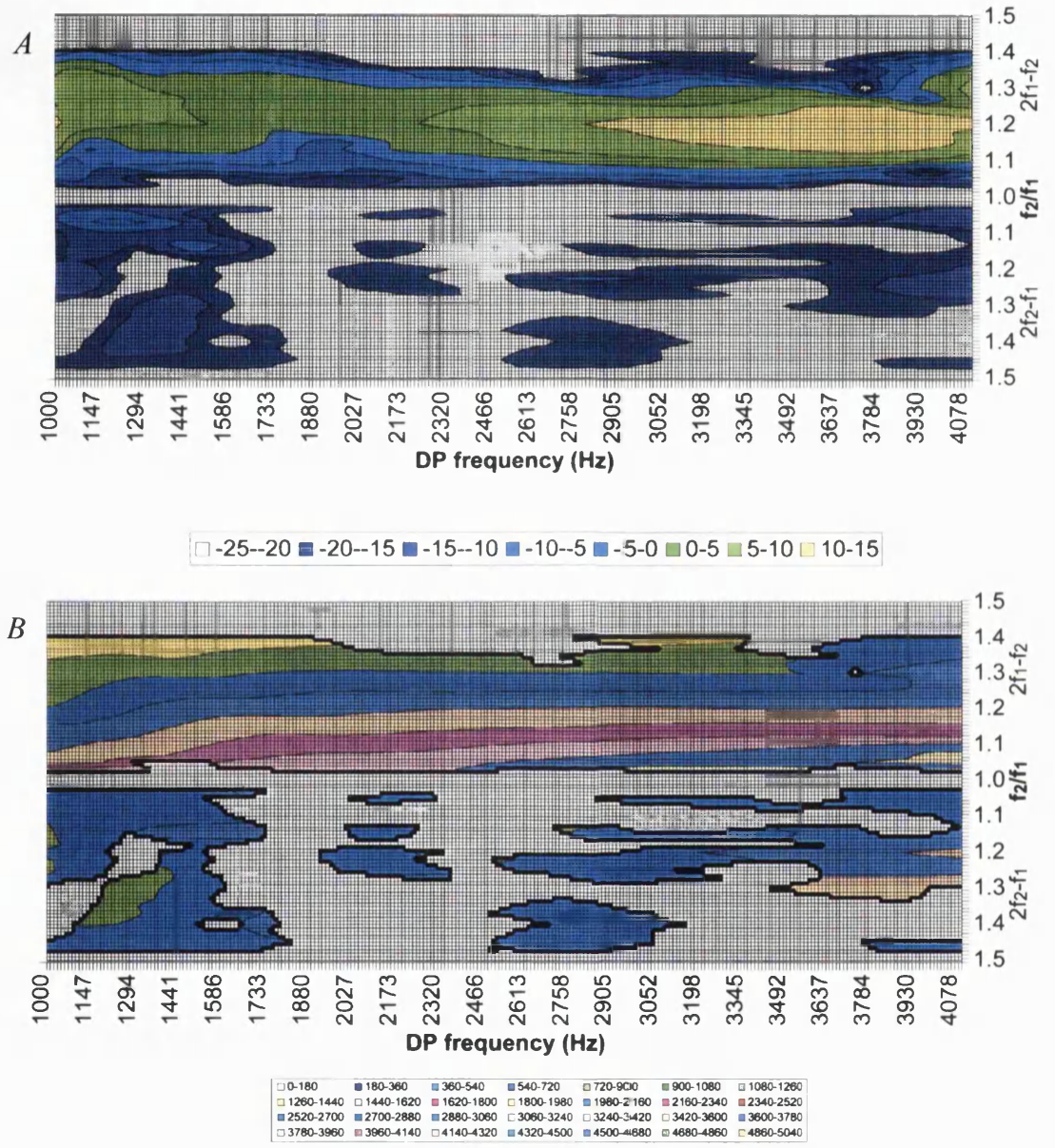

Figure 42. Low latency windowed $2f_1$-f_2 and $2f_2$-f_1 DPOAE data for subject RDK, taken from data in figure 27.

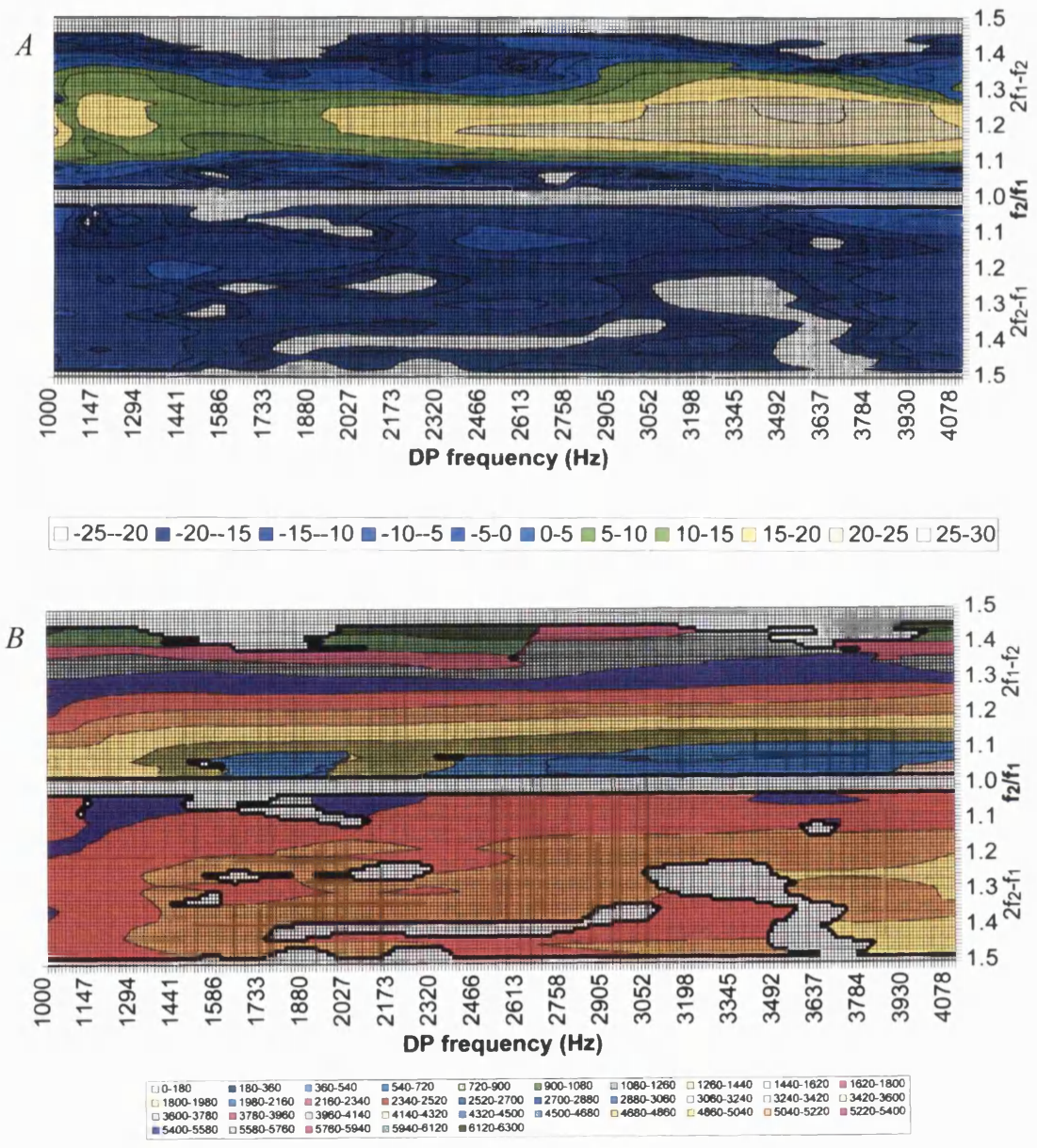

Figure 43. Low latency windowed $2f_1$-f_2 and $2f_2$-f_1 DPOAE data for subject RN, taken from data in figure 28.

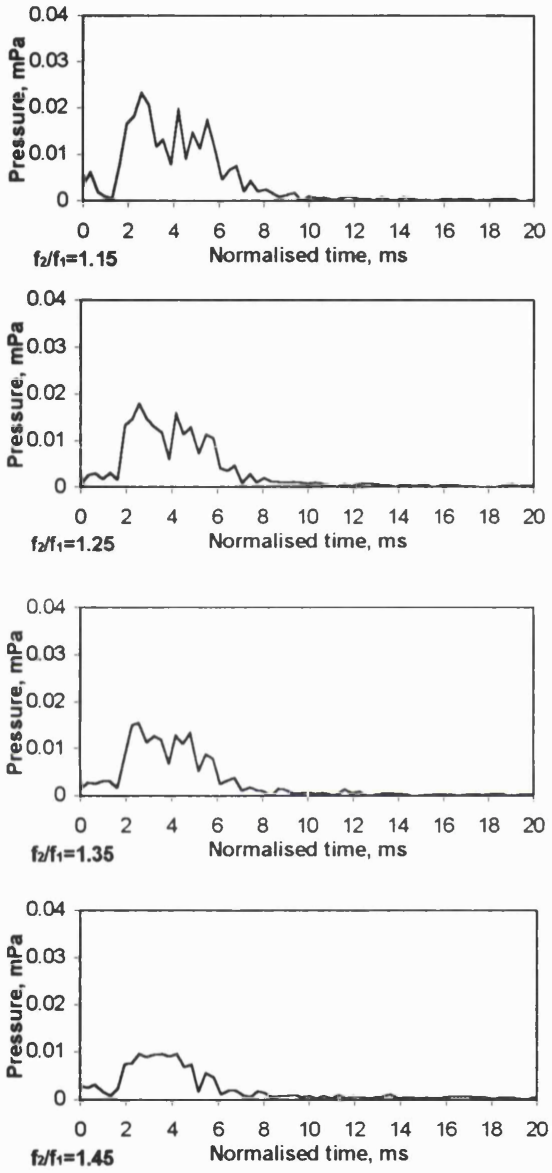

Figure 44. Magnitudes of inverse Fourier transforms of 256 point constant frequency ratio $2f_2$-f_1 DP sweeps with L_1=L_2=70 dB SPL (subject RN). f_1 was incremented in 12 Hz steps, starting at 1 kHz. The frequency intervals were converted to a log scale prior to the Fourier transform to remove an underlying gradual change in phase gradient.
A small peak is seen around 0-1 ms which is consistently above the level of the noise, (the noise is indicated by the level at the end of the trace after the OAE has died down).

c. Frequency domain view of the high latency (figures 45 and 46)

The phase pattern of the high latency part was predominantly dictated by the DP frequency, in contrast to the low latency DPOAE. The level of the high latency component was less sensitive than the low latency component to f_2/f_1 changes with the DP frequency held constant (vertical movement on the figures). The level of the place fixed DP is sensitive to f_2/f_1 and this may be related to the amount of apical propagation from the site of DP generation and the amount of suppression of the onward DP by the proximity of f_1 and f_2.

There are interesting secondary relationships with the frequency ratio visible in the data. At high frequencies (above about 2 kHz) the upper sideband DPOAE phase from both subjects shows a slight, accelerating negative drift towards smaller ratios (indicated by the phase contours bending to the left). The phase of the lower sideband high latency DPOAE was, at small frequency ratios, a continuation of the upper sideband phase. However, above f_2/f_1 ~1.07 the phase was steadily more positive at wider frequency ratios (contours leaning to the right).

The unprocessed data contained fine structure throughout where the place fixed emission appeared to dominate. The retention of this pronounced fine structure in the separated high latency DPOAE indicates that this is not caused by interactions with a low latency emission.

d. The $3f_1$-$2f_2$ and $3f_2$-$2f_1$ DPOAEs

Similar patterns were seen in the $3f_1$-$2f_2$ and $3f_2$-$2f_1$ DPOAE data from subject RDK, except that the DP's were only present when f_2/f_1 was small (figures 47, 48).

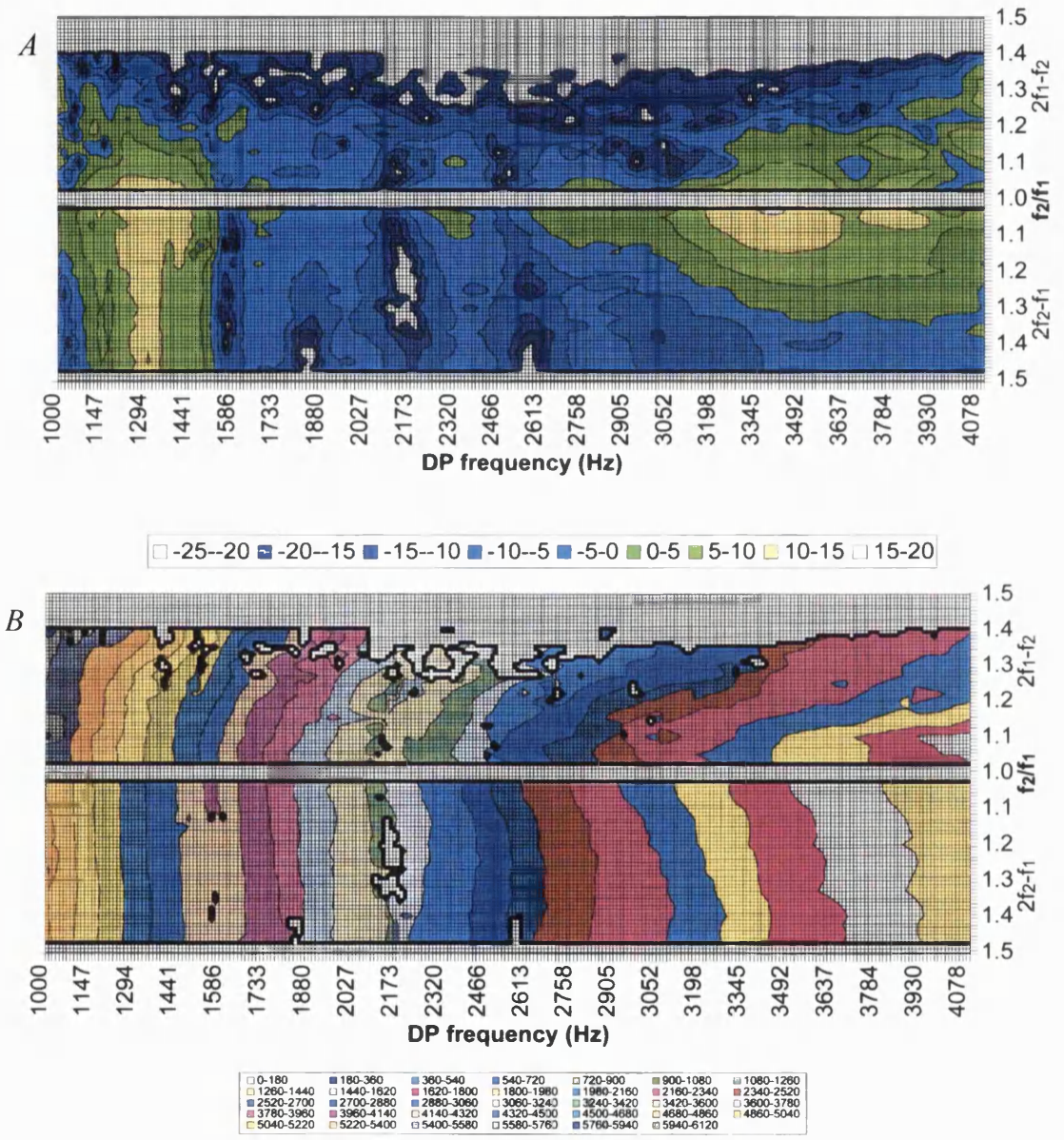

Figure 45. High latency windowed $2f_1$-f_2 and $2f_2$-f_1 DPOAE data for subject RDK, taken from data in figure 27.

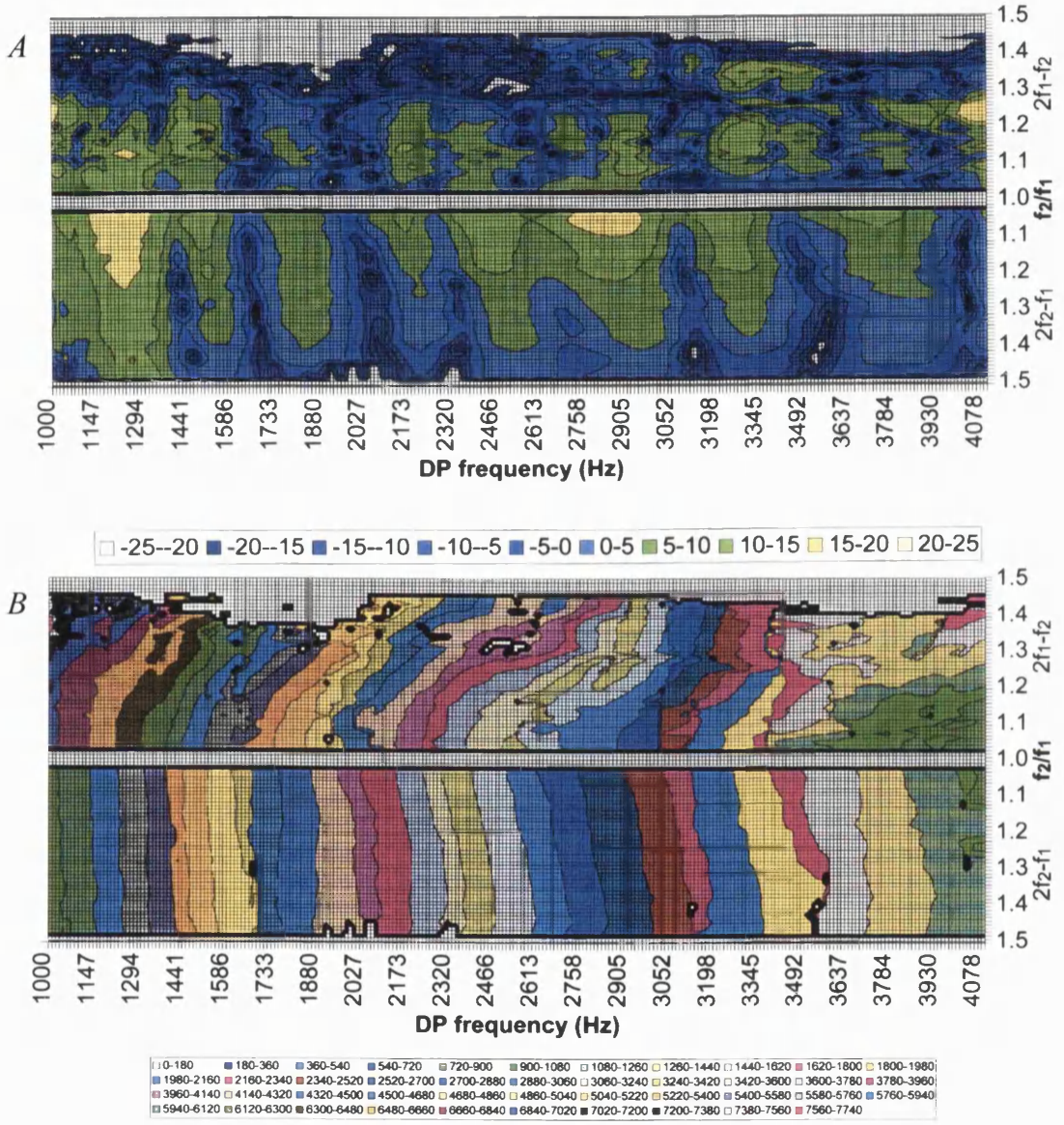

Figure 46. High latency windowed $2f_1$-f_2 and $2f_2$-f_1 DPOAE data for subject RN, taken from data in figure 28.

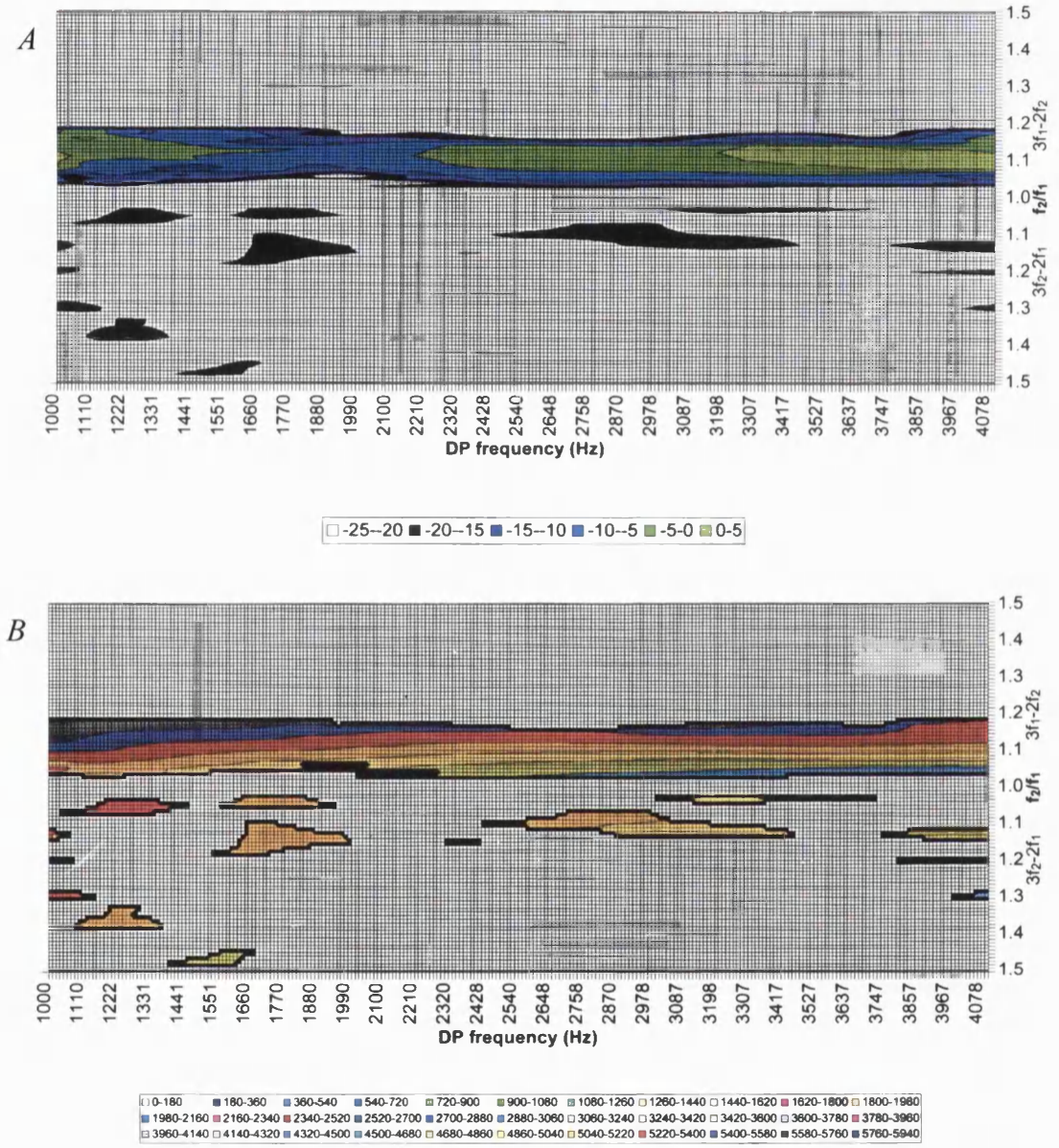

Figure 47. Low latency windowed $3f_1$-$2f_2$ and $3f_2$-$2f_1$ DPOAE data for subject RDK, taken from data in figure 29.

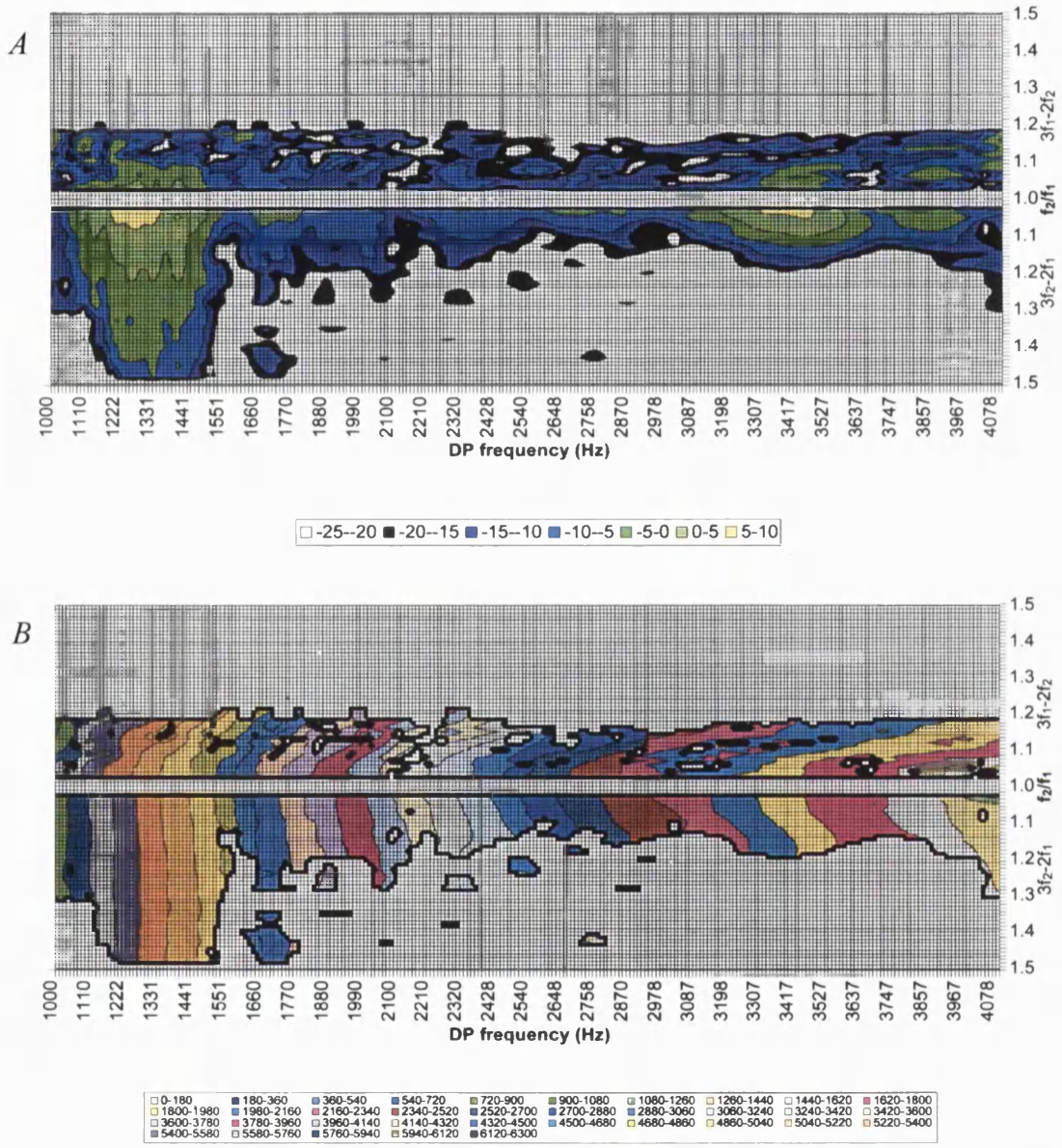

Figure 48. High latency windowed $3f_1$-$2f_2$ and $3f_2$-$2f_1$ DPOAE data for subject RDK, taken from data in figure 29.

e. Wave and place fixed level, averaged across DP frequency

In order to see clearly the preferred frequency ratio for the 'wave' and 'place fixed' DPOAE separately, a power average of the DPOAE level from figures 42, 43, 45 and 46 was calculated across DP frequency and plotted against frequency ratio (figure 49).

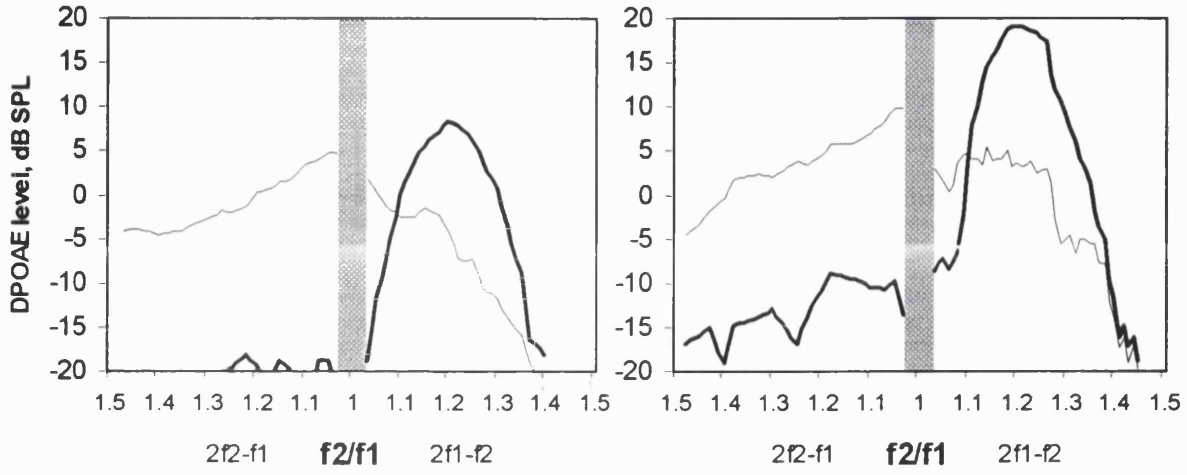

Figure 49. Wave fixed (thick line) and place fixed (thin line) DPOAE level for subject RN (left) and RDK (right) plotted against frequency ratio, calculated as a power average from the data in figures 42, 43, 45 and 46. The shaded region where f_2/f_1 is small indicates where data could not be obtained because of limitations on the smallest frequency spacing at which the DPOAE could be resolved from the stimuli.

The results show clearly that the 'wave fixed' emission favours a restricted ratio range from f_2/f_1=1.1-1.35 in the lower sideband only, whereas the 'place fixed' emission is present in both sidebands much more widely with the strongest emission when f_2/f_1 is small. The residual upper sideband 'wave fixed' emission can be seen from subject RN, typically at –10 to –15 dB SPL.

In the lower sideband when f_2/f_1 is large, the rapid fall seen in the 'wave fixed' level as f_2/f_1 increases beyond 1.3 and the more gradual fall in the 'place fixed' level with increasing f_2/f_1 means that the levels of the two components become similar. Tubis et al (2000) have suggested that at wide ratios, the lower sideband 'place fixed' DPOAE level may exceed the 'wave fixed' level (as is also the case when f_2/f_1>1.1). The present data suggests that this is indeed possible as the levels of the two emissions become similar when f_2/f_1~1.5. Perhaps with different stimulus conditions the 'place fixed' emission may exceed the 'wave fixed' emission when f_2/f_1 is large.

f. Suppression of the DP frequency place by a third tone, viewed in the 'time' domain

Further DP sweeps were obtained using 128 points in the $2f_1$-f_2 DP frequency range of 1087-2381 Hz with a frequency ratio of 1.15 and a stimulus level of L_1=L_2=55 dB SPL. The measurement was then repeated with a third tone of 55 dB SPL introduced at 50 Hz above the DP frequency.

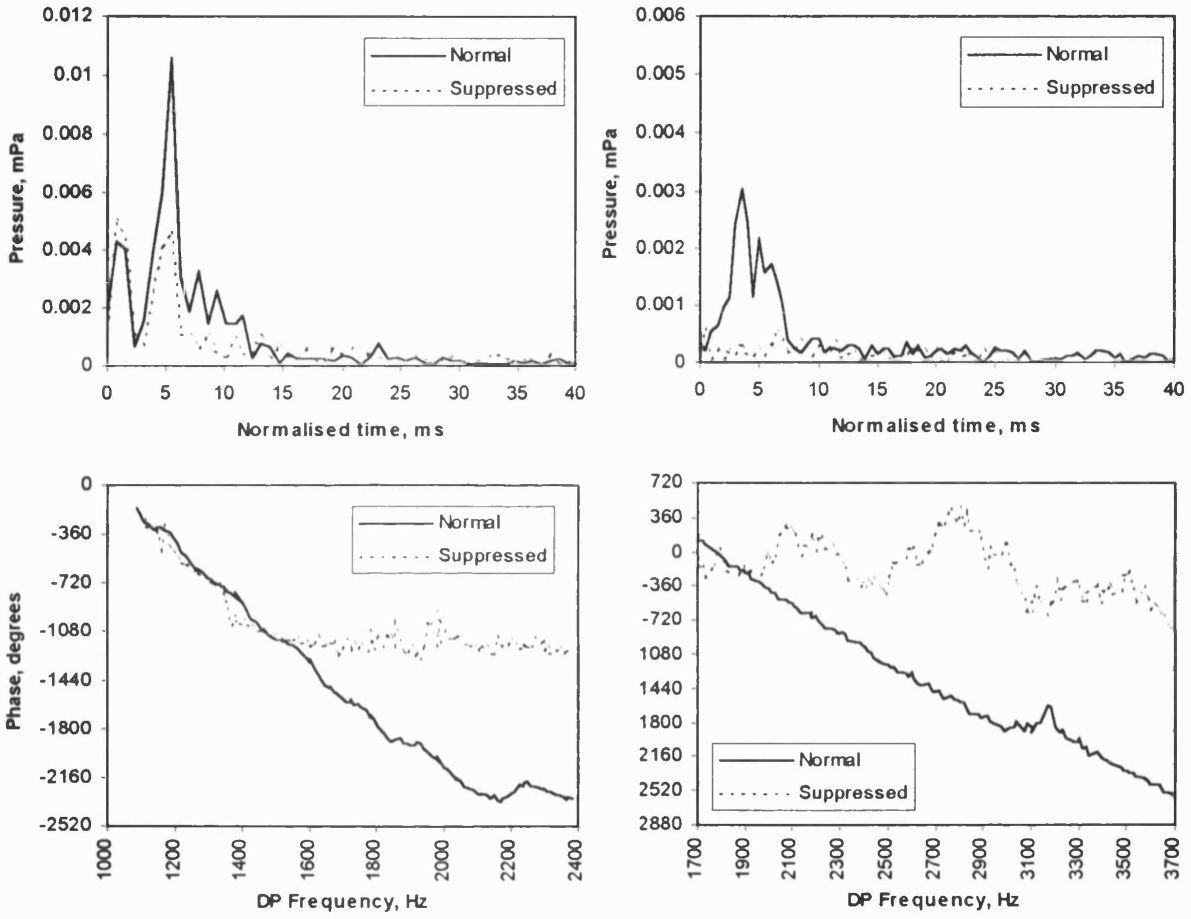

a) $2f_1$-f_2 DP b) $2f_2$-f_1 DP

Figure 50. Magnitude of inverse Fourier transform data (top) and phase (bottom) from constant frequency ratio DP sweeps (before the Fourier transformation) with L_1=L_2=55 dB SPL and with f_2/f_1 fixed at 1.15 (subject RDK). (a) $2f_1$-f_2 DP: Insertion of a third stimulus tone of 55 dB SPL at 50 Hz above the DP frequency selectively suppresses the high latency emission and results in a predominantly flat phase characteristic. (b) $2f_2$-f_1 DP: The 'suppressor' tone suppresses the entire DP, leaving only noise.

Figure 50 contains both a time domain response and the unwrapped phase data. With the $2f_1$-f_2 DPOAE (fig 50 (a)), it can be seen that the third tone selectively 'suppresses' the more delayed component of the DP and the overall phase gradient changes from a steep gradient to a shallow gradient. No such gradient change could be induced by introducing a third stimulus tone at frequencies close to the frequencies of f_1 and f_2.

(Following the publication of these data (Knight and Kemp, 1999b), Konrad-Martin et al, 2001 have published a similar finding with f_1 sweeps (fixed f_2)).

Figure 50(b) shows the corresponding data for the $2f_2$-f_1 DPOAE. In this case, the suppressor close to the DP frequency obliterates the entire DP, leaving just noise.

IV Discussion

Inverse Fourier transformations of constant f_2/f_1 DPOAE frequency sweeps have been demonstrated to result in the efficient separation of two emission types (figure 49). These have been windowed in the 'time' domain and then returned separately to the frequency domain.

In general, the phase of the low latency derived DPOAE components (figures 42 and 43) is dependent on the ratio f_2/f_1 but changes only slowly with DP frequency (so phase contours run left to right across the figures). The phase of the high latency derived DPOAE changes far more rapidly with DP frequency (figures 45, 46). This difference between the low and high latency DPOAE phase behaviour with DP frequency is precisely what would be expected due to the windowing employed in the time domain, because windowing at low latency excludes components with a steep phase gradient with respect to DP frequency. Of far greater interest is the way in which the phase contours behave with respect to the frequency ratio (vertical in the map) when the sweeps are recombined. The agreement of the phase of adjacent sweeps when combined to form the maps confirms that the patterns seen in the data do not arise from merely an artefact. It is significant that a substantial amplitude of DP above the noise level was obtained for both modes under most stimulus conditions.

The levels of the 'wave' and 'place fixed' emissions have very different relationships to f_2/f_1, as shown clearly in figure 49. The 'wave fixed' emission is emitted strongly only in a restricted range of the lower sideband although a residual emission is present more widely. With a small primary frequency ratio there is almost no trace of the 'wave fixed' (low latency) emission in the $2f_1$-f_2 DP. This suggests that the distortion source is not uniformly bidirectional, because if DP energy was always sent equally towards the base and the apex of the cochlea, a 'wave fixed' component to the $2f_1$-f_2 DP would always be present. In addition, the high latency emission reduces in amplitude as the ratio f_2/f_1 increases. While the intensity of DP generation might be expected to decrease with increasing frequency separation of equal level primaries, an increase in place fixed emission amplitude relative to wave fixed emission could be expected because of a

reduction in suppression of the DP frequency 'amplifier' region by the primaries. This result implies that less DP energy is directed towards the apex from the f_2 region when stimulated with larger ratios of f_2/f_1. Kemp and Knight (1999) have proposed that the distortion source may be variably directional, dependent on the ratio f_2/f_1 (discussed in section A II i).

The 'place fixed' emission is emitted most strongly when f_2/f_1 is close to 1 in either sideband but the ratio is less critical. As f_2/f_1 increases, the level of the 'place fixed' emission falls faster in the lower sideband than the upper sideband. This may be because the phase gradient switches from favouring apical propagation to favouring basal propagation as the DPOAE generating region leaves the DP frequency place and moves with the f_2 envelope.

The analysis method has successfully uncovered the full extent of the two modes of emission. The basic features seen in the unprocessed data are preserved and the continuity between the upper and lower sidebands remains. However, there is some evidence of small artefacts being generated at wide ratios and high frequency, where some DPOAE is seen after windowing when none was present beforehand. Such 'blurring' of the data is a result of applying short windows in the time domain. The possibility of random noise arising from the whole sweep is discussed later with respect to the significance of the low latency $2f_2$-f_1 emission data.

Further support for the idea of the DP frequency place region being the site of re-emission for the 'place fixed' component is provided by the inverse Fourier transform and suppression data (figure 50). The suppressor tone close to f_{DP} suppressed the high latency part of the DPOAE, but not the low latency part. This shows that the high latency part of the DPOAE is from the DP frequency region, but the low latency part is not. Recently, Kalluri and Shera (2001) have also shown that similar results can be obtained by using either the suppression or Fourier transform methods to separate the wave and place fixed emissions, also indicating that the place fixed emission is associated with the DP frequency place.

a. Possible general explanation for the high latency DPOAE phase behaviour.

(place fixed mechanism)

The following arguments consider the case of a constant f_{DP} sweep and attempt to explain the difference in the phase behaviour of the high latency DPOAE between the lower and upper sidebands. It is helpful to consider a constant DP frequency sweep when considering place fixed DPOAE phase as the presumed reflection site doesn't

move, leaving only the changing phases of the inward and outward journeys to cause a DPOAE phase gradient. Such a sweep corresponds to vertical slices of the results in figures 45 and 46. The descriptions below consider only the case of a place fixed emission.

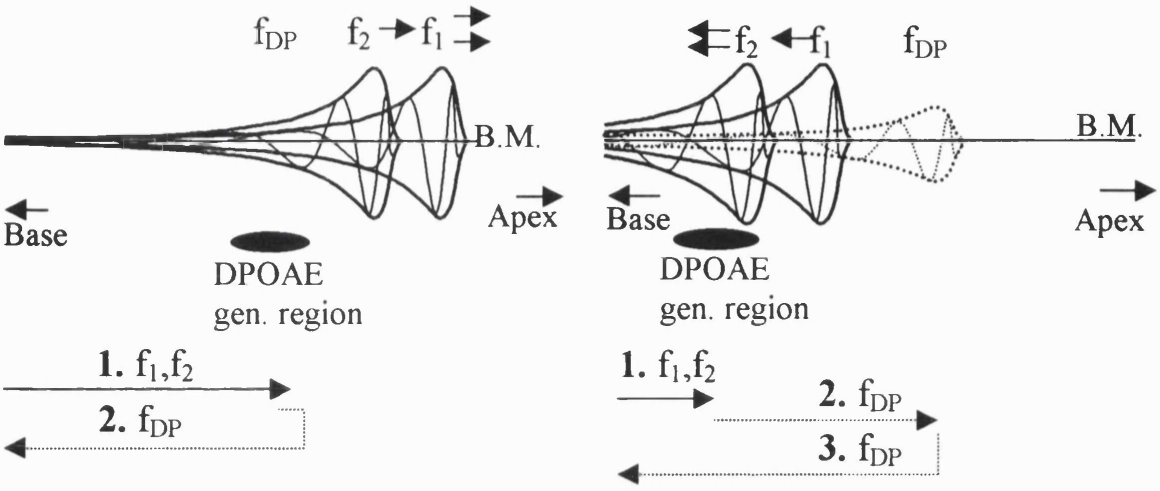

a) Place fixed upper sideband DP (e.g. $2f_2$-f_1)

b) Place fixed lower sideband DP (e.g. $2f_1$-f_2)

Figure 51. Illustrations of the path taken by place fixed DPOAE, considering a constant DP frequency sweep in which the peaks of the f_1 and f_2 travelling waves expand away from the DP frequency place as the frequency ratio increases. (a) Upper sideband DPOAE, and (b) Lower sideband DPOAE.

i) Upper sideband DP (e.g. $2f_2$-f_1)

DP generation and emission from the region of f_{DP} (figure 51a).

1. In a constant DP frequency sweep, as the ratio f_2/f_1 is increased and both f_1 and f_2 decrease, the f_1 and f_2 places move apically away from the f_{DP} place. The phase lag of both f_1 (ϕ_1) and f_2 (ϕ_2) at the DP generating site must decrease with respect to the input stimulus. The f_1 frequency place must move away at twice the rate of f_2 as $2f_2$-f_1 remains constant. However the phase of the $2f_2$-f_1 DP as it is generated changes twice as much in response to changes in ϕ_2 as to changes in ϕ_1. The phase gradient of ϕ_1 is more gradual than ϕ_2 at the DP generating site. As $\phi_{DP}=2\phi_2-\phi_1$, this means that the DP phase at its generation site will not change much with changing f_2/f_1 because changes in ϕ_1 and ϕ_2 have opposing effects.
2. The phase change resulting from the return journey is unchanged with changing stimulus frequency ratio. Therefore the return journey doesn't contribute to the phase gradient.

As the upper sideband experimental data has an almost flat phase gradient when DP frequency is fixed (a vertical section through figures 45 and 46), the opposing factors described appear to be roughly equal (and opposite) in magnitude.

The argument above suggests that any offset from flat phase in a constant DP frequency sweep (vertical phase contours on the charts) is associated with the difference in the gradients of the stimulus phases ϕ_1 and ϕ_2 at the DP generating site.

ii) Lower sideband high latency DP (e.g. $2f_1-f_2$)

DP generation is in the region of f_2, but the emission travels via the f_{DP} region (figure 51b).

1. In a constant DP frequency sweep, the phase lag of f_1 (ϕ_1) at the DP generating site decreases with increasing ratio, whereas the phase of f_2 (ϕ_2) at the DP generating site remains largely unchanged. This is because the site moves with the f_2 travelling wave envelope. Therefore the phase lag of the DP as it is generated decreases by $2\phi_1$.
2. As the stimulus ratio increases and the DP generating site moves basally away from the DP place, the phase lag of the journey onwards to the DP place increases. However of necessity the phase gradient of f_{DP} at f_2 is less than the f_1 phase gradient at f_2. Also, in point (1) above, the DP phase change due to the change in ϕ_1 was multiplied by 2. Therefore the change in DP phase due to (1) will be greater than the opposing change in (2).
3. The phase of the return journey is not affected by the stimulus frequency ratio. Therefore (3) doesn't contribute to the DPOAE phase gradient.

The factors involved here (1, 2 and 3) do not cancel, so there is a net reduction in DP phase lag as the frequency ratio increases with DP frequency constant, contrary to the upper sideband. This is consistent with the lower sideband experimental data when the frequency ratio exceeded about 1.1.

However, it has been shown that the lower sideband high latency phase doesn't follow this pattern at the smallest frequency ratios, indicating a divergence from the argument above.

The phase is continuous between the lower sideband and the upper sideband, suggesting continuity of mechanism. For the upper sideband the DPOAE generating region is associated with the DP frequency place, which is basal to the f_2 place. So for the lower sideband DPOAE at close ratios, where f_2 and f_{DP} become close, the

generating site may also be more associated with the f_{DP} site than with the f_2 site. Alternatively, the lower sideband DP generating region may simply be changing shape when f_2/f_1 is small. Changes in the phase gradients within the DP generating region (discussed by Kemp and Knight, 1999) may be significant.

This behaviour would be consistent with a tendency for DPs to always be generated somewhat basal to the f_2 peak.

b. Possible Explanations for the low latency $2f_2$-f_1 emission

As a secondary observation, a small low latency upper sideband DPOAE has been observed in one of the two subjects. The low latency emission, which was seen in the $2f_2$-f_1 DP from subject RN, is of interest as it has not previously been reported in humans. The level of the emission was typically –20 to –5 dB SPL, whereas the high latency emission was typically 0 to 15 dB SPL. The low latency upper sideband emission has a slight and consistent dependence of phase on the frequency ratio but little dependence on DP frequency. This is consistent with a low latency wave fixed emission, so the emission may be from the DP frequency region of the cochlea. The charts in figure 44, showing inverse- Fourier-transformed data of constant f_2/f_1 sweeps, indicate that a low latency peak is consistently present in the $2f_2$-f_1 data for subject RN.

c. Where is the noise floor?

As the data have been considerably processed, it is difficult to directly infer a noise floor for individual data points. In order to obtain an estimate of where the noise floor lies after the DPOAE separation processing, 'pseudo-time' windows were drawn from the data at a latency well after the DPOAE had died away. These samples of data were then subjected to a forward Fourier transform to provide an estimate of the noise level in the frequency domain. The average across the frequency range of the noise level estimate was obtained for the $2f_2$-f_1 DP with f_2/f_1=1.03 and 1.1 (Table V).

	RDK	*RN*
Short window	*-30.4*	*-29.3*
Long window	*-26.2*	*-24.6*

Table V. Mean noise level estimates, dB SPL, obtained from the normalised time domain responses of the $2f_2$-f_1 DP with f_2/f_1=1.03 and 1.1. The 'short window' was employed to isolate the low latency emission, the 'long window' was used for the high latency emission.

In each example, the noise estimate occasionally exceeded –20 dB SPL (exceptionally up to –13 dB SPL), so small regions of data points exceeding –20 dB SPL can be explained by random noise (e.g. the 'low latency' $2f_2$-f_1 data of RDK). However the 'low latency' $2f_2$-f_1 data of RN consistently exceed this level by 5 - 15 dB and so this cannot be explained by random noise.

d. How typical are the results?

Regarding the general features of the separated DPOAE, both subjects follow the same patterns, despite having different underlying latencies and DP levels. The general patterns can be accounted for on the basis of the description given in the earlier section 'Possible general explanation for the high latency DPOAE phase behaviour'.

In both subjects the low latency emission was only strong when f_2/f_1 was between 1.1-1.3. The peak occurred at around f_2/f_1=1.2-1.25, which is consistent with results in chapter C and other published data (Harris et al, 1989; Moulin, 2000).

It is likely, therefore, that the general features are typical of normal-hearing ears. The more localised features are not correlated between the two subjects and it seems that these will be different for each subject.

The balance between the levels of the low and high latency emissions with L_1=L_2=70 dB SPL may be different with other stimulus levels but the results in chapter C suggest that the overall pattern of behaviour is similar. Use of stimuli with L_1>L_2 can be expected to favour the lower sideband (Kemp, 1987).

The possibility has arisen of a 'wave fixed' emission being present in the $2f_2$-f_1 data, approximately 20 dB SPL lower in level than the place fixed emission. It is not known whether this will emerge as a 'normal feature' of normally-hearing ears as it has only been successfully identified as being above noise in one of the two subjects.

The comparative sensitivity of wave and place fixed emissions to cochlear hearing loss is beyond the scope of this study and would require further research including subjects with hearing loss.

V Summary

Separate 'wave' and 'place fixed' DPOAE maps with DP frequency and f_2/f_1 have been derived for two human ears using a phase gradient based method of separation. The 'wave fixed' output is maximal over a restricted f_2/f_1 range in the lower sideband (e.g. $2f_1-f_2$), but it remains present at a wide range of f_2/f_1 at much reduced levels. Slight evidence was found that a very small 'wave fixed' upper sideband (e.g. $2f_2-f_1$) component may be present but if present is less dependent on f_2/f_1. Unlike the lower sideband, its source may be in the region of or basal to the DP frequency place in the cochlea.

A 'place fixed' emission has been found at most stimulus frequency combinations, including the entire upper sideband region and the region in the lower sideband where it is normally obscured by the larger 'wave fixed' component. The 'place fixed' emission level was greatest at the smallest frequency ratios.

The phase pattern of the 'place fixed' DPOAE supports the common view that the source of DP contributing to upper sideband DPOAE is a region related to the DP frequency place for all f_2/f_1 ratios. For lower sideband DPOAE the initial DP source must be related to the f_2 peak excitation region when f_2/f_1 is large. However the excellent continuity of phase behaviour between the lower and upper sidebands suggests that when f_2/f_1 is small the lower sideband place fixed DPOAE is a continuation of the upper sideband DPOAE with its source region associated with the DP frequency place. Selective suppression of the high latency DPOAE by a third tone added close to f_{DP} provides further evidence for this.

G. Formal validation of the single source/two routes DPOAE hypothesis

I Introduction

a. The one source/two routes DPOAE hypothesis

In the preceding chapters, a plausible qualitative explanation has been developed in order to explain the observed phase behaviour of the two components of $2f_1$-f_2 DPOAE based on the primary characteristics of the cochlear travelling wave. The hypothesis (stated at the end of Chapter D) assumes one initial DP source region but two possible emission routes and can be summarised as follows.

Path 1. (Wave fixed) The DP is generated in the region of the stimulus travelling wave peaks and emitted directly towards the base.

Path 2. (Place fixed) The DP is generated in the region of the stimulus travelling wave peaks or the DP frequency place (whichever is more basal) but then travels apically as a travelling wave before being 'reflected' at the region of the DP frequency place and travelling back towards the base.

Here the hypothesis is formulated as a mathematical model to test whether this hypothesis is a workable explanation of the experimental DPOAE observations made here. If so, it could form the basis of a cochlear model of the processes involved in DPOAE generation.

In the previous chapter (Section F), the separation of wave fixed and place fixed DPOAE in humans has been demonstrated using a frequency domain editing method. The distinctive features that have actually been observed in the phase behaviour of DPOAEs appear consistent with the qualitative explanation offered, which was based on the general characteristics of the cochlear travelling wave and the anticipated effect of nonlinearity and 'reflectors'.

The appropriateness of the general explanation would be proved if it were possible to formally predict the main experimentally observed DPOAE phase patterns. A simple transmission line model of travelling wave interactions was constructed and used to generate maps of backward-travelling DP amplitude and phase to compare with the experimental DPOAE data. A region of DP generation was introduced, by adding nonlinearity to a localised region of gain leading up to the travelling wave peaks. The intensity and phase of the summated DP propagating back to the input of the model

(middle ear) was computed as a function of primary stimulus frequency and frequency ratio using the transmission parameters of the model. A series of partial reflectors were then introduced into the transmission line and the phase and intensity of DP that these reflectors caused to be propagated back to the input were also computed. It was reasoned that if the model reproduced the main features seen in the experimental results in a manner not critically dependant on the choice of parameters it would support the general explanation offered and its underlying assumptions.

II Implementation

a) Phase Curve

Signal propagation within the frequency domain transmission line model is based on a frequency dependent propagation phase curve similar to that found in basilar membrane observations. It has an exponential acceleration of phase accumulation with distance and a logarithmic spacing of characteristic frequencies. The phase lag from the input to the model is calculated for each stimulus frequency at each incremental distance along the transmission line. For each model element a parameter determines the phase delay at that element for each frequency. This is termed the 'frequency parameter'. The 'frequency parameter' for each element of the model is set up in a logarithmic relationship covering frequencies from 25 kHz down to 600 Hz. The incremental change between each model element is such that each element approximately represents two hair cells in a human ear.

The phase lag from the base of the cochlea is calculated for each stimulus frequency at each incremental distance along the basilar membrane. The phase lag is logarithmically related to the frequency parameter (See equations 1 and 2 in Appendix I). Figure 52 shows the envelope of the travelling wave and the associated phase curve. Figure 53 shows the phase curve used in this model compared with the phase measured in Chinchilla (Robles et al, 1986; Recio et al, 1998) and squirrel monkeys (Rhode, 1971). It is not possible to obtain such data in live human cochleae, but the data is probably similar, mainly differing only by a scaling factor.

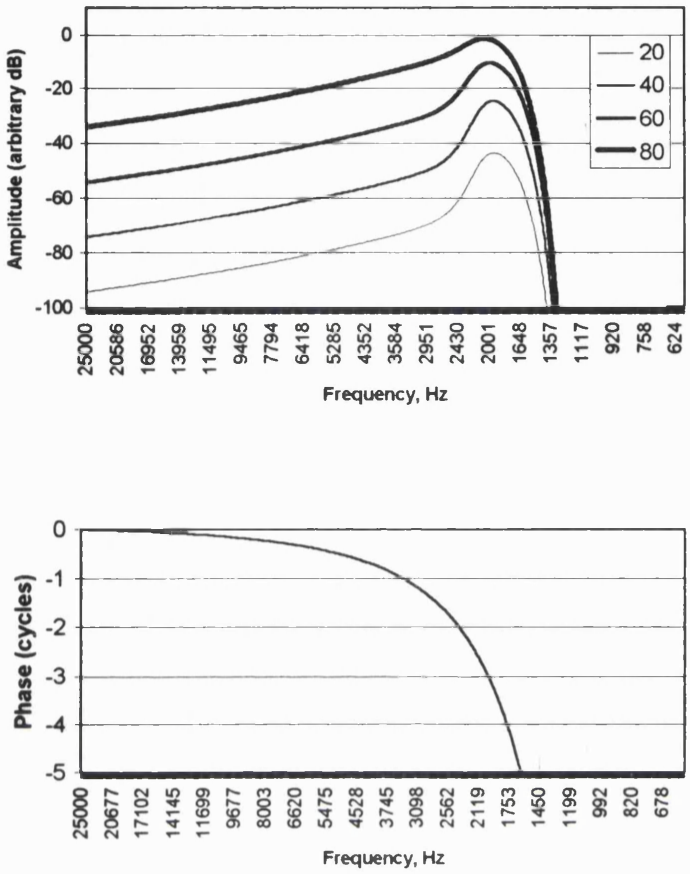

Figure 52. Amplitude (top chart) and phase (lower chart) of the model travelling wave. The amplitude envelope is shown with the stimulus level ranging from 20 dB SPL to 80 dB SPL to demonstrate the compressive growth of the travelling wave peak. The phase is unaffected by the stimulus level.

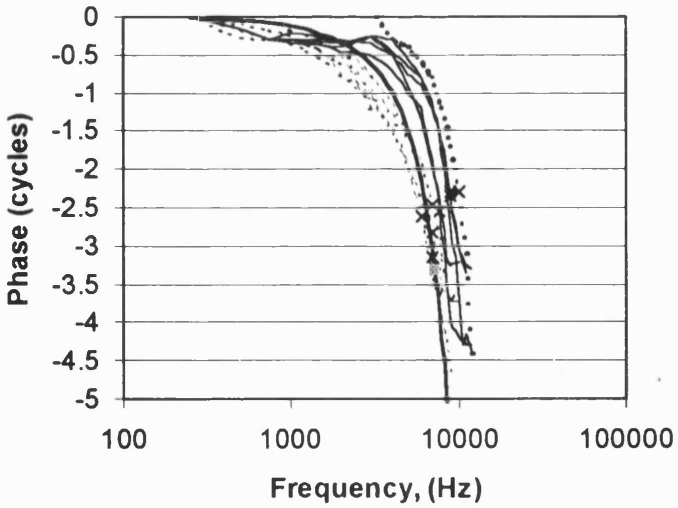

Figure 53. Comparison of the phase curve adopted in the model with basilar membrane data. Data sources: Dashed lines –Rhode, 1971, squirrel Monkey. Dotted line –Recio et al, 1998, chinchilla. Solid thin lines –Robles et al 1986, chinchilla. Solid thick line – model data. Crosses indicate the frequency which produced the maximum displacement in the experimental data, the square indicates the frequency which produced the maximum amplitude in the model. Data are zeroed at the lowest frequency point but are not frequency re-scaled.

b) Gain and damping

Transmission characteristics of this model, which include frequency dependent gain and damping functions, are designed to produce travelling wave envelopes which exhibit growth with distance up to a peak, followed by a rapid decline. A nonlinear gain function is introduced in order to achieve compressive growth at the travelling wave peak relative to input intensity, but linear growth further towards the start of the transmission line. The nonlinear gain also results in the generation of distortion products.

In this formulation, gain is necessary in the model so that the travelling waves grow to form sharp peaks (Neely and Kim, 1986; Geisler, 1993; de Boer 1983a,b). The gain is configured such that the total maximum linear gain along the basilar membrane (which would be delivered if the travelling wave amplitude was small) increases the amplitude of the travelling wave peak by 25 dB. This value is in comparison to the model operating without gain – i.e. the comparison is to a passive and damped model. The gain is frequency dependent and is restricted to a region which was centred just to the basal side of the travelling wave peak. The region of gain covers approximately $1/3^{rd}$ of an octave (-6 dB) of place frequencies in the model. The gain delivered by each model element is level dependent and is reduced by a factor related to the total stimulus travelling wave amplitude (f_1+f_2) at that point (this also includes self-suppression in the case of the propagating DP). Suppression by the small DP on the stimuli is presumed to be not significant. (See equations 3-5 in Appendix I)

The model included gain only for forward-propagating waves. Inclusion of gain for reverse-propagating waves in this model resulted in considerable undesirable growth of place fixed DPOAE in the lower sideband at wide frequency ratios which is not found experimentally. This was because the DP gain region was suppressed by the stimulus tones when f_2/f_1 was small but not when f_2/f_1 was large, so the place fixed DP would be amplified twice by the gain region at large frequency ratios (as it travelled through the gain region both ways).

The amplitude of the propagating travelling wave is diminished by a damping function which became increasingly significant at and beyond the travelling wave peak. Damping is applied as a function of the phase gradient with a constant added. The phase dependent part controls the sharpness and the location of the apical end of the travelling wave envelope. The additional constant tends to control the general growth of the travelling wave envelope basal to the travelling wave peak, outside of the gain region (Equation 6 in Appendix I). The travelling wave amplitude shape is shown in figure 52

at a range of stimulus levels. Linear growth is seen towards the start of the transmission line, with compressive growth near the peak.

c) DP generation and propagation

DP levels were obtained by applying the computed levels of f_1 and f_2 to the nonlinear input/output function. The model assumes that at each point a fixed proportion of the DP generated is converted into a bi-directional travelling wave and therefore that a fixed proportion of the DP is either absorbed or directed in a mode which doesn't readily set up a travelling wave. The phase of the DP generated at each incremental point along the basilar membrane is simply defined by the phase of f_1 and f_2 at that point.

The model supports propagation of the DP in both directions along the basilar membrane without preference, the DP generated at each model element being vectorally added to the propagating DP travelling wave as it passes. This differs from the approach used by Sun et al (1994a) who summed the DP sources to the point of maximum overlap between the stimulus tones and then radiated the DP as a point source from there.

Transmission of the DP from the DP generating region, propagated directly back to the start of the transmission line, was examined to see if it behaved like 'wave fixed' DPOAE. These data were generated over a range of stimulus frequencies, comparable to that used to obtain the experimental data.

d) Introduction of reflectors

In stage two of the model the onward-propagating DP signal encounters fixed, randomly spaced partial reflectors.

The onward-propagating component results in a travelling wave which proceeds to the DP frequency place. In order that a DP emission results from this component, randomly spaced place fixed reflectors have been introduced. These reflect a proportion of the travelling wave amplitude but without a phase shift which would be generally expected with an impedance irregularity. Each model element had a 1 in 5 chance of being a reflector, except that adjacent reflectors were not allowed. The reflecting factor was linked to the linear gain window associated with f_{DP} – therefore the significant reflectors are limited to the region leading up to the DP travelling wave peak. Summation of these reflected DP signals in the reverse direction gives rise to a DP component at the input which was examined to see if it was similar to 'place fixed' DPOAE generation.

The reflected reverse-propagating travelling wave is kept numerically separate from the reverse propagating 'wave fixed' DP to avoid the difficulties of separating them later.

The model does not include reflections back into the cochlea from the stapes, so repeated reflections between the base and the DP frequency place are not supported and this potential source of fine structure is not modelled.

Essentially the same procedure is performed to obtain $2f_2$-f_1 DPOAEs, but the model was found to produce very little $2f_2$-f_1 DPOAE via the wave-fixed mode due to cancellation. For place-fixed $2f_2$-f_1 DPOAE, the reflectors placed around the DP frequency place were also in the DP generation region so that the distance of apical DP travel before a reflector was encountered was minimal.

III. Results

The phase and amplitude of this direct component is presented in figure 54 (a and b) in a similar format to the DPOAE data of figures 42 and 43. The 'directly emitted' data reproduce both the wave fixed phase pattern and the general dependence of level on the ratio f_2/f_1. The dependence on f_2/f_1 appeared to be determined by the vector summation of the DP across its generating region. For the $2f_2$-f_1 DP component, this was largely self-cancelling in the basal direction for all f_2/f_1. With the $2f_1$-f_2 DP, cancellation was significant only when f_2/f_1 was small. The directly emitted model DP peaked at a wider ratio than in the experimental wave fixed DPOAE data (figure 42 and 43). This difference is likely to be due to the precise shape of the phase curve, specifically the phase gradients of f_1 and f_2 in the region at which the DP is generated.

Figure 55 (a and b) indicates the level and phase of the reflected DP generated by the model. The general patterns are very similar to the experimental DPOAE data in figures 45 and 46.

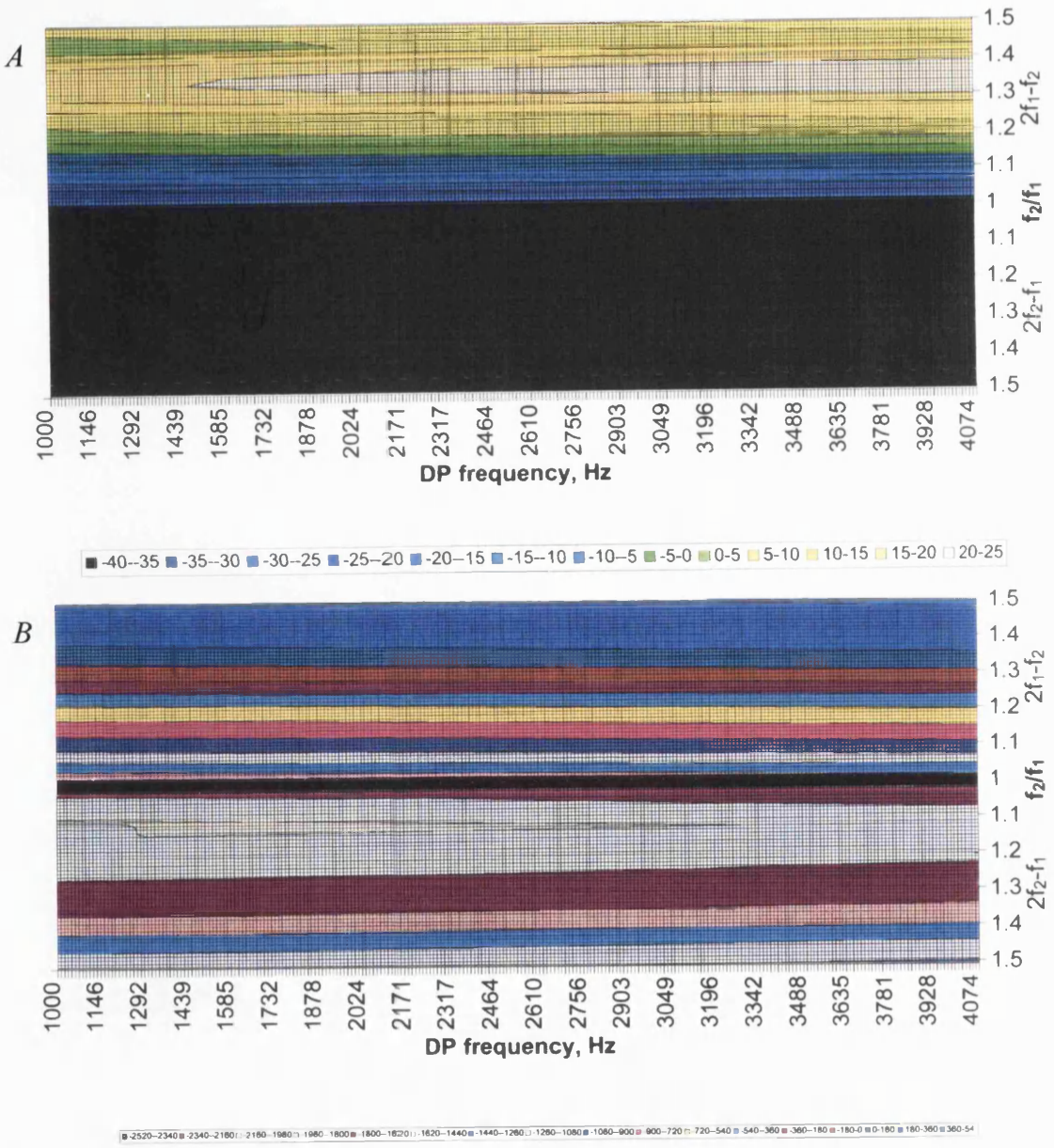

Figure 54. Wave fixed DP from a transmission line model. The DP is only strongly present over a limited range of ratios in the lower sideband. This and the horizontal phase contours are very similar to those of the low latency DPOAE of figures 42 and 43.

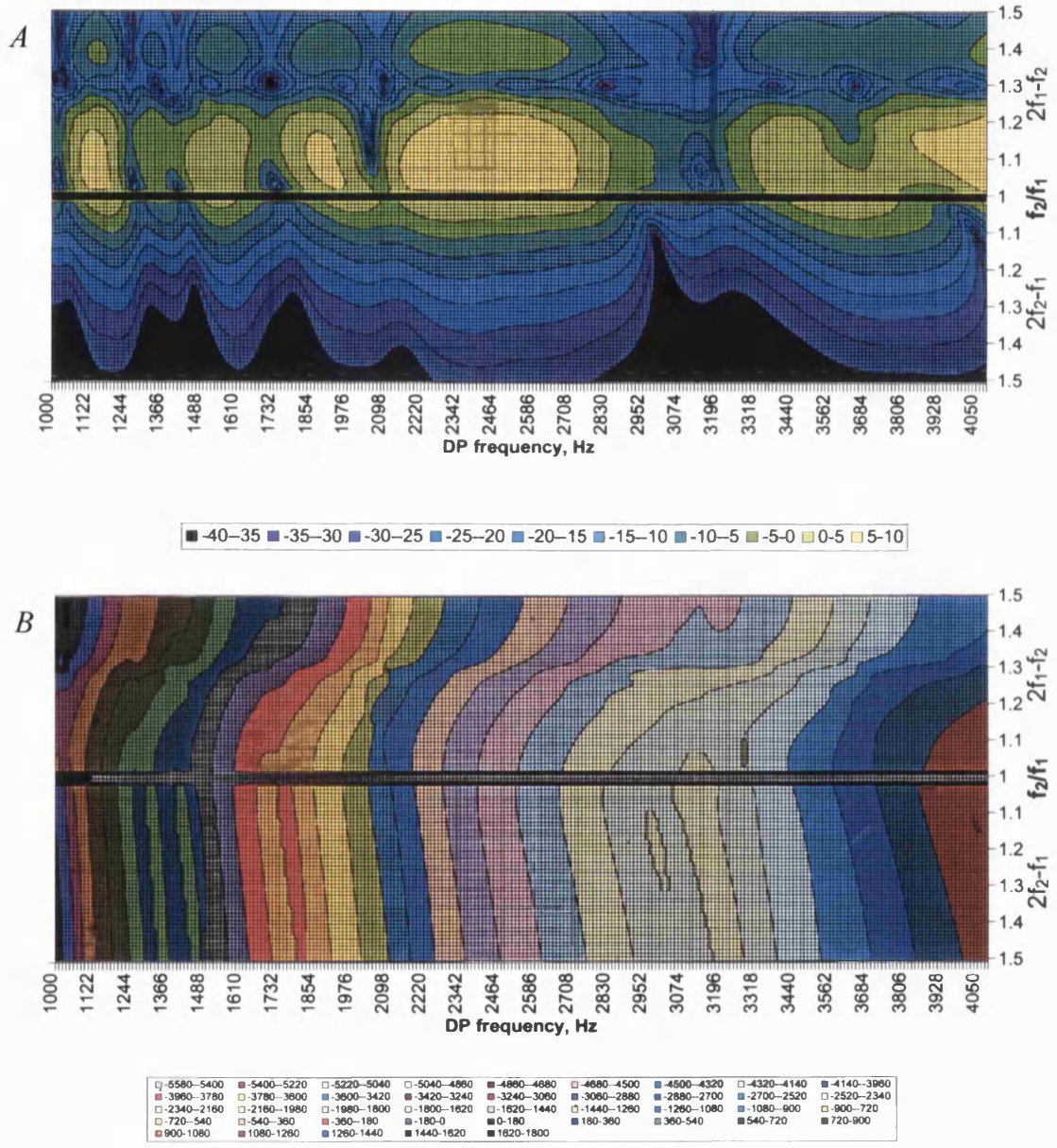

Figure 55. Place fixed DP from a transmission line model. The overall pattern of both level and phase is similar to measured place fixed DPOAE (compare to figures 45 and 46).

IV Discussion

The model level and phase data follow the general patterns of actual DP data. The model wave fixed data replicate both the dependence of the DP level on the stimulus frequency ratio and the phase dependence on the stimulus frequency ratio but independence of the emission frequency. Slight dependence of wave fixed phase on the emission frequency can sometimes be found in real DPOAE data, probably because of slight imperfections in cochlear frequency scaling and the propagation time of sound in the ear canal, both of which are not included in the present model.

The restricted range of ratios of f_2/f_1 for which the wave fixed DP is emitted strongly appears to be controlled by the phase gradient across the DP-generating region of the DP as it is generated, which reverses depending on whether f_2/f_1 is large or small. This results in the contributions from across the distributed DP source tending to preferentially sum constructively in an apical or basal direction depending on the stimulus frequency ratio. This mechanism for a variable directivity of the DP source has been proposed by Kemp and Knight (1999).

The model place fixed data also have similar patterns to the actual DPOAE data, with the upper sideband phase contours being slightly off vertical, whilst the lower sideband contours were curved and deviated more strongly from vertical than the upper sideband. The model phase data also reproduce the notchy level characteristic of experimentally obtained place fixed DPOAE, and this originates in interference between contributions from the random distribution of reflectors. It is notable success of the model that by simply adding reflections the experimental data was so closely reproduced.

In the model data, the place fixed DPOAE intensity is greater in the lower sideband than the upper sideband, whereas in the experimental data it is the other way round. The model DP level also falls more rapidly at wider ratios in the upper sideband in the model data compared to the experimental data. These features are affected by the parameters of the model such as the shape of the stimulus phase curves in the region of DP generation, the location of the gain and the input/output shape of the non-linearity.

There is a consistent notch in the lower sideband place fixed model DP level at a ratio of approximately $f_2/f_1=1.3$. Detailed inspection of spatial distribution of signal levels in the model indicated that this is caused by cancellation across the DP generation region in the forward direction. This feature is mostly not present in the experimental DPOAE data, which may be because the phase gradients and DP generating regions are less consistent in a real cochlea so the 'notch' doesn't always occur at the same frequency

ratio so is less obvious. Alternatively the notch may occur at a wider frequency ratio in experimental data at which the place fixed DPOAE has a small amplitude, making the notch less noticeable.

The parameters and details of the formulation were varied extensively within reasonable limits and the general features were found to be robust and comparable with the experimental data.

The simple model used here is not a physical model. Instead, 'cochlear like' transmission characteristics and compressive nonlinearity were built into the computational model which was then used to predict the reverse propagation of DPOAEs. Because of the formulation, the distortion products generated in the model were inevitably emitted with very similar phase and amplitude characteristics to the 'wave fixed' experimental data. However, it was necessary to insert 'reflectors' in order to create any place fixed DPOAE. Only a small number of discrete reflectors, which were active over the region of significant gain, were used. The detailed reflection model of Zweig and Shera (1995) demonstrates that even if an extensive random distribution had been used, complete cancellation among the reflectors would not occur so that a reflection is always to be expected from any distribution of reflectors. It is anticipated that other more physical cochlear models, which include a place-fixed reflection mechanism most effective in the region leading up to the DP frequency peak, would also reproduce the experimental level and phase DPOAE characteristics presented in this study.

The model is not a cochlear model but provides a means of computing the consequences of the various assumptions and simplifications about the creation of distortion products in the cochlea made in developing a qualitative explanation of observed DPOAE behaviour. The model's capacity to simulate realistic DPOAE maps serves only to support the qualitative explanation of the phenomenon observed in the previous chapter. It would not be appropriate to use the model to make quantitative predictions. However the model does support the contention that DPOAE behaviour can be simply understood to a first approximation and the qualitative model is useful for this purpose.

V. Summary and Conclusions

In the previous chapter it was shown that the separate wave and place fixed DPOAE results can be qualitatively accounted for on the basis of some reasonable assumptions about travelling wave behaviour in the cochlea and the mechanical nonlinear interaction which must take place. These assumptions have been formulated into a transmission line model consisting of a wave fixed DP source in the region of the primaries and randomly-spaced place fixed reflections in the region of the DP frequency place.

Good agreement between the model and experimental data was achieved indicating that the basic assumptions on which it is built can produce results that are compatible with DPOAE data. Differences between the model and experimental data could probably be further reduced by modifications to the modelling of the phase curve of the travelling wave and to the nonlinear interactions in the region of the stimulus tone peaks but this would add little to the understanding gained.

This study has demonstrated that the apparently complex behaviour of DPOAE phase when primary frequencies are altered can be readily understood and even predicted on the basis of a small number of reasonable assumptions about the cochlea.

The data do not support the concept of two DP generator regions, but rather one generation region with two emission routes. They clearly illustrate that interference across a distributed source controls both the observed primary ratio dependence of wave fixed DPOAEs and also the input to the reflection mechanism which is responsible for the place fixed DPOAE. When they are mixed, interference between direct and indirectly emitted DPOAEs results in additional DPOAE fine structure.

The careful separation of DPOAE components in experimental data, as demonstrated here, should simplify the task of extracting consistent physiologically significant information from DPOAE data by removing interference between the wave and place fixed emissions. However the two emission modes may contain complementary information, so neither one should be discarded.

H. Summary

a) Conclusions

The aim of this study was to investigate the underlying mechanisms involved in otoacoustic emissions.

A close relationship was found between TEOAE and DPOAE in both level and phase-versus-frequency gradient (but only if a limited set of DPOAE stimulus parameters are employed). This result provided strong evidence that the TEOAE emission mechanism is closely linked to the DPOAE place fixed emission mechanism.

Detailed DPOAE frequency maps developed during this study supported the wave and place fixed emission mechanisms proposed by Kemp in 1986. In addition to this the lower and upper DPOAE sidebands were shown to be a continuation of each other at small frequency ratios. The maps have demonstrated that not only is the upper sideband DPOAE site is linked to the DP frequency place, the place fixed part of the lower sideband DPOAE is also linked to the DP frequency place. Two mechanisms for DPOAE 'fine structure' have been identified: (1) a mixing of wave and place fixed components, which disappears when the two components are separated and (2) interference effects involved in the place fixed emission, which are still present in the place fixed DPOAE component after separation from the wave fixed component.

In order to investigate the locations of DPOAE sources on the basilar membrane, measurements of DPOAE suppression by a third stimulus tone were obtained. The method was not helpful for this purpose because the suppression tuning curves were complex and did not positively identify the source of the place fixed emission. This appeared to be because of complications due to interference effects.

The wave and place fixed emission components were successfully separated by a Fourier transform and windowing method. The individual relationships which the wave and place fixed emissions have with the stimulus frequency and ratio have been demonstrated. The detail of the place fixed phase component sheds new light on the possible mechanism for its emission. It appears that for the upper sideband the initial source for the place fixed emission is linked to the DP frequency place, and this is also the case with the lower sideband with a small frequency ratio. However, the lower sideband DP emission is linked to f_2 when stimulated with a wide frequency ratio.

The DPOAE mapping, the separated wave and place fixed DPOAE and the mathematical model all support a hypothesis for the creation of otoacoustic emissions. This consists of a single DP generator region which has variable directivity, depending largely on f_2/f_1 and which may direct the DP energy apically and basally. Energy directed apically requires a separate mechanism to reverse the direction of propagation in order for the DP to be emitted to the ear canal. This hypothesis has been supported by a simple mathematical model which produced results containing many of the features seen in experimental DPOAE.

This work has further clarified that instead of there being many mechanisms of otoacoustic emissions, all emissions can be identified with one of two mechanisms.

b) Confidence in the findings of this study

In order to unwrap the DPOAE phase for the frequency maps it was necessary to insert 360° phase steps in the lower sideband phase data at small frequency ratios. This was necessary because of the divergent phase behaviour of this data set. This process can result in an incorrect number of whole cycles being indicated between different parts of some of the data field, but the orientation of the iso-phase contours is not compromised.

The calibration of the different probe microphones agreed typically to within 3 dB. The calibration drifted by less than 1 dB over the course of the measurements. Ear canal standing waves raised calibration difficulties at high frequencies, these were minimised by optimising the probe fitting and by suspending the automatic frequency response correction in frequency regions where the ear canal frequency response was uneven. However, small departures from absolute calibration were not vital for the conclusions which have been drawn from the trends observed in this study.

The parts of this study involving detailed DPOAE frequency maps were performed on only two ears. However the data contain many features that are known to be typical of normally-hearing ears such as the divergence of phase behaviour of the lower sideband and the frequency ratio giving the maximum level of DPOAE. These and other features were seen in both ears investigated. There is therefore no reason to doubt that the results obtained here are typical of normally-hearing ears in terms of the general patterns observed in the data. Fine details will differ with each ear.

Data were generally obtained over the frequency range 1 kHz to 4.1 kHz. It remains possible that different patterns may occur outside this frequency range.

Windowing effects may have arisen in the Fourier transformation process which was employed to separate the wave and place fixed DPOAE components. The windowing employed in the frequency domain was not ideal and will have added noise in the time domain. However this noise will be of a continuous nature and therefore has been quantified by observing a window of data in the time domain after the DPOAE had died away, so the contents of this window were entirely noise. This noise estimate also includes the effect of random noise present in the original data. The noise floor calculated in this way was generally below −15 dB SPL in the frequency domain. Narrow windowing in the time domain results in 'smearing' of the data when returned to the frequency domain, but has the advantage of removing noise outside of the selected time window. Some evidence of this 'smearing' was seen in the processed data but only at low level in regions of absent DP in the original data. The data were little changed by windowing if one emission was strongly dominating in the original data, demonstrating that the processing method retained the true overall data patterns.

c) Further study

It would be of interest to observe the effect of mild hearing loss on the DPOAE frequency map, to see which parts of the map are most sensitive to cochlear damage. To achieve this, subjects with mild hearing loss would be required, or ideally a subject with progressive hearing loss to be observed in a longitudinal study.

The prevalence of certain minor details in the data, for example the fine structure of the place fixed DPOAE and the tendency of the upper sideband DPOAE to have occasional 'favoured frequencies' in which an emission can be emitted strongly even at very wide stimulus frequency ratios, could be explored by studying a larger number of normally-hearing subjects.

Acknowledgements

I would like to thank David Kemp for his assistance and advice during this project. Dave Brass and Siobhan Ryan also provided valuable advice and encouragement in the early stages. Peter Bray provided modifications to the software to allow additional functions to the macro control of DPOAE. The project was funded by the Institute of Laryngology and Otology. I am grateful to Otodynamics Ltd. for paying the tuition fees and for providing the OAE equipment.

Some of the data collected during this study have been published (Knight and Kemp, 1999b, 2000a, 2001). These papers are appended to the back of this thesis (Appendix II).

Some data has been presented at conferences (Knight and Kemp, 1999a, 2000b).

References

Aibara, R., Welsh, J.T., Puria, S. and Goode, R.L. 2001 Human middle ear transfer function and cochlear input impedance. Hearing Res. 152, 100-109.

Allen, J.B. 1980 Cochlear micromechanics: A physical model of transduction. J. Acoust. Soc. Am. 68, 1660-1670.

Allen, J.B. 1997 OHCs shift the excitation pattern via BM tension. In 'Diversity in auditory Mechanics', eds. H Duifhuis, J.W. Horst, P. van Dijk, S.M. Netten. (World scientific, Singapore) pp 167-175.

Allen, J.B. and Fahey, P.F. 1992 Using acoustic distortion products to measure the cochlear amplifier gain on the basilar membrane. J. Acoust. Soc. Am. 92, 178-188.

Allen, J.B. and Fahey, P.F. 1993 A second cochlear-frequency map that correlates distortion product and neural tuning measurements. J. Acoust. Soc. Am. 94, 809-816.

Allen, J.B. and Neely, S.T. 1992 Micromechanical models of the cochlea. Physics Today, 45 (7), 40-47.

Ashmore, J.F. 1987 A fast motile event in outer hair cells isolated from guinea pig cochlea. J. Physiol. 388, 323-347.

Avan, P., Elbez, M and Bonfils, P. 1997 Click-evoked otoacoustic emissions and the influence of high-frequency hearing losses in humans. J. Acoust. Soc. Am. 101, 2771-2777.

von Bekesy, G. 1960 Experiments in hearing. McGraw-Hill, New York.

Bell, A. 1992 Circadian and menstrual rhythms in frequency variations of spontaneous otoacoustic emissions from human ears. Hearing Res. 58, 91-100.

Boer, E. de 1983a. No sharpening? A challenge for cochlear mechanics. J. Acoust. Soc. Am. 73, 567-573.

Boer, E. de 1983b. On active and passive cochlear models – Towards a generalized analysis. J. Acoust. Soc. Am. 73, 574-576.

Bonfils, P. and Uziel, A. 1989 Clinical applications of evoked acoustic emissions: results in normally hearing and hearing-impaired subjects. Ann. Otol. Rhinol. Laryngol. 98, 326-331.

Borg, E. 1968 A quantitive study of the effect of the acoustic stapedius reflex on sound transmission through the middle ear of man. Acta oto-laryngologica 66, 461-472.

Brass, D. and Kemp, D.T. 1993a Suppression of Stimulus frequency otoacoustic emissions. J. Acoust. Soc. Am. 93, 920-939.

Brass, D. and Kemp, D.T. 1993b Analyses of Mossbauer mechanical measurements indicate that the cochlea is mechanically active. J. Acoust. Soc. Am. 93, 1502-1515.

Bray, P.J. 1989 Click evoked otoacoustic emissions and the development of a clinical otoacoustic hearing instrument. PhD thesis, University of London.

Bray, P. and Kemp, D.T. 1987 An advanced cochlear echo technique suitable for infant screening. Br. J. Audiol. 21, 191-204.

Bright, K.E. 1997 Spontaneous otoacoustic emissions. In 'Otoacoustic emissions: clinical applications.' Eds. Robinette, M.S. and Glattke, T.J. Thiele, New York. pp 46-52.

Brown, A.M. 1987 Acoustic distortion from rodent ears: A comparison of responses from rats, guinea pigs and gerbils. Hearing Res. 31, 25-38.

Brown, A.M. 1988 Continuous low level sound alters cochlear mechanics: An efferent effect? Hearing Research 34, 27-38.

Brown, A.M., McDowell, B. and Forge, A. 1989 Acoustic distortion products can be used to monitor the effects of chronic gentamicin treatment. Hearing Res. 42, 143-156.

Brown, A.M., Harris, F.P. and Beveridge, H.A. 1996 Two sources of acoustic distortion products from the human cochlea. J. Acoust. Soc. Am., 100, 3260-3267.

Brown, A.M. and Kemp, D.T. 1984 Suppressibility of the $2f_1$-f_2 stimulated acoustic emissions in gerbil and man. Hear. Res. 13, 29-37.

Brownell, W.E. 1983 Observations on a motile response in isolated outer hair cells, in 'Mechanisms of hearing', eds. Webster, W.R. and Aitken, L.M., Monash University Press, pp 5-10.

Brownell, W.E. 1990 Outer hair cell electromotility and otoacoustic emissions. Ear Hear. 11, 82-92.

Carmel, P.W. and Starr, A. 1963 Acoustic and non-acoustic factors modifying middle-ear muscle activity in waking cats. J. Neurophysiol. 26, 598-616.

Clemis, J.D. and Sarno, C.N. 1980 The acoustic reflex latency test: clinical application. The Laryngoscope 90, 601-611.

Collet, L., Kemp, D.T., Veuillet, E., Duclaux, R., Moulin, A. and Morgon, A. 1990 Effect of contralateral auditory stimuli on active cochlear micro-mechanical properties in human subjects. Hearing Res. 43, 251-261.

Collet, L., Veuillet, E., Chanal, J.M. and Morgon, A. 1991 Evoked otoacoustic emissions: Correlates between spectrum analysis and audiogram. Audiology 30, 164-172.

Dallos, P.J. 1964 Dynamics of the acoustic reflex: phenomenological aspects. J. Acoust. Soc. Am. 36, 2175-2183.

Dallos, P. 1992 The active cochlea. J. Neurosci 12, 4575-4585.

Dancer, A. 1992 Experimental look at cochlear mechanics. Audiology 31, 301-312.

Dancer, A. and Franke, R. 1980 Intracochlear sound pressure measurements in guinea pigs. Hearing Res. 2, 191-205.

Dancer, A, Avan, P and Magnan, P. 1997 Can the travelling wave be challenged by direct intracochlear pressure measurements? In 'Diversity in auditory Mechanics', eds. H Duifhuis, J.W. Horst, P. van Dijk, S.M. Netten. (World scientific, Singapore) pp 340-346.

Davis, H 1983 An active process in cochlear mechanics Hearing Res. 9, 79-90.

Dirks, D.D. and Kincaid, G.E. 1987 Basic acoustic considerations of ear canal probe measurements. Ear and Hearing 8, 60S-67S.

Dorn, P.A., Piskorski, P., Gorga, M.P., Neely, S.T. and Keefe, D.H. 1998 Predicting audiometric status from distortion product otoacoustic emissions using discriminant analysis. ARO Abst., 21, 594.

Dreisbach, L.E. and Seigel, J.H. 1999 Level and phase relationships of distortion-product otoacoustic emission sources with varied primary frequency ratios in humans. ARO Abst., 22, 392.

Elliot, E. 1958 A ripple effect in the audiogram. Nature 181, 1076.

Erminy, M., Avan, P., Baril, P., Bonfils, P. 1996 Caractéristiques du produit de distorsion $2f_2$-f_1 chez l'homme normo-entendant. Ann. Otolaryngol. Chir. Cervicofac., 113, 321-327.

Evans, E.F. 1972 The frequency response and other properties of single fibers in the guinea pig cochlea nerve. J. Physiol. 226, 263-287.

Evans, E.F. 1975 The sharpening of cochlear frequency selectivity in the normal and abnormal cochlea. Audiology 14, 419-442.

Fahey, P.F. and Allen, J.B. 1997. Measurement of distortion product phase in the ear canal of the cat. J. Acoust. Soc. Am., 102, 2880-2891.

Fahey, P.F., Stagner, B.B., Lonsbury-Martin, B.L. and Martin, G.K. 2000 Theory for two new routes of distortion product generation. ARO Abst., 23, 478.

Fawcett, D.W. 1986 A textbook of histology. W.B Saunders, Philadelphia.

Fernández, C. 1952 Dimensions of the cochlea (Guinea Pig). J. Acoust. Soc Am. 24, 519, 523.

Frank, G. and Kössl, M. 1996 The acoustic two-tone distortions 2f1-f2 and f2-f1 and their possible relation to changes in the operating point of the cochlear amplifier. Hearing Res. 98, 104-115.

Furst, M., Rabinowitz, W.M. and Zurek, P.M. 1988 Ear canal acoustic distortion at 2f1-f2 from human ears: Relation to other emissions and perceived combination tones. J. Acous. Soc. Am., 84, 215-221.

Gaskill, S.A. and Brown, A.M. 1990 The behavior of the acoustic distortion product, $2f_1$-f_2, from the human ear and its relation to auditory sensitivity J. Acoust. Soc. Am., 88, 821-839.

Gaskill, S.A. and Brown, A.M. 1996 Suppression of human acoustic distortion product: Dual origin of 2f1-f2. J. Acoust. Soc. Am. 100, 3268-3274

Geisler, C.D. 1993. A realizable cochlear model using feedback from motile outer hair cells. Hearing Res. 68, 253-262.

Gifford, M.L. and Guinan, J.J. 1987 Effect of electrical stimulation of medial olivocochlear neurons on ipsilateral and contralateral cochlear responses. Hearing Res. 29, 179-194.

Gold, T. 1948 Hearing II The physical basis of the action of the cochlea. Proceeding of the Royal Society of Biological Sciences, 135, 492-498.

Gorga, M.P., Neely, S.T., Bergman, B.M., Beauchaine, K.L., Kaminski, J.R., Peters, J., Schulte, L. and Jesteadt, W. 1993 A comparison of transient-evoked and distortion product otoacoustic emissions in normal-hearing and hearing-impaired subjects. J. Acoust. Soc. Am. 94, 2639-2648

Gorga, M.P., Neely, S.T., Ohlrich, B., Hoover, B., Redner, J. and Peters, J. 1997 From laboratory to clinic: a large scale study of distortion product otoacoustic emissions in ears with normal hearing and ears with hearing loss. Ear Hear. 18, 440-455.

Harris, F.P., Lonsbury-Martin, B.L., Stagner, B.B., Coats, A.C. and Martin, G.K. 1989 Acoustic distortion products in humans: systematic changes in amplitude as a function of f_2/f_1 ratio. J. Acoust. Soc. Am., 85, 220-229.

Harris, F.P., Probst, R. and Wenger, R. 1991 Repeatability of transiently evoked otoacoustic emissions in normally hearing humans. Audiology, 30, 135-141.

Hauser, R., and Probst, R. 1991 The influence of systematic primary-tone level variation L_2-L_1 on the acoustic distortion product emission $2f_1$-f_2 in normal human ears. J. Acoust. Soc. Am., 89, 280-286.

He, N. and Schmiedt, R.A. 1993 Fine structure of the $2f_1$-f_2 acoustic distortion product: Changes with primary level. J. Acoust. Soc. Am., 94, 2659-2669.

He, N. and Schmiedt, R.A. 1997 Fine structure of the $2f_1$-f_2 acoustic distortion product: effects of primary level and frequency ratios. J. Acoust. Soc. Am., 101, 3554-3565.

Heitmann, J., Waldmann, B., Schnitzler, H., Plinkert. P.K. and Zenner, H. 1998 Suppression of distortion product otoacoustic emissions (DPOAE) near $2f_1$-f_2 removes DP-gram fine structure - Evidence for a secondary generator. J. Acoust. Soc. Am., 103, 1527-1531.

Holube, I., Kinkel, M. and Kollmeier, B. 1998 Binaural and monaural auditory filter bandwidths and time constants in probe tone detection experiments. J. Acoust. Soc. Am. 104, 2412-2425.

Hudspeth, A.J. 1989 How the ear's works work. Nature 341, 397-404.

Johnstone, B.M, Patuzzi, R. and Yates, G.K. 1986 Basilar membrane measurements and the travelling wave. Hearing Res. 22, 147-153.

Kalluri, R. and Shera, C. 2000 Are DPOAEs a mixture of emissions generated by different mechanisms? ARO Abst. 23, 480.

Kemp, D.T. 1978 Stimulated acoustic emissions from within the human auditory system. J. Acoust. Soc. Am., 64(5), 1386-1391.

Kemp, D.T. 1979a Evidence of mechanical nonlinearity and frequency selective wave amplification in the cochlea. Arch. Otorhinolaryngol. 224, 37-45.

Kemp, D.T. 1979b The evoked cochlear mechanical response and the auditory microstructure – Evidence for a new element in cochlear mechanics. Scand. Audiol. Suppl. 9, 35-47.

Kemp, D.T. 1980 Towards a model for the origin of cochlear echoes. Hear. Res. 2, 533-548.

Kemp, D.T. 1986 Otoacoustic emissions, travelling waves and cochlear mechanisms. Hear. Res., 22, 95-104.

Kemp, D.T. 1987 Otoacoustic emission characteristics during moderate continuous stimulation- intermodulation. 12th International Congress of Acoustics B7-1.

Kemp, D.T. 1997 "Otoacoustic emissions in perspective." In Otoacoustic emissions, Clinical perspectives, edited by M.S. Robinette and T.J. Glattke (New York, Thiele) pp 1-21.

Kemp, D.T. 1998 "Otoacoustic emissions: distorted echoes of the cochlea's travelling wave." in Otoacoustic emissions basic science and clinical applications, edited by C.I. Berlin (Singular Publishing Group, San Diego) Chap. 1, pp 1-59, fig. 1-12.

Kemp, D.T., Bray, P., Alexander, L. and Brown, A. M. 1986 Acoustic emission cochleography - practical aspects. Scand. Audiol. Suppl. 25 71-95.

Kemp, D.T. and Brown, A.M. 1983 An integrated view of cochlear mechanical nonlinearities observable from the ear canal. Cochlear Mechanics (De Boer, E., Viergever M.,A. eds), Delft University Press, Holland.

Kemp, D.T. and Brown, A.M. 1984 Ear canal acoustic and round window electrical correlates of 2f1-f2 distortion generated in the cochlea. Hearing Res 13, 39-46.

Kemp D.T. and Chum, R.A. 1980a Properties of the generator of stimulated acoustic emissions. Hear. Res. 2, 213-232

Kemp D.T. and Chum, R.A. 1980b Observations on the generator mechanism of stimulus frequency acoustic emissions - two tone suppression, in Psychophysical, physiological and behavioural studies in hearing. (van den Brink and Bilsen eds), Delft University Press, Holland. pp 34-42.

Kemp, D.T. and Knight, R.D. 1999 Virtual DP reflector explains DPOAE wave and place fixed dichotomy. ARO Abst., 22, 396.

Kemp, D.T., Ryan, S. and Bray, P. 1990 A guide to the effective use of Otoacoustic Emissions. Ear Hear., 11(2), 93-105.

Kennedy, C.R., Kimm, L., Cafarelli Dees, D., Campbell, M.J. and Thornton, A.R.D. (Wessex Universal Neonatal Hearing Screening Trial Group) 1998 Controlled trial of universal neonatal screening for early identification of permanent childhood hearing impairment. The Lancet, 352, 1957-1964.

Kennedy, C.R., Kimm, L., Thornton, R. and Davis, A. 2000 False positives in universal neonatal screening for permanent childhood hearing impairment The Lancet, 35, 1903-1904.

Kessel R.G. and Kardon R.H. 1979 'Tissues and Organs: A Text-Atlas of scanning Electron Microscopy', W.H. Freeman and Co., San Francisco)

Khanna, S.M. and Tonndorf, J. 1972 Tympanic membrane vibrations in cats studied by time-averaged holography. J. Acoust. Soc. Am. 51, 1904-1920.

Kiang, N.Y.S., Moxon, E.C. and Levine R.A. 1970 Auditory-nerve activity in cats with normal and abnormal cochleas. In 'Sensorineural hearing loss', eds. G.E.W. Wolstenholme and J. Knight. CIBA Foundation symposium, Churchill, London. pp 241-268.

Kim, D.O. 1980. Cochlea mechanics: Implications of electrophysiological and acoustical observations. Hear Res. 2, 297–317.

Kimberley, B.P, Brown, D.K. and Eggermont, J.J. 1993 Measuring human cochlear travelling wave delay using distortion product emission phase responses. J. Acoust. Soc. Am. 94, 1343-1350.

Kinsler, L.E., Frey, A.R., Coppens, A.B. and Sanders, J.V. 1982 Fundamentals of acoustics. Wiley, New York.

Kleine, E. de, Wit, H.P., van Dijk, P. and Avan, P. 2000 The behavior of spontaneous otoacoustic emissions during and after postural changes. J. Acoust. Soc. Am. 107, 3308-3316.

Knight, R.D. 1997 Relationships between DPOAE and TEOAE in normal subjects. MSc project, University College London.

Knight, R.D. and Kemp, D.T. 1999a f_1, f_2 area representations of DPOAEs indicate that the clinical 2f1-f2 DPOAE is an atypical form of OAE. Brit. J. Audiol. 33, 87.

Knight, R.D. and Kemp, D.T. 1999b Relationships between DPOAE and TEOAE characteristics. J. Acous. Soc. Am. 106, 1420-1435.

Knight, R.D. and Kemp, D.T. 2000a Indications of different DPOAE mechanisms from a detailed f1, f2 area study. J. Acoust. Soc. Am., 107, 457 – 473.

Knight, R.D. and Kemp, D.T. 2000b Separation of "wave" and "place" fixed $2f_1$-f_2 DPOAE. ARO Abst., 23, 987.

Knight, R.D. and Kemp, D.T. 2001 Wave and place fixed maps of the human ear. J. Acoust. Soc. Am 109, 1513-1525.

Kollmeier, B. and Holube, I. 1992. Auditory filter bandwidths in binaural and monaural listening conditions. J. Acoust. Soc. Am., 92, 1889-1901.

Konrad-Martin, D., Neely, S.T., Keefe, D.H., Dorn, P.A and Gorga, M.P. 2001 Sources of distortion product otoacoustic emissions revealed by suppression experiments and inverse fast Fourier transforms in normal ears. J. Acoust. Soc. Am. 109, 2862-2879.

Kummer, P., Janssen, T. and Arnold, W. 1995 Suppression tuning characteristics of the 2fl-f2 distortion-product otoacoustic emission in humans. J. Acoust. Soc. Am. 98, 197-210.

Kusuki, M., Sakashita, T., Kubo, T., Kyunai, K., Ueno, K., Hikawa, C., Wada, T and Nakai, Y. 1998 Changes in distortion product otoacoustic emissions from ears with Meniere's disease. Acta Otolaryngol Suppl 538, 78-89.

Kvaerner, K.J., Engdahl, B., Aursnes, J., Arnesen, A.R. and Mair, I.W.S. 1996 Transient-evoked otoacoustic emissions, helpful tool in the detection of pseudohypacusis. Scand. Audiol. 25, 173-177.

Liberman, M.C. and Kiang, N.Y-S. 1978 Acoustic trauma in cats. Acta Otolaryngol. (Suppl 358), 1-63.

Lim, D.J. 1980 Cochlear anatomy related to cochlear micromechanics. A review. J. Acoust. Soc. Am. 67, 1686-1695.

Lim, D.J. 1986a Effects of noise and ototoxic drugs at the cellular level in the cochlea: A review. Am. J. Otolaryngol. 7, 73-99.

Lim, D.J. 1986b Functional structure of the organ of Corti: a review. Hearing Res. 22, 117-146.

Lonsbury-Martin, B.L., Martin, G.K., Probst, R. and Coats, A.C. 1988 Spontaneous otoacoustic emissions in a non-human primate. II Cochlear Anatomy. Hear. Res. 33, 69-94.

Lonsbury-Martin, B.L., Harris, F.P., Stagner, B.B., Hawkins, M.D. and Martin, G.K. 1990 Distortion product emissions in humans II Relations to acoustic immittance and stimulus frequency and spontaneous otoacoustic emissions in normally hearing subjects. Ann. Otol. Rhinol. Laryngol. Suppl. 147, 99, 15-29.

Lutman, M.E., Mason, S.M., Sheppard, S. and Gibbin, K.P. 1989 Differential diagnosis potential of otoacoustic emissions: A case study. Audiology, 28, 205-210.

Lutman, M.E., Davis, A.C., Fortnum, H.M. and Wood, S. 1997 Field sensitivity of targeted neonatal hearing screening by transient-evoked otoacoustic emissions. Ear and Hearing, 18, 265-276.

Lynch, T.J., Nedzelnitsky, V. and Peake, W.T. 1982 Input impedance of the cochlea in cat. J. Acoust. Soc. Am. 72, 108-130.

Magnan, P., Avan, P., Dancer, A., Probst, R. and Smurzynski, J. 1997 A new approach to cochlear mechanics and cubic distortion tones by intracochlear acoustic pressure measurements in the guinea pig. In 'Diversity in auditory Mechanics', eds. H Duifhuis, J.W. Horst, P. van Dijk, S.M. Netten. (World scientific, Singapore) pp 333-339.

Mammano, F. and Nobili, R. 1993 Biophysics of the cochlea: Linear approximation. J. Acoust. Soc. Am. 93, 3320-3332.

Martin, G.K., Lonsbury-Martin B.L., Probst, R., Scheinin, S.A. and Coats, A.C. 1987 Acoustic distortion products in rabbit ear canal. II. Sites of origin revealed by suppression contours and pure tone exposures. Hear. Res., 28, 191-208.

Martin, G.K., Jassir, D., Stagner, B.B., Whitehead, M.L. and Lonsbury-Martin B.L. 1998 Locus of generation for the $2f_1$-f_2 vs. $2f_2$-f_1 distortion-product otoacoustic emissions in normal-hearing humans revealed by suppression tuning, onset latencies, and amplitude correlations. J. Acoust. Soc. Am. 103, 1957-1971.

Martin, G.K., Stagner, B.B., Fahey, P.F. and Lonsbury-Martin B.L. 1999a Influence of even-order nonlinearities on the suppression and enhancement of DPOAEs above f_2 in rabbits. Association for Research in Otolaryngology Abstracts 22, 382.

Martin, G.K., Stagner, B.B., Jassir, D., Telischi, F.F. and Lonsbury-Martin B.L. 1999b Suppression and Enhancement of distortion-product otoacoustic emissions by interference tones above f_2. I Basic findings in rabbits. Hear Res. 136, 105-123.

Martin, G.K., Stagner, B.B. and Lonsbury-Martin B.L. 2000 Harmonic otoacoustic emissions in normal and noise-exposed rabbits. ARO Abst., 23, 231.

Mauermann, M., Uppenkamp, S., van Hengel, P.W. and Kollmeier, B. 1999a Evidence for the distortion product frequency as a source of distortion product otoacoustic emission (DPOAE) fine structure in humans. I. Fine structure and higher-order DPOAE as a function of the frequency ratio f_2/f_1. J. Acoust. Soc. Am. 106, 3473-3482.

Mauermann, M., Uppenkamp, S., van Hengel, P.W. and Kollmeier, B. 1999b Evidence for the distortion product frequency as a source of distortion product otoacoustic emission (DPOAE) fine structure in humans. II. Fine structure for different shapes of cochlear hearing loss. J. Acoust. Soc. Am. 106, 3473-3482.

Merchant, S.N., Ravicz, M.E. and Rosowski, J.J. 1996 Acoustic input impedance of the stapes and cochlea in human temporal bones. Hearing Res. 97, 30-45.

Moulin, A. 2000 Influence of primary frequencies ratio on distortion product otoacoustic emissions amplitude. I. Intersubject variability and consequences on the DPOAE-gram. J. Acoust. Soc. Am. 107, 1460-1470.

Moulin, A, Collet, L., Delli, D. and Morgon, A. 1991 Spontaneous otoacoustic emissions and sensori-neural hearing loss. Acta Otolaryngol 111, 835-841.

Moulin, A., Collet, L., Veuillet, E., and Morgon, A. 1993 Interrelations between transiently evoked otoacoustic emissions and acoustic distortion products in normally hearing subjects. Hear. Res.65, 216-233.

Moulin, A., Bera, J.C. and Collet, L. 1994 Distortion product otoacoustic emissions and sensorineural hearing loss. Audiol., 33, 305-326.

Moulin, A. and Kemp, D.T. 1996 Multicomponent acoustic distortion product otoacoustic emission phase in humans. I. General characteristics. J. Acoust. Soc. Am., 100, 1617-1639.

Moulin, A., Jourdain, F. and Collet, L. 1999 Using acoustic distortion product otoacoustic emissions in clinical applications: Influence of f_2/f_1 on DPOAE gram. Br. J. Audiol. 33, p89.

Mountain, D.C. 1980 Changes in endolymph potential and crossed olivocochlear bundle stimulation alter cochlear mechanics. Science 210, 71-72.

Narayan, S.S., Temchin, A.N., Recio, A and Ruggero, M.A. 1998 Frequency tuning of basilar membrane and auditory nerve fibers in the same cochleae. Science 282, 1882-1884.

Neely, S.T. and Kim, D. O. 1986 A Model for active elements in cochlear biomechanics. J. Acoust. Soc. Am. 79, 1472 - 1480.

Norton, S.J. 1993 Application of transient evoked otoacoustic emissions to pediatric populations. Ear. Hear. 14, 64-73.

Norton, S.J. and Rubel, E.W. 1990 "Active and passive ADP components in mammalian and avian ears", in "The mechanics and Biophysics of hearing", Lecture

notes in biomathematics, (eds. P Dallos, C.D. Geisler, J.W. Matthews, M.A Ruggero and C.R. Steele (Springer-Verlag, Berlin) 87, 219-226.

Norton, S.J. Gorga, M.P., Widen, J.E., Folsom, R.C., Sininger, Y. Cone-Wesson, B., Vohr, B.R., Mascher, K and Fletcher, K. 2000a Identification of neonatal hearing impairment: Evaluation of transient evoked otoacoustic emission, distortion product otoacoustic emission and auditory brain stem response test performance. Ear Hear. 21, 508-528.

Norton, S.J. Gorga, M.P., Widen, J.E., Folsom, R.C., Sininger, Y. Cone-Wesson, B., Vohr, B.R. and Fletcher, K. 2000b Identification of neonatal hearing impairment: Summary and recommendations. Ear Hear. 21, 529-535.

O Mahoney, C.F. and Kemp, D.T. 1995 Distortion product otoacoustic emission delay measurement in human ears. J. Acoust. Soc. Am., 97, 3721-3735.

Otodynamics Ltd. 1994 The Otodynamics ILO92 DPOAE software research manual.

Patterson, R.D. 1976 Auditory filter shapes derived with noise stimuli. J. Acoust. Soc. Sm., 59, 640-654.

Penner, M.J. 1988 Audible and annoying spontaneous otoacoustic emissions. Archives of otolaryngology, head and neck surgery. 114, 150-153.

Penner, M.J. and Zhang, T. 1997 Prevalence of spontaneous otoacoustic emissions in adults revisited. Hearing Res. 103, 28-34.

Pickles, J.O., Comis, S.D. and Osborne, M.P. 1984 Cross-links between stereocilia in the guinea-pig organ of Corti and their possible relation to sensory transduction. Hearing Res. 15, 103-112.

Pickles, J.O 1988 An introduction to the physiology of hearing. (2nd Ed.) Academic Press, London.

Preyer, S., Hemmert, W., Zenner, H.P. and Gummer, A.W. 1995 Abolition of the receptor potential response of isolated mammalian outer hair cells by hair-bundle treatment with elastase: a test of the tip-link hypothesis. Hearing Res. 89, 187-193.

Prieve, B. A., Gorga, M. P., Schmidt, A., Neely, S., Peters, J., Schules, L. and Jesteadt, W. 1993 Analysis of transient-evoked otoacoustic emissions in normal hearing and hearing-impaired ears. J. Acoust. Soc. Am., 93, 3308-3319.

Probst, R. and Harris, R. 1993 Transiently evoked and distortion-product otoacoustic emissions. Arch. Otolaryngol. Head Neck Surg., 119, 858-860.

Recio, A., Rich, N.C., Narayan, S.S. and Ruggero, M.A. 1998 Basilar-membrane responses to clicks at the base of the chinchilla cochlea. J Acoust. Soc. Am. 103, 1972-1988.

Rhode, W.S. 1971 Observations of the vibration of the basilar membrane in squirrel monkeys using the Mossbauer technique. J. Acoust. Soc. Am. 49, 1218-1231.

Robinette, M.S. 1992 Clinical observations with transient evoked otoacoustic emissions with adults. Seminars in hearing, 13, 23-36.

Robinette, M.S. and Facer, G.W. 1991 Evoked otoacoustic emissions in differential diagnosis: A case report. Otolaryngology – head and neck surgery. 105, 120-123.

Robinette, M.S. and Durrant, J.D. 1997 Contributions of evoked otoacoustic emissions in differential diagnosis of retrocochlear disorders, in 'Otoacoustic emissions: clinical applications.' Eds. Robinette, M.S. and Glattke, T.J. Thiele, New York. pp. 205-232.

Robinson, D.W. and Dadson, R.S. 1956 A re-determination of the equal-loudness relations for pure tones. Brit. J. of Appl. Physics 7, 166-181.

Robles, L, Ruggero, M.A. and Rich, N.C. 1986 Basilar membrane mechanics at the base of the cochlea. I. Input-output functions, tuning curves and response phases. J. Acoust. Soc. Am. 80, 1364-1374.

Ruggero, M.A., Rich, N.C., Robles, L. and Shivapuja B.G. 1990 Middle ear response in the chinchilla and its relationship to mechanics at the base of the cochlea. J. Acoust. Soc. Am. 87, 1612-1629.

Ruggero, M.A., Narayan, S.S., Temchin, A.N. and Recio, A. 2000 Mechanical bases of frequency tuning and neural excitation at the base of the cochlea: Comparison of basilar-membrane vibrations and auditory-nerve-fiber responses in chinchilla. Proceedings of the National Academy of Sciences of the United States of America. 97, 11744-11750.

Rutten, W.L.C. 1980 Evoked acoustic emissions from within normal and abnormal human ears: Comparison with audiometric and electrocochleographic findings. Hearing Res. 2, 263-271.

Ryan A.F. and Dallos, P. 1984 Physiology of the cochlea. In 'Hearing disorders', pp 253-266 (ed J.L. Northern). Little Brown, Boston.

Sellick, P.M., Patuzzi, R. and Johnstone, B.M. 1982 Measurement of basilar membrane motion in the guinea pig using the Mossbauer technique. J. Acoust. Soc. Am. 72, 131-141.

Sellick, P.M., Patuzzi, R and Johnstone, B.M. 1983 Comparison between the tuning properties of inner hair cells and basilar membrane motion. Hearing Res. 93-1000.

Shaw, E.A.G. 1974 The external ear. In 'Handbook of Sensory Physiology', Vol 5/1, pp 455-490. (eds W.D. Keidel and W.D. Neff) Springer, Berlin.

Shera, C.A and Guinan, J.J. 1998 Reflection emissions and distortion products arise by fundamentally different mechanisms. Association for Research in Otolaryngology Abstracts 344.

Shera, C.A. and Guinan, J.J. 1999 Evoked otoacoustic emissions arise by two fundamentally different mechanisms: A taxonomy for mammalian OAEs. J. Acoust. Soc. Am., 105, 782-798.

Shera, C.A. and Zweig, G. 1993 Noninvasive measurement of the cochlear traveling-wave ratio. J. Acoust. Soc. Am., 93, 3333-3352.

Siegel, J.H. 1994 Ear-canal standing waves and high-frequency sound calibration using otoacoustic emission probes. J. Acoust. Soc. Am. 95, 2589-2597.

Siegel, J.H. and Hirohata, E.T. 1994 Sound calibration and distortion product otoacoustic emissions at high frequencies. Hearing Res. 80, 146-152.

Siegel, J. and Kim, D.O. 1982 Efferent neural control of cochlear mechanics? Olivocochlear bundle stimulation affects cochlear biomechanical nonlinearity. Hearing Res. 6, 171-182.

Siegel, J., Borneman, A. and Dreisbach, L. 2000 Suppressor conditions for optimal separation of distortion product otoacoustic emission sources. ARO Abst., 23, 983.

Simmons, 1964 Perceptual theories of middle ear muscle function. Ann. Otol. Rhinol. Laryngol. 73, 724-740.

Smurzinsky, J. and Kim, D.O. 1992 Distortion-product and click-evoked otoacoustic emissions of normally-hearing adults. Hear. Res. 58, 227-240.

Smurzinsky, J., Jung, M.D., Lafreniere, D., Kim, D.O., Kamath, M.V., Rowe, J.C., Holman, M.C. and Leonard, G. 1993 Distortion-product and click-evoked otoacoustic emissions of preterm and full-term infants. Ear Hear. 14, 258-274.

Stein, L., Tremblay, K., Pasternak, J., Banerjee, S., Lindemann, K. and Kraus, N. 1996 Brainstem abnormalities in neonates with normal otoacoustic emissions. Seminars in hearing, 17, 197-213.

Steinberg, J.C. and Gardner, M.B. 1937 The dependence of hearing impairment on sound intensity. J. Acoust. Soc. Am. 9, 11-23.

Stover, L.J., Neely, S.T. and Gorga, M.P. 1996a. Latency and multiple sources of distortion product otoacoustic emissions J. Acoust. Soc. Am., 99, 1016-1024.

Stover, L., Gorga, M.P., Neely, S.T. and Montoya, D. 1996b Toward optimising the clinical utility of distortion product otoacoustic emission measurements. J. Acoust. Soc. Am. 100(2), 956-967.

Strube, H.W. 1989. Evoked otoacoustic emissions as cochlear Bragg reflections. Hear. Res., 38, 35-46.

Sun, X., Schmiedt, R.A., He, N. and Lam, C.F. 1994a Modeling the fine structure of the $2f_1$-f_2 acoustic distortion product. I. Model Development. J. Acoust. Soc. Am., 96, 2166-2174.

Sun, X., Schmiedt, R.A., He, N. and Lam, C.F. 1994b Modeling the fine structure of the $2f_1$-f_2 acoustic distortion product. II. Model Evaluation. J. Acoust. Soc. Am., 96, 2175-2183.

Talmadge, Long, G.R., C.L., Tubis, A. and Dhar, S. 1999 Experimental confirmation of the two-source interference model for the fine structure of distortion product otoacoustic emissions. J. Acoust. Soc. Am., 105, 275-292.

Talmadge, C.L., Tubis, A., Long, G.R. and Tong, C. 2000 Modelling the combined effects of basilar membrane nonlinearity and roughness on stimulus frequency otoacoustic emission fine structure. J. Acoust. Soc. Am. 108, 2911-2932.

Tavartkiladze, G.A., Frolenkov, G.I., Kruglov, A.V. and Artamasov, S.V. 1994a Ipsilateral suppression effects on transient evoked otoacoustic emission. Brit. J. Audiol. 28, 193-204.

Tavartkiladze, G.A., Frolenkov, G.I., Kruglov, A.V. and Artamasov, S.V. 1994b Ipsilateral suppression of transient evoked otoacoustic emissions. In 'Otoacoustic emissions: Clinical applications', eds M.S. Robinette and T.J. Glattke (Thiele, New York).

Tavartkiladze, G.A., Frolenkov, G.I., and Artamasov, S.V. 1996 Ipsilateral suppression of transient evoked otoacoustic emission: Role of the medial olivovovhlear system. Acta Otolaryngol. 116, 213-218.

Tubis, A., Talmadge, C., Long, G.R., Dhar, S. and Tong, C. 2000 Amplitude and group-delay finestructures of distortion product otoacoustic emissions as functions of primary levels and frequency ratios. ARO Abst., 23, 483.

Wable, J., Collet, L. and Chéry-Croze, S. 1996 Phase delay measurements of distortion product otoacoustic emissions at $2f_1$-f_2 and $2f_2$-f_1 in human ears. J. Acoust. Soc. Am. 100(4), 2228-2235.

Watkin, P.M. 1996a Neonatal otoacoustic screening and the identification of deafness. Arch. Dis. Child (Fetal Neonatal Ed.) 74, F16-25.

Watkin, P.M. 1996b Outcomes of neonatal screening for hearing loss by otoacoustic emission. Arch. Dis. Child (Fetal Neonatal Ed.) 75, F158-168.

Watkin, P.M. and Baldwin, M. 1999 Confirmation of deafness in infancy. Arch. Dis. Child 81, 380-389.

Wever, E. G. 1938 The width of the basilar membrane in man. The annals of otology, rhinology and laryngology. 47, 37-47.

Wever, E. G. and Vernon, J.A. 1955 The effects of the tympanic muscle reflexes upon sound transmission. Acta Otolaryngol. 45, 433-439.

White, K.R., Vohr, E.R. and Behrens, T.R. 1993 Universal newborn hearing screening using transient evoked otoacoustic emissions: results of the Rhode Island hearing assessment project. In: The Rhode Island hearing assessment project: Implications for universal newborn hearing screening. Seminars in Hearing 14, 18-27.

Whitehead, M.L., Lonsbury-Martin, B.L. and Martin, G.K. 1990 "Actively and passively generated acoustic distortion at $2f_1$-f_2 in rabbits", in "The mechanics and Biophysics of hearing", Lecture notes in biomathematics, (eds. P Dallos, C.D. Geisler, J.W. Matthews, M.A Ruggero and C.R. Steele (Springer-Verlag, Berlin) 87, 243-250.

Whitehead, M.L., McCoy, M.J., Lonsbury-Martin, B.L. and Martin, G.K. 1995 Dependence of distortion-product otoacoustic emissions on primary levels in normal and impaired ears. I. Effects of decreasing L_2 below L_1. J. Acous. Soc. Am., 97, 2346-2358.

Whitehead, M.L., Stagner. B.B., Martin, G.K. and Lonsbury-Martin, B.L. 1996. Visualization of the onset of distortion-product emissions and measurement of their latency. J. Acoust. Soc. Am., 100, 1663-1679.

Widick, M.P., Telischi, F.F., Lonsbury-Martin, B.L. and Stagner, B.B. 1994 Early effects of cerebellopontine angle compression on rabbit distortion-product otoacoustic emissions: a model for monitoring cochlear function during acoustic neuroma surgery. Otolaryngol. Head Neck Surg. 111, 407-416.

Wilson, J.P. 1980 Evidence for a cochlear origin for acoustic re-emissions, threshold fine-structure and tonal tinnitus. Hear. Res., 2, 233-252.

Wright, A. 1984 Dimensions of the cochlear stereocilia in man and the guinea pig. Hearing Res. 13 89-98.

Wright, A, Davis, A., Bredberg, G., Ulehlova, L and Spencer, H. 1987 Hair cell distributions in the normal human cochlea. Acta Otolaryngol. Suppl. 444, 1-48.

Yardley, M.P.J., Davies, C.M and Stevens, J.C. 1998 Use of transient evoked otoacoustic emissions to detect and monitor cochlear damage caused by platinum-containing drugs. Brit. J. Audiol. 32, 305-316

Yates, G.K and Johnstone, B.M. 1979 Measurement of basilar membrane movement, in 'Auditory Investigation: The scientific and technological basis', edited by H.A. Beagley (Clarendon, Oxford) pp 418-430.

Yates, G.K. and Withnell, R.H. 1999 The role of intermodulation distortion in transient-evoked otoacoustic emissions. Hearing Research 136, 49-64.

Zakrisson, J.E. and Borg, E. 1974 Stapedius reflex and Auditory fatigue. Audiology 13, 231-235.

Zhang, M. and Abbas, P.J. 1997 Effects of middle ear pressure on otoacoustic emission measures. J. Acoust. Soc Am., 102, 1032-1037.

Zurek, P.M. 1981 Spontaneous narrowband acoustic signals emitted by human ears. J. Acoust. Soc. Am. 69, 514-523.

Zweig, G. and Shera, C.A. 1995 The origin of periodicity in the spectrum of evoked otoacoustic emissions. J. Acoust. Soc. Am., 98, 2018-2047.

Zwicker, E. and Schloth, E. 1984 Interrelation of different otoacoustic emissions. J. Acoust. Soc. Am. 75, 1148-1153.

Zwislocki, J. 1962 Analysis of middle ear function. Part 1: Input impedance. J Acoust. Soc. Am. 34, 1514-1523.

Appendix I - Model formulation

The main formulae for the model are listed below.

Frequency parameter array

For the purpose of this model, an array of 'frequency parameters' were ascribed to the model elements. A phase delay of 3 cycles was incurred by a stimulus in travelling to the place of its corresponding 'frequency parameter'. At a stimulus level of 70 dB SPL, the travelling wave amplitude peaked at the appropriate 'frequency parameter'. For lower stimulus levels, the travelling wave peak would be slightly beyond the 'frequency parameter'.

The 'frequency parameter' of each model element is calculated as follows:

$$\text{Frequency parameter}(f_p)=25000\times 0.995595^{(n-1)} \quad -(1)$$

Where n=the number of the model element

The 'frequency parameter' is used in the calculation of the phase gradients and the gain characteristics. The gain and damping is balanced such that, at low levels, the travelling wave envelope peaks at the frequency parameter corresponding to the stimulus frequency.

Phase curve

$$\text{Phase lag (radians)}=6\pi\left\{\frac{(e^{(2f/fp)})-(e^{(2f/25111)})}{2.3e}\right\} \quad -(2)$$

Where f= the stimulus frequency of the travelling wave

f_p= frequency parameter

The second part of the numerator ensures that the phase lag at the first model element is 0. Where this term is ≈ 0, there are 3 phase cycles to the frequency place. With high frequencies, the number of phase cycles reduces slightly because part of the phase curve is 'lost' at the basal end of the model. The phase gradient at the peak of the travelling wave is the same for all frequencies.

Conversion of Stimulus level to travelling wave amplitude

The stimulus level is entered into the model in dB SPL, which is converted to pascals.

In order to obtain the initial amplitude of the travelling wave the sound pressure in pascals is multiplied by the phase difference between the first two model elements for

that frequency and arbitrarily by 100. The travelling wave amplitude is of arbitrary units.

Gain

The non-linear gain is defined as follows:

$$G=1+(g_L/C) \quad - (3)$$

Where g_L defines the place envelope of the maximum gain (the gain which would be obtained if the travelling wave amplitude were small). C is a compression function which reduces the gain which is achieved depending on the travelling wave amplitude.

g_L is calculated as follows:

$$g_L= \frac{(0.12(1.1f/f_p)^{10})}{(1+(1.1f/f_p)^{25})} \quad - (4)$$

Where f=travelling wave frequency

f_p= frequency parameter

The gain is therefore restricted to a region centred just before the travelling wave peak.

$$C= (3L_T)^{1.2}+1 \quad - (5)$$

Where L_T=total apical-going travelling wave amplitude of f_1 and f_2 (for suppression of DP gain, self-suppression by f_{DP} is also included.)

Damping

The damping is based on the travelling wave phase gradient and is therefore proportional to the time spent at that element, with a constant added:

$$\text{Damping (D)}=0.0003(300\Delta\phi)^2+0.001 \quad - (6)$$

Where $\Delta\phi$=phase change between adjacent model elements.

The new travelling wave amplitude after gain and damping is then as follows:

$$\text{New amplitude}=\frac{A_oG}{1+D} \quad - (7)$$

Where A_o= travelling wave amplitude input to the present model element

G= nonlinear gain

D= damping

In each model element the travelling wave is modified by functions of the gain, damping and phase gradient. The amplitude is divided by the present phase gradient and then multiplied by the next phase gradient in order to re-scale it for the incremental phase gradient change.

DP generation formula level/phase

The generation of DP is calculated by applying the non-linear gain to the waveform of L_1 and L_2 at each model element. For computational convenience, a table of values was generated and from this an approximate function was created which was used in the model.

The phase lag of the DP at each point at which it is generated is $2\phi_1-\phi_2$ in the case of the $2f_1-f_2$ DP, or $2\phi_2-\phi_1$ in the case of the $2f_2-f_1$ DP.

Where ϕ_1 and ϕ_2 are the phase lags of f_1 and f_2 at the point of DP generation.

Reflections

Each model element is given a reflectivity factor equal to zero or to the frequency dependent gain multiplied by a constant. Each element has a 1 in 5 random chance of being a reflector, except adjacent reflectors were not allowed. The envelope of the reflections of the fixed reflectors on the basilar membrane is therefore linked to the linear gain window related to the DP frequency. Typically there may be around 10 reflectors within the –6 dB limits of the gain region.

Appendix II

Relationships between DPOAE and TEOAE amplitude and phase characteristics

Richard D. Knight and David T. Kemp
Auditory Biophysics Group, ILO, University College London, RNTNE Hospital, 330/332 Gray's Inn Road, London WC1X 8EE, United Kingdom

(Received 30 December 1998; accepted for publication 3 June 1999)

Most published data comparing the amplitudes of transient evoked otoacoustic emissions (TEOAEs) and bi-tonally evoked otoacoustic emissions (DPOAEs) indicate a low level of correlation, raising the question to what extent do the two responses share the same relationship with hearing function. However, DPOAE intensities are sensitive to stimulus parameters and comparisons with TEOAE have mostly been made with the specific range of DPOAE parameters found to optimize DP output level. To determine if other DPOAE stimulus parameter domains give closer correspondence between TEOAE and DPOAE characteristics, $2f_1-f_2$ and $2f_2-f_1$ DPOAE intensity and phase measurements were made across a sample 1/2-octave frequency range centered on 2 kHz in nine normally hearing subjects using a wide range of stimulus parameter configurations. The DP fine structure was resolved by detailed measurements and the mean DP levels were compared to those in the corresponding frequency range from TEOAE measurements obtained with the same probe fitting. The closest relationships between TEOAE and DPOAE amplitude were obtained with the smallest DPOAE stimulus frequency ratios and with lower DPOAE stimulus levels. For these conditions, the DPOAE intensity for individuals in this subject group could be predicted from TEOAE with a standard deviation of 1 dB, similar to the test–retest difference. The $2f_1-f_2$ DPOAE phase versus frequency gradients for fixed f_2/f_1 corresponded closely with phase gradients in TEOAE data when a small DP primary stimulus frequency ratio was used. They differed markedly at wider frequency ratios. In contrast, $2f_2-f_1$ DP phase agreement with TEOAE was good for all stimulus parameters, where measurable. These data suggest that the detailed mechanism of TEOAE and all DPOAEs is very similar when close stimulus tones are used to stimulate DP's. Significant divergence exists with the $2f_1-f_2$ DP with the wider stimulus ratios typically employed for clinical testing. The reasons are discussed. [S0001-4966(99)03309-3]

PACS numbers: 43.64.Jb, 43.64.Kc, 43.64.Ri [BLM]

INTRODUCTION

Sound emission from the ear is well established as a sign of healthy cochlear status and evoked otoacoustic emission (OAE) testing is widely used both for screening and as a diagnostic indicator. It is generally accepted that otoacoustic emissions originate in the physiological response of the cochlea's sensory mechanism to mechanical stimulation and that outer hair cells play a major part in this. (For a general review, see Robinette and Glattke, 1997.) The exact mechanism for the escape of sound energy from the cochlea has not been established in detail, but the creation of OAEs appears to be intimately associated with the cochlear traveling wave from which OAEs inherit a substantial part of their characteristic latency.

The OAEs are in general evoked by any acoustic stimulus, but the most appropriate method and the relative difficulty of response extraction varies with the type of stimulus given. The two techniques most commonly used to study OAEs and which are most often used in clinical practice are the transient evoked OAE method (TEOAE) and the distortion product OAE method (DPOAE). These techniques are superficially very different so that it is reasonable to expect that the OAEs recovered by the techniques will also differ in their relation to hearing function.

With TEOAE recording, a wideband click stimulus is repeatedly presented to the closed ear canal. The cochlea is therefore observed repeatedly "returning" to its rest state following brief stimulation. Synchronous averaging is applied to recover low-level delayed ear canal acoustic signals which include the OAE. The acoustic response component attributable to cochlear activity is separable from that of the ear canal and the middle ear by signal processing techniques sensitive to the time delay and nonlinearity of the OAE (Kemp *et al.*, 1986). The linear components of the cochlear response are sacrificed in this process.

With the DPOAE method, stimulation can be continuous, consisting of two simultaneously applied tones with frequencies f_1 and f_2, with f_2/f_1 usually set to between 1.3:1 and 1.2:1 for maximum output. Nonlinearity in the cochlear mechanism means that OAE components are produced not only at the stimulus frequencies f_1 and f_2, but also at intermodulation frequencies given by $f_2+N(f_2-f_1)$, where N may be a small positive or negative integer. Only those frequency components not coincident with f_1 and f_2 are extractable by spectral analysis and of these $2f_1-f_2$ and to a much lesser extent $2f_2-f_1$ are most commonly selected for examination. While mechanical nonlinearity may be expected to cause $2f_1-f_2$ and $2f_2-f_1$ distortion products at

any point in the f_2 traveling wave envelope, it is thought that the $2f_1-f_2$ DPOAE arises primarily from the region of the f_2 peak on the basilar membrane, whereas the higher frequency $2f_2-f_1$ DPOAE is emitted from a more basal region near the DP frequency place (Martin *et al.*, 1987; Kemp, 1998; Martin *et al.*, 1998).

Irrespective of differences in the signal recovery method, DPOAE production contrasts markedly with TEOAE production because (a) with DPOAE, the portion of the cochlea stimulated is restricted to the excitation pattern of the two close tones f_1 and f_2 whereas a click applies all frequencies to the cochlea simultaneously, (b) because TEOAEs and DPOAEs are different subsets of the total OAE response present, (c) because the DPOAE response is produced in the "steady stimulation" state whereas TEOAE is recorded after stimulation has ceased, and (d) TEOAE is obtained across frequencies simultaneously, whereas DPOAE is obtained sequentially. Point (c) is moderated by the fact that the combined DPOAE stimulus of f_1 and f_2 is pulsatile with a period of f_2-f_1.

The OAEs are accepted as an audiological tool, however it is not self-evident which of these two convenient means of evoking and extracting an OAE yields a signal most closely linked to the functional status of the sensory mechanism.

Also, it is not clear that the intensity of OAEs, which is only a byproduct of sensory activity, is the measure most likely to be closely related to function. Furthermore, DPOAE intensity depends not only on the stimulus intensity, but it also varies very substantially with the particular stimulus frequency and amplitude ratios used. It is sometimes assumed that the frequency-specific nature of DPOAE stimulation will logically lead to DPOAEs being more closely associated with function, but a close relationship to auditory threshold has yet to be found (e.g., Gorga *et al.*, 1993; Moulin *et al.*, 1994; Gorga *et al.*, 1997; Dorn *et al.*, 1998).

A relationship between TEOAE and $2f_1-f_2$ DPOAE amplitude has been shown (Moulin *et al.*, 1993; Probst and Harris, 1993; Smurzinsky and Kim, 1992; Smurzinsky *et al.*, 1993), but the results only indicate weak correlations. However, these studies for the most part only covered the small range of DP stimulus parameters which are in clinical use. For example, f_2/f_1 ratios only ranged from 1.17–1.23. They also used little or no averaging across the OAE fine structure, which is prominent in both DPOAE and TEOAE. There has been no comparable study between the $2f_2-f_1$ DP and TEOAE.

The TEOAE and DPOAE arise from such different spatial and temporal excitation patterns of stimulation within the cochlea that relative differences between the levels of each is to be expected between individuals. Interference between elemental contributions distributed along the cochlea must affect the ear canal signal greatly and this may vary between individuals. One would therefore expect at least to have to average OAE activity over a range of stimulus parameters in order to arrive at a reliable indicator of cochlear status, but this is not common practice. Also, the very different stimuli used for TE and DP OAE measurements must, to some extent, exercise different aspects of the sensory mechanism's input–output characteristic and this may also differ from ear to ear.

These considerations raise a question: which set of OAE stimulation and measurement parameters is least influenced by any intra- and intersubject differences which do not alter hearing sensitivity but may be significant to OAEs? Such parameters would be most appropriate for the purpose of obtaining an index of cochlear status.

As noted above, most comparative work on OAEs has used limited ranges of parameters because of the interest in clinical and screening applications. For DPOAE the stimulus amplitude and frequency ratios giving maximum DP output levels have been preferred in order to optimize testing time and test specificity (e.g., Harris *et al.*, 1989; Gaskill and Brown, 1990; Hauser and Probst, 1991) and to maximize differences between hearing and hearing impaired ears (e.g., Stover *et al.*, 1996; Moulin *et al.*, 1994). Reductions in the absolute stimulus levels which give increased sensitivity to cochlear disorder are traded against increased testing time within the environment of a clinic. As a result, levels exceeding 60 dB SPL are commonly used to achieve adequate specificity and speed. With TEOAE, sensitivity is generally maintained even with the highest click levels compatible with minimal transducer artifact levels (around 90 dB SPL peak) and these higher levels optimize the specificity (Prieve *et al.*, 1993).

Central to this paper is the consideration that stimulus parameters typically used for DP and TEOAE in audiological investigation may not necessarily be optimal for describing the functional differences between two cochleae. The influence of spurious factors may or may not be minimized by the adoption of stimulus conditions yielding maximum DPOAE intensity. They may also not be optimal for deciding how closely the two OAE response modes (TEOAE and DPOAE) are physiologically related.

There are more fundamental reasons for expecting a divergence between even averaged TEOAE and DPOAE intensity levels and auditory threshold. First, the otoacoustic reemission mechanism itself is a by-product of cochlear function and is not directly part of the hearing process, and, second, the vital process of transduction at the inner hair cell which leads to audition does not participate in OAE production. The relationship between OAEs and hearing threshold is beyond the scope of this paper.

The OAEs arise from functionally important elements of the cochlea—almost certainly the outer hair cells. This paper is concerned with the relationship between two modes of OAE detection: TEOAE and DPOAE. Clearly there are many unexplained sources of variance in OAEs, for example, those between OAE detection modes, between parameter configurations, and between individuals which may not all be related to hearing function. If, by the selection of appropriate stimulation parameters, very closely correlated OAE characteristics were obtainable by two different and independent OAE measurement techniques across a subject population, it is likely that those particular OAE detection modes are equally influenced by the intervening variables. More specifically, if for any stimulus configuration the DPOAE and TEOAE characteristics are found to agree

across a population, then it becomes less likely that, for that stimulus configuration, TEOAE and DPOAE generation relates to very different aspects of cochlear function.

The purpose of the present study is therefore to establish the relationship between TEOAE and DPOAE characteristics over a broader range of stimulus parameters than is presently represented in the literature and from the results to draw inferences of the functional relationships between the two modes of OAE observation. To this end we have included measurements of OAE phase gradients with frequency and also measurements of the less studied $2f_2-f_1$ DPOAE.

I. METHOD

A DPOAE and TEOAE study was designed to enable a detailed investigation of the relationships between the two OAE forms without demanding an excessive amount of time from each subject. As the phase and general waveform of TEOAE are not critically dependent on stimulus level, a single stimulus amplitude was used for TEOAE measurements. A narrow frequency spacing of DPOAE measurements was desired to allow averaging across the OAE fine structure and derivation of phase gradients. Therefore, to remain within the time constraints the f_2 frequency of the DPOAE measurements was limited to approximately a 1/2 octave range centered on 2 kHz, within which a range of stimulus frequency ratios and stimulus levels were explored.

A. Subjects

Nine left ears from subjects ranging in age from 22–41 years (mean 31.4 years) were given the OAE test battery (eight female and one male). All ears, when tested via standard audiometry, demonstrated normal hearing threshold sensitivity ($\leq$20 dB HL) from 125 Hz to 8 kHz with the exception of one ear, which gave a threshold of 25 dB HL at 4 kHz. All ears complied with normal tympanometry patterns.

B. OAE recordings

1. TEOAE

For TEOAE, the stimulus was presented at 20.5-ms intervals using the ILO 88 DPI in the nonlinear mode (Kemp *et al.*, 1986; Kemp *et al.*, 1990). Each measurement was derived from 260 nonlinear subaverages using a 2.5–20.5-ms time window with a 2.5-ms risetime. Use of a 512-point fast Fourier transform (FFT) yielded spectral harmonic values at 48.8-Hz intervals.

In order to calibrate the probe fitting in the ear prior to recording, the click stimulus, measured with the microphone contained within the probe, was assessed to confirm an absence of excessive ringing or other evidence of a poor probe fit (Kemp *et al.*, 1990) and the frequency spectrum (obtained by Fourier transform of the stimulus click) was essentially flat in the frequency range from 1 to 4 kHz. For each subject, the stimulus amplitude was adjusted to register a peak close to 0.3 Pa at the probe in the ear canal.

2. DPOAE

Short DP sweeps (i.e., DP intensity versus frequency) were constructed using 16 f_2 frequencies in the frequency range 1660–2393 Hz, which was adequate to cover an auditory filter bandwidth. The frequencies of f_2 were chosen to coincide with each harmonic of the TEOAE response in this range.

The parameters chosen for the DP sweeps were selected to cover as wide a range of conditions as possible within the constraint of a reasonable time period for the subject. The DPOAE stimulus parameters are defined by L_1 (sound pressure level of lower stimulus tone of frequency f_1) and L_2 (sound pressure level of higher stimulus tone of frequency f_2).

L_1: Levels of 65, 70, and 75 dB SPL were used, which are similar to those used by Harris *et al.* (1989). Gaskill and Brown (1990) used stimulus levels from 40 to 65 dB SPL, but these lower levels were not included in this study as the lower amplitude responses which would have resulted would have necessitated a longer averaging period for each measurement, reducing the range of conditions which could be studied within the time period.

L_1-L_2 (level difference): measurements were made with L_2 reduced below L_1 by 0, 5 and 10 dB, so including the condition $L_1=L_2$ and also the conditions with L_2 reduced below L_1 which can result in larger amplitude $2f_1-f_2$ emissions. The latter has been preferred for clinical applications, e.g., by Whitehead *et al.* (1995) and Stover *et al.* (1996).

f_2/f_1 (frequency ratio): Ratios of 1.05, 1.2, 1.27, and 1.32 were used, the latter three being clustered around the ratios 1.2–1.3 known to give maximum-amplitude DPOAEs (Harris *et al.*, 1989; Gaskill and Brown, 1990), and the first ratio investigating a much smaller frequency ratio which has been shown to have different $2f_1-f_2$ DP phase properties (Kemp, 1986) and which may produce a larger amplitude $2f_2-f_1$ distortion product response (Erminy *et al.*, 1996).

The DPOAE test sequence was programmed to run semi-automatically under the control of a macro. Both the $2f_1-f_2$ and $2f_2-f_1$ DPs were recorded simultaneously and automatically saved from within the macro. Measurements were made using the ILO 88 DPi, with software version 5.6Z. Before each DP sweep, a calibration procedure was undertaken in which three stimuli were presented cyclically: a 250-Hz sinewave and a broadband click presented to each of the two probe output transducers. The 250-Hz sine wave was used to provide an estimate of the ear canal volume by comparing the measurement from the probe microphone with data obtained from a 1 cc cavity. The responses to the broadband clicks obtained by the probe microphone were Fourier transformed and it was ensured that the two spectra obtained were approximately equal and essentially flat in the frequency range 1–4 kHz. Once this stage had been accepted, the broadband clicks were presented a further 16 times to obtain a reference spectrum of the accepted fit. This reference was used to balance and normalize the two stimuli at each of the test frequencies of the DP sweep. Normally, where the software detects wide variations in the spectrum with frequency, a standing wave effect within the

ear canal is suspected and the compensation is not performed. However, in this study, this condition was not accepted within the frequency range of interest at the calibration stage and so the level compensation always took place.

For each stimulus condition, one full frequency sweep was completed and then individual points were repeated at frequencies at which the signal-to-noise ratio was judged to be the lowest. Each DP measurement was terminated manually, usually after all $2f_1-f_2$ responses exceeded $2\times$ the standard deviation of the noise.

The DPOAE test sequence typically lasted approximately 45 min, depending on the signal-to-noise ratio of the responses. The equipment was situated in a quiet office in which the ambient noise was typically 40 dBA SPL.

C. OAE measurement procedure

Following the audiometric tests, for each subject the OAE probe was fitted with a foam tip and inserted into the ear canal and the TEOAE calibration procedure was performed. The same adult probe was used (with a different foam tip) for each subject. A TEOAE measurement was then obtained.

Following this, the complete series of DP sweeps was collected. Generally the original probe position was retained throughout the session. The probe was only reinserted on occasions when it moved during the test sequence. Where this occurred during a DP sweep, the DPOAE calibration procedure was repeated and the DP sweep measurement was rerun.

For each subject the DP measurements were obtained in the same order. Initially, with $L_1=L_2=65$, dB SPL, four DP sweeps were obtained with frequency ratios of 1.05, 1.20, 1.27, and 1.32. Here L_2 was reduced by 5 dB and the DP sweeps with the four frequency ratios were repeated. Then L_2 was reduced by a further 5 dB and the four DP sweeps were repeated again. This sequence was then repeated, beginning with $L_1=L_2=70$ dB SPL and then with $L_1=L_2=75$ dB SPL. In addition, at the start and end of the test sequence an additional DP measurement was obtained using the test parameters $L_1=L_2=70$ dB SPL and $f_2/f_1=1.2$. These two extra measurements were used to check the stability of the responses.

D. Analysis and calculations

1. Comparison of TEOAE and DPOAE amplitudes

In order to allow a straightforward comparison between TEOAE and DPOAE levels, a single figure was required which would represent the OAE level obtained across the frequency range for each OAE stimulus configuration. A different calculation method was adopted for TEOAE and DPOAE because the TEOAE measurement presents all frequencies to the cochlea simultaneously, whereas the DPOAE measurement tests each frequency sequentially. This means that for TEOAE the capacity for OAE generation is divided across frequency, whereas for DPOAE the full capacity of OAE generation is available for every frequency in the DP sweep. It is therefore appropriate to average DPOAE across frequency, but to sum TEOAE across a suitable frequency range.

For this study, the sum of the 16 TEOAE levels from 1660 to 2393 Hz was calculated and compared to the average level of each 16-point DP sweep:

$$\mathrm{DPOAE}_{\mathrm{ave}}=10\log\left(\left(\sum_{i=1}^{16}10^{\mathrm{DPOAE}/10}\right)\Big/16\right),$$

$$\mathrm{TEOAE}_{\mathrm{sum}}=10\log\left(\sum_{i=1}^{16}10^{\mathrm{TEOAE}/10}\right).$$

This calculation difference makes the reasonable assumption that the frequency range under investigation covers approximately one auditory filter and increases the numerical value for TEOAE levels relative to DPOAE by $10\log(16)$, i.e., 12 dB. The difference in calculation method has no effect on the subsequent data analysis of relationships between TEOAE and DPOAE.

2. Interrelations between TEOAE and DPOAE

For each configuration of DPOAE stimulus parameters, a scattergraph was generated in which the frequency-averaged DPOAE level was plotted against the band-limited frequency averaged TEOAE level of each subject.

The $2f_1-f_2$ DPOAE was plotted against the TEOAE frequency band corresponding to the f_2 frequency range, whereas the $2f_2-f_1$ DPOAE was plotted against the TEOAE band corresponding to the $2f_2-f_1$ DP frequency.

For each set of DPOAE stimulus parameters, a linear regression line was calculated from the paired DPOAE and TEOAE level data and the standard deviation of the data from the regression line was calculated. This measure was used as the main descriptor of the relationship between the measurements as it indicates the uncertainty associated with using the regression line to predict the DPOAE level from the TEOAE measurement.

The standard deviation calculated in this way will be referred to as the prediction standard deviation (prediction s.d.).

In order to investigate the influence of the across frequency averaging on the closeness of the relationship between TEOAE and DPOAE level, prediction s.d. was also calculated using single point TEOAE and DPOAE data without cross-frequency averaging for two DPOAE stimulus configurations, with $L_1=L_2=70$ dB SPL and $f_2/f_1=1.05$ and 1.32. To ensure that the optimum frequency alignment of the TEOAE and DPOAE fine structure was achieved, the TEOAE data was shifted by successive frequency steps and a series of prediction s.d. values were calculated. The lowest calculated value for prediction s.d. was then compared to the corresponding figure for the averaged data. The difference indicated the extent to which the apparent relationship between TEOAE and DPOAE was weakened by the fine structure mismatch of the OAE's when unaveraged data was compared.

The gradient (ΔDP/ΔTE) of the best fit line was also obtained as an indicator of the relationship between TEOAE

and DPOAE as a gradient close to 1 means that intersubject factors affecting OAE level effect both OAE forms in equal proportion, implying similarities between the underlying mechanisms of TEOAE and DPOAE.

3. Phase and phase gradients

The phase of the OAE response relative to the stimulus is readily measurable and may help to characterize the origin of an emission. The phase versus frequency gradient associated with $2f_1-f_2$ DPOAE with stimulus sweeps of a constant frequency ratio has previously been shown to be fairly flat when f_2/f_1 exceeds approximately 1.1, but to develop a much steeper gradient at smaller frequency ratios (Kemp, 1986; Knight and Kemp, 1999). This may indicate a difference in the means by which the $2f_1-f_2$ DPOAE is emitted at small and large f_2/f_1 ratios, perhaps the wave-fixed and place-fixed behavior first described by Kemp and Brown (1983). There is limited data in the literature regarding the phase behavior of the $2f_2-f_1$ DP. Wable *et al.* (1996) used an f_2 sweep test and found that the $2f_2-f_1$ DP group delay was less than that of the $2f_1-f_2$ DP if the emission frequencies were matched, and Moulin and Kemp (1996) found no difference in $2f_2-f_1$ DP group delay obtained from f_1 or f_2 sweeps.

The TEOAE measurements have associated latencies of 5–15 ms (depending on frequency) measured both in the delay seen in the time domain (Kemp, 1978) and derived from the phase gradient (Wilson, 1980).

The phase data obtained from the OAE recordings were only defined within the range ±180 degrees. The data sequences were "unwrapped" using the following procedure to yield the phase gradient. First, to deal with instances in which the data jumped up from −180 to +180 degrees, 360 degrees was subtracted if the phase of a data point differed from adjacent data points by more than 2× the typical variance for a data series plus the maximum variation due to noise at each point (based on 2×s.d. above the noise mean). Second, to correct downward jumps from +180 to −180 degrees, 360 degrees was added if the phase gradient fell below the overall line gradient by more than 360 degrees minus the maximum noise and 2× the typical variance.

These criteria were chosen as they are logical and also appear to select the most appropriate phase correction without being triggered excessively by data points with a poor signal-to-noise ratio.

Subsequently, the phase gradient (relative to the change in emission frequency) was used to provide a calculation of the group delay. The full data series from each DP gram was utilized provided that all points exceeded the mean noise by at least 1×s.d. Where this was not the case, the data sequence was shortened to include the longest continuous sequence of acceptable data. For a gradient to be recorded, a minimum of three consecutive data points were required.

The phase gradient of the $2f_1-f_2$ DP was compared to the TEOAE phase gradient across the frequency range of f_2, whereas the $2f_2-f_1$ DP was compared to the TEOAE phase across the frequency range corresponding to the emission frequency.

II. RESULTS

A. DPOAE levels

The $2f_1-f_2$ distortion product exceeded the mean noise by 1× the s.d. across the measured frequency range in all ears for all stimulus conditions with the exception of a few isolated points. The $2f_2-f_1$ distortion product was also measurable in all ears, but some parameter configurations gave low-amplitude responses containing a large number of points within the DP sweep which failed to meet the S/N criteria. Figure 1 shows all DPOAE data obtained with $L_1=70$ dB SPL from one subject. The levels of each DP to each stimulus condition, averaged across the frequency range and across the nine subjects, are shown in the graph in Fig. 2.

The overall trends seen in the amplitudes of the $2f_1-f_2$ distortion product responses with stimulus frequency ratio and stimulus level are similar to those reported by Harris *et al.* (1989).

The lowest amplitude $2f_1-f_2$ DP responses were obtained when $f_2/f_1=1.05$, whereas the frequency ratio to give the maximum amplitude response increased from 1.2 to 1.32 as L_1 increased and L_1-L_2 increased. The level difference resulting in the largest response level also increased from 5 to 10 dB as the frequency ratio increased.

The highest growth rate with increasing stimulus level seen in the $2f_1-f_2$ responses was 1.4 dB/dB and occurred when $f_2/f_1=1.32$ and $L_1=L_2$, while the lowest growth rate was 0.1 dB/dB and occurred when $f_2/f_1=1.05$ and $L_1=L_2+10$ dB.

In contrast to the $2f_1-f_2$ DP, the highest level $2f_2-f_1$ DP responses were obtained when $f_2/f_1=1.05$ and $L_1=L_2$. Reducing L_2 below L_1 resulted in reductions in $2f_2-f_1$ DP response, the greatest being 1.4 dB per 1-dB change in L_2 when $f_2/f_1=1.05$ and $L_1=75$ dB SPL.

Increasing the frequency ratio above 1.05 also reduced the level of the $2f_2-f_1$ response, especially at low stimulus levels.

The greatest growth rates in $2f_2-f_1$ DPOAE with increasing stimulus level occurred when $f_2/f_1=1.32$, although the response level generally remained lower than corresponding measurements with lower frequency ratios. As with the $2f_1-f_2$ DP, there was little growth in the $2f_2-f_1$ DP when $f_2/f_1=1.05$, especially with $L_2<L_1$, when virtually no response growth occurred.

The $2f_1-f_2$ DP level was always greater than the $2f_2-f_1$ DP level except when $L_1=L_2$ and $f_2/f_1=1.05$, in which case the $2f_2-f_1$ DP exceeded the $2f_1-f_2$ DP by 2–2.5 dB. The $2f_1-f_2$ DP, however, was up to 20 dB greater than the $2f_2-f_1$ DP with large stimulus frequency ratios and when L_2 was reduced below L_1.

B. Comparison of TEOAE and DPOAE levels

The TEOAE responses exceeded the noise within the frequency region under investigation in all ears tested, with the exception of a few isolated points in some subjects. The sum of the TEOAE level within the frequency range varied from −2.0 to 12.6 dB SPL between subjects, with the mean being 6.2 dB SPL. The mean was close to the mean, for example, of the averaged DPOAE sweeps with $L_1=L_2=65$

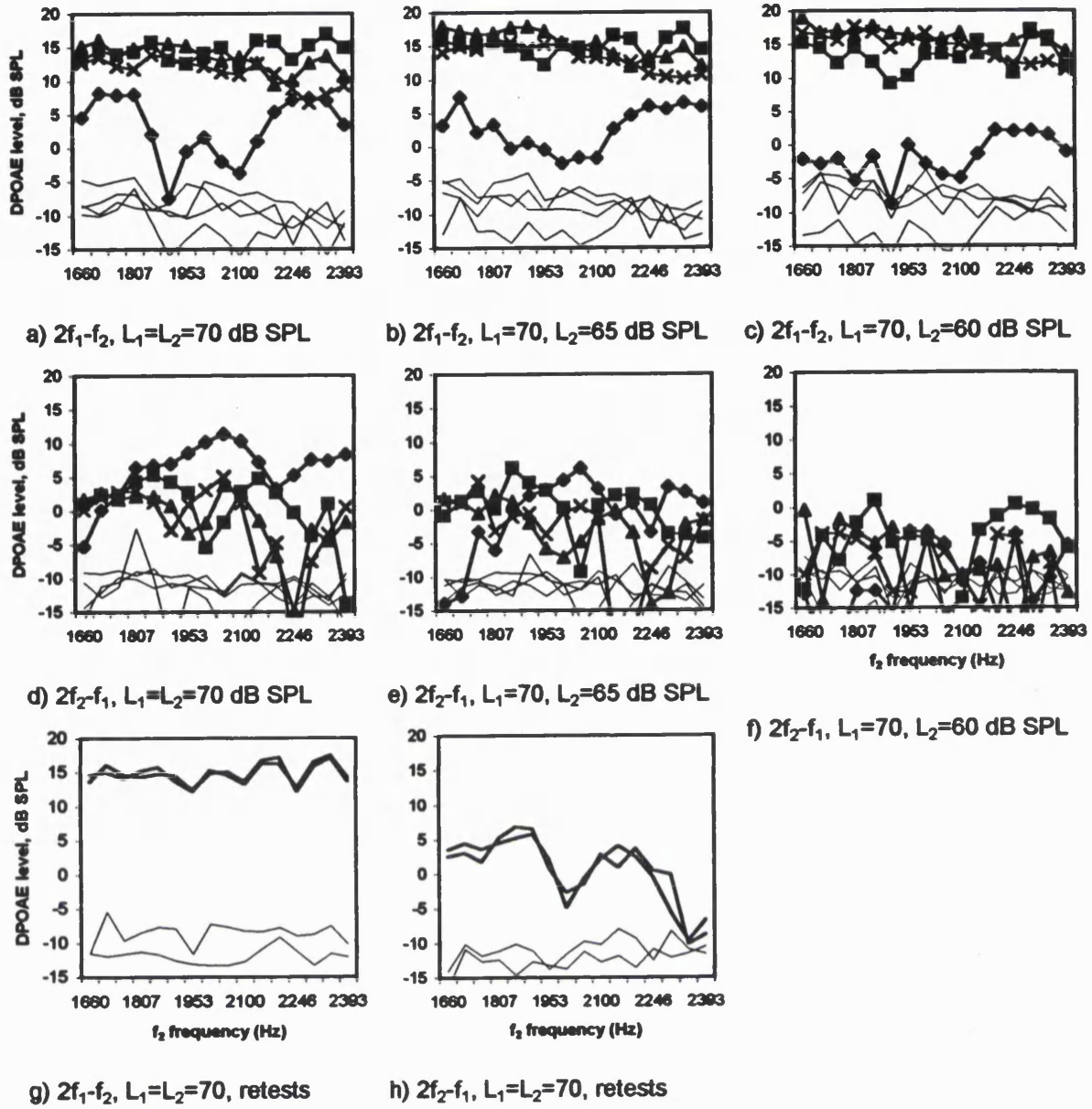

FIG. 1. DPOAE amplitude data for subject *D* with $L_1 = 70$ dB SPL. ◆ $= f_2/f_1 = 1.05$, ■ $= f_2/f_1 = 1.2$, ▲ $= f_2/f_1 = 1.27$, × $= f_2/f_1 = 1.32$. (a)–(c) shows the $2f_1 - f_2$ DP, (d)–(f) the corresponding $2f_2 - f_1$ DP, and (g) and (h) repeat tests with $L_1 = L_2 = 70$ dB SPL and $f_2/f_1 = 1.2$ from the beginning and end of the DPOAE test sequence. Thin lines show the mean noise estimates from the adjacent ten spectral frequency bands to the DP. The standard deviation associated with each noise estimate was typically 2–3 dB.

dB SPL and $f_2/f_1 = 1.2$ or 1.27. For each subject, the standard error in the mean TEOAE level was calculated from the set of individual TEOAE data points (this measure is likely to reflect the amount of fine structure, although it could also indicate an underlying smooth trend across the frequency range under test). The average of these was 1.3 dB, comparable with standard errors of all the $2f_2 - f_1$ DPOAE measurements and $2f_1 - f_2$ DPOAE measurements with $f_2/f_1 = 1.05$, which were typically in the range 1.2–1.6 dB. The mean $2f_1 - f_2$ DPOAE measurements with larger f_2/f_1 had smaller standard errors, mostly in the range 0.5–0.9 dB.

C. Relationships between TEOAE and DPOAE amplitude

For each DP parameter configuration, a scattergram was generated on which the TEOAE total level was plotted against the average DPOAE response for each subject. Examples of the scattergrams are shown in Fig. 3 with best-fit lines calculated by linear regression.

The standard deviation of the DPOAE level predicted from the TEOAE level with respect to the actual DPOAE level ("prediction s.d.") was calculated for each of the 72 data sets. The calculated values are shown in Table I(a) and (b).

Considering the $2f_1 - f_2$ DP, the general trend was for the closest relationships to TEOAE to be with smaller frequency ratios. Paired *t* tests from whole columns of data in Table I(a) indicate that the prediction s.d. values with stimulus frequency ratios of 1.27 or 1.32 were significantly higher ($p < 0.05$) than with any lower ratios.

When $f_2/f_1 = 1.05$ or 1.2, there was also a trend for the prediction s.d. values to be lower with lower stimulus levels. Therefore, the closest amplitude relationship between the

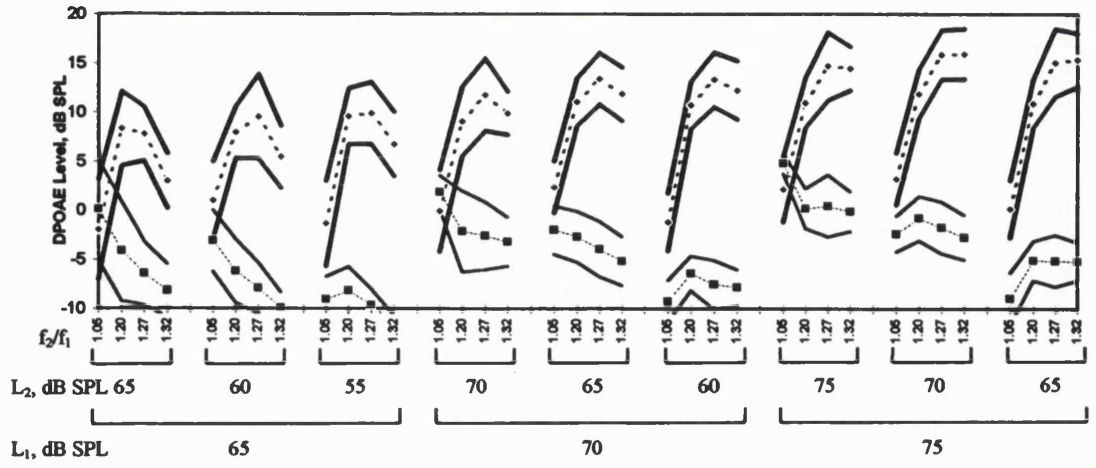

FIG. 2. Average $2f_1-f_2$ and $2f_2-f_1$ DPOAE levels obtained with each combination of stimulus parameters in the frequency range 1660–2393 Hz. Errors shown are 2×s.e. from the mean of nine ears. The average noise floor for each condition was always below −10 dB SPL. ◆ $=2f_1-f_2$ DP, ■ $=2f_2-f_1$ DP.

$2f_1-f_2$ DP and TEOAE occurred when $L_1=65$ dB SPL and $f_2/f_1=1.05$ or 1.2. The lowest single result (1.66 dB) was obtained with $L_1=65$ dB SPL, $L_2=60$ dB SPL, and $f_2/f_1=1.2$.

The $2f_2-f_1$ DP also showed an overall trend to have closest relationships to TEOAE level with lower stimulus frequency ratios. Paired t tests from whole columns of data in Table I(b) indicate that the prediction s.d. values obtained with $f_2/f_1=1.05$ are significantly lower ($p<0.05$) than any other frequency ratio. When $L_1=65$ dB SPL, the prediction s.d. values were also lower with L_2 reduced below L_1, although with a very small response level. However, when $L_1=70$ or 75 dB SPL, $L_1=L_2$ produced lower values of prediction s.d. Comparing rows of data from Table I(b), $L_1=L_2=75$ dB SPL gave prediction s.d. values significantly lower ($p<0.005$) than with L_2 reduced by 5 or 10 dB.

When L_1 and L_2 were equal, higher stimulus levels gave closer relationships between the $2f_2-f_1$ DP and TEOAE except when $f_2/f_1=1.05$, in which case there was no clear trend as the relationship was always close. Stimulus levels of $L_1=L_2=65$ dB SPL gave significantly higher values of prediction s.d. than $L_1=L_2=70$ or 75 dB SPL ($p<0.05$). Meanwhile, when $L_1=L_2+10$, a lower stimulus level produced lower prediction s.d. values but with very low level DPOAE's. Comparing rows of data in Table I(b), the stimulus level combination which gave the highest values for prediction s.d. was $L_1=75$ dB SPL and $L_2=65$ dB SPL. The tests indicate a high statistical significance ($p<0.05$) to the difference between this and all other stimulus level combinations except $L_1=L_2=65$ dB SPL.

The $2f_2-f_1$ prediction s.d. values close to 1 dB were obtained with $L_1=L_2=70$ dB SPL and $f_2/f_1=1.05$ and with $L_1=L_2=75$ dB SPL and $f_2/f_1=1.2$. The lowest single value (0.69 dB) was obtained with $L_1=65$ dB SPL, $L_2=55$

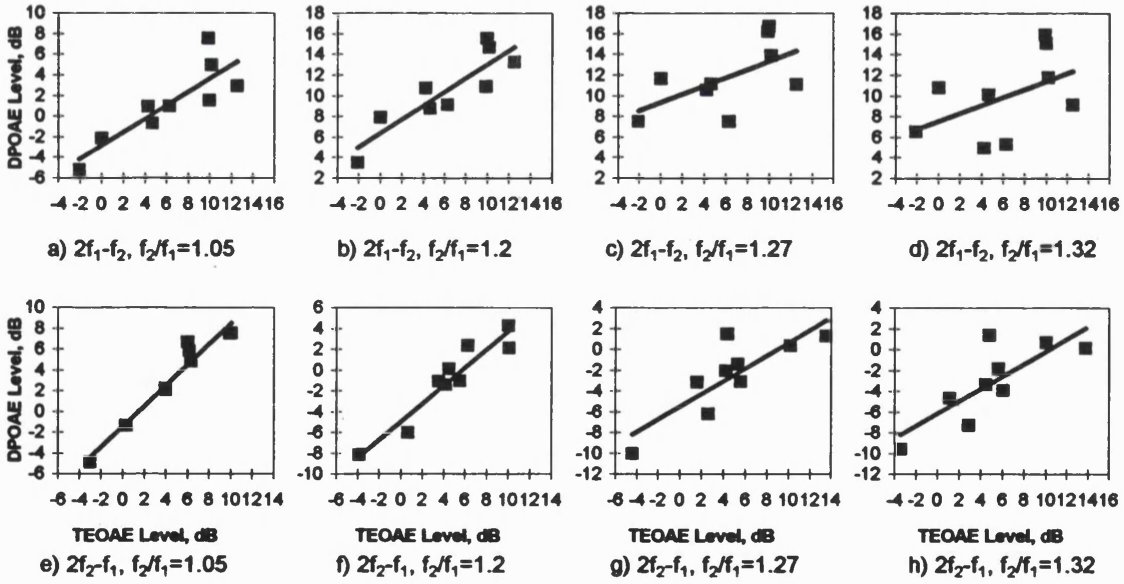

FIG. 3. Comparison of average DPOAE and total TEOAE level in the frequency range 1660–2392 Hz for nine ears, with the best-fit line calculated by linear regression. The TEOAE response is plotted against the f_2 frequency range of the $2f_1-f_2$ distortion product and the emission frequency of the $2f_2-f_1$ distortion product. The examples shown were obtained with stimulus amplitudes $L_1=L_2=70$ dB SPL and frequency ratios: (a) $2f_1-f_2$, $f_2/f_1=1.05$, (b) $2f_1-f_2$, $f_2/f_1=1.2$, (c) $2f_1-f_2$, $f_2/f_1=1.27$, (d) $2f_1-f_2$, $f_2/f_1=1.32$, (e) $2f_2-f_1$ $f_2/f_1=1.05$, (f) $2f_2-f_1$, $f_2/f_1=1.2$, (g) $2f_2-f_1$, $f_2/f_1=1.27$, and (h) $2f_2-f_1$, $f_2/f_1=1.32$. Both the $2f_1-f_2$ and the $2f_2-f_1$ DPs appear more closely related to TEOAE when the stimulus frequency ratio is smaller.

TABLE I. The relationship between DPOAE and TEOAE level indicated by standard deviation and the gradient associated with the best fit line for each configuration of DPOAE parameters. (a) and (b) Standard deviations of (a) $2f_1-f_2$ and (b) $2f_2-f_2$ DPOAE level (dB) predicted from best-fit line relationship with TEOAE (defined as prediction s.d.). Heavy shading indicates prediction s.d.>3.0 dB, light shading indicates 1.5<prediction s.d.<3.0 dB, no shading indicates prediction s.d. below 1.5 dB. (c) and (d) Gradients ($\Delta DP/\Delta TE$) of best fit lines between TEOAE and (c) $2f_1-f_2$ and (d) $2f_2-f_1$ DPOAE amplitudes. Heavy shading indicates gradient <0.6, light shading indicates 0.6<gradient<0.8, no shading indicates gradient above 0.8. (e) and (f) Standard errors of the gradients between TEOAE and (e) $2f_1-f_2$ and (f) $2f_2-f_1$ DPOAE levels.

Stim(dB SPL)		1.05	1.2	1.27	1.32
L1	L2	2f1-f2	2f1-f2	2f1-f2	2f1-f2
65	65	1.7	1.8	3.4	4.8
	60	1.8	1.7	3.5	5.1
	55	1.9	1.9	3.4	4.8
70	70	2.1	1.9	2.8	3.7
	65	2.0	1.9	3.3	4.0
	60	2.2	2.3	3.3	3.9
75	75	1.8	1.9	2.9	3.7
	70	2.3	2.4	3.1	3.8
	65	2.5	4.2	3.0	3.4

a) Prediction S.D., $2f_1$-f_2

Stim(dB SPL)		1.05	1.2	1.27	1.32
L1	L2	2f2-f1	2f2-f1	2f2-f1	2f2-f1
65	65	1.4	2.4	2.7	3.9
	60	1.2	2.3	2.1	2.7
	55	0.7	1.9	1.4	2.0
70	70	1.1	1.3	2.2	2.4
	65	1.2	2.1	2.6	1.9
	60	1.6	2.7	2.3	1.7
75	75	1.3	1.0	1.6	1.6
	70	2.1	1.9	2.4	2.8
	65	2.3	2.9	3.0	3.0

b) Prediction S.D., $2f_2$-f_1

Stim(dB SPL)		1.05	1.2	1.27	1.32
L1	L2	2f1-f2	2f1-f2	2f1-f2	2f1-f2
65	65	0.82	0.76	0.56	0.78
	60	0.72	0.81	0.70	0.90
	55	0.78	0.88	0.77	0.88
70	70	0.65	0.67	0.40	0.39
	65	0.63	0.71	0.54	0.48
	60	0.60	0.71	0.65	0.69
75	75	0.68	0.63	0.40	0.40
	70	0.63	0.62	0.51	0.51
	65	0.57	0.67	0.60	0.62

c) Gradient, $2f_1$-f_2

Stim(dB SPL)		1.05	1.2	1.27	1.32
L1	L2	2f2-f1	2f2-f1	2f2-f1	2f2-f1
65	65	1.25	1.04	0.84	0.94
	60	1.12	0.66	0.37	0.64
	55	0.85	0.38	0.06	0.48
70	70	0.99	0.91	0.84	0.81
	65	0.89	0.89	0.75	0.69
	60	0.52	0.60	0.50	0.10
75	75	0.67	0.76	0.68	0.62
	70	0.66	0.84	0.69	0.77
	65	0.51	0.68	0.28	0.54

d) Gradient, $2f_2$-f_1

Stim(dB SPL)		1.05	1.2	1.27	1.32
L1	L2	2f1-f2	2f1-f2	2f1-f2	2f1-f2
65	65	0.12	0.13	0.24	0.34
	60	0.13	0.12	0.25	0.36
	55	0.14	0.13	0.24	0.34
70	70	0.15	0.13	0.20	0.26
	65	0.15	0.13	0.23	0.28
	60	0.16	0.17	0.24	0.28
75	75	0.13	0.14	0.20	0.26
	70	0.16	0.17	0.22	0.27
	65	0.18	0.30	0.21	0.24

e) Gradient standard error, $2f_1$-f_2

Stim(dB SPL)		1.05	1.2	1.27	1.32
L1	L2	2f2-f1	2f2-f1	2f2-f1	2f2-f1
65	65	0.12	0.20	0.19	0.28
	60	0.10	0.19	0.14	0.20
	55	0.06	0.15	0.10	0.14
70	70	0.09	0.11	0.15	0.17
	65	0.10	0.17	0.18	0.13
	60	0.13	0.22	0.16	0.12
75	75	0.11	0.08	0.11	0.11
	70	0.18	0.15	0.17	0.20
	65	0.19	0.23	0.21	0.22

f) Gradient standard error, $2f_2$-f_1

TABLE II. A comparison of prediction s.d. calculated from single frequency points and the average prediction s.d. values drawn from Table I (a) and (b). Stimulus levels are $L_1=L_2=70$ dB SPL.

f2/f1	D.P.	Single Point	Average
1.05	2f1-f2	5.21	2.08
	2f2-f1	4.65	1.09
1.2	2f1-f2	4.22	1.87
	2f2-f1	6.24	1.30
1.32	2f1-f2	4.00	3.71
	2f2-f1	5.45	2.39

dB SPL, and $f_2/f_1=1.05$, but this is a parameter combination which may not be very useful to pursue as it gives a very low level $2f_2-f_1$ DPOAE.

The overall magnitude of the prediction s.d. values obtained for both the $2f_1-f_2$ and $2f_2-f_1$ distortion products has been confirmed by an additional study in which five of the DP sweeps were investigated for a further ten subjects and prediction s.d. values of a similar magnitude were obtained.

D. Averaging across frequency and the relationship between TEOAE and DPOAE

Prediction s.d. was also calculated using single point TEOAE and DPOAE data without cross-frequency averaging for three DPOAE stimulus configurations; with $L_1=L_2=70$ dB SPL and $f_2/f_1=1.05$, 1.2, and 1.32. The calculation was repeated with successive steps in the frequency alignment between DPOAE and TEOAE, and the minimum prediction s.d. was recorded. The results are shown in Table II.

In general, a much closer relationship was found between TEOAE and DPOAE when the data was averaged across frequency, with the exception of the $2f_1-f_2$ DP with $f_2/f_1=1.32$ in which case the averaging only resulted in a small reduction in prediction s.d. This implies that when the $2f_1-f_2$ DPOAE was stimulated by a wide frequency ratio, the poor correlation of the OAE fine structures was not the main limiting factor in the prediction s.d. calculated without averaging. With a frequency ratio of 1.05, the prediction s.d. was lowest with both the $2f_1-f_2$ and $2f_2-f_1$ DPs when the TEOAE frequency was matched the DP frequency. However, with a frequency ratio of 1.32, the exact frequency alignment was much less critical, suggesting that the fine structure pattern of the wide ratio DPOAE responses differed more from that of the TEOAE responses so that frequency misalignment was less significant. With $f_2/f_1=1.2$, the frequency alignment of the $2f_1-f_2$ DP was of little significance (suggesting that the DPOAE fine structure was not correlated with that of TEOAE), but with the $2f_2-f_1$ DP the prediction s.d. was lowest when the TEOAE frequency was aligned with the DP frequency.

E. Comparison of $2f_2-f_1$ and f_2 TEOAE frequency mapping

The prediction s.d. associated with the $2f_2-f_1$ distortion product was also calculated using the TEOAE component corresponding to the DPOAE f_2 stimulus frequency and compared to the prediction s.d. values shown in Table I(b), which were calculated using the TEOAE component corresponding to the DPOAE $2f_2-f_1$ emission frequency.

When $f_2/f_1=1.05$, the prediction s.d. values were significantly lower ($p<0.005$) when based on matching the emission frequencies of TEOAE and DPOAE, consistent with the $2f_2-f_1$ DPOAE level being defined in the region of the emission frequency place on the basilar membrane. However when $f_2/f_1=1.27$ or $1.32(p<0.005)$, the prediction s.d. was lower when the TEOAE band was matched to the DPOAE f_2 frequency. With a frequency ratio of 1.2, the prediction s.d. values showed a nonsignificant tendency to be lower at the f_2 frequency. It is surprising that the upper sideband DPOAE with $f_2/f_1=1.27$ or 1.32 may be related to the f_2 region on the basilar membrane, as the DP is not expected to be able to propagate efficiently along the basilar membrane in this region. It may be that the relevant frequencies of the TEOAE come from a basilar membrane region more basal than their frequency place, and so the $2f_2-f_1$ DPOAE also corresponds to a region more basal than f_2.

F. Amplitude best-fit line gradients

The gradients of the best fit lines can also be considered to be indicators of the similarities between the DPOAE and TEOAE levels, a gradient of 1 being indicative of a close agreement. This is distinct from a comparison of OAE growth rates, as it is an intersubject measure and each gradient is derived from only one stimulus level for DPOAE and TEOAE. Instead it is a measure of whether intersubject factors causing a difference in TEOAE amplitude result in the same proportional difference in DPOAE amplitude. (In the stimulus parameter ranges used in this study, TEOAE growth rate is normally lower than that of DPOAE.) The level best-fit line gradients are shown in Table I(c) and (d). The standard errors associated with these gradients are shown in Table I(e) and (f).

The best fit line gradients of the level relationship between $2f_1-f_2$ DPOAE and TEOAE ranged from 0.39 to 0.90 (the gradient of the amplitude relationship is defined as ΔDPOAE/ΔTEOAE), but were generally closer to 1 at lower stimulus levels and smaller stimulus frequency ratios. At larger stimulus frequency ratios, the maximum reduction of L_2 below L_1 also produced gradients closer to 1. Paired t tests of whole rows of data from Table I(c) indicate a strong significance ($p<0.05$) for the tendency of the gradients with stimulus levels of $L_1=65$ dB SPL and $L_2=60$ or 55 dB SPL (rows 2 and 3) to be higher than with any combination with $L_1=70$ or 75 dB SPL (rows 4–9).

At higher stimulus levels the gradients were higher with smaller stimulus frequency ratios, and comparing whole columns of data, the best fit line gradients with $f_2/f_1=1.05$ or 1.2 were significantly higher ($p<0.05$) than with f_2/f_1

$=1.27$ and the gradients with $f_2/f_1=1.2$ were also significantly higher than with $f_2/f_1=1.32$.

All gradients over 0.8 associated with the $2f_1-f_2$ DP occurred with $L_1=65$ dB SPL but were spread across the frequency ratios and the highest single figure (0.90) occurred with $f_2/f_1=1.32$. The highest best fit line gradients with the $2f_2-f_1$ DP occurred with $L_1=L_2$ [Table I(d)]. Equilevel stimuli at 65 or 70 dB SPL (rows 1 and 4) had significantly higher best-fit line gradients than any combination with a 10 dB stimulus level difference (rows 3, 6, and 9).

Higher gradients also occurred with smaller stimulus frequency ratios, with gradients with $f_2/f_1=1.05$ or 1.2 (columns 1 and 2) being higher than with $f_2/f_1=1.27$ or 1.32 (columns 3 and 4, $p<0.005$). With $f_2/f_1=1.05$, the gradient was also higher at low stimulus levels, but at higher frequency ratios this only remained true when $L_1=L_2$.

Although the highest gradients occurred with lower stimulus levels and $f_2/f_1=1.05$, there were also some gradients over 0.9 with $L_1=L_2=65$ or 70 dB SPL at the larger stimulus frequency ratios.

G. Comparison of repeat DPOAE measurements

Verification that the response level was consistent throughout the test sequence was achieved by repeating one DP sweep at the start and end of the DPOAE test series as well as in sequence halfway through the series. The repeated test used the following stimulus parameters: $L_1=L_2=70$ dB SPL and $f_2/f_1=1.2$. For each subject the levels of DPOAE were determined for the first and last tests and the differences between the two measurement levels were calculated. The standard deviation of the differences for the $2f_1-f_2$ DPOAE was 0.9 dB, whereas for the $2f_2-f_1$ DPOAE it was 1.4 dB.

The higher variations seen in the $2f_2-f_1$ distortion product are likely to result from a greater influence of noise, as the two distortion products were measured simultaneously and the greatest retest differences for the $2f_2-f_1$ distortion product were seen in subjects with the lowest amplitude responses. There was no significant trend for the DPOAEs to increase or decrease during the test sequence, although the $2f_2-f_1$ distortion product showed a slight tendency to have a higher level in the later test (mean difference 0.4 dB).

H. Phase gradients and delays

The results for all subjects (Fig. 4) fell into two distinct categories, with the $2f_1-f_2$ DP at wide frequency ratios producing very shallow phase gradients and hence a small group delay while the $2f_1-f_2$ DP with $f_2/f_1=1.05$ and all $2f_2-f_1$ DP measurements produced steep phase gradients, similar to the TEOAE phase.

The TEOAE group delays in Fig. 4(b) are calculated in the frequency band corresponding to the DPOAE f_2 frequency range and also at the frequencies corresponding to the $2f_2-f_1$ emission frequency for each of the stimulus frequency ratios. The TEOAE group delays corresponding to the $2f_2-f_1$ DP frequency with wider stimulus frequency ratios are slightly shorter as they are derived from slightly higher frequency bands.

The $2f_2-f_1$ results with $L_1=65$, $L_2=55$, and $f_2/f_1=1.27$ and 1.32 are based on one subject because of low level responses resulting in a failure to meet the signal-to-noise ratio criteria in at least three consecutive frequencies in most subjects. All other data is based on at least five subjects.

The phase of the DPOAE and TEOAE data from one subject is shown in Fig. 5(a)–(d). The phase gradient of the $2f_1-f_2$ DP at stimulus frequency ratios of 1.2 and greater was considerably less than that of all other DPOAE and the TEOAE measurements.

The behavior of the $2f_1-f_2$ DP phase confirms the earlier findings of Kemp (1986). In the case of the $2f_2-f_1$ DP meanwhile, the steep phase gradient which is seen only at small frequency ratios in the $2f_1-f_2$ DP is retained out to ratios of at least $f_2/f_1=1.32$.

III. DISCUSSION OF RESULTS

A. DPOAE amplitudes

1. $2f_1-f_2$

The amplitudes of the $2f_1-f_2$ DPOAE measurements passed through a maximum at a stimulus frequency ratio which increased from 1.2 to 1.32 as the stimulus level increased. This finding is in agreement with results presented by Harris *et al.* (1989) and other workers.

All stimulus configurations used in the test sequence gave responses which exceeded the mean noise by at least $1\times$ the s.d. with the exception of a few isolated points. However, measurements with ratios of stimulus frequency 1.2, 1.27, and 1.32 gave larger amplitude responses than the 1.05 ratio and were therefore quicker and easier to measure.

The lower growth rates with stimulus level seen in the DPOAE measurements with a stimulus frequency ratio of 1.05 imply that the generation or emission mechanisms may be more saturated. The relatively low level of response indicates that under these stimulus conditions either the distortion product does not easily escape back to the ear canal or the response induced in the basilar membrane produces less energy at that DP frequency.

Conversely, the high growth rates seen with a frequency ratio of 1.32 (of up to 1.4 dB/dB) suggest that the DP generation or emission mechanisms for wider spaced tones are not so easily saturated leading to the higher DP level.

2. $2f_2-f_1$

The levels of the $2f_2-f_1$ DPOAEs are sensitive to changes in frequency ratio and differences between L_1 and L_2, particularly at lower stimulus levels, with the highest level responses being obtained with smaller frequency ratios and equal stimulus levels. This is the opposite of the $2f_1-f_2$ DP behavior, for which a larger frequency ratio and $L_1>L_2$ increased the OAE level. The trend shown by Erminy *et al.* (1996) for a larger $2f_2-f_1$ DP level to be obtained with $f_2/f_1=1.12$ than with $f_2/f_1=1.22$ has been shown to continue at both higher and lower ratios.

As with the $2f_1-f_2$ distortion product, the $2f_2-f_1$ DP growth rates were smallest when $f_2/f_1=1.05$, implying a

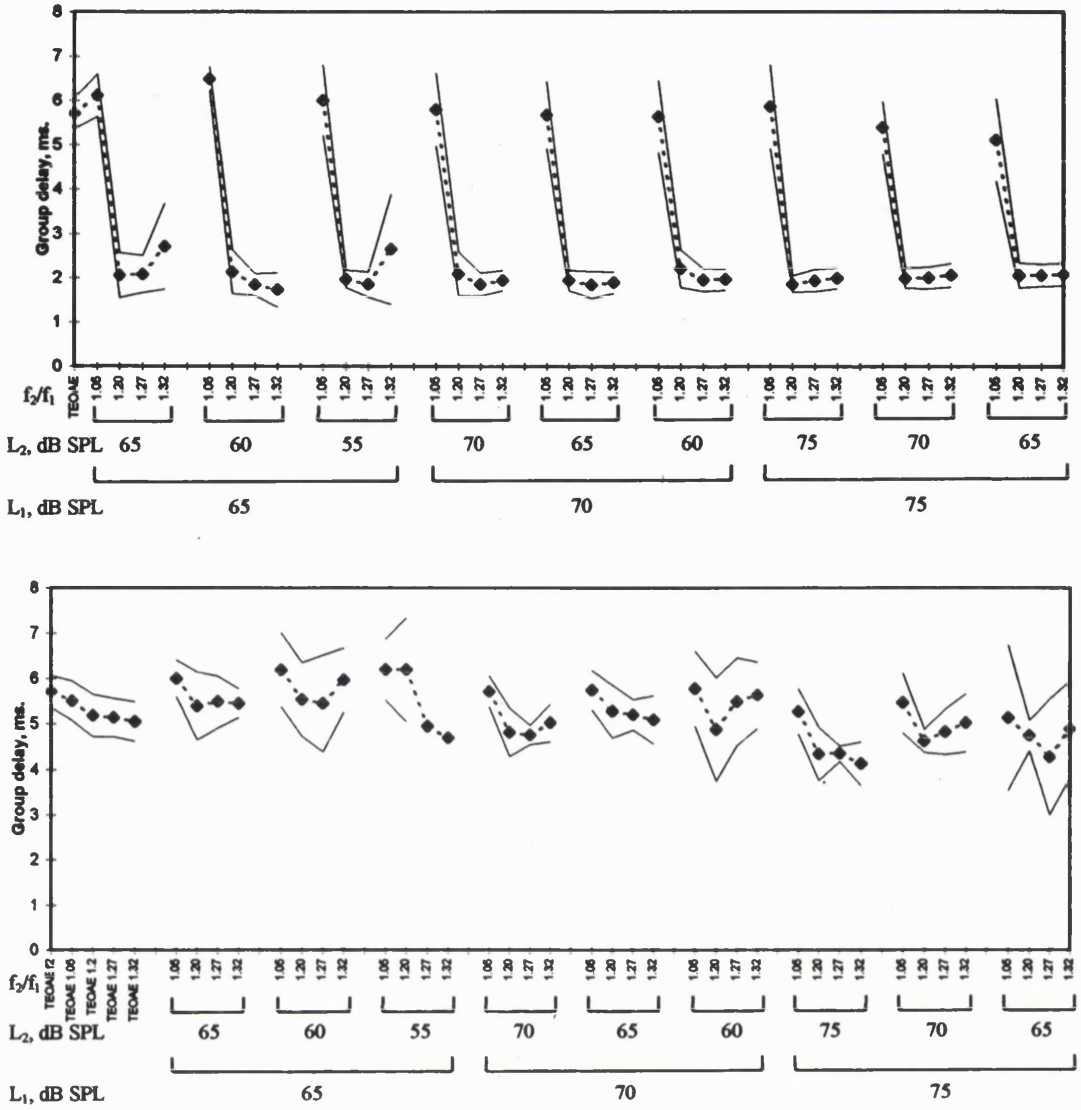

FIG. 4. Group delay, derived from the DPOAE phase gradients obtained from sweeps with constant f_2/f_1. Results are an average from nine subjects. Errors shown are 2×s.e. from the mean. The corresponding TEOAE data is shown for comparison: (a) $2f_1-f_2$ DP and (b) $2f_2-f_1$ DP. In (b), the TEOAE data is shown corresponding to the f_2 frequency of the DP measurements and also the frequency of the $2f_2-f_1$ DP at each frequency ratio. Group delay is considerably lower for the $2f_1-f_2$ DP with $f_2/f_1=1.2$–1.32 than with the $2f_1-f_2$ DP with $f_2/f_1=1.05$ or the $2f_2-f_1$ DP or TEOAE.

more saturated generation or emission mechanism, and greatest when $f_2/f_1=1.32$, implying a less saturated response.

B. Relationships between TEOAE and DPOAE amplitude

1. $2f_1-f_2$

A close relationship was found between the frequency averaged levels of the $2f_1-f_2$ DPOAE and TEOAE, particularly when the frequency ratio was small.

With larger stimulus ratios, there was a tendency for the prediction s.d. to be smaller with higher stimulus levels, a condition which coincided with lower DPOAE versus TEOAE level gradients [Table I(c)]. A smaller DPOAE versus TEOAE level gradient would reduce the values obtained for prediction s.d. and so the lower prediction s.d. values obtained with higher stimulus levels may not in this case indicate a closer relationship between DPOAE and TEOAE. The relationships found in the present study are closer than expected from literature. Calculations from data presented by Smurzinsky and Kim (1992) and Smurzinsky *et al.* (1993) produced approximate $2f_1-f_2$ prediction s.d. values at 2 kHz of 3.7 dB (preterm infants), 3.6 dB (fullterm infants), and 2.7 dB (adults) using DPOAE stimulus parameters of $L_1=L_2=65$ dB SPL, $f_2/f_1=1.18$–1.23 with $\frac{1}{4}$-octave steps between points ($\frac{1}{2}$-octave averaging in analysis). It is likely that a closer agreement was seen between TEOAE and DPOAE with adult subjects than with infants because of easier measurement conditions. A difference remains between the adult prediction s.d. (2.7 dB) and the corresponding result using a comparable stimulus frequency ratio and level from the present study (1.8 dB). This is likely to be because of the finer frequency interval within the DP sweeps of the present study and hence the greater degree of across frequency averaging and also the use of the same probe fitting for both DPOAE and TEOAE measurements in the present study resulting in the removal of possible variance arising from variations in probe fitting.

The corresponding calculated prediction s.d. associated with the work of Moulin *et al.* (1993) and Probst and Harris

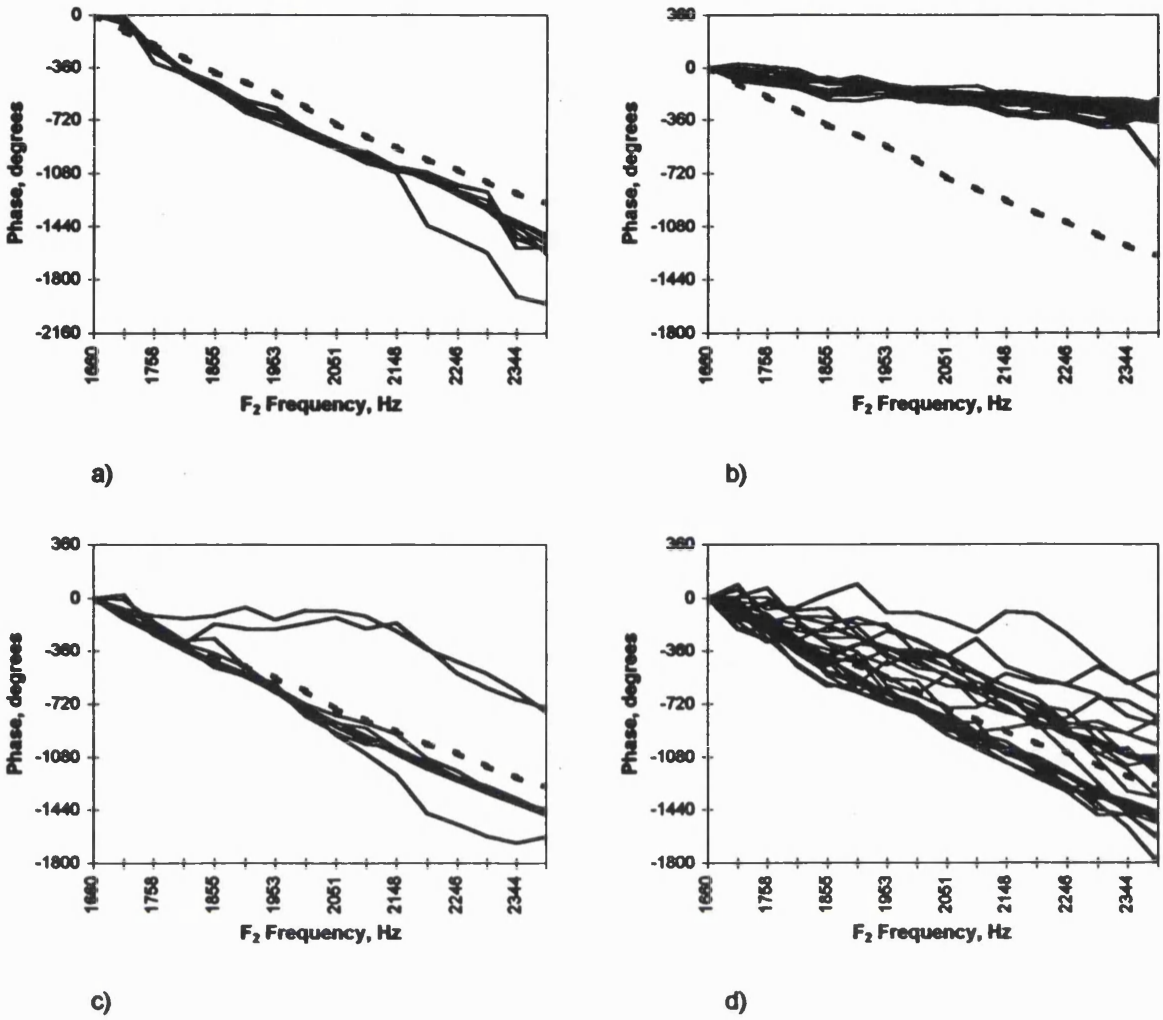

FIG. 5. The DPOAE phase (solid lines) plotted with TEOAE phase (broken lines) corresponding to the f_2 frequency of the DPOAE measurements for one subject. (a) $2f_1-f_2$ DP, $f_2/f_1=1.05$. (b) $2f_1-f_2$ DP, $f_2/f_1=1.2$, 1.27, and 1.32. (c) $2f_2-f_1$ DP, $f_2/f_1=1.05$. (d) $2f_2-f_1$ DP, $f_2/f_1=1.2$, 1.27, and 1.32. The gradient of the $2f_1-f_2$ DP phase in (b) is considerably shallower than all other DP data and the TEOAE. Scattering seen in (d) occurs in data with a poor signal-to-noise ratio.

(1993) are 4.1 and 3.9 dB, respectively, which correspond to prediction s.d. values of 1.8 and 1.7 dB obtained with comparable stimulus parameters in the present study. Moulin *et al.* used DPOAE stimulus parameters of $L_1=L_2=60$ dB SPL and $f_2/f_1=1.17$ and compared unaveraged single DPOAE points to 200-Hz averaged TEOAE bands. The larger prediction s.d. seen in the Moulin data presumably arises from the reduced averaging in both the TEOAE and DPOAE data. Probst and Harris used a frequency ratio of 1.22 and a stimulus level difference of 6 dB SPL and compared the TEOAE and DPOAE levels across the full frequency range and so the TEOAE and DPOAE mean responses may have been dominated by different frequency regions.

Therefore, it appears that there are two main reasons why closer relationships have been observed between the levels of TEOAE and DPOAE in the present study than had been previously shown:

(a) The averaging process across a frequency range removes to a large extent the effect of the OAE fine structure, and

(b) the DPOAE configurations which give the closest agreements are not those which have the largest amplitude and so have not previously been investigated so extensively.

2. Relationships between TEOAE and DPOAE amplitude, $2f_2-f_1$

As with the $2f_1-f_2$ DP, the $2f_2-f_1$ DP was also most closely related to TEOAE when evoked by smaller frequency ratios and stimulus levels, although the relationship did not deteriorate at wider DP stimulus frequency ratios to as great an extent as was the case with the $2f_1-f_2$ distortion product. Interestingly, although when $L_1=70$ or 75 dB SPL it was preferable for the stimuli to be of equal level, when $L_1=65$ dB SPL the values of prediction s.d. were lower when $L_1>L_2$. However, these have very low levels and are associated with very shallow amplitude gradient relationships and, therefore, in this case the association with TEOAE may not be as close as it may appear.

C. Comparison of $2f_1-f_2$ and $2f_2-f_1$ prediction s.d. values

A comparison of the average $2f_1-f_2$ and $2f_2-f_1$ prediction s.d.'s in Table I(a) and (b) at each frequency ratio is shown in Table III.

TABLE III. A comparison of the average prediction s.d. of the $2f_1-f_2$ and $2f_2-f_1$ distortion products for each frequency ratio from Table I(a) and (b). A positive difference indicates that the $2f_1-f_2$ prediction s.d. values were larger than the corresponding $2f_2-f_1$ values. *P* values are derived via a paired *t* test.

	Stimulus frequency ratio			
DPOAE	1.05	1.2	1.27	1.32
2f1-f2	2.04	2.21	3.18	4.12
2f2-f1	1.42	2.05	2.25	2.44
Difference	0.62	0.16	0.93	1.68
p value	<0.001	≈0.25	<0.001	<0.001

The data confirms the apparent trend seen in Table I(a) and (b) that the $2f_2-f_1$ distortion product measurements were more closely related to the TEOAE level than the $2f_1-f_2$ distortion product. The differences were statistically highly significant with frequency ratios of 1.05, 1.27, and 1.32.

D. Gradient of DPOAE/TEOAE amplitude relationship

Gradients close to 1 imply that intersubject differences affecting OAE level act in equal proportion on both DPOAE and TEOAE, thus suggesting similarities in generation and/or emission. There are various factors which could effect the amplitudes of TEOAE and DPOAE. Variation in the efficiency of sound conduction through the middle ear would maintain a 1:1 relationship between TEOAE and DPOAE and would probably affect TEOAE and DPOAE level equally. Changing the DP parameters may change the DPOAE level, but would not necessarily of itself alter the 1:1 gradient unless the change led to unequal saturation of TEOAE and DPOAE. However, if DPOAE and TEOAE were of unequal sensitivity to the condition of the outer hair cells or if they arose from different emission mechanisms, the 1:1 gradient would probably be lost. As both DPOAE and TEOAE measured with the nonlinear stimulus method are both a result of nonlinear cochlear processes, their amplitudes could be expected to behave similarly.

1. Gradient of DPOAE/TEOAE amplitude relationship, $2f_1-f_2$

The DPOAE/TEOAE amplitude gradients associated with the $2f_1-f_2$ DP results were generally closer to 1 with lower stimulus levels and when $L_1>L_2$ [Table 1(c)]. This indicates that inter subject factors affecting OAE level have a proportionate effect on DPOAE and TEOAE with these stimulus conditions, implying that the mechanisms involved in generating the two OAE types are related. At higher stimulus levels there was also a tendency for the gradients to be higher with smaller frequency ratios, in spite of the lower DP growth rates associated with these stimulus parameters. These findings generally agree with the prediction s.d. data with the exception of the level difference: Reducing L_2 tended to increase the best-fit line gradient (implying closer agreement), but also increased the prediction s.d. (implying worse agreement) when f_2/f_1 was small.

2. Gradient of DPOAE/TEOAE amplitude relationship, $2f_2-f_1$

The $2f_2-f_1$ gradients were near to 1 with low stimulus levels, small frequency ratios, and $L_1=L_2$ and were lower with other DPOAE stimulus parameters. The pattern of results is therefore consistent with the prediction s.d. data. The tendency for the gradients obtained with a low stimulus level to be high may be a result of avoidance of a saturated DP response, whereas high gradients obtained with small frequency ratios and $L_1=L_2$ are associated with higher DPOAE levels and may therefore arise from the avoidance of the influence of noise.

Comparing the average DPOAE/TEOAE amplitude gradients of the two distortion products at each frequency ratio, the gradients associated with the $2f_2-f_1$ DP were closer to 1 than those of the $2f_1-f_2$ DP when $L_1=L_2$, but the $2f_1-f_2$ DP gradients were closer to 1 when $L_1=L_2+10$.

Considering the prediction s.d. and amplitude gradients together, both the $2f_1-f_2$ DP and the $2f_2-f_1$ DP levels appear to be generally most closely related to TEOAE with smaller frequency ratios and lower stimulus levels. Additionally, the $2f_2-f_1$ DP is also more closely related to TEOAE when $L_1=L_2$.

E. Retest error

The test–retest difference for the $2f_1-f_2$ distortion product was found to be 0.9 dB, so the values of prediction s.d. would not reliably fall below this even if there is no difference at all in the mechanisms involved in the TEOAE and DPOAE. Additionally, if a similar test–retest error is present in the TEOAE measurements, the combined effect would result in a prediction s.d. floor of 1.25 dB. Several of the $2f_2-f_1$ DP test configurations have produced prediction s.d. values which are of this order, and so there may not be any significant difference between the TEOAE measurement form and some configurations of DPOAE.

Possible additional random error arises from the possibility that the fine structure ripple may not be completely eliminated by the frequency averaging over only approximately $\frac{1}{2}$ of an octave and may not match perfectly between the frequency regions adopted from the TEOAE and DPOAE responses.

F. Phase gradients and delays

Derivation of the group delay from the phase data associated with the TEOAE and DPOAE measurements (Figs. 4 and 5) has indicated that $2f_1-f_2$ measurements with $f_2/f_1=1.05$ and all $2f_2-f_1$ measurements have phase gradients close to that of the corresponding TEOAE measurements, implying that the mechanisms by which the two forms of OAE are emitted are related. Stimulus frequency otoacoustic emissions (SFOAE) are also known to have similar steep phase versus frequency gradients (Shera and

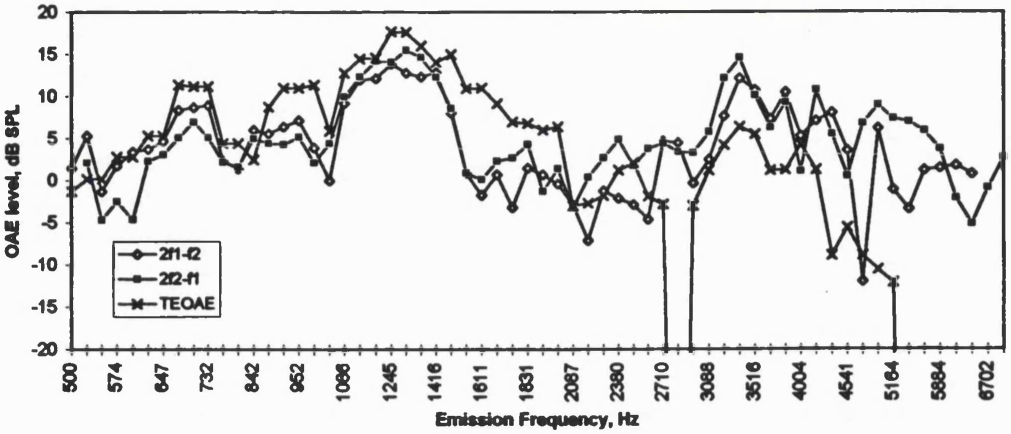

FIG. 6. Extended fine structure DP grams with corresponding TEOAE response on a logarithmic frequency scale. Each OAE is plotted against its emission frequency. The TEOAE amplitude is increased by 12 dB to correspond with the summation method used elsewhere in this study. The DPOAE stimulus parameters are $L_1 = L_2 = 70$ dB SPL $f_2/f_1 = 1.05$. Close agreement is seen in the fine structure of the three OAE forms.

Guinan, 1999). However, the phase gradients of the $2f_1 - f_2$ distortion product with larger frequency ratios were considerably reduced, suggesting that these emissions differ fundamentally from TEOAE.

G. Extension to full frequency range

In order to investigate the relationship of DPOAE to TEOAE across a full frequency range with a small DPOAE frequency ratio, an extended fine structure DP sweep was obtained with stimulus parameters $f_2/f_1 = 1.05$ and $L_1 = L_2 = 70$ dB SPL for one subject covering the frequency range 500–7000 Hz. The $2f_1 - f_2$ and $2f_2 - f_1$ DPs are shown in Fig. 6 with a corresponding standard TEOAE, with each response plotted against the frequency of the emitted response on a logarithmic scale. The level of the TEOAE response in Fig. 6 was increased by 12 dB to correspond with the summation method used in the averaging of the responses earlier in this study.

It can be seen that both of the distortion products shown were measurable across the complete frequency range, whereas as expected the TEOAE response level decreased sharply above 4 kHz as a result of the time windowing to remove low latency artifacts. The behavior of the $2f_2 - f_1$ distortion product with these parameters therefore differs from the wider frequency ratios used by Erminy *et al.* (1996), who observed a reduction in $2f_2 - f_1$ level towards higher frequencies. It can also be seen that the fine structures of the three responses show excellent agreement, indicating that with these stimulus parameters the fine structure of each OAE is determined by the emitted frequency rather than the stimulating frequency.

He and Schmiedt (1997) have shown that the fine structure of the $2f_1 - f_2$ DPOAE shifts in frequency with changes in stimulus level at frequency ratios of $f_2/f_1 = 1.11$, 1.2, and 1.33. Therefore, the finding presented here indicates that either the frequency shifting effect does not occur when $f_2/f_1 = 1.05$ or that the DPOAE parameters chosen coincidentally are subject to the same frequency shift as TEOAE, allowing the accurate relationship with TEOAE to occur.

IV. ORIGINS OF TEOAE AND DPOAE

The frequency ratio which produced the maximum level of the $2f_1 - f_2$ DPOAE was in the region of $f_2/f_1 = 1.2–1.3$ and it is largely for this reason that ratios between 1.2 and 1.3 have tended to be preferred for clinical use as the larger response results in a clearer differentiation between normal and hearing impaired ears.

In the case of the $2f_2 - f_1$ DP, the largest levels were obtained with a small stimulus frequency ratio and with $L_1 = L_2$. This pattern could be expected as a small frequency ratio brings the $2f_2 - f_1$ frequency closer to the stimulus frequencies where the transverse displacement on the basilar membrane due to the traveling wave is greater, while reducing L_2 below L_1 may reduce the travelling wave modulation depth in the $2f_2 - f_1$ frequency region and so reduce the effect of nonlinear distortion associated with the basilar membrane movement. Indeed, it is a general property of compressive nonlinearities that upper sideband distortion product generation is enhanced if L_2 exceeds L_1 by a small amount (Kemp, 1987).

The $2f_2 - f_1$ DP growth with stimulus level was faster with larger frequency ratios. This may be because the $2f_2 - f_1$ DP frequency is moved further to the base from the primary tones on the basilar membrane with larger stimulus ratios to a region where the primary tone traveling wave amplitudes grow linearly with increasing stimulus level as opposed to the compressive growth seen in the basilar membrane motion in the region of the traveling wave peak.

The amplitude relationships between TEOAE and DPOAE in some stimulus configurations have been found to be unexpectedly close despite the many obvious differences in the manner in which each emission is stimulated and extracted, supporting the view that with these stimulus conditions the same information is provided by results obtained by either OAE method and that the same underlying mechanism is responsible for both.

Both the $2f_1 - f_2$ and $2f_2 - f_1$ DP levels were more closely related to TEOAE when stimulated with a frequency ratio of $f_2/f_1 = 1.05$ than with the wider ratios of 1.2–1.32. Therefore DPOAE is more like TEOAE when stimulated with a small frequency ratio in which the emission frequency is close to that of the stimuli than when stimulated with a wide frequency ratio in which the emission frequency differs more markedly from the stimulus frequencies.

The amplitude relationship between TEOAE and DPOAE was closer with the $2f_1 - f_1$ DP than the $2f_1 - f_2$ DP. There are fundamental differences between these two DPOAEs which may indicate why the $2f_2 - f_1$ DP is more closely related to TEOAE. (1) The $2f_2 - f_1$ DPOAE genera-

tion site must be linked to the emission frequency place on the basilar membrane rather than the region of the stimulus frequencies. (2) The $2f_2-f_1$ DPOAE has only one possible emission region whereas the $2f_1-f_2$ DPOAE has two. (3) The phase behavior of the $2f_1-f_2$ and $2f_2-f_1$ DPOAEs differs.

Close agreement between the TEOAE and the $2f_2-f_1$ DP and also the low ratio $2f_1-f_2$ DP was seen in the phase data. The shallower phase gradient seen in the $2f_1-f_2$ DP at wider stimulus frequency ratios suggests that the $2f_1-f_2$ DPOAE may have a different mechanism of generation and/or emission depending on the ratio f_2/f_1.

The two distinct phase gradient categories are consistent with the two emission creating modes described as "place fixed" and "wave fixed" (e.g., Kemp, 1986; O Mahoney and Kemp, 1995; Kemp and Knight, 1999) or "reflection" and "distortion" (Shera and Guinan, 1998, 1999). The wave-fixed model, in which the emission source is locked to the traveling wave envelopes and so moves smoothly with frequency, would produce an almost flat phase gradient because of the approximate geometric frequency scaling of the cochlea. This is seen in the wide ratio $2f_1-f_2$ DP sweeps. The place fixed model, which requires a series of fixed impedance irregularities on the basilar membrane to reflect or scatter OAE energy back towards the base of the cochlea, would result in a comparatively steep phase gradient in a constant frequency ratio sweep, formed by the traveling wave envelopes of the stimulus tones passing over the reflectors as the stimulus frequencies change. This steep phase gradient behavior is consistent with TEOAE, SFOAE, the $2f_2-f_1$ DP, and the $2f_1-f_2$ DP behavior when f_2/f_1 is small.

Yates and Withnell (1998) have suggested that TEOAE may consist mostly of intermodulation distortion components, but it nevertheless has the phase characteristic of the reflection-based place-fixed model and therefore is not dominated by wide stimulus ratio, low-phase gradient, lower sideband components. If TEOAEs included a component like the $2f_1-f_2$ DP at wide ratios, this would be a low-latency component. It remains possible that low-latency components of the TEOAE exist, but are lost in the time windowing employed to extract the OAE from the stimulus and middle ear response.

The results raise the question of whether it would be valuable to change the DPOAE parameters used in clinical applications in order for the response to fall within the place fixed category. However, the issue of whether the wave fixed or place fixed category of OAE is more closely linked to auditory function remains unresolved, and so currently the only reason to change DP parameters would be to allow reliable interchangeability between DPOAE and TEOAE measurements. This would be at the expense of a loss of DPOAE intensity, resulting in a less efficient DPOAE measurement.

V. CONCLUSIONS

A closer agreement has been observed between TEOAE and DPOAE amplitude than has been previously presented.

This is thought to be because

(a) averaging over a frequency range has been used to reduce the variance which arises from the fine structure in DPOAE and TEOAE, and
(b) DPOAE parameters which are seldom used clinically have been found to produce the closest relationships.

The phase gradients of the TEOAE, $2f_2-f_1$ DPOAE, and $2f_1-f_2$ DPOAE with $f_2/f_1=1.05$ are similar and are consistent with a place-fixed reflection-based emission mechanism. Also, SFOAE is known to have a steep phase versus frequency characteristic. The phase of the $2f_1-f_2$ DP with a larger stimulus frequency ratio deviates markedly from this and instead is consistent with a wave fixed emission mechanism. It therefore seems that the DPOAE parameters chosen for clinical use result in an emission which is different from all other evoked OAEs.

ACKNOWLEDGMENTS

The authors would like to thank Peter Bray and Otodynamics Ltd. for customizing the software and each of the subjects who generously gave their time.

Dorn, P. A., Piskorski, P., Gorga, M. P., Neely, S. T., and Keefe, D. H. (**1998**). "Predicting audiometric status from distortion product otoacoustic emissions using discriminant analysis," Association for Research in Otolaryngology Abstracts 594.

Erminy, M., Avan, P., and Baril, P., and Bonfils, P. (**1996**). "Caractéristiques du produit de distorsion $2f_2-f_1$ chez l'homme normo-entendant," Ann. Otolaryngol. Chir. Cervicofac. **113**, 321–327.

Gaskill, S. A., and Brown, A. M. (**1990**). "The behavior of the acoustic distortion product, $2f_1-f_2$, from the human ear and its relation to auditory sensitivity," J. Acoust. Soc. Am. **88**, 821–839.

Gorga, M. P., Neely, S. T., Bergman, B. M., Beauchaine, K. L., Kaminski, J. R., Peters, J., Schulte, L., and Jesteadt, W. (**1993**). "A comparison of transient-evoked and distortion product otoacoustic emissions in normal-hearing and hearing-impaired subjects," J. Acoust. Soc. Am. **94**, 2639–2648.

Gorga, M. P., Neely, S. T., Ohlrich, B., Hoover, B., Redner, J., and Peters, J. (**1997**). "From laboratory to clinic: a large scale study of distortion product otoacoustic emissions in ears with normal hearing and ears with hearing loss," Ear Hear. **18**(6), 440–455.

Harris, F. P., Lonsbury-Martin, B. L., Stagner, B. B., Coats, A. C., and Martin, G. K. (**1989**). "Acoustic distortion products in humans: systematic changes in amplitude as a function of f_2/f_1 ratio," J. Acoust. Soc. Am. **85**, 220–229.

Hauser, R., and Probst, R. (**1991**). "The influence of systematic primary-tone level variation L_2-L_1 on the acoustic distortion product emission $2f_1-f_2$ in normal human ears," J. Acoust. Soc. Am. **89**, 280–286.

He, N., and Schmiedt, R. A. (**1997**). "Fine structure of the $2f_1-f_2$ acoustic distortion product: effects of primary level and frequency ratios," J. Acoust. Soc. Am. **101**, 3554–3565.

Kemp, D. T. (**1978**). "Stimulated acoustic emissions from within the human auditory system," J. Acoust. Soc. Am. **64**, 1386–1391.

Kemp, D. T. (**1986**). "Otoacoustic emissions, travelling waves and cochlear mechanisms," Hearing Res. **22**, 95–104.

Kemp, D. T. (**1987**). "Otoacoustic emission characteristics during moderate continuous stimulation-intermodulation," 12th International Congress of Acoustics B7-1.

Kemp, D. T. (**1998**). "Otoacoustic emissions: distorted echoes of the cochlea's travelling wave," in Otoacoustic Emissions Basic Science and Clinical Applications, edited by C. I. Berlin (Singular, San Diego), Chap. 1, pp 1–59, fig. 1-12.

Kemp, D. T., and Brown, A. M. (**1983**). "An integrated view of cochlear mechanical nonlinearities observable from the ear canal," in *Cochlear Mechanics*, edited by E. DeBoer and M. A. Viergever (Delft U. P., Delft, Holland).

Kemp, D. T., and Knight, R. D. (**1999**). "Virtual DP reflector explains DPOAE wave and place fixed dichotomy," Association for Research in Otolaryngology Abstracts **22**, 99–100, number 396.

Kemp, D. T., Ryan, S., and Bray, P. (**1990**). "A guide to the effective use of Otoacoustic Emissions," Ear Hear. **11**(2), 93–105.

Kemp, D. T., Bray, P., Alexander, L., and Brown, A. M. (**1986**). "Acoustic emission cochleography-practical aspects," Scand. Audiol. Suppl. **25**, 71–95.

Knight, R. D., and Kemp, D. T. (**1999**). "f_1, f_2 area representations of DPOAEs indicate that the clinical $2f_1$-f_2 DPOAE is an atypical form of OAE," Br J. Audiol. **33**, 87.

Martin, G. K., Jassir, D., Stagner, B. B., Whitehead, M. L., and Lonsbury-Martin, B. L. (**1998**). "Locus of generation for the $2f_1-f_2$ vs $2f_2-f_1$ distortion-product otoacoustic emissions in normal-hearing humans revealed by suppression tuning, onset latencies, and amplitude correlations," J. Acoust. Soc. Am. **103**, 1957–1971.

Martin, G. K., Lonsbury-Martin, B. L., Probst, R., Scheinin, S. A., and Coats, A. C. (**1987**). "Acoustic distortion products in rabbit ear canal. II. Sites of origin revealed by suppression contours and pure tone exposures," Hearing Res. **28**, 191–208.

Moulin, A., Bera, J. C., and Collet, L. (**1994**). "Distortion product otoacoustic emissions and sensorineural hearing loss," Audiology **33**, 305–326.

Moulin, A., Collet, L., Veuillet, E., and Morgon, A. (**1993**). "Interrelations between transiently evoked otoacoustic emissions and acoustic distortion products in normally hearing subjects," Hearing Res. **65**, 216–233.

Moulin, A., and Kemp, D. T. (**1996**). "Multicomponent acoustic distortion product otoacoustic emission phase in humans. I. General characteristics," J. Acoust. Soc. Am. **100**, 1617–1639.

O Mahoney, C. F., and Kemp, D. T. (**1995**). "Distortion product otoacoustic emissions," Arch. Otolaryngol. Head Neck Surg. **119**, 858–860.

Prieve, B. A., Gorga, M. P., Schmidt, A., Neely, S., Peters, J., Schules, L., and Jesteadt, W. (**1993**). "Analysis of transient-evoked otoacoustic emissions in normal hearing and hearing-impaired ears." J. Acoust. Soc. Am. **93**, 3308–3319.

Probst, R., and Harris, R. (**1993**). "Transiently evoked and distortion-production otoacoustic emissions," Arch. Otolaryngol. Head Neck Surg. **119**, 858–860.

Robinette, M. S., and Glattke, T. J. (eds.) (**1997**). *Otoacoustic Emissions: Clinical Applications* (Thiele, New York).

Shera, C. A., and Guinan, J. J. (**1998**). "Reflection emissions and distortion products arise by fundamentally different mechanisms," Association for Research in Otolaryngology Abstracts 344.

Shera, C. A., and Guinan, J. J. (**1999**). "Evoked otoacoustic emissions arise by two fundamentally different mechanisms: A taxonomy for mammalian OAEs," J. Acoust. Soc. Am. **105**, 782–798.

Smurzinsky, J., and Kim, D. O. (**1992**). "Distortion-product and click-evoked otoacoustic emissions of normally-hearing adults," Hearing Res. **58**, 227–240.

Smurzinsky, J., Jung, M. D., Lafreniere, D., Kim, D. O., Kamath, M. V., Rowe, J. C., Holman, M. C., and Leonard, G. (**1993**). "Distortion-product and click-evoked otoacoustic emissions of preterm and full-term infants," Ear Hear. **14**(4), 258–274.

Stover, L., Gorga, M. P., Neely, S. T., and Montoya, D. (**1996**). "Toward optimising the clinical utility of distortion product otoacoustic emission measurements," J. Acoust. Soc. Am. **100**, 956–967.

Wable, J., Collet, L., and Chéry-Croze, S. (**1996**). "Phase delay measurements of distortion product otoacoustic emissions at $2f1-f2$ and $2f2-f1$ in human ears," J. Acoust. Soc. Am. **100**, 2228–2235.

Whitehead, M. L., McCoy, M. J., Lonsbury-Martin, B. L., and Martin, G. K. (**1995**). "Dependence of distortion-product otoacoustic emissions on primary levels in normal and impaired ears. I. Effects of decreasing L_2 below L_1," J. Acoust. Soc. Am. **97**, 2346–2358.

Wilson, J. P. (**1980**). "Evidence for a cochlear origin for acoustic re-emissions, threshold fine-structure and tonal tinnitus," Hearing Res. **2**, 233–252.

Yates, G. K., and Withnell, R. H. (**1998**). "Intermodulation distortion in click-evoked otoacoustic emissions," Association for Research in Otolaryngology Abstracts 17.

Indications of different distortion product otoacoustic emission mechanisms from a detailed f_1,f_2 area study

Richard D. Knight and David T. Kemp
Auditory Biophysics Group, Institute of Laryngology and Otology, University College London, 330/332 Gray's Inn Road, London WC1X 8EE, United Kingdom

(Received 2 March 1999; revised 26 August 1999; accepted 1 September 1999)

The primary site of generation on the basilar membrane for the $2f_1-f_2$ distortion product (DP) is generally considered to be near where the higher-frequency stimulus tone peaks. This site has also been shown to be a source of DP otoacoustic emission (DPOAE) in the ear canal, but a second source of emission is known to exist in the region of the DP frequency place. The DPOAE phase versus frequency gradient provides a means of investigating the emission mechanisms. "Wave-fixed" and "place-fixed" mechanisms have been proposed to account for the very different phase gradients found depending on whether the $2f_1-f_2$ DPOAE is evoked by a small or large stimulus-frequency ratio. DPOAE phase versus frequency gradients can be investigated either by sweeping f_1,f_2 or by sweeping both frequencies maintaining a constant frequency ratio. Each manipulation gives only a partial description of DP behavior. In this study, the place-fixed/wave-fixed dichotomy is analyzed using extensive $2f_1-f_2$ and $2f_2-f_1$ DP stimulus-frequency sweep data presented on matrices of f_1 vs f_2 and f_2/f_1 ratio versus DP frequency. These show how the DPs are related and provide a more complete picture of $2f_1-f_2$ and $2f_2-f_1$ DPOAE phase and amplitude versus frequency behavior. The phase data contain evidence for a systematic variation in the proportions of wave- and place-fixed emission. The results suggest that $2f_1-f_2$ DPOAEs with a wide stimulus frequency ratio are wave fixed, while all other DPOAEs are place fixed. A transition occurs within the $2f_1-f_2$ DP data region at a frequency ratio of about $f_2/f_1=1.1$. The $2f_1-f_2$ DP and $2f_2-f_1$ DP phase behavior is continuous across the $f_2/f_1=1$ boundary. As the $2f_2-f_1$ DP generation region must be strongly influenced by the DP frequency place, the results imply that the place-fixed component of the $2f_1-f_2$ DP is also linked to its frequency place. A similar pattern was obtained with the $3f_1-2f_2$ and $3f_2-2f_1$ DPs. The results support the following model: For the limited set of stimulus conditions that gives rise to $2f_1-f_2$ wave-fixed emissions, DP energy is largely generated in the f_2 region and is emitted directly. All other DPOAEs are place-fixed emissions, and while nonlinearity within the f_2 stimulus envelope remains the generator, the DP is not directly emitted but travels apically until it is re-emitted basally via a separate reflection mechanism in the region of the DP place.
[S0001-4966(99)05212-1]

PACS numbers: 43.64.Jb, 43.64.Kc, 43.64.Ri [BLM]

INTRODUCTION

All evoked otoacoustic emissions (OAEs) exhibit delay relative to the stimulus; therefore, OAE phase is dependent on frequency. Phase versus stimulus frequency gradients have been shown, for example, with transient-evoked otoacoustic emissions (TEOAE) (e.g., Kemp and Chum, 1980a; Wilson, 1980), distortion product otoacoustic emissions (DPOAE) (Kemp and Brown, 1983), and stimulus frequency otoacoustic emissions (SFOAE) (Kemp and Chum, 1980b). The group delay implied by these phase gradients (often referred to as "OAE latency") is believed to contain information about the mechanism underlying otoacoustic emissions.

The possibility of two cochlear sources of lower sideband DPOAE was suggested by Kim (1980). Two modes of distortion product emission mechanism were first put forward by Kemp and Brown (1983), and Kemp (1986) introduced the terms wave- and place-fixed to describe these two modes. These have recently been discussed by Shera and Guinan (1998, 1999), who referred to the wave-fixed and place-fixed modes of emission as "distortion" or "reflection" emissions and emphasized fundamental differences between them.

In the case of the wave-fixed mode, the emission site is supposed to be an integral part of and to move smoothly with the stimulus traveling wave envelope as stimulus frequency is swept. Since the cochlear frequency scaling is approximately geometric, with the result that frequency shifts cause little change to the traveling wave shape, when a stimulus pattern is swept in frequency the phase at any point moving with the traveling wave envelope changes little. Therefore, any OAE contribution from that point would have a very shallow phase gradient. With the place-fixed model, a series of reflecting or scattering sites is supposed to exist at fixed locations along the basilar membrane. As a stimulus is swept in frequency and its excitation pattern moved along the basilar membrane, the stimulus phase at each reflector will change, thus changing the OAE phase and creating a steep phase gradient.

Shera and Guinan (1999) showed that the wave-fixed

mechanism was consistent with the shallow DPOAE phase gradient obtained with the most commonly used stimulus parameters in a constant frequency ratio sweep, but was incapable of generating the steep phase gradients obtained with stimulus frequency (SF) OAE and transiently evoked (TE) OAE. Therefore, they argued, OAEs fell into two entirely separate categories—a distortion-emission class and a reflection-emission class.

However, the steep and shallow phase-gradient characteristics can both be observed in $2f1-f2$ distortion product OAEs obtained with constant stimulus frequency ratio sweeps. Kemp (1986) and Knight and Kemp (1999) have shown that the $2f_1-f_2$ DPOAE has a shallow phase gradient consistent with the wave-fixed model when stimulated using typical clinical stimulus parameters (f_2/f_1 is usually between 1.2 and 1.25 for clinical use), but has a steep phase gradient when stimulated using a small stimulus frequency ratio, e.g., $f_2/f_1=1.05$. Therefore, the $2f_1-f_2$ DP appears to change emission mode depending on whether a wide or small stimulus frequency ratio is used.

DPOAE phase gradients are not entirely smooth and monotonic. In addition to an overall gradual change in phase gradient from low to high frequency, there are also small scale irregularities. These irregularities are not only due to the effects of noise, as they occur when the DPs are well above the noise floor. The irregularities are permanent and repeatable and are often associated with the fine structure of DPOAE amplitude (Moulin and Kemp, 1996). The irregularities could arise from interference caused by multiple reflections between the DP frequency place in the cochlea and the middle ear (Stover *et al.*, 1996), or by interference between either two DP sources (e.g., Brown *et al.*, 1996; Talmadge *et al.*, 1999), or between different parts of a distributed source region (e.g., Zweig and Shera, 1995; Sun *et al.*, 1994). It may be that more than one of these effects can occur, either simultaneously or under different stimulus conditions.

Usually, test strategies are adopted for obtaining DP phase gradients with either f_1 (e.g., Kimberley *et al.*, 1993) or f_2 (e.g., O Mahoney and Kemp, 1995) being swept in frequency while the other is held constant. In the case of the "f_1 sweep," the $2f_1-f_2$ DP generation region [which is related to the f_2 frequency place (e.g., Brown and Kemp, 1984)] remains stationary, whereas with an "f_2 sweep," the $2f_1-f_2$ DP generation region moves. It has been shown that in the case of the $2f_1-f_2$ DP, f_2 sweeps result in a higher value for group delay than f_1 sweeps (Kimberley *et al.*, 1993; O Mahoney and Kemp, 1995). The $2f_2-f_1$ DP behaves differently. No significant difference between f_1 and f_2 sweep latencies is reported (Moulin and Kemp, 1996).

DPOAE latency does not directly indicate the site of generation. Using an f_2 sweep paradigm, the group delay of the $2f_2-f_1$ DP has been reported by Wable *et al.* (1996) to be shorter than that of the $2f_1-f_2$ DP; this finding was used to support the generally accepted view that the generation region of the $2f_2-f_1$ DP is more basal than the $2f_1-f_2$ DP (Martin *et al.*, 1998). However, this result is in fact dependent on the test paradigm—the opposite result could have been found using a sweep with a constant frequency ratio (Knight and Kemp, 1999). The "latency" derived from DPOAE phase versus frequency gradients requires careful interpretation as an indicator of true time delay because of the dispersive nature of the cochlea and because the path length varies with frequency. The phase gradient also does not directly indicate the relative source locations of the DPs along the basilar membrane, as the DPs have different frequencies and would therefore travel at different speeds at the same location in the cochlea and also because different mechanisms may be involved in generating the reverse traveling waves. The onset delays measured by Whitehead *et al.* (1996) are an alternative method of evaluating DP delay and the result is a more physically meaningful time delay, although the onset can be gradual, resulting in uncertainty regarding the exact onset time. Despite the difficulties in interpretation, phase gradient-derived delays are useful as comparative probes of the mechanisms involved in cochlear function.

Logically, the $2f_1-f_2$ DP must be generated in a region where both stimulus tones are present, which in practice means within the f_2 envelope, probably near the f_2 traveling wave peak. Once the DP is generated it may travel in either direction—either straight back out or onwards to the DP place. From the DP place it may be re-emitted back to the base as a "stimulus-frequency" emission. Group delays consistent with both wave- and place-fixed emission modes have been found in $2f_1-f_2$ DPOAE measurements. The place-fixed part would be consistent with a stimulus-frequency OAE from the DP place, and the wave-fixed part would be consistent with a direct emission from the region of the f_2 frequency place as suggested by Whitehead *et al.* (1996), Fahey and Allen (1997), and Brown *et al.* (1996).

The emitted $2f_2-f_1$ DP, meanwhile, must originate in the region of the f_2 envelope which embraces the DP characteristic frequency place on the basilar membrane, since frequencies propagate very poorly from positions apical to their characteristic place. These conclusions are supported by suppression studies (e.g., Martin *et al.*, 1987, 1998; Kemp, 1998). The DP could be produced at the sites of the reflectors and immediately travel basally, or it may be generated at a site removed from the reflectors and initially travel apically until a reflector is encountered.

Inverse Fourier transform techniques have been used to view complex DPOAE data obtained with f_1 stimulus frequency sweeps in the time domain. This has revealed coexisting DP components with different latencies whose relative strength varies depending on stimulus level (Fahey and Allen, 1997; Stover *et al.*, 1996). Stover *et al.* also found that with low stimulus amplitudes a series of DPOAE amplitude peaks is sometimes seen in the time domain, which could be an indication of multiple reflections between the DP place and the stapes.

Generally, the literature has centered on the wide-frequency ratio case with the $2f_1-f_2$ DP, and tended to avoid small and intermediate frequency ratios and phase data with the $2f_2-f_1$ DP.

As discussed above, the use of f_1 and f_2 sweeps to investigate latency, while useful, provides an incomplete picture of DP phase behavior and the true significance of the

"partial" latencies obtained via these methods remains unclear. The aim of this study was to reach a better understanding of which stimulus conditions result in DPOAE of the wave-fixed and the place-fixed type and determine how the production of $2f_2-f_1$ DPOAE is similar to or different from the $2f_1-f_2$ DP in this respect. Previous reports on DPOAE phase behavior have been fragmentary and invariably presented as isolated sweeps of either f_1, f_2 or occasionally constant f_2/f_1 sweeps. In the present study, we adopt a new representation in which multiple sweeps are combined within two-dimensional stimulus domains, providing a more complete picture of DPOAE phase versus frequency behavior.

Phase gradients over the stimulus-frequency surfaces rather than over isolated linear sweeps allow the delineation all of the conditions in which the DPOAE behavior is consistent with the wave-fixed mechanism and when it matches the place-fixed emission mechanism. Also, the transition region between the two domains can be visualized, previously only known from single-sweep data. Direct comparison of the $2f_1-f_2$ and $2f_2-f_1$ DPs allows exploration of the links between them and identification of any common characteristics.

A. Two-dimensional DP data representation

1. Phase behavior expected from wave- and place-fixed emissions

Because of the near-geometric frequency scaling of the cochlea, the phase of a wave-fixed DPOAE would be expected to be roughly constant through a frequency sweep maintaining a constant stimulus-frequency ratio.

If the frequency ratio changes, the relative phases of f_1 and f_2 must change over the whole excitation region and the DP phase must also change. In the case of an f_1 change, even if the DP generator itself were fixed to the f_2 wave envelope the DP generator would still "read" the changing phase of f_1 at the generator site. Similarly, for an f_2 frequency change the generator site would be moved to a new location where the phase of f_1 would be different. Therefore, for either an f_1 or f_2 sweep the DPOAE phase would change smoothly with a changing frequency ratio.

In the case of a place-fixed lower-sideband DPOAE, DP energy is released from a region inside the f_2 excitation envelope basal to the DP frequency place and propagates apically towards the DP frequency place, from where it is then re-emitted. (Upper-sideband DPOAE may also travel apically before being reflected basally in this way, or may be generated at fixed points already traveling in a basal direction.) Much of the latency would be associated with the traveling wave behavior near the DP place. In this case, it is helpful to consider a constant DP frequency sweep as the phase of a place-fixed DPOAE may remain relatively constant during such a sweep.

For the $2f_2-f_1$ DP at wide frequency ratios, the inward travel time of the stimulus tones to the DP place would be very short and almost constant with f_1 and f_2 frequency changes because the f_1 and f_2 peaks would be far removed apically from the DP place. The DPOAE phase would therefore depend only on the DP frequency, and so the phase contours for the $2f_2-f_1$ DP would be expected to closely follow lines of equal DP frequency. In the case of a constant-DP-frequency sweep (for which, in the case of the $2f_2-f_1$ DP, f_1 changes at twice the rate of f_2) a flat phase characteristic would in this case be observed. With a smaller frequency ratio, some inward f_1 and f_2 delay could accumulate and so the DPOAE phase may then develop a steeper gradient in a constant-DP-frequency sweep. However, the DP may be generated basal to the DP place and propagated apically before being reflected at the DP place. The amount of inward delay would depend on how close the DP generator is to the DP frequency place on the basilar membrane: the closer to the DP place, the more the inward travel time would increase.

For the $2f_1-f_2$ DP, in the case of a place-fixed emission, substantial phase delays for the primaries would be expected to accumulate by the DP generation site which would add to the phase delay contributed by the re-emission from the DP place. $2f_1-f_2$ DPOAE phase contours would not necessarily, therefore, be expected to lie along lines of constant DP frequency.

2. f_1, f_2 area

Figure 1(a) defines the first way in which we will present DPOAE data in this study. In this representation we can show what phase-contour pattern can be expected for different DPOAE emission mechanisms. Constant ratio frequency sweeps are straight lines in this representation radiating from the 0, 0-Hz point. Phase contours would be expected to follow this pattern in the case of a wave-fixed emission mechanism.

Lines of constant DP frequency are a family of parallel lines and cross the chart with a gradient of 2 (because the stimulus frequency which is more distant to the DP frequency must change at twice the amount of the closer stimulus frequency in order to maintain a constant DP frequency). Phase contours would be expected to follow this pattern in the case of a place-fixed emission mechanism.

3. f_2/f_1 ratio, DP frequency area

Figure 1(b) defines the second way in which we will present DPOAE data in this study. Amplitude data have been shown using a related presentation method by Moulin *et al.* (1999) (but with $f2/f1$ vs f_2 instead of DP frequency). In this case, by definition, lines of constant frequency ratio are horizontal and lines of constant DP frequency are vertical. Therefore, phase contours which are horizontal on this chart are consistent with a wave-fixed emission mechanism and phase contours which are vertical are consistent with a place-fixed emission mechanism.

I. METHOD

A. Subjects

Data presented in this paper are drawn from an exhaustive study of DPOAE conducted using the left ears of two subjects: a male (RDK), aged 29 and a female (RN), aged 24. Prior to commencing the DPOAE study, the ears were confirmed as having normal auditory thresholds and middle-ear function. In addition, standard DP grams ($f_1/f_2=1.22$, L_1

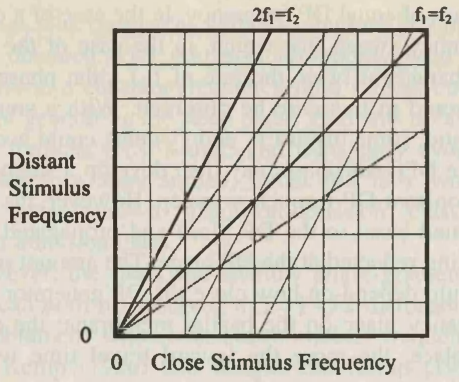

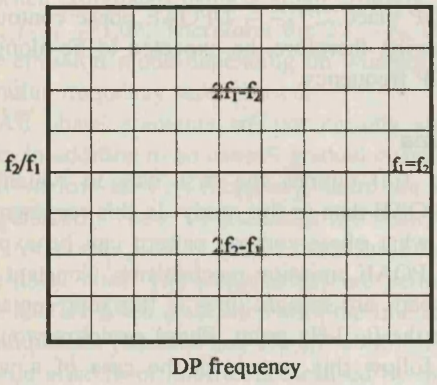

FIG. 1. (a) The f_1, f_2 scheme for presenting DPOAE data. The frequency scales are linear and the x and y axes are the "close" and "distant" stimulus frequencies, respectively. These terms refer to the stimulus frequencies which are closer to or further away from the DP frequency, i.e., the close stimulus frequency to the $2f_1-f_2$ DP is f_1 and the close stimulus frequency to the $2f_2-f_1$ DP is f_2. The reason for employing this definition for the axes rather than simply using f_1 and f_2 is that it allows both upper-sideband and lower-sideband DP data to be combined on one chart. The leading diagonal line on the chart is $f_1=f_2$, a condition at which DP measurements are not possible. Above this line is the $2f_1-f_2$ DP area; below the line is the $2f_2-f_1$ DP area. The line running from the origin with a gradient of 2 is $f_2=2f_1$. At this line, the $2f_1-f_2$ DP frequency falls to 0 Hz and therefore becomes mathematically impossible. In practice, the DP becomes unmeasurable well before this. No similar limitation exists with the $2f_2-f_1$ DP, although the DP also becomes unmeasurable if f_1 and f_2 are very widely separated. Dotted lines show the orientation of constant f_2/f_1 and constant DP frequency sweeps. (b) The f_2/f_1 versus DP frequency scheme for presenting DPOAE data. $f_1=f_2$ is a horizontal line at the center of the chart (i.e., $f_2/f_1=1$). Above this is the $2f_1-f_2$ DP; below it is the $2f_2-f_1$ DP.

$=65$, $L_2=55$ dB SPL) were obtained which were within normal limits (Gorga *et al.*, 1997). RDK was one of a small normal-hearing group investigated for TEOAE and DPOAE phase characteristics and was typical of that group (Knight and Kemp, 1999).

B. Experimental method

An ILO88 DPi instrument was used with a standard adult two port probe (RDK) and a standard child probe (RN), which deliver the two stimulus tones via separate amplification and loudspeakers. Custom stimulus "sweeps" could be preprogramed with either f_1, f_2 or f_1 and f_2 in increments with time. Each measured DP sweep data point was obtained from averaging of 64 (RDK) or 32 (RN) signal samples, each of 80-ms duration. The equipment has a noise rejection facility in which individual 80-ms samples were excluded if the noise exceeded a preset noise threshold. This was set to between 2 or 4 mPa depending on the ear fitting and on the frequency range to be tested. The equipment was situated in a quiet room with a typical background noise level of 40 dBA SPL.

Level differences between L_1 and L_2 were not explored as these are usually devised to optimize $2f_1-f_2$ DPOAE amplitude for a specific frequency ratio. For measurements with RDK with $L_1=L_2=60$ or 75 dB SPL, sequential measurements were mostly in the form of f_2 sweeps with 12-Hz steps, supplemented by some f_1 sweeps and constant frequency ratio sweeps. Successive f_2 sweeps were separated by f_1 intervals of approximately 50 Hz. Subsequently, where required to clarify detail, additional f_2 sweeps were added which halved the frequency spacing between adjacent sweeps to approximately 25 Hz. For RDK and RN with $L_1=L_2=70$ dB SPL, the data were obtained in constant f_2/f_1 sweeps, with the ratio in increments of 0.25 for adjacent sweeps. The overall stimulus-frequency range studied extended from 1300 Hz to approximately 3 kHz for the f_1, f_2 area representation, which was extended to a DP frequency range of 1–4.1 kHz for the f_2/f_1 versus DP frequency area representation.

In order to be accepted, each DP sweep data measurement was required to exceed the mean measured noise level in the adjacent ten harmonic frequencies of the 80-ms data sample by at least 1 s.d. In order to be visible above the floor in the amplitude chart, the DP amplitude also needed to exceed -15 dB SPL. Constant frequency ratio sequences swept from low frequency towards higher frequencies.

The stimulus levels used were $L_1=L_2=75$, 70, and 60 dB SPL. The 75-dB SPL level was chosen because of the large amplitude and therefore better signal-to-noise (S/N) ratio of the DPs. The stimulus levels also facilitated successful measurements at wider frequency ratios than could have been obtained using smaller-amplitude stimuli. This level is higher than that typically employed for clinical assessment but did not lead to a significant risk of artifactual DP contamination and did not generate measurable DPs in a 1-cc test cavity. Similar sets of measurements were obtained using lower stimulus levels for comparison. At each frequency point, the data for the first pair of DPs were obtained simultaneously, i.e., the $2f_1-f_2$ and $2f_2-f_1$ DP data were obtained simultaneously for frequency points on the chart with the stimulus frequencies transposed.

C. Testing procedure

The probe was sealed in the external auditory meatus with a disposable foam tip. Each DP sweep was preceded by a "checkfit" procedure in which the frequency response of the ear canal was measured using wideband clicks. In the event of the response not being substantially flat in the fre-

quency region to be tested, the probe was removed and reinserted. The f_1 or f_2 sweep sequences began with a small frequency ratio, with either f_2 in successive increments or f_1 in decrements until several successive $2f_1-f_2$ and $2f_2-f_1$ DPOAEs were unobtainable or until the limits of the frequency range under investigation were reached. Constant frequency ratio sweeps began at low frequency and swept towards higher frequencies.

D. Data analysis

DP amplitude and phase data from every DP sweep were entered into the two-dimensional frequency plane in EXCEL spreadsheets. To complete a single area chart, up to approximately 3500 data points were obtained per DP from up to approximately 70 f_1 and f_2 sweeps. On occasion, single points were repeated at intersections of f_1 and f_2 sweeps and in these cases an average was taken. Typically, repeated points agreed to within 2 dB or 20°. Linear interpolation was employed between unmeasured data points. However, no interpolation was allowed across data points which failed to meet the S/N criteria or at data points where adjacent measured data implied that a DPOAE would not have met the S/N criteria if attempted. This restriction was to prevent excessive "filling in" of amplitude notches or smoothing of irregularities in the phase data.

The phase was unwrapped by adding or subtracting multiples of 360° so as to minimize adjacent phase steps. The absolute number of whole 360° cycles is unknown for each DP. With the $2f_1-f_2$ DP, a choice was necessary whether to optimize the smoothing of the phase at small or large stimulus-frequency ratios. This was because optimizing the smoothing of the phase with small f_2/f_1 led to some large phase steps with large f_2/f_1, and vice versa. This curious feature of the phase data is described in more detail in Results, Sec. II C.

E. Data analysis in the time domain

In order to observe the relative contributions of the various components of the DPOAEs, long sweeps of DPOAE data were obtained and subsequently analyzed in the time domain via an inverse Fourier transform. This resulted in the different DPOAE components being separated by their latencies. This is similar to the method of Stover *et al.* (1996) except that they used f_2 sweeps. Two hundred-and-fifty-six-point constant frequency ratio sweeps of the $2f_1-f_2$ DP were obtained with $L_1=L_2=70$ dB SPL using 12-Hz steps through an f_1 frequency range from 1 to 4 kHz. Before the data were inverse-Fourier transformed to enter the time domain, the frequency intervals within the DP sweeps were converted to a log scale. This was in order to linearize the underlying phase gradient, which would otherwise gradually change from low to high frequency as a result of the logarithmic frequency scaling of the cochlea and give rise to a broad peak in the time domain with different parts of the peak representing different parts of the frequency sweep. Use of a logarithmic frequency scale counteracts the effect of cochlear frequency scaling and results in a linearized underlying phase gradient and therefore well-defined peaks in the time domain. The time scales in the time domain were derived from the average DP frequency step size in each of the logarithmic frequency scales.

II. RESULTS

A. f_1, f_2 area representation

1. Subject RDK

a. $L_1=L_2=75$ dB SPL

i. Amplitude features. The amplitude data for the $2f_1-f_2$ and $2f_2-f_1$ DPs are shown in Fig. 2(a). In general, the maximum amplitude tended to occur with the $2f_1-f_2$ DP using a frequency ratio of 1.3–1.35, consistent with the results of Harris *et al.*, 1989. In addition, for this ear the DP amplitude was generally raised in two broad areas, one in the $2f_1-f_2$ DP below $f_1=1.8$ kHz and one in both DPs above approximately $f_1=2.2$ kHz.

Also in this ear, two well-defined valleys with a depth of 10–15 dB can be seen in the $2f_2-f_1$ DP data. The notches occur at constant DP frequencies and possibly continue into the $2f_1-f_2$ DP data. The $2f_2-f_1$ DP was measurable at very wide frequency ratios away from the center line, extending up to $f_2/f_1=1.9$. This contrasts with the $2f_1-f_2$ DP, which was not measurable at frequency ratios greater than $f_2/f_1=1.5$. Notches are typically seen in DP gram data and the 2D representation shows how these notches would shift position for DP grams constructed with different primary ratios. The amplitude data of the $2f_1-f_2$ DP contain a smooth plateau along the maximum amplitude region of $f_2/f_1=1.3-1.4$, whereas at smaller frequency ratios a series of valleys occurred which followed lines of approximately constant DP frequency. There are missing data in both DPs at $f_2/f_1=1.5$, which was caused in the $2f_1-f_2$ DP by the fact that the difference tone was coincident, and in the $2f_2-f_1$ DP by harmonic distortion at $2f_1$ (most likely from the transducers) appearing in the noise spectrum.

ii. Phase. Overall, the 2D representation shows lines of equal phase running from lower left to upper right bending to become less steep as they do so.

It is highly significant that the $2f_2-f_1$ DP phase contours (lower-right region) all lie along constant DP frequencies [Fig. 2(b)] in contrast to the $2f_1-f_2$ DP region (upper left).

The $2f_2-f_1$ DP data also contained phase steps which occurred at constant DP frequencies and coincided with the amplitude notches described in Sec. *i.* above.

With a small frequency ratio (close to the diagonal $f_1=f_2$ line), the $2f_1-f_2$ DP phase contours tend to be a continuation of the $2f_2-f_1$ DP phase contours with isophase lines crossing directly between the two DP regions. At larger frequency ratios the $2f_1-f_2$ DP phase contours turn to follow constant frequency ratios. The transition occurs at a frequency ratio of around $f_2/f_1=1.1-1.15$.

b. Reduced stimulus levels, $L_1=L_2=60$ dB SPL

The overall pattern of results obtained at $L_1=L_2=75$ dB SPL was not specific to that stimulus level, although signifi-

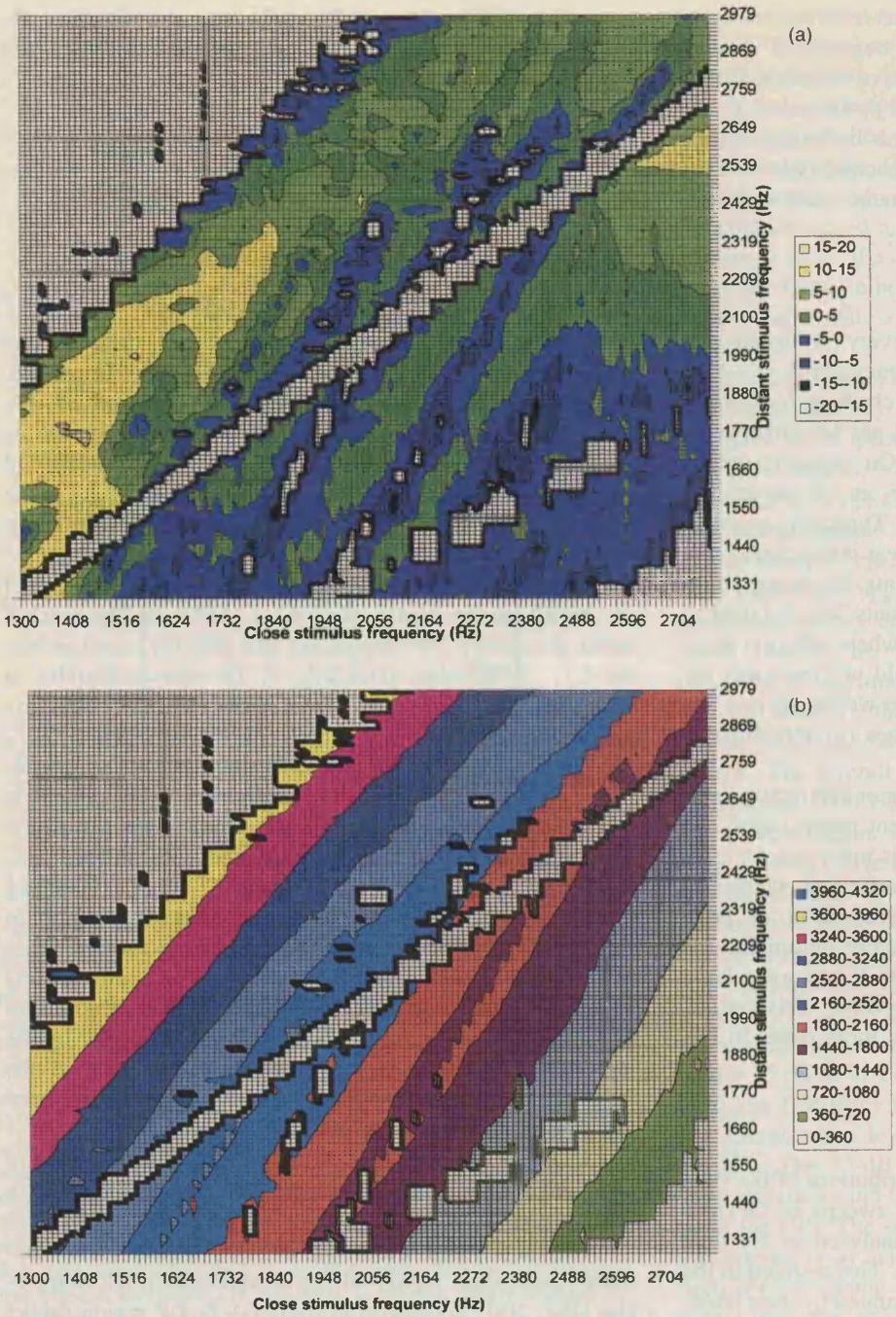

FIG. 2. f_1, f_2 area representations of (a) level, dB SPL (upper chart), and (b) phase, deg (lower chart) of $2f_1-f_2$ and $2f_2-f_1$ DPOAE with $L_1=L_2=75$ dB SPL with subject RDK. In each chart, $2f_1-f_2$ DP data are above the leading diagonal line; $2f_2-f_1$ DP data are below the line. Major amplitude features include two valleys in the $2f_2-f_1$ DP data which follow approximately constant DP frequencies, and in the $2f_1-f_2$ DP data there are complex amplitude patterns when f_2/f_1 is small, but a smooth amplitude function when f_2/f_1 is between 1.2 and 1.4. Phase contours typically follow lines of constant DP frequency, but there is a transition within the $2f_1-f_2$ DP data at approximately $f_2/f_1=1.1-1.15$, above which the phase contours follow lines of constant stimulus-frequency ratio.

cant differences were found with stimulus level, mainly in the amplitude data.

i. Amplitude differences. The measurements were repeated with the stimulus reduced to $L_1=L_2=60$ dB SPL. The amplitude data obtained using a lower stimulus amplitude [Fig. 3(a)] are much more complex. The two pronounced valleys in the $2f_2-f_1$ DP data are no longer present, but have been replaced by another at approximately 3 kHz. The $2f_2-f_1$ DP amplitude is still strong at small frequency ratios, but at frequency ratios above $f_2/f_1=1.2$ there has been a larger reduction in amplitude, resulting in difficulty obtaining measurements. The $2f_1-f_2$ DP data also appear more complex, with valleys which are not always straight following approximately constant DP frequencies. The valleys in some cases appear to divide into two, for example when the close stimulus frequency (f_1) is 1700 and 1900 Hz. The amplitude features are not just noise, as the data are well above the noise floor (except the very lowest amplitude points), are repeatable, and related patterns occur across adjacent data sweeps. No smooth plateau occurs in the $2f_1-f_2$ DP data and the maximum amplitude occurs at a smaller frequency ratio than was the case with the stimulus levels at 75 dB SPL (approximately $f_2/f_1=1.2$ instead of 1.3).

ii. Phase. The phase data [Fig. 3(b)] essentially follow the same patterns as with the higher stimulus levels, where the data met the S/N criteria. In the case of the $2f_1-f_2$ DP, the transition at which the phase contours turn from follow-

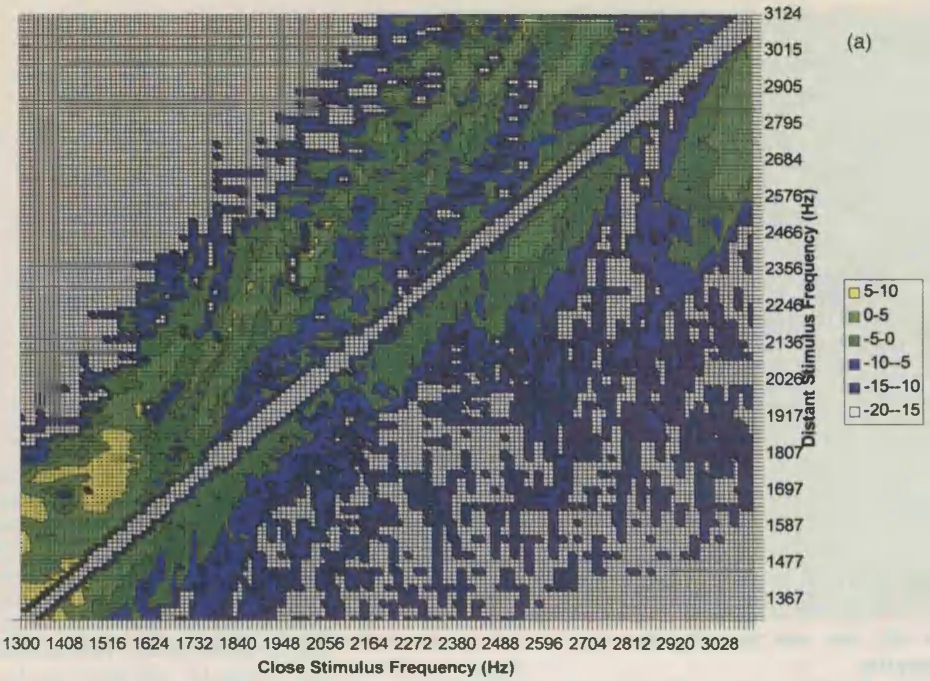

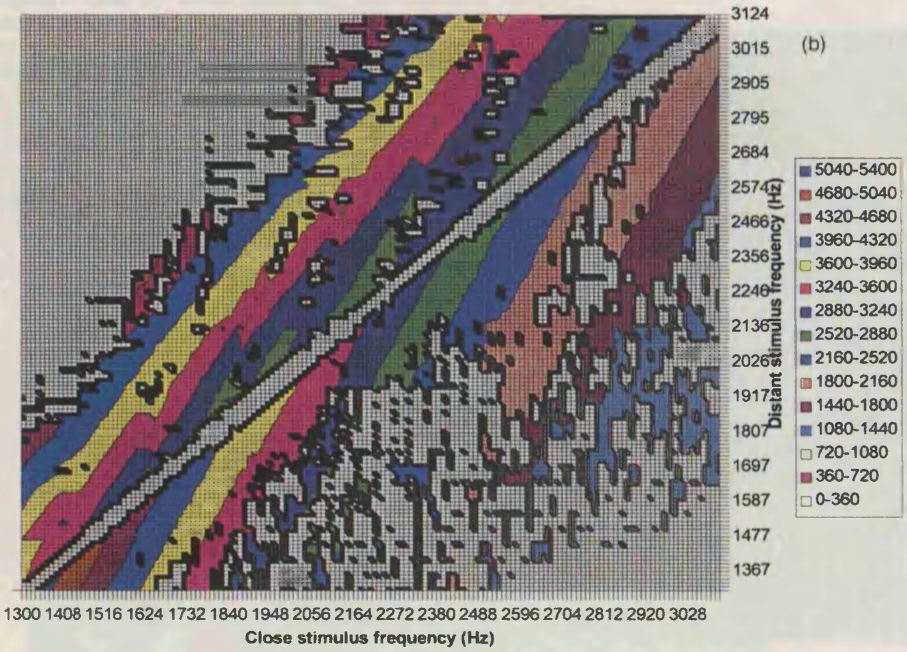

FIG. 3. f_1, f_2 area representations of (a) level, dB SPL (upper chart), and (b) phase, deg (lower chart) of $2f_1-f_2$ and $2f_2-f_1$ DPOAE with $L_1=L_2=60$ dB SPL with subject RDK. In each chart, $2f_1-f_2$ DP data are above the leading diagonal line; $2f_2-f_1$ DP data are below the line. Compared to Fig. 2, the $2f_1-f_2$ DP amplitude is much more complicated with no smooth plateau at any ratio of f_2/f_1. The $2f_2-f_1$ DP is difficult to measure at wide stimulus-frequency ratios, and the two amplitude valleys which were found when $L_1=L_2=75$ dB SPL are no longer present, but another valley has appeared at a higher frequency. The phase behavior is similar to that seen in Fig. 2, except that the transition region within the $2f_1-f_2$ DP data occurs at a slightly larger stimulus-frequency ratio.

ing a constant DP frequency to following a constant frequency ratio occurs at a slightly larger frequency ratio of approximately $f_2/f_1=1.15$.

c. Higher-order DPOAEs $3f_1-2f_2$ and $3f_2-2f_1$

The data obtained using stimulus levels $L_1=L_2=75$ dB SPL are shown in Fig. 4(a) and (b). As with the $2f_2-f_1$ DP, the $3f_2-2f_1$ DP phase contours always tend to follow constant DP frequencies; however, in this case the lines of constant DP frequency have an aspect ratio of 3:2 because of the different order of the DP components. The "transition" region at which the phase contours turn from following DP frequencies to following frequency ratios occurs at a smaller frequency ratio with the $3f_1-2f_2$ DP ($f_2/f_1=1.05$) than was the case with the $2f_1-f_2$ DP ($f_2/f_1=1.1-1.15$), and the DPs are not measurable with ratios greater than $f_2/f_1=1.1-1.15$. However, as the emission frequency of the $3f_1-2f_2$ DP is twice as far from f_2 as that of the $2f_1-f_2$ DP for the same stimulus frequencies, the transition is occurring at comparable frequency spacings from f_2 for both DPs.

2. $L_1=L_2=70$ dB SPL, subject RN

a. Amplitude

The amplitude data, shown in Fig. 5(a), contain many of the features which were seen with subject RDK. Amplitude "valleys" are seen in the $2f_2-f_1$ DP data, which follow

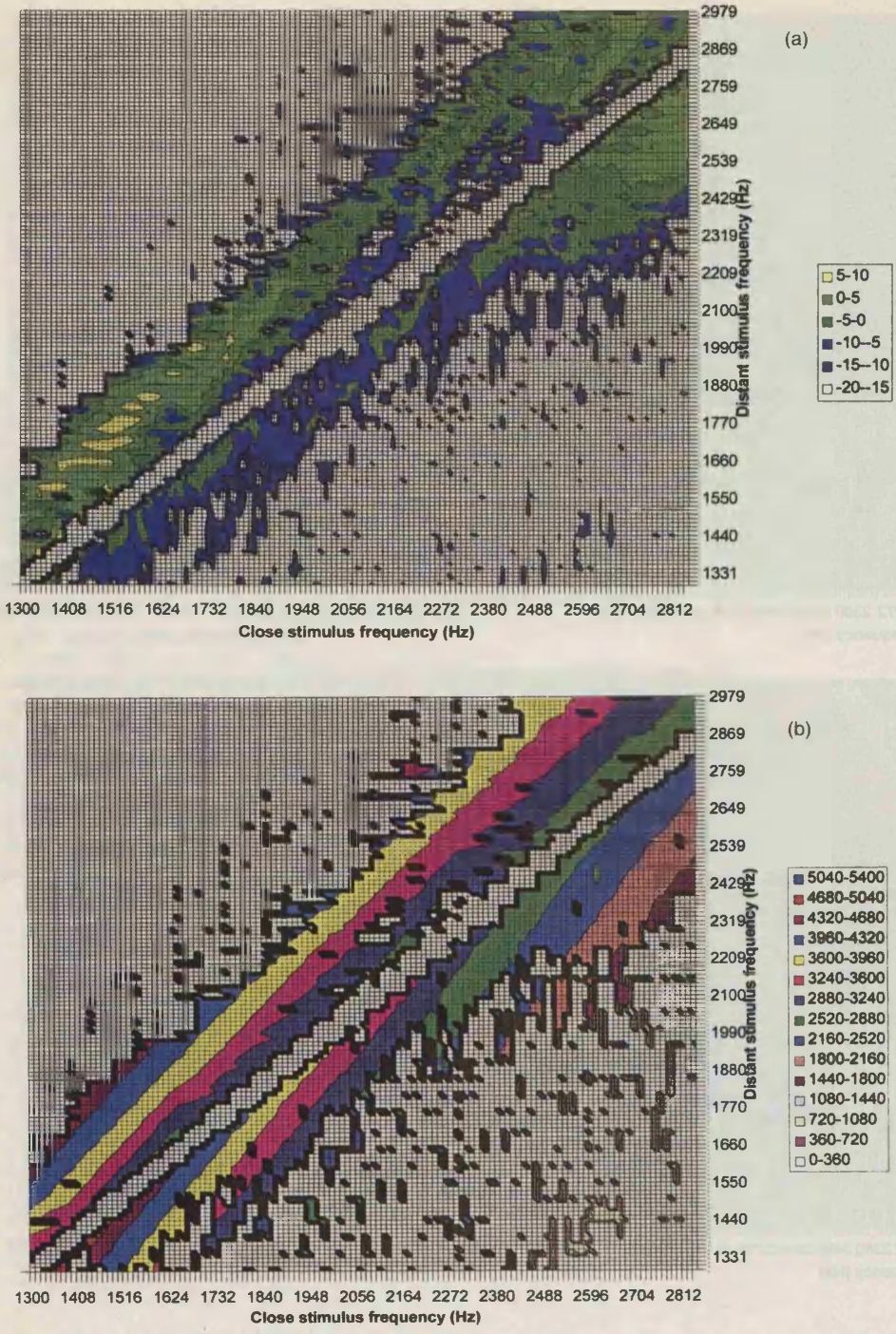

FIG. 4. Area representations of (a) level, dB SPL (top), and (b) phase, deg (lower) of $3f_1-2f_2$ and $3f_2-2f_1$ DPOAE with $L_1=L_2=75$ dB SPL with subject RDK. In each chart, $3f_1-2f_2$ DP data are above the leading diagonal line; $3f_2-2f_1$ DP data are below the line. These DPs are only measurable with small stimulus-frequency ratios. The phase is comparable to Fig. 2, except that where the phase contours follow constant DP frequencies, the direction has an aspect of 3:2 instead of 2:1 because of the different DP. The transition between phase contours following constant DP frequency or following constant f_2/f_1 occurs at a smaller stimulus-frequency ratio.

constant DP frequencies and continue into the $2f_1-f_2$ DP. The $2f_1-f_2$ data become smoother at wider frequency ratios, rising to a peak at a ratio of approximately $f_2/f_1=1.25$ before falling into the noise floor at approximately $f_2/f_1=1.4-1.45$. The $2f_2-f_1$ DP, meanwhile, reduces in amplitude gradually towards wider frequency ratios, but remains above the noise floor up to frequency ratios of 1.7–1.8.

There are differences in the detail of the results from the two subjects. The results from RN are of higher amplitude and contain more valleys in the $2f_2-f_1$ DP data. The amplitude ridge and valley features do not occur at the same frequencies in the two subjects.

b. Phase

The phase data from RN [Fig. 5(b)] follow the same pattern as RDK, with $2f_2-f_1$ DP phase contours following constant DP frequencies and crossing to the $2f_1-f_2$ DP. The $2f_1-f_2$ DP phase contours also follow constant DP frequencies when f_2/f_1 is small, but switch to following constant frequency ratios when $f2/f1$ exceeds approximately 1.1–1.15.

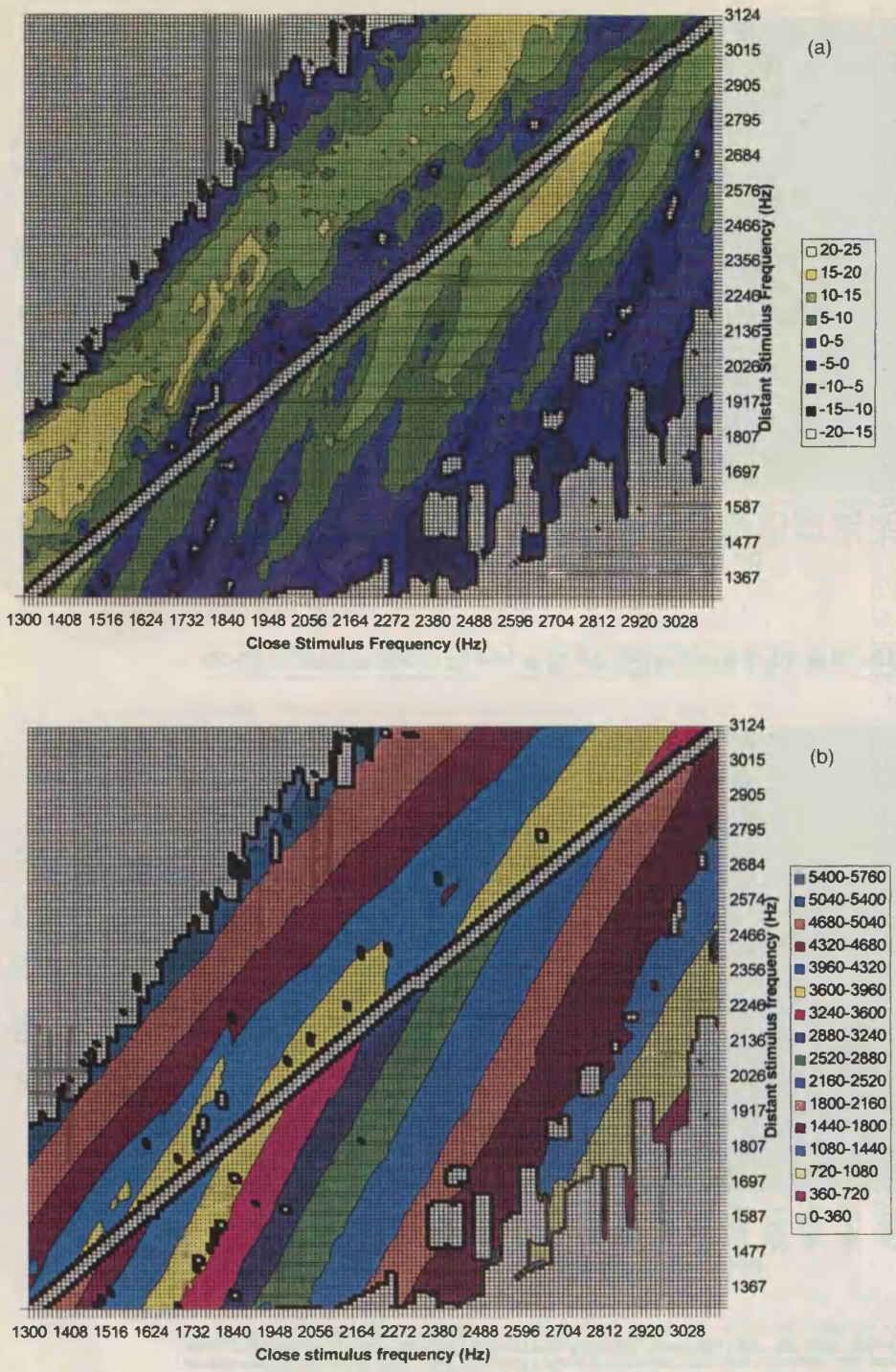

FIG. 5. f_1, f_2 area representations of (a) level, dB SPL (upper chart), and (b) phase, deg (lower chart) of $2f_1-f_2$ and $2f_2-f_1$ DPOAE with $L_1=L_2=70$ dB SPL with subject RN. In each chart, $2f_1-f_2$ DP data are above the leading diagonal line; $2f_2-f_1$ DP data are below the line. Data were obtained in constant f_2/f_1 sweeps. Compared to RDK, there is a greater amount of fine structure in the $2f_2-f_1$ DP with valleys and ridges occurring across the whole frequency range; the level of the DPs is also a little higher generally, but otherwise the overall pattern of the results is very similar.

B. f_2/f_1 versus DP frequency representation

1. $L_1=L_2=70$ dB SPL, RDK and RN

Figures 6 and 7 show data for each subject with $L_1=L_2=70$ dB SPL using the alternative presentation format, plotting stimulus-frequency ratio f_2/f_1 against DP frequency.

a. Amplitude

With this format [Figs. 6(a) and 7(a)] the amplitude valleys in the $2f_2-f_1$ DP are approximately vertical, indicating that they are defined by the DP frequency. The valleys cross to the $2f_1-f_2$ DP. The amplitude fine structure in the $2f_1-f_2$ DP at frequency ratios above 1.1 is not fixed to emission frequency, but instead drifts towards lower frequencies at larger frequency ratios. With subject RDK, the amplitude data become more smooth when the DP frequency is above 3 kHz, whereas with RN the fine structure continues across the whole frequency range investigated.

b. Phase

The $2f_2-f_1$ phase contours [Figs. 6(b) and 7(b)] are almost vertical, with a slight drift towards lower DP fre-

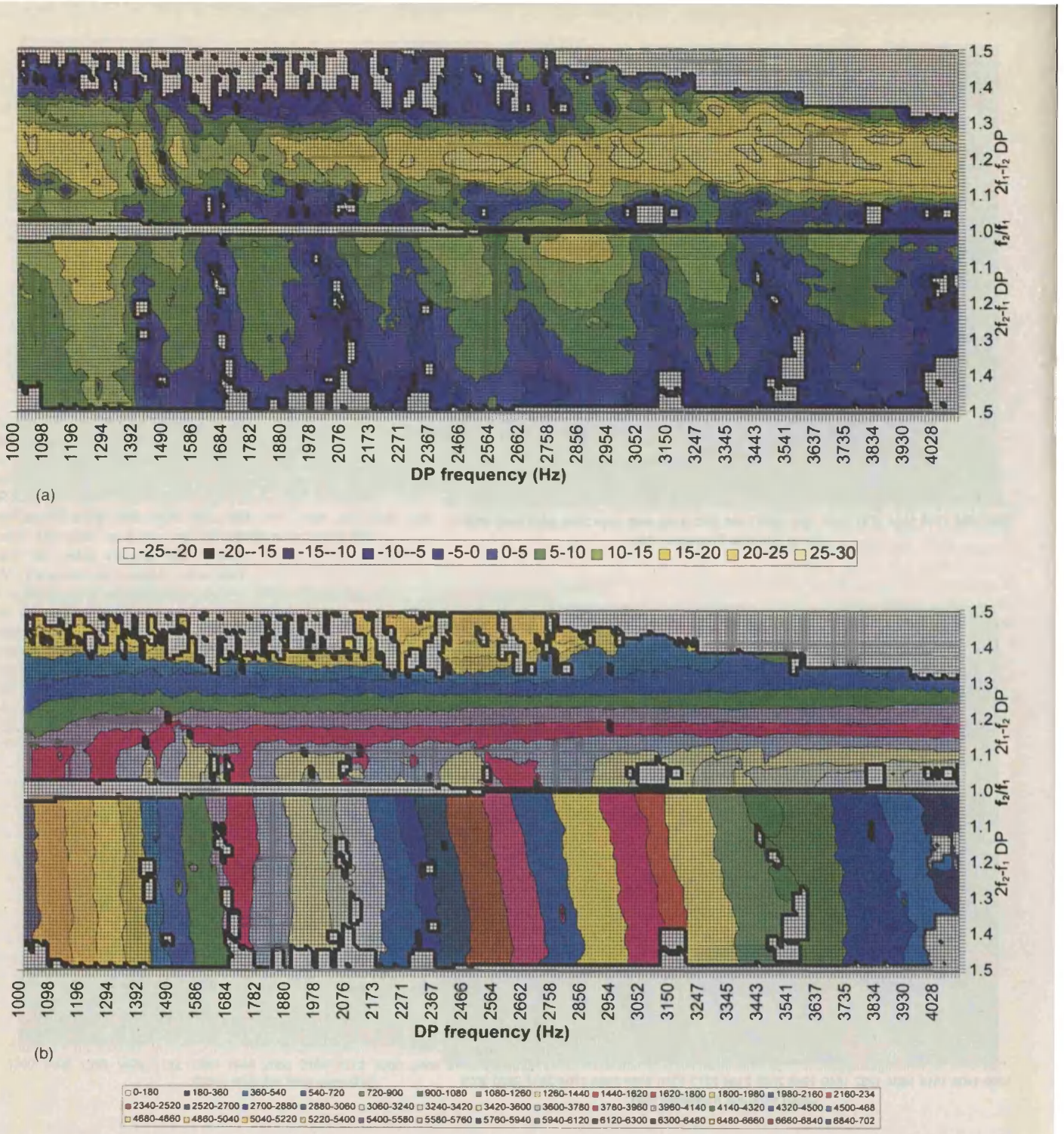

FIG. 6. f_2/f_1 versus DP frequency area representations of (a) level, dB SPL (upper chart), and (b) phase, deg (lower chart) of $2f_1-f_2$ and $2f_2-f_1$ DPOAE with $L_1=L_2=70$ dB SPL with subject RN. The data in Fig. 5 are drawn from these charts. Using this presentation, the transition within the $2f_1-f_2$ data between the wave-fixed and place-fixed behavior can clearly be seen.

quency at small f_2/f_1 which is more marked above approximately 2 kHz. This is to be expected from Figs. 2, 3, and 5 and is consistent with a place-fixed emission mechanism. The slight deviation from vertical indicates a very small influence of the stimulating frequencies on the resulting phase of the DPOAE. It is unclear whether this results from greater inward delay in the cochlea to the DP place because of the smaller frequency ratio (and hence the DP place is closer to $f2$), a small movement of the DP generating region, or whether it merely reflects greater inward phase change of the stimuli as they travel along the ear canal because of the higher frequency and therefore shorter wavelength of the primaries.

The phase contours clearly cross directly between the $2f_2-f_1$ and $2f_1-f_2$ DPs in both subjects, suggesting a continuity of emission mechanism, but with the $2f_1-f_2$ DP the

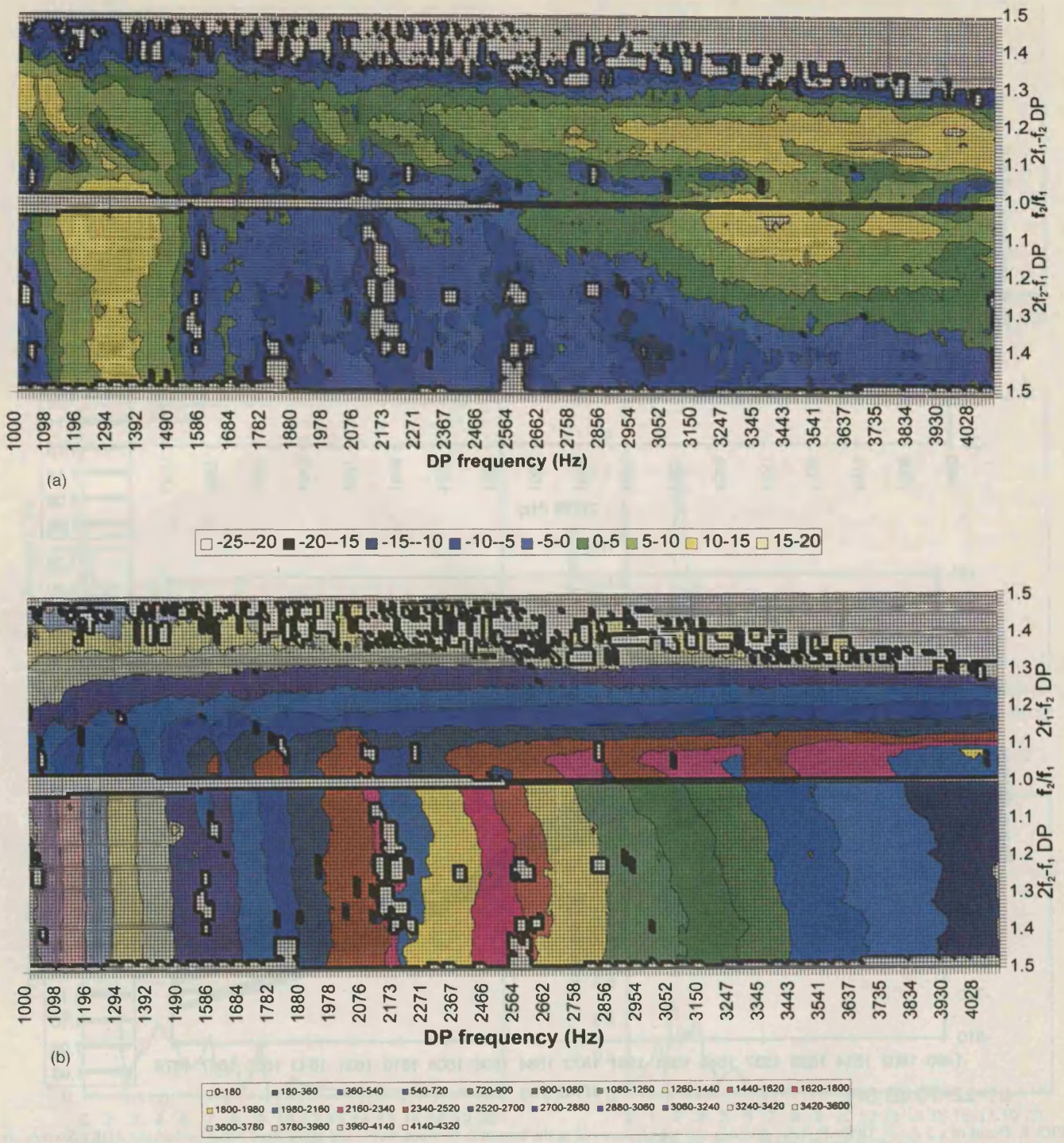

FIG. 7. f_2/f_1 versus DP frequency area representations of (a) level, dB SPL (upper chart), and (b) phase, deg (lower chart) of $2f_1-f_2$ and $2f_2-f_1$ DPOAE with $L_1=L_2=70$ dB SPL with subject RDK. The same general pattern is seen as in Fig. 6, except that no notches in level are seen above 2.5 kHz in the $2f_2-f_1$ DP.

phase contours switch from vertical (phase determined by DP frequency) to horizontal (phase determined by f_2/f_1) at larger ratios. This is consistent with a change from the place-fixed to the wave-fixed emission mechanism.

C. The $2f_1-f_2$ DP transition

In order to investigate the $2f_1-f_2$ DP transition between the wave- and place-fixed mechanisms, successive short constant frequency ratio sweeps were obtained with the frequency ratio in increments for each sweep. Each sweep covered the $2f_1-f_2$ DP frequency range 1490–1678 Hz. The stimulus level was $L_1=L_2=70$ dB SPL, and the frequency ratio was varied from $f_2/f_1=1.08$ up to 1.2 (Fig. 8).

When the frequency ratio was large, the DP sweeps had shallow phase gradients. As the frequency ratio reduced, the phase gradient became steeper with an upward step. When

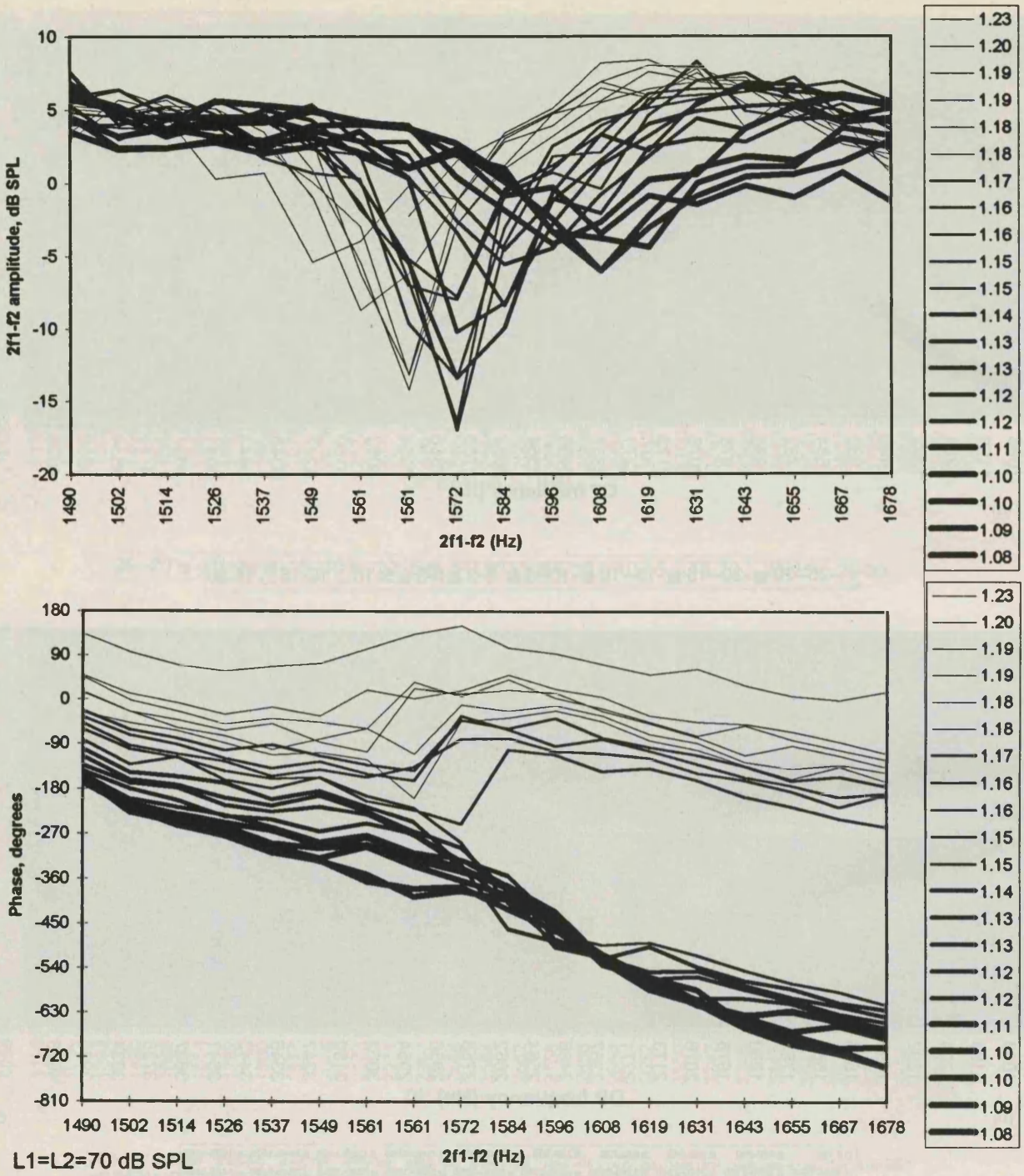

FIG. 8. Detail of a $2f_1-f_2$ DPOAE phase discontinuity which occurred in the transition between wave- and place-fixed behavior (subject RDK). Sweeps are constant f_2/f_1 and successive sweeps are in increments of f_2/f_1. Phase is seen to switch between a steep or a shallow gradient by gaining or losing a 360°-step. A corresponding level notch comes and goes during this transition, moving slightly towards lower frequencies at larger f_2/f_1.

the frequency ratio reached 1.15, the upward step exceeded 180° and so was logically stepped downwards. Ultimately, at the narrowest ratios ($f_2/f_1 \approx 1.1$) the step approached 360° and the phase resolved to a new steep gradient. The frequency at which the step occurred increased slightly with smaller stimulus-frequency ratios. There was a corresponding amplitude notch which came and went during this transition.

This process by which 360° is "lost" as the stimulating-frequency ratio is increased explains the necessity in the area DP data for either downward 360° steps at low-frequency ratios or upward 360° steps at high ratio when attempting to join the phase data in a 2D frequency array.

D. Time-domain analysis

In order to observe the relative contributions of the various components of the DPOAEs, we transformed the data into the time domain.

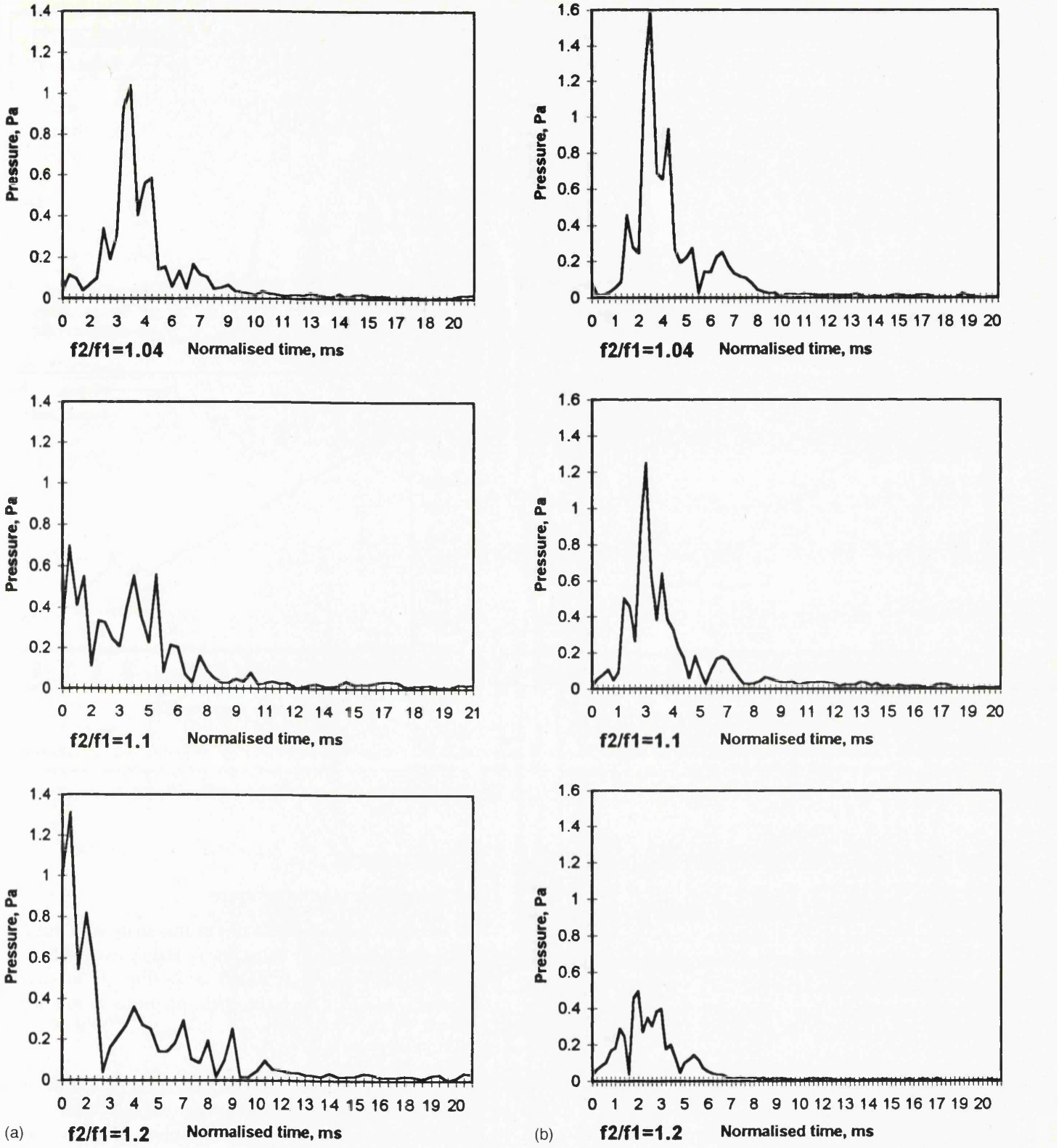

FIG. 9. Magnitudes of Fourier transforms of 256-point constant frequency ratio DP sweeps with $L_1 = L_2 = 70$ dB SPL (subject RDK). f_1 was in increments of 12-Hz steps, starting at 1 kHz. The frequency intervals were converted to a log scale prior to the Fourier transform to remove an underlying gradual change in phase gradient. (a) $2f_1 - f_2$ DP—A low-latency and a high-latency component can be identified. When $f_2/f_1 = 1.04$, there is almost no trace of the low-latency component; when $f_2/f_1 = 1.1$, both components are present and approximately equal in amplitude, and when $f_2/f_1 = 1.2$, the low-latency component dominates although higher-latency elements are also present. (b) $2f_2 - f_1$ DP—The level is lower with wider frequency ratios, but the latency remains about the same.

The magnitudes of the inverse Fourier transforms derived from three DPOAE sweeps are shown in Fig. 9(a), using stimulus-frequency ratios of $f_2/f_1 = 1.04$, 1.1, and 1.2. Each peak has an implied group delay, derived from the rate of change of phase in the DP sweep. The group delay associated with the frequency ratio of $f_2/f_1 = 1.04$ is 3–4 ms, compared to 0.5–1 ms with a frequency ratio of 1.2. When the frequency ratio is 1.1, components with both group delays are seen, rather than a single peak with an intermediate time delay. Therefore, two components of DPs are identified,

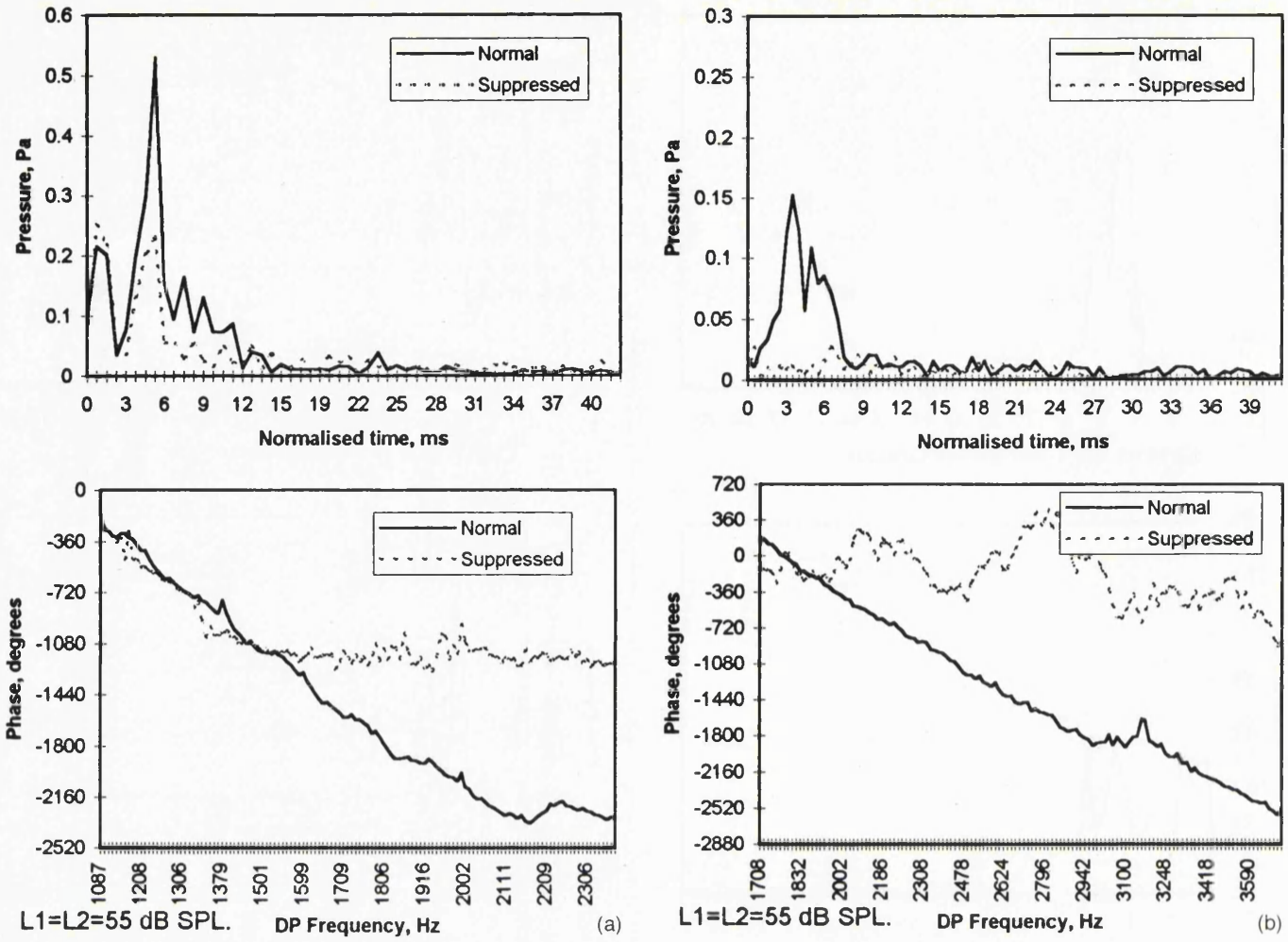

FIG. 10. Phase and amplitude of Fourier transform data from constant frequency ratio DP sweeps with $L_1=L_2=55$ dB SPL and with f_2/f_1 fixed at 1.15 (subject RDK). (a) $2f_1-f_2$ DP: Insertion of a third stimulus tone of 55 dB SPL at 50 Hz above the DP frequency selectively suppresses the high-latency emission and results in a predominantly flat phase characteristic. (b) $2f_2-f_1$ DP: The suppressor tone suppresses the entire DP, leaving only noise.

with two distinct group delays. As the sweeps had constant stimulus-frequency ratios, the peak with a small group delay is consistent with the wave-fixed emission mechanism, whereas the later peak is consistent with the place-fixed emission mechanism. Which one dominates the measured DPOAE depends on the ratio f_2/f_1.

Similar data have been obtained for the $2f_2-f_1$ DP [Fig. 9(b)]. In this case, there is no sign of the low-latency peak that was seen with the $2f_1-f_2$ DP.

Further DP sweeps were obtained using 128 points in the $2f_1-f_2$ DP frequency range of 1087–2381 Hz with a frequency ratio of 1.15 and a stimulus level of $L_1=L_2=55$ dB SPL. The measurement was then repeated with a third tone of 55 dB SPL introduced at 50 Hz above the DP frequency. Figure 10(a) contains both a time-domain response and the unwrapped phase data. It can be seen that the third tone selectively "suppresses" the more delayed component of the DP and the overall phase gradient changes from a steep gradient to a shallow gradient. No such gradient change could be induced by introducing a third stimulus tone at frequencies close to the frequencies of f_1 and f_2. Figure 10(b) shows the corresponding data for the $2f_2-f_1$ DPOAE. In this case, the suppressor close to the DP frequency obliterates the entire DP, leaving just noise.

III. DISCUSSION

A. Comparison with literature

We can compare the results of this study with that available in the literature by using our f_1 and f_2 sweep-phase data obtained with $L_1=L_2=60$ dB SPL (Fig. 3) to calculate "partial" latencies from the phase gradients as follows:

$$\text{Latency} = -\delta(\phi/2\pi)/\delta(f),$$

where ϕ is the DP phase in radians and f is the DP frequency in Hz. The frequency ranges of the examples were selected to avoid discontinuous data or data containing large irregularities.

In the case of the $2f_2-f_1$ DP the latencies calculated via the f_2 sweep method were only marginally greater than the f_1 sweep latencies (ratio of f_1 sweep/f_2 sweep latency $=0.92-1.00$). In this respect the results are consistent with those of Moulin and Kemp (1996), who used stimulus parameters of $L_1=65$, $L_2=60$ dB SPL $f_2/f_1=1.2-1.22$, and reported no significant difference between f_1 and f_2 sweep latencies for the $2f_2-f_1$ DPOAE. Each individual latency found here is also consistent with those found by Moulin and Kemp [which in the frequency range 1–3 kHz ranged from 9.5 to 6 ms ($2f_1-f_2$, f_2 sweep), 7.7 to 4 ms ($2f_1-f_2$, f_1

sweep), 9 to 4.5 ms ($2f_2-f_1$, f_2 sweep)), and 7 to 4.5 ms ($2f_2-f_1$, f_1 sweep)]. For our $2f_1-f_2$ data, the f_2 sweep-derived latencies exceed the f_1 sweep latencies when measured using large frequency ratios (ratio of f_1 sweep/f_2 sweep latency=0.75–0.86). This was consistent with studies by Kimberley *et al.* (1993) and O Malhoney and Kemp (1995), who found that f_1 sweeps were 20% lower than f_2 sweeps. However, when f_2/f_1 was small,, the latencies calculated via the f_2 sweep method were only marginally greater than the f_1 sweep latencies (ratio of f_1 sweep/f_2 sweep latency=0.89–1.02), as was the case with the $2f_2-f_1$ DP.

B. Emission modes

In describing the DP frequency versus f_2/f_1 ratio representation of DP data, we indicated that wave-fixed emission mechanisms would result in horizontal phase contours. It can be seen from the results in Figs. 6 and 7 that the $2f_1-f_2$ DP does follow this trend when $f_2/f_1>1.1-1.15$. Meanwhile, place-fixed DPs would tend to result in vertical phase contours, following lines of constant DP frequency. The $2f_2-f_1$ DP and the $2f_1-f_2$ DP with $f_2/f_1<1.1-1.15$ tend to be of this form. The division is not simply between the upper- and lower-sideband distortion products (where $f_2/f_1=1$ on the charts), but instead the transition occurs within the $2f_1-f_2$ DP data at a frequency ratio of approximately 1.1, with a transition region in which both mechanisms coexist and give rise to interference effects.

To summarize, at large frequency ratios the $2f_1-f_2$ DP phase behavior implies a wave-fixed emission mode, whereas the $2f_1-f_2$ DP with a small frequency ratio and the $2f_2-f_1$ DP are consistent with a place-fixed emission mode.

As TEOAE and SFOAE phase behavior is also consistent with the place-fixed model (Kemp and Chum, 1980a; Wilson, 1980; Kemp and Chum, 1980b), the clinical $2f_1-f_2$ DPOAE, for which the frequency ratio is normally approximately 1.2, is part of a subset of wave-fixed OAEs which includes only lower-sideband DPOAEs stimulated with a wide frequency ratio. All other stimulated OAEs appear to be place-fixed.

C. The origins of DPOAE fine structure

The issue of whether the fine structure associated with the $2f_1-f_2$ DP is caused by interference between two distinct regions of DP emission or a local effect of interactions within one source region remains controversial. Clearly, two sources of differing latency would give rise to fine structure by interference, but repeated reflections between the base and a single DP place-fixed reflector could also produce a fine structure (as in SFOAE). Mechanisms have been proposed by which interference could also arise from within a single distributed source region. Initially, the place-fixed reflectors were thought of as single scattering points (Kemp, 1978). Subsequently, to explain the extended segmented nature of the reflector-phase behavior, models requiring regularly spaced impedance changes along the basilar membrane (e.g., Strube, 1989) were introduced, although no physiological anatomical correlate was known. More recently, Zweig and Shera (1995) have shown that OAE fine structure could be generated with a random spacing of impedance irregularities which could, for example, be linked to the irregularities in primate outer hair-cell (OHC) arrangements. Evidence that part of the $2f_1-f_2$ DPOAE may be from the DP place under some conditions has been provided by suppression tuning curves (Kummer *et al.*, 1995) and suppression of the fine structure (Heitmann *et al.*, 1998). The mechanism underlying such a "re-emission" or reflection is expected to be place-fixed by logical argument, because the situation with a forward-going DP from the region of the stimulus frequencies proceeding to its frequency place and then returning as an OAE is essentially the same as a stimulus-frequency otoacoustic emission, which has a phase characteristic consistent with a place-fixed mechanism.

D. Wave- and place-fixed emissions

The results presented in the present study provide further evidence that the high-latency place-fixed part of the $2f_1-f_2$ DP arises from the region of the DP frequency place. At small ratios, the continuation of the phase contours between the $2f_1-f_2$ and $2f_2-f_1$ DPs across the $f_1=f_2$ or $f_2/f_1=1$ line suggests a continuation of the same emission mechanism between the upper and lower sidebands. As the $2f_2-f_1$ DP must be primarily emitted from the region of or basal to the DP frequency place, this result strongly suggests that the place-fixed $2f_1-f_2$ DP is also emitted largely from the region of its DP frequency place via a reflection mechanism. In the case of the $2f_1-f_2$ DP, this is a re-emission of a DP which was originally generated in the frequency region of the primary tones on the basilar membrane.

Further support for the theory of the DP frequency place region being the site of reflection for the place-fixed emission is provided by the inverse Fourier transform and suppression data (Figs. 9 and 10).

With a small primary frequency ratio, the inverse Fourier-transformed DP data contain almost no trace of the wave-fixed (low latency) emission in the $2f_1-f_2$ DP, which suggests that the distortion source may not be simply bidirectional. If DP energy was always sent equally towards the base and the apex of the cochlea, a wave-fixed component to the $2f_1-f_2$ DP would always be present. In addition, the high-latency emission reduces in amplitude as the ratio f_2/f_1 increases. While the intensity of DP generation might be expected to decrease with increasing frequency separation of equal-level primaries, an increase in place-fixed emission amplitude relative to wave-fixed emission could be expected because of a reduction in suppression of the DP frequency "amplifier" region by the primaries. This result implies that less DP energy is directed towards the apex from the f_2 region when stimulated with larger ratios of f_2/f_1. A mechanism by which the distortion source may be directional and dependent on the ratio f_2/f_1 is presented by Kemp and Knight (1999).

E. Characteristics of DPOAE fine structure

The $2f_1-f_2$ DP showed a quite smooth amplitude function with wide frequency ratios when stimulated by $L_1=L_2$

=75 dB SPL (Fig. 2), but when the stimulus tones were reduced to 60 dB SPL the amplitude function remained complex at all frequency ratios, up until the DP sank into the noise floor at approximately $f_2/f_1=1.4$ (Fig. 3). The uneven amplitude of the $2f_1-f_2$ DPOAE at wide ratios with lower stimulus levels could be a result of the wave-fixed emission failing to completely dominate the place-fixed emission, or an increase in interference between out-of-phase elements within a single DP-generating region, or multiple reflections between the base of the cochlea and the DP place becoming more significant.

The most striking feature of the $2f_2-f_1$ DP (upper sideband) amplitude data from RDK in Fig. 2 is the two valleys which approximately follow constant DP frequencies (2150 and 2550 Hz). Similar features were also seen with RN across the whole frequency range under investigation. The possible causes would seem to be an interference effect or localized cochlear anatomical features; however, the notches disappear at lower stimulus levels (RDK) and so localized anatomical irregularities are unlikely. As there is one obvious region on the basilar membrane from which this DP is emitted (unlike lower-sideband DPs), i.e., the DP frequency place, the remaining possible sources of interference are from different parts of a large region of generation or reflection, or from cancellation between multiple reflections between the DP place and the stapes. The latter is less likely as the reflections would be unlikely to become relatively more significant with higher stimulus levels. Recently, Martin *et al.* (1999) have suggested that a source of the $2f_2-f_1$ DP exists basal to the DP frequency place due to the interference of the harmonic $2f_2$ with f_1 to produce another source of the $2f_2-f_1$ DP, reintroducing the possibility of interference between two DP-generating sites. The situation is therefore potentially quite complex.

F. Location of the $2f_2-f_1$ DP generator in this data

It is interesting that the $2f_2-f_1$ DP phase contours in our data do not deviate much from following lines of equal DP frequency even with a very low frequency ratio, despite the expectation that under these conditions the DPOAE would gain delay from the increased traveling time of the stimuli to the DP place. The two possible reasons for this are (1) The outward traveling time reduces at the same rate as the inward traveling time increases, or (2) The inward traveling time doesn't increase.

Option 1 would require that the region from which a DP reflection occurs should move depending on the frequency ratio by which the DP was generated, being further towards the base with smaller frequency ratios. Option 2 would require that the $2f_2-f_1$ DP generation region is significantly basal to the DP frequency place (Martin *et al.*, 1998, 1999), therefore remaining far enough from the region of the stimulus frequencies so as not to accumulate much inward traveling time even when the DP frequency is close to f_2. The region of place-fixed reflections could occur anywhere between the DP generation region and the DP frequency place, maintaining a fixed relationship with the DP frequency place.

G. Are the results typical?

The results presented in this study contain some features that have been previously shown, and others that are new. Both subjects had a change in phase behavior in the $2f_1-f_2$ DP in constant f_2/f_1 frequency sweeps, with steep phase gradients recorded with f_2/f_1 below approximately 1.1 and shallow phase gradients at wider frequency ratios. This has been shown previously (Kemp, 1986; Knight and Kemp, 1999) and is undoubtably a normal feature. The exact ratio at which the changeover occurs is known to be variable across subjects and also to be slightly frequency- and stimulus-level dependent. Both subjects also produced maximum levels of $2f_1-f_2$ DPOAE with frequency ratios of approximately 1.2–1.25 [Figs. 6(a), 7(a)] and this is also known to be typical (Harris *et al.*, 1989). The exact ratio at which the maximum level occurs is also known to vary between subjects and is also frequency- and stimulus-level dependent.

Where data are dominated by place-fixed behavior, the phase is almost entirely dependent on the DP frequency. As this occurs in both subjects, this interesting result is likely to be typical of normal ears. The continuity of the amplitude and phase contours between the lower- and upper-sideband DPOAEs also occurs in both subjects and appears to indicate a continuity of emission mechanism which would be true of all normal ears.

The presence of amplitude ridges and valleys in the $2f_2-f_1$ DP data appears to be less certain in other subjects, as in subject RDK they didn't occur across the whole frequency range or at all stimulus levels. This is therefore likely to be a common but not necessarily universal feature. Data from both subjects with the $2f_1-f_2$ DP wave-fixed emission show evidence of amplitude valleys which drift towards lower emission frequencies at wider frequency ratios. However, the exact location of specific amplitude features are not correlated between the two subjects.

IV. SUMMARY

For lower-sideband DPOAEs, whether the wave- or place-fixed mechanism dominates depends on the stimulus-frequency ratio, the DP, order and the stimulus amplitude. Therefore, the wave-fixed emission mode cannot be explained as the uncomplicated leakage of DP energy and may depend on a source region which has variable directivity. Upper-sideband DPOAEs are always dominated by the place-fixed emission mode.

The phase of corresponding place-fixed upper- and lower-sideband DPs appeared to be continuous between the DPs at small frequency ratios, suggesting continuity of mechanism. Whilst the presence of two separate emission regions for the $2f_1-f_2$ DP is presumably the cause of much of the amplitude fine structure seen in this DP, the presence of amplitude notches in the $2f_2-f_1$ DP indicates that fine structure may also arise from either multiple reflections within the cochlea or from interference within a distributed DP generating or reflecting region.

The emission model which is suggested by these results can be summarized as follows. For the wave-fixed emission, distortion in the basilar-membrane motion is the generator

and the DP is emitted directly. For the place-fixed emission, distortion occurring within the f_2 envelope is still the generator of the DP, but DP energy is projected apically and is emitted via a separate reflection process in the region of the DP frequency place.

The two-dimensional and time-domain analysis methods have been shown to be valuable. Further work is required to investigate variability among other ears and the effect of using other stimulus levels.

ACKNOWLEDGMENTS

The authors would like to thank Ruchi Narang for her considerable patience as a subject for this study and the Auditory Biophysics Laboratory at the Institute of Laryngology and Otology, London for financially supporting this project.

Brown, A. M., Harris, F. P., and Beveridge, H. A. (**1996**). "Two sources of acoustic distortion products from the human cochlea," J. Acoust. Soc. Am. **100**, 3260–3267.

Brown, A. M., and Kemp, D. T. (**1984**). "Suppressibility of the $2f1-f2$ stimulated acoustic emissions in gerbil and man," Hearing Res. **13**, 29–37.

Fahey, P. F., and Allen, J. B. (**1997**). "Measurement of distortion product phase in the ear canal of the cat," J. Acoust. Soc. Am. **102**, 2880–2891.

Gorga, M. P., Neelly, S. T., Ohlrich, B., Hoover, B., Redner, J., and Peters, J. (**1997**). "From laboratory to clinic: a large scale study of distortion product otoacoustic emissions in ears with normal hearing and ears with hearing loss," Ear Hear. **18**(6), 440–455.

Harris, F. P., Lonsbury-Martin, B. L., Stagner, B. B., Coats, A. C., and Martin, G. K. (**1989**). "Acoustic distortion products in humans: systemic changes in amplitude as a function of f_2/f_1 ratio," J. Acoust. Soc. Am. **85**, 220–229.

Heitmann, J., Waldmann, B., Schnitzler, H., Plinkert, P. K., and Zenner, H. (**1998**). "Suppression of distortion product otoacoustic emissions (DPOAE) near $2f1-f2$ removes DP-gram fine structure—Evidence for a secondary generator," J. Acoust. Soc. Am. **103**, 1527–1531.

Kemp, D. T. (**1978**). "Stimulated acoustic emissions from within the human auditory system," J. Acoust. Soc. Am. **64**, 1386–1391.

Kemp, D. T. (**1986**). "Otoacoustic emissions, travelling waves and cochlear mechanisms," Hearing Res. **22**, 95–104.

Kemp, D. T. (**1998**). "Otoacoustic emissions: distorted echoes of the cochlea's travelling wave," *in Otoacoustic Emissions Basic Science and Clinical Applications*, edited by C. I. Berlin (Singular, San Diego), Chap. 1, pp. 1–59, Figs. 1–12.

Kemp, D. T., and Brown, A. M. (**1983**). "An integrated view of cochlear mechanical nonlinearities observable from the ear canal," *in Cochlear Mechanics*, edited by E. DeBoer and M. A. Viergever (Delft University Press, Holland).

Kemp, D. T., and Chum, R. A. (**1980a**). "Properties of the generator of stimulated acoustic emissions," Hearing Res. **2**, 213–232.

Kemp, D. T., and Chum, R. A. (**1980b**). "Observations on the generator mechanism of stimulus frequency acoustic emissions—two tone suppression," in *Psychophysical, Physiological and Behavioural Studies in Hearing*, edited by van den Brink and Bilsen (Delft University Press, Holland), pp. 34–42.

Kemp, D. T., and Knight, R. D. (**1999**). "Virtual DP reflector explains DPOAE wave and place fixed dichotomy," in *Association for Research in Otolaryngology Abstracts* 396.

Kim, D. O. (**1980**). "Cochlea mechanics: Implications of electrophysiological and acoustical observations," Hearing Res. **2**, 297–317.

Kimberley, B. P., Brown, D. K., and Eggermont, J. J. (**1993**). "Measuring human cochlear travelling wave delay using distortion product emission phase responses," J. Acoust. Soc. Am. **94**, 1343–1350.

Knight, R. D., and Kemp, D. T. (**1999**). "Relationships between DPOAE and TEOAE characteristics," J. Acoust. Soc. Am. **106**, 1420–1435.

Kummer, P., Janssen, T., and Arnold, W. (**1995**). "Suppression tuning characteristics of the $2f1-f2$ distortion-product otoacoustic emission in humans," J. Acoust. Soc. Am. **98**, 197–210.

Martin, G. K., Lonsbury-Martin, B. L., Probst, R., Scheinin, S. A., and Coats, A. C. (**1987**). "Acoustic distortion products in rabbit ear canal. II. Sites of origin revealed by suppression contours and pure tone exposures," Hearing Res. **28**, 191–208.

Martin, G. K., Jassir, D., Stagner, B. B., Whitehead, M. L., and Lonsbury-Martin, B. L. (**1998**). "Locus of generation for the $2f_1-f_2$ vs $2f_2-f_1$ distortion-product otoacoustic emissions in normal-hearing humans revealed by suppression tuning, onset latencies, and amplitude correlations," J. Acoust. Soc. Am. **103**(4), 1957–1971.

Martin, G. K., Stagner, B. B., Fahey, P. F., and Lonsbury-Martin, B. L. (**1999**). "Influence of even-order nonlinearities on the suppression and enhancement of DPOAEs above $f2$ in rabbits," in *Association for Research in Otolaryngology Abstracts* 22, p. 382.

Moulin, A., and Kemp, D. T. (**1996**). "Multicomponent acoustic distortion product otoacoustic emission phase in humans. I. General characteristics," J. Acoust. Soc. Am. **100**, 1617–1639.

Moulin, A., Jourdain, F., and Collet, L. (**1999**). "Using acoustic distortion product otoacoustic emissions in clinical applications: Influence of $f2/f1$ on DPOAE gram," Br. J. Audiol. **33**, 89.

O Mahoney, C. F., and Kemp, D. T. (**1995**). "Distortion product otoacoustic emission delay measurement in human ears," J. Acoust. Soc. Am. **97**(6), 3721–3735.

Shera, C. A., and Guinan, J. J. (**1998**). "Reflection emissions and distortion products arise by fundamentally different mechanisms," in *Association for Research in Otolaryngology Abstracts* 21, p. 344.

Shera, C. A., and Guinan, J. J. (**1999**). "Evoked otoacoustic emissions arise by two fundamentally different mechanisms: A taxonomy for mammalian OAEs," J. Acoust. Soc. Am. **105**, 782–798.

Stover, L. J., Neely, S. T., and Gorga, M. P. (**1996**). "Latency and multiple sources of distortion product otoacoustic emissions," J. Acoust. Soc. Am. **99**, 1016–1024.

Strube, H. W. (**1989**). "Evoked otoacoustic emissions as cochlear Bragg reflections," Hearing Res. **38**, 35–46.

Sun, X., Schmiedt, R. A., He, N., and Lam, C. F. (**1994**). "Modelling the fine structure of the $2f1-f2$ acoustic distortion product. I. Model development," J. Acoust. Soc. Am. **96**, 2166–2174.

Talmadge, C. L., Long, G. R., Tubis, A., and Dhar, S. (**1999**). "Experimental confirmation of the two-source interference model for the fine structure of distortion product otoacoustic emissions," J. Acoust. Soc. Am. **105**, 275–292.

Wable, J., Collet, L., and Chéry-Croze, S. (**1996**). "Phase delay measurements of distortion product otoacoustic emissions at $2f1-f2$ and $2f2-f1$ in human ears," J. Acoust. Soc. Am. **100**, 2228–2235.

Whitehead, M. L., Stagner, B. B., Martin, G. K., and Lonsbury-Martin, B. L. (**1996**). "Visualization of the onset of distortion-product emissions and measurement of their latency," J. Acoust. Soc. Am. **100**, 1663–1679.

Wilson, J. P. (**1980**). "Evidence for a cochlear origin for acoustic re-emissions, threshold fine-structure and tonal tinnitus." Hearing Res. **2**, 233–252.

Zweig, G., and Shera, C. A. (**1995**). "The origin of periodicity in the spectrum of evoked otoacoustic emissions," J. Acoust. Soc. Am. **98**, 2018–2047.

Wave and place fixed DPOAE maps of the human ear

Richard D. Knight and David T. Kemp
Auditory Biophysics Group, Institute of Laryngology and Otology, University College London, 330/332 Gray's Inn Road, London WC1X 8EE, United Kingdom

(Received 3 July 2000; revised 27 December 2000; accepted 3 January 2001)

Human intermodulation distortion product otoacoustic emissions (DPOAE) can be a mixture of low and high latency components. They have different level, phase, and suppression characteristics, which indicate that emissions arise both from the frequency region of the primary tones directly and indirectly via the DP frequency place. Which component dominates the measured DPOAE in the ear canal depends on the stimulus parameters, especially the frequency ratio, f_2/f_1. Interference between the two emissions adds complexity to measurements of DPOAE. The behavior and even existence of whichever emission route is lower in level often cannot directly be deduced from the raw DPOAE data because the other emission covers it. It is therefore not known whether both emissions are present for all stimulus parameters or whether the trends seen in each emission when they are the dominant emission route continue under stimulus conditions when they are not dominant. In this study, the two DPOAE components are separated by a post-processing method. Previously, maps of raw DPOAE data against f_2/f_1 and DP frequency have been obtained. To separate the components, sets of data consisting of f_2/f_1 sweeps were transformed by an inverse Fourier transform into the time domain. The low and high latency components appeared as two distinct peaks because of their different phase gradients. These peaks were separated by windowing in the time domain and two frequency domain maps were reconstructed, representing the low and high latency DPOAEs. It was found that the low latency component of the $2f_1-f_2$ DP was only emitted strongly with f_2/f_1 between approximately 1.1 and 1.3. The removal of the high latency component revealed the low ratio edge of this region, at which the level falls sharply. However, the low latency emission has been traced at reduced amplitude over a wide range of stimulus parameters. Although previously only observed at small frequency ratios, the high latency component was found to be present widely in the lower sideband, its level reducing slowly at larger f_2/f_1. Its phase behavior changes in the lower sideband, being approximately constant with DP frequency at small ratios of f_2/f_1, but deviating from this at wider ratios. These results support the hypothesis that a DPOAE component which propagates to and is re-emitted from the DP frequency place (place fixed emission) is present across a wide parameter range. However, for all but the close primary condition the lower sideband DPOAE is dominated by direct emission from the region of f_2 and f_1 wave interaction (wave fixed emission). A simple transmission line model is presented to illustrate how the observed DPOAE maps can arise on the basis of this hypothesis. [DOI: 10.1121/1.1354197]

PACS numbers: 43.64.Jb, 43.64.Kc, 43.64.Ri [BLM]

I. INTRODUCTION

Distortion product otoacoustic emission (DPOAE) are of great research and clinical interest. Recent research interest has focused attention on the two possible paths by which lower sideband DPOAE [of the form $(a+1)f_1-af_2$, $a=1,2,3$, etc.] may travel to the ear canal once generated within the region of f_2 excitation.

A. PATH 1: The DP travels directly to the base from the generation site

Kemp and Knight (1999) have suggested that the mechanism of DP generation may, for certain f_2/f_1, preferentially direct energy basally. Kemp (1986) described $2f_1-f_2$ DP production with $f_2/f_1>1.1$ as "wave fixed" because its phase characteristics required the generator to move smoothly with the f_2 traveling wave in a frequency sweep.

Shera and Guinan (1999) labeled the same phenomenon "distortion emission" to emphasize that only nonlinearity (not a reflection) is required for an ear canal DP to be produced. Path 1 results in "low latency" DPOAEs.

B. PATH 2: The DP travels initially toward the apex, until it is reflected back toward the base

This mode of DPOAE, seen in the $2f_1-f_2$ DPOAE for small f_2/f_1, was separated by Kemp and Brown (1983) who suppressed activity at the DP place by adding an extra stimulus tone close to the DP frequency. It was described as "place fixed" by Kemp (1986), because the phase characteristics required reflectors to be fixed in position on the basilar membrane. TEOAEs have similar phase characteristics and have been said to require an impedance discontinuity (Kemp, 1978) or impedance irregularities along the basilar membrane to cause the reflection (Kemp, 1986; Lonsbury-Martin *et al.*, 1988; Zweig and Shera, 1995). Shera and Guinan (1999) described this mode of DPOAE as "reflection DPs" to emphasize that the "turnaround" mechanism is a reflection. Path 2 results in "high latency" DPOAEs.

Upper sideband DPOAE differ from this as the initial generation region is thought to be around the DP frequency place and the DP will propagate poorly beyond this place. Upper sideband DPOAE are always emitted predominantly by a place fixed mechanism from around the DP frequency place (e.g., Martin *et al.*, 1987, 1998; Kemp, 1998), although a small wave fixed emission is theoretically possible.

Martin *et al.* (1999, 2000) and Fahey *et al.* (2000) have shown that there may also be alternative basal sites for DP generation. These require more complex generation mechanisms, for example, involving the generation of intermodulation distortion from harmonic distortion products and difference tones derived from the original stimulus tones.

The region of "reflection" in lower sideband DPOAE probably lies in the DP frequency place region, as suggested by suppression studies using a third stimulus tone (e.g., Kummer *et al.*, 1995; Gaskill and Brown, 1996; Heitmann *et al.*, 1998), observation of DPOAE fine structure in frequency limited hearing loss and relationships between the fine structure of different distortion products (Mauermann *et al.*, 1999a, b) and comparison of experimental data with mathematical models (Talmadge *et al.*, 1999). If outer hair cell activity adequately compensates for the transmission losses in propagating back to the base and in reflection back a second time to the DP place, then the distortion product also could reflect repeatedly between the DP characteristic place and the base of the cochlea resulting in a feedback system causing interference effects, fine structure and occasionally resulting in spontaneous otoacoustic emissions (Kemp, 1980; Zweig and Shera, 1995; Talmadge *et al.*, 2000).

Whichever DP emission path results in the higher DP amplitude in the ear canal will dominate the phase behavior of the measured DPOAE. This depends on various aspects of the stimulus parameters, particularly the ratio of f_2/f_1. Previous studies (Kemp, 1986; Knight and Kemp, 1999) have shown that there appears to be a modal change in the $2f_1-f_2$ DPOAE phase behavior. In a frequency sweep with f_2/f_1 held constant, if f_2/f_1 is less than about 1.1 the $2f_1-f_2$ DPOAE has a steep phase gradient (high latency), indicating that the DP is dominated by a place fixed emission. But if the ratio is larger a shallow phase gradient is found (low latency), indicating that the emission is wave fixed.

Knight and Kemp (2000a) investigated the relationship between DP frequency and the ratio of f_2/f_1 in detail and showed that the place fixed behavior of the $2f_1-f_2$ DP when f_2/f_1 is small is a continuation of the patterns that are seen in the $2f_2-f_1$ DP for all f_2/f_1. However, the ear canal $2f_1-f_2$ DP was dominated by a wave fixed emission mode when f_2/f_1 exceeded approximately 1.1. A similar relationship was also seen between the $3f_1-2f_2$ and $3f_2-2f_1$ DPs.

The DP source, in the region of the f_2 frequency place, has been assumed to have a constant directivity for all f_2/f_1 (e.g., Allen and Fahey, 1992). However, more recently it has been suggested that this directivity changes as the frequency ratio changes (Knight and Kemp, 2000a).

Kemp and Knight (1999) have suggested a mechanism by which this may occur. Essentially this involves analyzing the modeled phase of f_1 and f_2 in the presumed generating region around f_2 and calculating the phase gradient of the $2f_1-f_2$ distortion product across this region as it is generated. This gradient changes from positive to negative as the ratio between f_1 and f_2 changes, resulting in constructive summation of the $2f_1-f_2$ distortion product occurring either toward the base or the apex. Therefore the phase gradients in the region of DP generation may to a large extent control the relative amplitudes of the wave and place fixed emission mechanisms.

As the DPOAE behavior which is observed is dominated by whichever mode is stronger, it is not known whether the two DP paths both continue to be significant for all f_2/f_1 ratios or whether DP production tends to be bi-modal with only one mode usually present and just a small transition region at which both emissions can occur. If both modes were always present and could be separated then the phase behavior of the "residual" or "minority" emissions would be of great interest. The phase characteristic of such a "residual emission" could be seen in relation to the traveling wave excitation patterns and the systematic trends that have previously only been seen in restricted stimulus parameter conditions could be pursued over a wider range of frequency ratios. Observation of the "place fixed" phase behavior will be of particular interest. The crossover between the lower and upper sidebands, the lower sideband f_2/f_1 ratio at which the phase pattern which continues from the upper sideband changes, and the phase behavior in the lower sideband at moderately wide ratios would provide further clues regarding the locations of the initial DP generating region relative to the f_2 frequency place and the reflecting region relative to the f_{DP} place.

However, separating the wave and place fixed emissions is not a straightforward task. One way is to add a third stimulus tone to suppress activity at the DP place, leaving only the DP emitted directly from the f_2 region. Comparison of DPOAE measurements obtained with and without the third tone can yield the DP place contribution by vector subtraction (Dreisbach and Siegel, 1999). However, it can be difficult to ensure that the DP place is fully suppressed without the f_2 region, and hence DP generation, also being affected. This risk is greatest with small stimulus frequency ratios (Siegel *et al.*, 2000).

An alternative method is pursued here, in which DPOAE is evoked by two stimulus tones and the wave and place fixed DPOAE are separated by a phase gradient dependent post-processing method. Shera and Zweig (1993) and Zweig and Shera (1995) have used Fourier transforms to investigate the spectral oscillations in SFOAE. Stover *et al.* (1996), Fahey and Allen (1997), and Kalluri and Shera (2000) used Fourier transforms on DPOAE frequency sweeps to observe the phase gradient-derived latency. It has been shown by Knight and Kemp (2000a) that an inverse fourier transform of a DP sweep with constant f_2/f_1 results in a quasi-time domain representation with two distinct peaks, the relative sizes of the peaks depending on the ratio of f_2/f_1 at which the sweep is performed. In the present study, these low and high latency parts are windowed in the pseudo-time domain

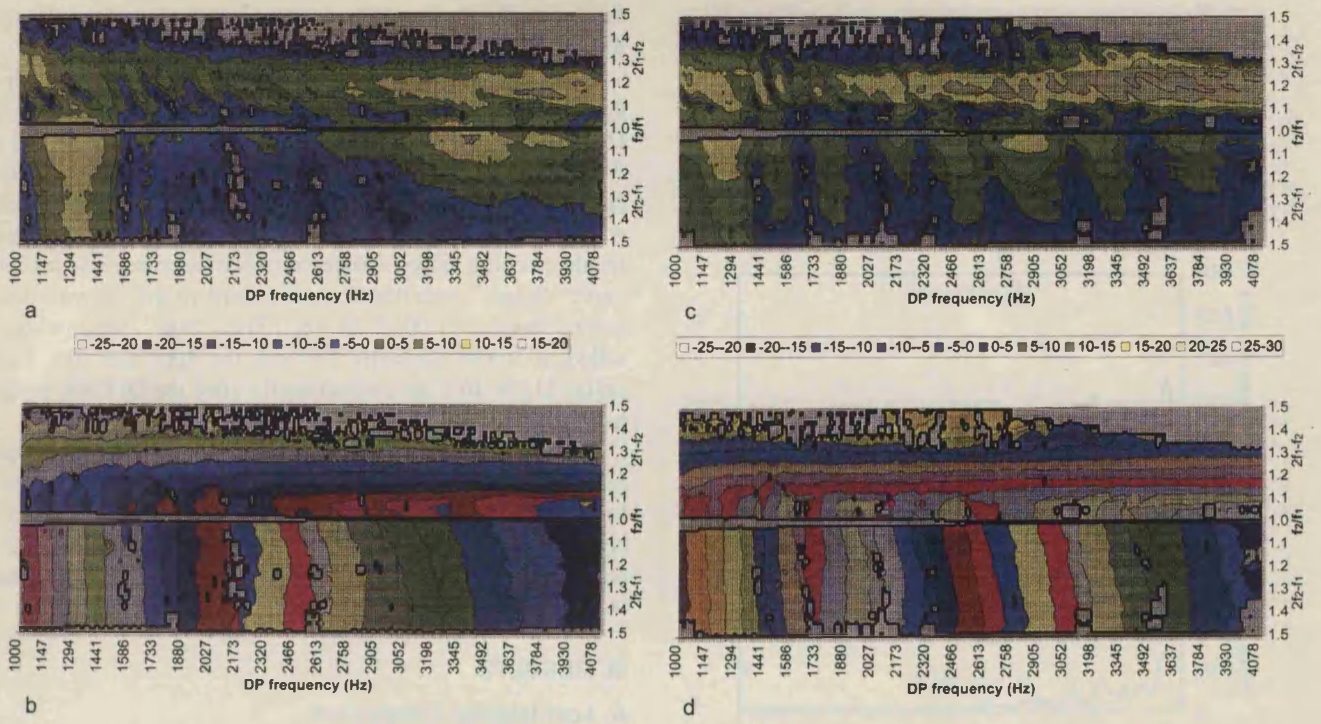

FIG. 1. $2f_1-f_2$ and $2f_2-f_1$ DPOAE data for subjects RDK in parts (a) and (b) and RN in parts (c) and (d) before the separation process [previously presented in J. Acoust. Soc. Am. **107**, 457–473 (2000)]. For each figure presented in this format, level (dB SPL) is shown in parts (a) and (c) in 5 dB steps and phase is shown in parts (b) and (d) in 180° steps. Phase becomes more positive toward the top and left of the chart.

and then transformed back to the frequency domain separately.

This method has the advantage of avoiding the unpredictable nonlinear effects of a third tone. A detailed and wide frequency sweep is required in order for the Fourier transformations to be adequately performed, from which definite separation of emissions with different phase behaviors can be achieved. This technique has been used to observe the ''wave'' and ''place'' fixed DPOAEs separately, allowing behavior which is usually masked to be uncovered.

There is an underlying difference in the third tone and the Fourier transform methods. The third tone separates the emission modes on the basis of place on the basilar membrane and it turns out that these emissions are different modes. The Fourier transform method separates the emission modes on the basis of their different phase gradients and it seems that they are from different places. The methods are comparable if the place fixed emission is from the region of the DP frequency place and the wave fixed emission is from elsewhere. Kalluri and Shera (2000) have shown an example in which similar results were obtained by the two methods, and Knight and Kemp (2000a) showed that the later peak in the time domain can be selectively suppressed by a third tone close to the DP frequency, supporting the theory that the two methods are comparable.

II. MEASUREMENTS AND DATA ANALYSIS

Data presented in this study have been obtained from an additional analysis of data presented by Knight and Kemp (2000a, reproduced in Fig. 1). The DPOAE measurements were obtained using the left ears of two subjects: a male (RDK) aged 29 and a female (RN) aged 24, both of whom had normal auditory thresholds and middle ear function.

DPOAE measurements were obtained with $L_1=L_2=70$ dB SPL with DP frequencies ranging from 1 kHz to 4.1 kHz in 12 Hz steps. Stimulus frequency ratios from 1.01 to 1.5 were employed. The DPOAE phase is corrected for the phase changes induced by the probe loudspeakers and microphone (the system detects the stimulus phase via the microphone and corrects automatically) but no phase correction is applied for acoustic delays along the ear canal.

From these data, the two emission components (wave and place fixed) have distinctly different latencies and therefore can be separated by the following post-processing method. A 512 point frequency array was set up, ranging from 0 to 3100 Hz, thereby preserving the original 3100 Hz range. An exponential frequency spacing was adopted in order to linearize the underlying curve in the phase versus frequency relationship of the place fixed DPOAE and therefore produce clearer peaks in the time domain (Zweig and Shera, 1995). The exponential frequency points were calculated as follows:

$$f_i = 1000 \times 4.1^{((i-1)/511)} - 1000,$$

where f_i = the frequency of the ith array point.

The measured data points were frequency shifted down 1000 Hz and inserted into this array with linear interpolation between data points where required. The level and phase data were converted to complex number format for the inverse Fourier transformation.

No frequency domain windowing was applied before the inverse Fourier transformation. Although there is a risk of

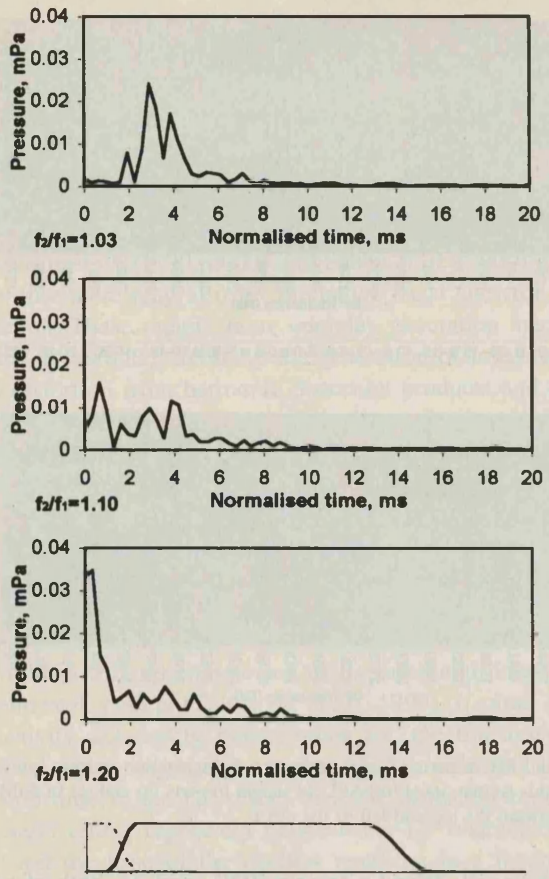

FIG. 2. Magnitude of inverse Fourier transforms of DPOAE constant frequency ratio sweeps selected from data in Fig. 1 (subject RDK, a and b). The time windowing employed to separate the early and late components is indicated at the bottom of the figure. In each case the total area under the curve corresponds to a DPOAE level of between 15 and 20 dB SPL.

artifacts resulting from this, the artifacts would be easily distinguishable from the signal in this case as the artefacts would be spread throughout the time window whereas the true signal would form peaks early in the time window. The time domain windowing which was subsequently employed would therefore largely remove any such artefacts. The advantage of this approach was that the data were not therefore weighted in favor of data from the middle of the frequency range and the final separated data were easy to compare directly with the original unprocessed data.

As the frequency array had an exponential characteristic, the meaning of the time scale of the inverse Fourier transform was not straightforward. The time scale in the time domain which is indicated in Fig. 2 was calculated as follows:

Time increment per point (ms)

$$= 1000/\text{frequency range (Hz)}.$$

This gives a time increment of approximately 0.32 ms per point. This calculated time interval most accurately reflects true time for data from the middle of the frequency range (2–3 kHz). It is an underestimate for the lower frequencies and an overestimate for the higher frequencies. The definition of this time scale is not relevant for the subsequent windowing and processing of the data. The transformation into the "time" domain produced separate amplitude peaks for the low and high latency components (Fig. 2).

The peaks were separated by time windowing, the windowing being designed to separate the wave and place fixed DPOAE at the point at which the magnitude function had a dip between the wave and place fixed peaks. The chosen crossover point for the "early" and "late" time windows was the fifth data point, which is about 1.6 ms. A flat topped window with a raised cosine edge was adopted. The cosine curve "edge" extended from the third to the seventh data points (approx. 1.00–2.25 ms). The "late" window was rolled off more gradually between the 40th and 50th data points (12.9–16.1 ms), comfortably after the DPOAE peaks had died down to the noise floor.

Each windowed part of the time domain response was returned to the frequency domain by a forward Fourier transform. The data were returned to level and phase format and converted back to the original 256 point linear frequency array. Separate area charts were then constructed for the wave and place fixed DPOAE.

III. RESULTS

A. Low latency component

The low latency portion of the $2f_1-f_2$ DPOAE had a high level when f_2/f_1 was between 1.1 and 1.3 [Figs. 3 and 4, parts (a) and (b)]. Outside this range the level fell rapidly. The DPOAE is likely to be restricted to a limited ratio range because the phases of the DP sources in the generating region of the basilar membrane can only positively sum in the basal direction with a limited range of ratios (Kemp and Knight, 1999). The phase contours were approximately horizontal, indicating that phase was dependent on the frequency ratio, but almost independent of DP frequency. There was good vertical agreement between successive constant f_2/f_1 sweeps, with phase being steadily more positive at larger stimulus frequency ratios.

The low latency portion of the $2f_2-f_1$ DPOAE (Figs. 3 and 4, parts a and b) was of very small amplitude. In one subject (RDK, Fig. 3) it was mostly below -20 dB SPL, but the other subject (RN, Fig. 4) had a clear low latency peak in the inverse Fourier transform (not shown) which was above -20 dB SPL in the frequency domain [the lower half of Fig. 4(a)] with most combinations of f_1 and f_2. In the frequency domain the associated phase, where measurable, had a tendency to gradually be more positive when f_2/f_1 was smaller, but the phase was less dependent on the DP frequency.

The absence after processing of the fine structure which had been seen in the unprocessed data of Fig. 1, even when the wave fixed emission appeared to dominate, suggests that the fine structure was caused by interference between the low and high latency DPOAE components.

B. High latency

The phase of the high latency part was predominantly dictated by the emission frequency, in contrast to the low latency DPOAE [Figs. 3 and 4, parts (c) and (d)]. The level of the high latency component was less sensitive to f_2/f_1 changes as DP frequency was held constant (vertical move-

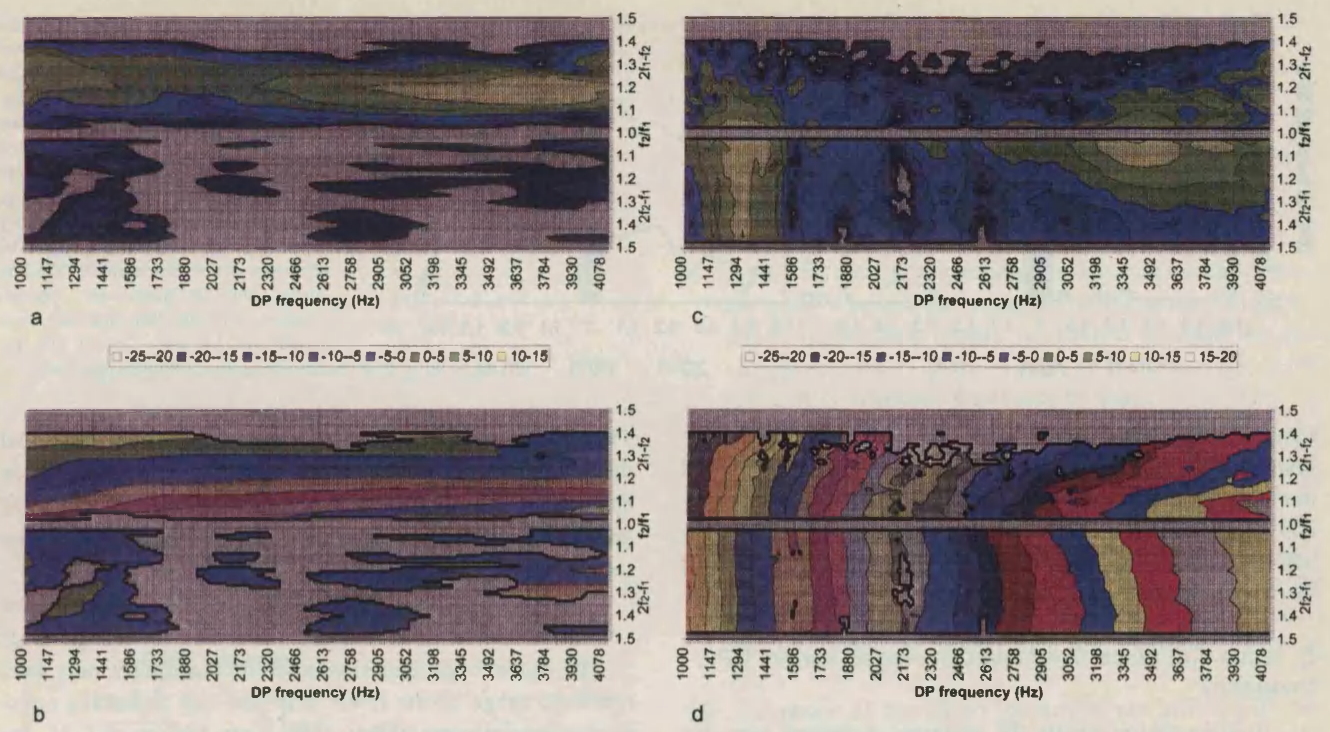

FIG. 3. Low (a and b) and high (c and d) latency windowed DPOAE for subject RDK, extracted from data in Fig. 1(a and b).

ment on the figures). Factors which affect the level of the place fixed DP and are sensitive to f_2/f_1 include the amount of apical propagation from the site of DP generation and the amount of suppression of the apically traveling DP by the proximity of f_1 and f_2.

There are interesting secondary relationships with the frequency ratio visible in the data. At higher frequencies (above about 2 kHz) the upper sideband DPOAE phase from both subjects shows a slight, accelerating negative drift toward smaller ratios (indicated by the phase contours bending to the left). The phase of the lower sideband high latency DPOAE was, at small frequency ratios, a continuation of the upper sideband phase. However, above $f_2/f_1 \sim 1.07$ the phase was steadily more positive at wider frequency ratios

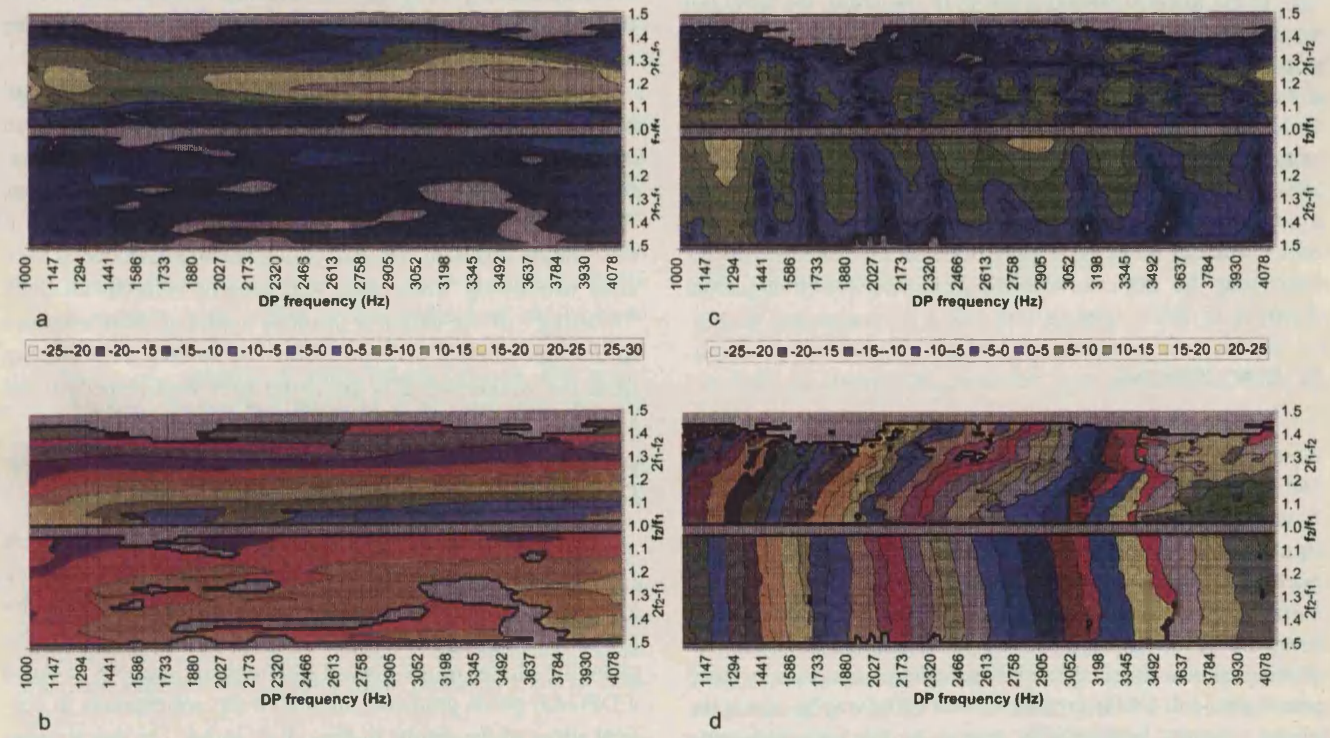

FIG. 4. Low (a and b) and high (c and d) latency windowed DPOAE for subject RN, extracted from data in Fig. 1(c and d).

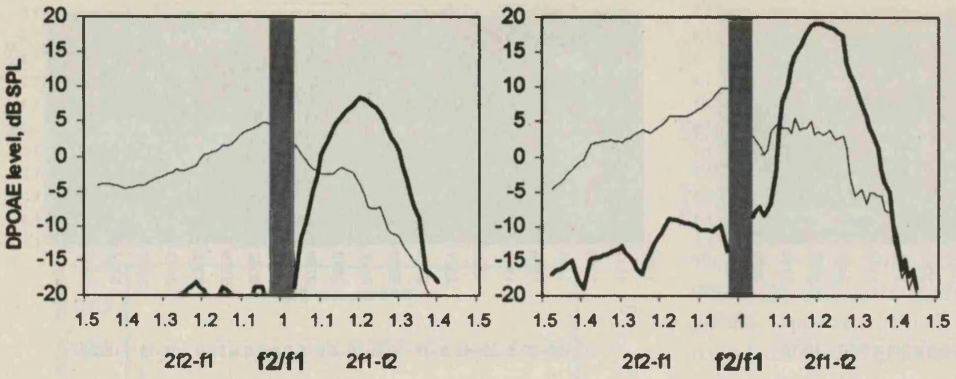

FIG. 5. Wave fixed (thick line) and place fixed (thin line) DPOAE level for subject RDK (left) and RN (right) plotted against frequency ratio, calculated as a power average from the data in Figs. 3 and 4. The shaded region where f_2/f_1 is small indicates where data could not be obtained because of limitations on the smallest frequency spacing at which the DPOAE could be resolved from the stimuli. Random noise floor estimates are approximately -30 dB SPL for the wave fixed DPOAE and -25 dB SPL for the place fixed DPOAE (see Table I).

(contours leaning to the right). The retention of the pronounced fine structure in the high latency DPOAE indicates that this is not caused by interactions with a low latency emission. Similar patterns were observed from $3f_1-2f_2$ and $3f_2-2f_1$ DPOAE data (not shown), except that the DPs were only present when f_2/f_1 was small.

C. Wave and place fixed level, averaged across DP frequency

In order to see clearly the preferred frequency ratio for the wave and place fixed DPOAE separately, a power average of the DPOAE level from Figs. 3 and 4 was calculated across DP frequency and plotted against frequency ratio (Fig. 5). The results show clearly that the wave fixed emission favors a restricted ratio range from $f_2/f_1=1.1-1.35$ in the lower sideband only, whereas the place fixed emission is present in both sidebands much more widely with the strongest emission when f_2/f_1 is small. The residual upper sideband wave fixed emission can be seen from subject RN, typically at -10 to -15 dB SPL.

In the lower sideband when f_2/f_1 is larger, the rapid fall seen in the wave fixed level as f_2/f_1 increases beyond 1.3 and the more gradual fall in the place fixed level with increasing f_2/f_1 means that the levels of the two components become similar. Tubis *et al.* (2000) have suggested that at wide ratios, the lower sideband place fixed DPOAE level may exceed the wave fixed level (as is also the case when $f_2/f_1>1.1$). The present data suggest that this is indeed possible although it does not quite occur in our data, the difference may be due to different stimulus conditions being adopted.

IV. DISCUSSION

In general, the low latency derived DPOAE phase is dependent on the ratio f_2/f_1 but changes only slowly with DP frequency (so phase contours run left to right across the figures). The high latency derived DPOAE phase changes far more rapidly with DP frequency (Figs. 3 and 4). This difference between the low and high latency DPOAE phase is not surprising and is precisely what would be expected due to the windowing employed in the time domain, because windowing at low latency excludes components with a steep phase gradient. Of far greater interest is the way in which the phase contours behave with respect to the frequency ratio (vertical in the figures) when the sweeps are recombined. The agreement of the phase of adjacent sweeps confirms that the patterns seen in the data do not arise from merely an artifact. It is significant that a substantial amplitude of DP above the noise level was obtained for both modes under most stimulus conditions.

The levels of the wave and place fixed emissions have very different relationships to f_2/f_1, as shown clearly in Fig. 5. The wave fixed emission is emitted strongly only in a restricted range of the lower sideband and a residual emission is present more widely. This limited range of f_2/f_1 for which the wave fixed DPOAE is strong may result from the phase gradient across the DPOAE generating region only being favorable for basal propagation under these conditions (Kemp and Knight, 1999).

The place fixed emission is emitted most strongly when f_2/f_1 is close to 1 in either sideband but the ratio is less critical. As f_2/f_1 increases the level of the place fixed emission falls faster in the lower sideband than the upper sideband, this may be because the phase gradient switches from favoring apical propagation to favoring basal propagation as the DPOAE generating region leaves the DP frequency place and moves with the f_2 envelope.

The analysis method has successfully uncovered the full extent of the two modes of emission. The basic features seen in the unprocessed data are preserved and the continuity between the upper and lower sidebands remains. However, there is some evidence of small artefacts being generated at wide ratios and high frequency, where some DPOAE is seen after windowing when none was present beforehand. Such "blurring" of the data is a result of applying short windows in the time domain. The possibility of random noise arising from the whole sweep is discussed later with respect to the significance of the low latency $2f_2-f_1$ emission data.

A. Possible general explanation for the high latency DPOAE phase behavior (place fixed mechanism)

The following arguments consider the case of a constant f_{DP} sweep. It is helpful to consider a constant DP frequency sweep when considering place fixed DPOAE phase, as the presumed reflection site does not move, leaving only the changing phases of the inward and outward journeys to cause a DPOAE phase gradient. Such a sweep corresponds to vertical slices of the results in Figs. 1, 3, and 4. The descriptions below consider only the case of a place fixed emission.

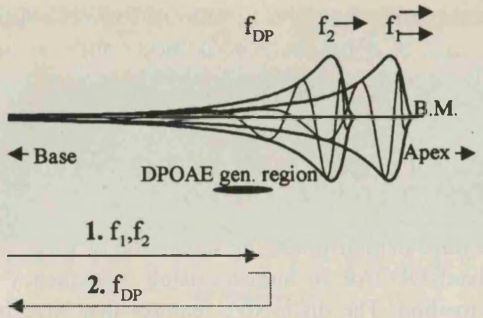

a) Place fixed upper sideband DP (e.g. $2f_2$-f_1)

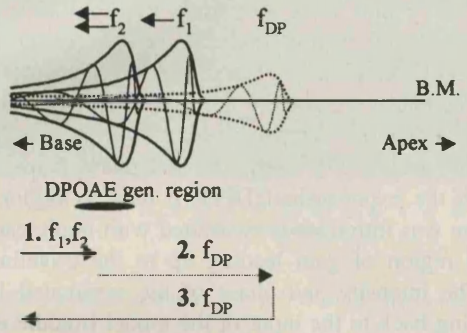

b) Place fixed lower sideband DP (e.g. $2f_1$-f_2)

FIG. 6. Illustrations of the path taken by place fixed DPOAE, considering a constant DP frequency sweep in which the peaks of the f_1 and f_2 traveling waves expand away from the DP frequency place as the frequency ratio increases. (a) Upper sideband DPOAE, and (b) lower sideband DPOAE.

1. Upper sideband DP (e.g., $2f_2-f_1$)

DP generation and emission are from the region of f_{DP} [Fig. 6(a)].

(1) In a constant DP frequency sweep, as the ratio f_2/f_1 is increased, the f_1 and f_2 places move apically away from the f_{DP} place, so the phase lag of both $f_1(\phi_1)$ and $f_2(\phi_2)$ at the DP generating site must decrease. The f_1 frequency place moves away at twice the rate of f_2. However, the phase of the $2f_2-f_1$ DP as it is generated changes twice as much in response to changes in ϕ_2 as to changes in ϕ_1. The phase gradient of ϕ_1 is more gradual than ϕ_2 at the DP generating site. Therefore there are opposing factors influencing the DP phase which means that the DP phase at its generation site will not change much with changing f_2/f_1.
(2) The phase change resulting from the return journey is unchanged with changing ratio. Therefore the return journey doesn't contribute to the phase gradient.

As the upper sideband experimental data has an almost flat phase gradient when DP frequency is fixed (a vertical section through Figs. 3 and 4, parts c and d), the opposing factors described appear to be roughly equal (and opposite) in magnitude.

The argument above suggests that any offset from flat phase (vertical phase contours on the charts) is associated with the difference in the gradients of ϕ_1 and ϕ_2 at the DP generating site.

2. Lower sideband DP (e.g., $2f_1-f_2$)

DP generation is in the region of f_2, but the emission travels via the f_{DP} region [Fig. 6(b)].

(1) In a constant DP frequency sweep, the phase lag of $f_1(\phi_1)$ at the DP generating site decreases with increasing ratio, whereas the phase of $f_2(\phi_2)$ at the DP generating site remains largely unchanged because the site moves with the f_2 place. Therefore the phase lag of the DP as it is generated decreases by $2\phi_1$.
(2) As the ratio increases and the DP generating site moves basally away from the DP place, the phase lag of the journey onward to the DP place increases. However, of necessity the phase gradient of f_{DP} at the f_2 place is less than the f_1 phase gradient at the f_2 place. Also, in point (1) above, the DP phase change due to the change in ϕ_1 was multiplied by 2. Therefore the change in DP phase due to (1) will be greater than the opposing change in (2).
(3) The phase of the return journey is not affected by the stimulus frequency ratio. Therefore (3) does not contribute to the DPOAE phase gradient.

The factors involved here (1, 2, and 3) do not cancel, so there is a net reduction in DP phase lag as the frequency ratio increases with DP frequency constant, contrary to the upper sideband. This is consistent with the lower sideband experimental data when the frequency ratio exceeded about 1.1.

However, it has been shown that the lower sideband high latency phase does not follow this pattern at the smallest frequency ratios, indicating a divergence from the argument above. The phase is continuous between the lower sideband and the upper sideband, suggesting continuity of mechanism. For the upper sideband the DPOAE generating region is associated with the DP frequency place, which is basal to the f_2 place. So for the lower sideband DPOAE at close ratios, where f_2 and f_{DP} become close, the generating site may also be more associated with the f_{DP} site than with the f_2 site. Alternatively, the lower sideband DP generating region may simply be changing shape when f_2/f_1 is small. Changes in the phase gradients within the DP generating region (discussed by Kemp and Knight, 1999) may be significant. This behavior would be consistent with a tendency for DPs to always be generated somewhat basal to the f_2 peak.

B. Possible explanations for the low latency $2f_2-f_1$ emission

As a secondary observation, a small low latency upper sideband DPOAE has been observed in one of the two subjects. The low latency emission, which was seen in the $2f_2-f_1$ DP from subject RN, is of interest as it has not previously been reported in humans. The level of the emission was typically -20 to -5 dB SPL, whereas the high latency emission was typically 0 to 15 dB SPL. The low latency upper sideband emission has a slight and consistent depen-

TABLE I. Mean noise level estimates, dB, SPL, obtained from the normalized time domain responses of the $2f_2-f_1$ DP with $f_2/f_1=1.03$ and 1.1. The "short window" was employed to isolate the low latency emission, the "long window" was used for the high latency emission.

	RDK	RN
Short window	−30.4	−29.3
Long window	−26.2	−24.6

dence of phase on the frequency ratio but little dependence on DP frequency. This is consistent with a low latency wave fixed emission, so the emission may be from the DP frequency region of the cochlea.

Where is the noise floor?

As the data have been considerably processed, it is difficult to directly infer a noise floor for individual data points. In order to obtain an estimate of where the noise floor lies after the DPOAE separation processing, "pseudo-time" windows were drawn from the data at a latency well after the DPOAE had died away. These samples of data were then subjected to a forward Fourier transform to provide an estimate of the noise level in the frequency domain. The average across the frequency range of the noise level estimate was obtained for the $2f_2-f_1$ DP with $f_2/f_1=1.03$ and 1.1 (Table I).

In each example, the noise estimate occasionally exceeded −20 dB SPL (exceptionally up to −13 dB SPL), so small regions of data points exceeding −20 dB SPL can be explained by random noise (e.g., the "low latency" $2f_2-f_1$ data of RDK). However, the "low latency" $2f_2-f_1$ data of RN consistently exceeds this level by 5–15 dB and so this cannot be explained by random noise.

C. How typical are the results?

Regarding the general features of the separated DPOAE, both subjects follow the same patterns, despite having different underlying latencies and DP levels. The general patterns can be accounted for on the basis of the description given in Sec. IV A. In both subjects the wave fixed emission was only strong when f_2/f_1 was between 1.1 and 1.3. The peak occurred at around $f_2/f_1=1.2-1.25$, which is consistent with other data (Harris *et al.*, 1989; Knight and Kemp, 1999; Moulin, 2000). It is likely, therefore, that the general features are typical of normal-hearing ears. The more localized features are not correlated between the two subjects and it seems that these will be different for each subject.

The balance between the levels of the wave and place fixed emissions with $L_1=L_2=70$ dB SPL may be different with other stimulus levels but the overall pattern of behavior is similar (Knight and Kemp, 1999). Use of stimuli with $L_1>L_2$ can be expected to favor the lower sideband (Kemp, 1987).

The possibility has arisen of a "wave fixed" emission being present in the $2f_2-f_1$ data, approximately 20 dB SPL lower in level than the place fixed emission. It is not known whether this will emerge as a "normal feature" of normally hearing ears as it has only been successfully identified as being above noise in 1 of the 2 subjects.

V. FURTHER ASSESSMENT OF THE TWO COMPONENT DP PHASE HYPOTHESIS

We have demonstrated the separation of wave fixed and place fixed DPOAE in humans using a frequency domain editing method. The distinctive features that have been observed in the phase behavior of DPOAEs appear consistent with the qualitative explanation offered, which was based on the general characteristics of the cochlear traveling wave and the anticipated effect of nonlinearity and reflectors.

In this section we demonstrate the appropriateness of our general explanation by deriving the main experimentally observed DPOAE phase patterns from a basic computational model. We constructed a simple transmission line model of traveling wave interactions and used this to generate maps of backward-traveling DP amplitude and phase maps to compare with the experimental DPOAE data. A region of DP generation was introduced, associated with nonlinearity of a localized region of gain leading up to the traveling wave peaks. The intensity and phase of the summated DPOAE propagating back to the input of the model (middle ear) was computed as a function of primary stimulus frequency and frequency ratio. We then introduced a series of partial reflectors into the transmission line and computed the phase and intensity of DPOAE that these reflectors caused to be propagated back to the input. We reasoned that if the model reproduced the main features seen in the experimental results in a manner not critically dependant on the choice of parameters, it would support the general explanation offered and its underlying assumptions.

Signal propagation within our frequency domain transmission line model is based on a propagation phase curve similar to that found in basilar membrane observations. It has an exponential acceleration of phase accumulation with distance and a logarithmic spacing of characteristic frequencies. Transmission characteristics, which include frequency dependent gain and damping functions, are designed to produce traveling wave envelopes with growth with distance up to a peak, followed by a rapid decline. A nonlinear gain function is introduced which achieved compressive growth with input intensity at the traveling wave peak but linear growth further toward the start of the transmission line and DP generation. Details of the model are given in Appendices A and B.

In our model the DP can propagate in both directions, the DP generated at each model element being vectorally added to the propagating DP traveling wave as it passes. This differs from the approach used by Sun *et al.* (1994) who summed the DP sources to the point of maximum overlap between the stimulus tones and then radiated the DP as a point source from there. Transmission of the DP from the DP generating region, propagated directly back to the start of the transmission line, was taken to represent "wave fixed" DPOAE generation. These data were generated over a range of stimulus frequencies, comparable to that used to obtain the experimental data.

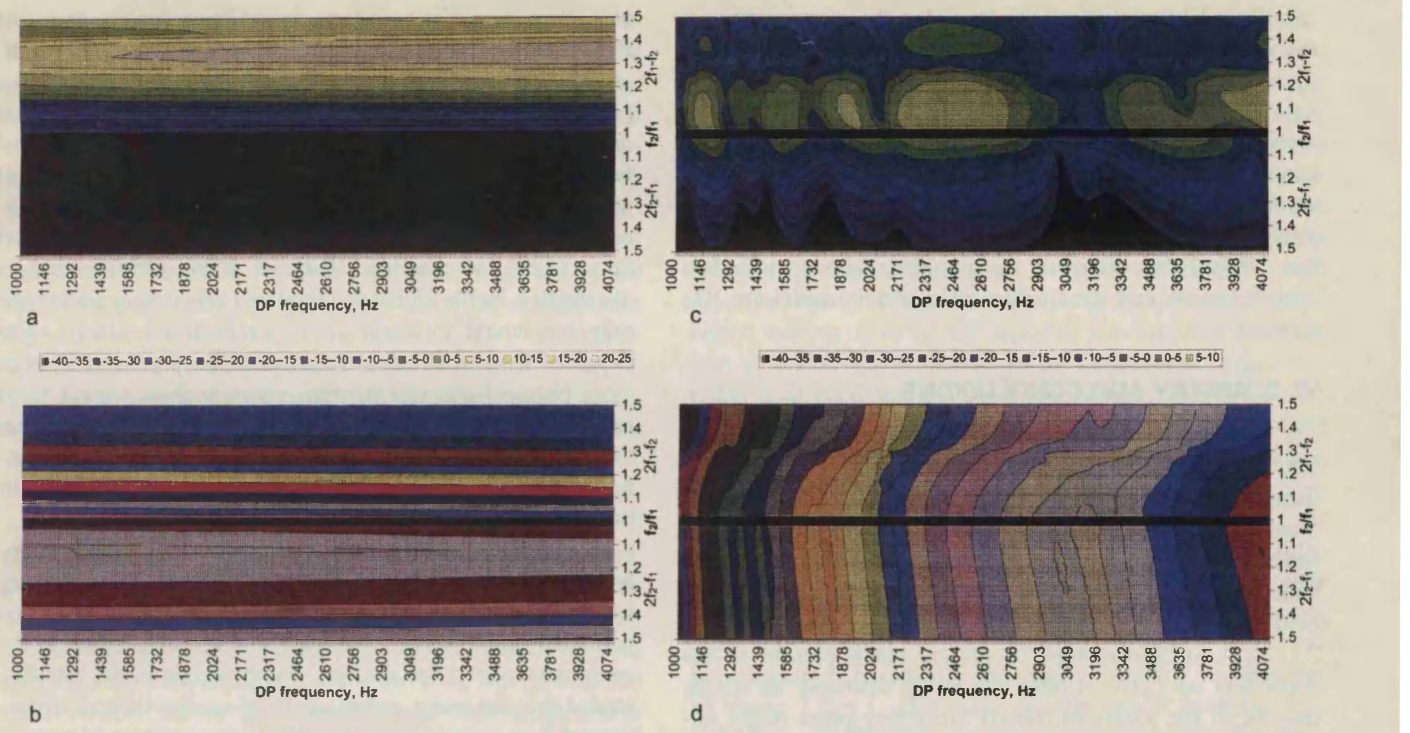

FIG. 7. Wave (a and b) and place (c and d) fixed DP from a transmission line model. The overall level and phase patterns are similar to those seen in measured DPOAE.

The phase and amplitude of this direct component is presented in Fig. 7 (a and b) in a similar format to the DPOAE data of Figs. 3 and 4 (a and b). The ''directly emitted'' data reproduce both the wave fixed phase pattern and the general dependence of level on the ratio f_2/f_1. The dependence on f_2/f_1 appeared to be determined by the vector summation of the DP across its generating region. For the $2f_2-f_1$ DP component, this was largely self-cancelling in the basal direction for all f_2/f_1. With the $2f_1-f_2$DP, cancellation was significant only when f_2/f_1 was small. The directly emitted model DP peaked at a wider ratio than in the experimental wave fixed DPOAE data [Figs. 3 and 4 (a and b)]. This difference is likely to be due to the precise shape of the phase curve, specifically the phase gradients of f_1 and f_2 in the region at which the DP is generated.

Introduction of reflectors

In stage two of our model the onward-propagating DP signal encounters fixed, randomly spaced partial reflectors. The reflection coefficient has been made a function of the level of gain present so that significant reflection occurs at the DP frequency only in the region leading up to and at the DP frequency place. Summation of these reflected DP signals in the reverse direction gives rise to a DP component at the input which is taken to represent ''place fixed'' DPOAE generation.

Figure 7 (c and d) indicates the level and phase of the reflected DP generated by the model. The general patterns are very similar to the experimental DPOAE data in Figs. 3 and 4 (c and d). The model phase data follow the general pattern of actual DP data, with the upper sideband phase contours being slightly off vertical and the lower sideband contours being curved and deviating more strongly from vertical. The model phase data also reproduce the notchy level characteristic of experimentally obtained place fixed DPOAE, and this originates in interference between contributions from the random distribution of reflectors.

In the model data the place fixed DPOAE intensity is greater in the lower sideband than the upper sideband, whereas in the experimental data it is the other way round. The model DP level also falls more rapidly at wider ratios in the upper sideband in the model data compared to the experimental data. These features are affected by the parameters of the model such as the shape of the stimulus phase curves in the region of DP generation, the location of the gain, and the input/output shape of the nonlinearity.

There is a consistent notch in the lower sideband place fixed model DP level at a ratio of approximately $f_2/f_1 = 1.3$. Detailed inspection of spatial distribution of signal levels in the model indicated that this is caused by cancellation across the DP generation region in the forward direction. This feature is mostly not present in the experimental DPOAE data, which may be because the phase gradients and DP generating regions are less consistent in a real cochlea so the ''notch'' does not always occur at the same frequency ratio so is less obvious. Alternatively the notch may occur at a wider frequency ratio in experimental data at which the place fixed DPOAE has a small amplitude, making the notch less noticeable.

We have extensively varied the parameters and details of the formulation within reasonable limits and found the general features to be robust and comparable with the experimental data. It should be noted that our model is not a co-

chlear model but a means of computing the consequences of the various assumptions and simplifications made in developing a qualitative explanation of observed DPOAE behavior. The models capacity to simulate realistic DPOAE maps serves only to support the authors deductions from their qualitative explanation of the phenomenon observed. It would not be appropriate to use the model to make specific predictions. However, the model does support the contention that DPOAE behavior can be simply understood to a first approximation and the qualitative model is useful for this purpose.

VI. SUMMARY AND CONCLUSIONS

Separate wave and place fixed DPOAE maps with DP frequency and f_2/f_1 have been derived for two human ears using a phase gradient based method of separation. The wave fixed output is maximal over a restricted f_2/f_1 range in the lower sideband (e.g., $2f_1-f_2$), but it remains present at a wide range of f_2/f_1 at much reduced levels. We found slight evidence that a very small wave fixed upper sideband (e.g., $2f_2-f_1$) component may be present but if present is less dependent on f_2/f_1. Unlike the lower sideband, its source may be in the region of the DP frequency place in the cochlea.

The place fixed emission has been found at most stimulus frequency combinations, including the entire upper sideband region and the region in the lower sideband where it is normally obscured by the larger wave fixed component. The place fixed emission level was greatest at the smallest frequency ratios.

The phase of the place fixed DPOAE supports the common view that the source of DP contributing to upper sideband DPOAE is a region related to the DP frequency place for all f_2/f_1 ratios. For lower sideband DPOAE the initial DP source must be related to the f_2 peak excitation region when f_2/f_1 is large. However, the excellent continuity of phase behavior between the lower and upper sidebands suggests that when f_2/f_1 is small the lower sideband place fixed DPOAE is a continuation of the upper sideband DPOAE with its source region associated with the DP frequency place.

The observed result can be qualitatively accounted for on the basis of some reasonable assumptions about traveling wave behavior in the cochlea and the mechanical nonlinear interaction which must take place. These assumptions have been formulated into a transmission line model consisting of a wave fixed DP source in the region of the primaries and randomly spaced place fixed reflections in the region of the DP frequency place. Good agreement between the model and experimental data could be achieved, indicating that the observed DP behavior can be simply understood. Differences between the model and experimental data could probably be further reduced by modifications to the modeling of the phase curve of the traveling wave and to the nonlinear interactions in the region of the stimulus tone peaks but this would add little to our main finding.

The simple model used here is not a physical model. Instead, ''cochlearlike'' transmission characteristics and compressive nonlinearity were built into the model which was then used to predict the reverse propagation of DPOAEs. DPOAE generation inherently resulted in a resultant reverse traveling wave with very similar phase and amplitude characteristics to the ''wave fixed'' experimental data. It was necessary to insert ''reflectors'' in order to simulate the place fixed DPOAE map. We used a relatively small number of discrete reflectors active over the region of significant gain. The detailed reflection model of Zweig and Shera (1995) demonstrates that even if an extensive random distribution had been used, complete cancellation among the reflectors would not occur so that a reflection is always to be expected from such an arrangement. We predict that other more physical cochlear models, which include a place fixed reflection mechanism most effective in the region leading up to the DP frequency peak, would also reproduce the experimental level and phase DPOAE characteristics presented in this study.

In conclusion, this study has demonstrated that the apparently complex behavior of DPOAE phase when primary frequencies are altered can be readily understood and even predicted on the basis of a small number of reasonable assumptions about the cochlea. Furthermore it has demonstrated that the wave and place fixed mechanisms of distortion product emission are generally active over a wider range of stimulation conditions than was indicated by Kemp (1986). Kemp presented data suggesting a bimodal generating mechanism, whereas data presented here demonstrate that both emission modes are simultaneously active, at least for the lower sideband DPs. Our analysis does not support the concept of two DP generator regions but does clearly illustrate that interference across a single distributed DP source controls both the observed primary ratio dependence of wave fixed DPOAEs and also the input to the reflection mechanism which is responsible for the place fixed DPOAE. When they are mixed, interference between direct and indirectly emitted DPOAEs results in additional DPOAE fine structure.

We believe the careful separation of DPOAE components in experimental data, as demonstrated here, simplifies the task of extracting consistent physiologically significant information from DPOAE data by removing interference between wave and place fixed emission. However, we are of the opinion that the two emission modes complement each other and that neither one should be studied in isolation.

ACKNOWLEDGMENTS

This project was financially supported by the Auditory Biophysics Lab. at the Institute of Laryngology and Otology. ILO 88 and ILO 96 equipment was provided by Otodynamics Ltd. A preliminary account of parts of this work has been presented at the ARO conference (Knight and Kemp, 2000b).

APPENDIX A: DESCRIPTION OF MODEL

The phase lag from the input to the model is calculated for each stimulus frequency at each incremental distance along the transmission line. For each model element a parameter determines the phase characteristic at that element

for each frequency. This is termed the "frequency parameter." The "frequency parameter" for each element of the model is set up in a logarithmic relationship covering frequencies from 25 kHz down to 600 Hz. The incremental change between each model element is such that each element approximately represents two hair cells. The phase lag from the base of the cochlea is calculated for each stimulus frequency at each incremental distance along the basilar membrane. The phase lag is logarithmically related to the frequency parameter [see Eqs. (B1) and (B2) in Appendix B].

In this formulation, gain is necessary in the model so that the traveling waves grow to form sharp peaks (Neely and Kim, 1986; Geisler, 1993; de Boer, 1983a, b). The gain is configured such that the total maximum linear gain along the basilar membrane (which would be delivered if the traveling wave amplitude was small) increases the amplitude of the traveling wave peak by 25 dB. This value is in comparison to the model operating without gain—i.e., the comparison is to a passive and damped model. The gain is frequency dependent and therefore restricted to a region which we have centred just to the basal side of the traveling wave peak. The gain window covers approximately one-third of an octave (−6 dB) of place frequencies in the model. The gain delivered by each model element is reduced by a factor related to the total stimulus travelling wave amplitude (f_1+f_2) at that point (this also includes self-suppression in the case of the propagating DP). Suppression by the small DP on the stimuli is therefore presumed to be not significant [see Eqs. (B3)–(B5) in Appendix B].

The model included gain only for forward-propagating waves. Inclusion of gain for reverse-propagating waves in this model would have resulted in considerable undesirable growth of place fixed DPOAE in the lower sideband at wide frequency ratios. This was because the DP gain region was suppressed by the stimulus tones when f_2/f_1 was small but not when f_2/f_1 was large, so the place fixed DP would be amplified twice by the gain region at large frequency ratios (as it traveled through the gain region both ways).

The amplitude of the propagating traveling wave is diminished by a damping function. Damping is applied as a function of the phase gradient with a constant added. The phase dependent part controls the sharpness and the location of the apical end of the traveling wave envelope. The additional constant tends to control the general growth of the traveling wave envelope basal to the traveling wave peak, outside of the gain region [Eq. (B6) in Appendix B].

DP levels were obtained by applying the computed levels of f_1 and f_2 to the nonlinear input/output function. The model assumes that a fixed proportion of the DP generated is converted into a traveling wave and therefore that a fixed proportion of the DP is either absorbed or directed in a mode which does not readily set up a traveling wave. The phase of the DP generated at each incremental point along the basilar membrane is defined by the phase of f_1 and f_2 at that point.

The model supports propagation of the DP in both directions along the basilar membrane. The DP generated at each model element is vectorally added to the propagating traveling wave as it passes.

The reverse-traveling part provided the "wave fixed" DPOAE component (path 1 described in our Introduction). The onward-propagating component results in a traveling wave which proceeds to the DP frequency place. In order that a DPOAE results from this component, randomly spaced place fixed reflectors have been introduced. Each model element had a 1 in 5 chance of being a reflector, except that adjacent reflectors were not allowed. The reflector strength is linked to the linear gain window associated with f_{DP}—therefore the significant reflectors are limited to the region leading up to the DP traveling wave peak. The reflection is defined by a proportion of the incident traveling wave, rather than being defined by an impedance irregularity.

The reflected DP propagates back toward the start of the model with contributions from each reflector being added to the traveling wave as it passes. The reflected reverse-propagating traveling wave is kept numerically separate from the reverse propagating "wave fixed" DP to avoid the difficulties of separating them later. The model does not include reflections back into the cochlea from the stapes, so repeated reflections between the base and the DP frequency place are not supported. Essentially the same procedure is performed to obtain $2f_2-f_1$ DPOAEs, but the model produces very little $2f_2-f_1$ DPOAE via the wave fixed mode. For place fixed DPOAE, the reflectors placed around the DP frequency place were also in the DP generation region so that the distance of apical DP travel before a reflector was encountered was minimal.

APPENDIX B

The main formulas for the model are listed below.

Frequency parameter array

For the purpose of this model, an array of "frequency parameters" was ascribed to the model elements. A phase delay of three cycles was incurred by a stimulus in traveling to the place of its corresponding "frequency parameter." At a stimulus level of 70 dB SPL, the traveling wave amplitude peaked at the appropriate "frequency parameter." For lower stimulus levels, the traveling wave peak would be slightly beyond the "frequency parameter."

The "frequency parameter" of each model element is calculated as follows:

$$\text{Frequency parameter } (f_p) = 25\,000 \times 0.995\,595^{(n-1)}, \tag{B1}$$

where n = the number of the model element. The "frequency parameter" is used in the calculation of the phase gradients and the gain characteristics. The gain and damping is balanced such that, at 70 dB SPL, the traveling wave envelope peaks at the frequency parameter corresponding to the stimulus frequency.

Phase curve

The phase curve is:

$$\text{Phase lag (radians)} = \frac{6\pi\{(e^{(2f/f_p)}) - (e^{(2f/25\,111)})\}}{2.3e}, \tag{B2}$$

where f = the stimulus frequency of the traveling wave, and f_p = frequency parameter. The second part of the numerator ensures that the phase lag at the first model element is 0. Where this term is ≈0, there are three phase cycles to the frequency place. With high frequencies, the number of phase cycles reduces slightly because part of the phase curve is "lost" at the basal end of the model. The phase gradient at the peak of the traveling wave is the same for all frequencies.

Conversion of stimulus level to traveling wave amplitude

The stimulus level is entered into the model in dB SPL, which is converted to pascals. In order to obtain the initial amplitude of the traveling wave the sound pressure in pascals is multiplied by the phase difference between the first two model elements for that frequency and arbitrarily by 100. This calculation is reversed for the 'reverse propagating DP' when it arrives back at the start of the model to obtain a DP level in dB SPL. The traveling wave amplitude is of arbitrary units.

Gain

The nonlinear gain is defined as follows:

$$G = 1 + (g_L / C), \tag{B3}$$

where g_L defines the place envelope of the maximum gain (the gain which would be obtained if the traveling wave amplitude were small). C is a compression function which reduces the gain which is achieved depending on the traveling wave amplitude.
g_L is calculated as follows:

$$g_L = \frac{(0.12(1.1f/f_p)^{10})}{(1 + (1.1f/f_p)^{25})}, \tag{B4}$$

where f = traveling wave frequency, and f_p = frequency parameter. The gain is therefore restricted to a region centered just before the traveling wave peak:

$$C = (3L_T)^{1.2} + 1, \tag{B5}$$

where L_T = total apical-going traveling wave amplitude of f_1 and f_2 (for suppression of DP gain, self-suppression by f_{dp} is also included).

Damping

The damping is based on the traveling wave phase gradient and is therefore proportional to the time spent at that element, with a constant added:

$$\text{Damping (D)} = 0.0003(300\Delta\phi)^2 + 0.001, \tag{B6}$$

where $\Delta\phi$ = phase change between adjacent model elements. The new traveling wave amplitude after gain and damping is then as follows:

$$\text{New amplitude} = \frac{A_0 G}{1 + D}, \tag{B7}$$

where A_0 = traveling wave amplitude input to the present model element, G = nonlinear gain, and D = damping. In each model element the traveling wave is modified by functions of the gain, damping, and phase gradient. The amplitude is divided by the present phase gradient and then multiplied by the next phase gradient in order to re-scale it for the incremental phase gradient change.

DP generation formula level/phase

The generation of DP is calculated by applying the nonlinear gain to the waveform of L_1 and L_2 at each model element. For computational convenience, a table of values was generated and from this an approximate function was created which was used in the model. The phase lag of the DP at each point at which it is generated is $2\phi_1 - \phi_2$ in the case of the $2f_1 - f_2$ DP, or $2\phi_2 - \phi_1$ in the case of the $2f_2 - f_1$ DP, where ϕ_1 and ϕ_2 are the phase lags of f_1 and f_2 at the point of DP generation.

Reflections

Each model element is given a reflectivity factor equal to zero or to the frequency dependent gain multiplied by a constant. Each element has a 1 in 5 random chance of being a reflector, except adjacent reflectors were not allowed. The envelope of the reflections of the fixed reflectors on the basilar membrane is therefore linked to the linear gain window related to the DP frequency. Typically there may be around 10 reflectors within the −6 dB limits of the gain region.

Allen, J. B., and Fahey, P. F. (**1992**). "Using acoustic distortion products to measure the cochlear amplifier gain on the basilar membrane," J. Acoust. Soc. Am. **92**, 178–188.

de Boer, E. (**1983a**). "No sharpening? A challenge for cochlear mechanics," J. Acoust. Soc. Am. **73**, 567–573.

de Boer, E. (**1983b**). "On active and passive cochlear models—Toward a generalized analysis," J. Acoust. Soc. Am. **73**, 574–576.

Dreisbach, L. E., and Seigel, J. H. (**1999**). "Level and phase relationships of distortion-product otoacoustic emission sources with varied primary frequency ratios in humans," Assoc. Res. Otorhinolaryngol. Abstracts **22**, 392.

Fahey, P. F., and Allen, J. B. (**1997**). "Measurement of distortion product phase in the ear canal of the cat," J. Acoust. Soc. Am. **102**, 2880–2891.

Fahey, P. F., Stagner, B. B., Lonsbury-Martin, B. L., and Martin, G. K. (**2000**). "Theory for two new routes of distortion product generation," Assoc. Res. Otorhinolaryngol. Abstracts **23**, 478.

Gaskill, S. A., and Brown, A. M. (**1996**). "Suppression of human acoustic distortion product: Dual origin of 2 $f1 - f2$," J. Acoust. Soc. Am. **100**, 3268–3274.

Geisler, C. D. (**1993**). "A realizable cochlear model using feedback from motile outer hair cells," Hear. Res. **68**, 253–262.

Harris, F. P., Lonsbury-Martin, B. L., Stagner, B. B., Coats, A. C., and Martin, G. K. (**1989**). "Acoustic distortion products in humans: systematic changes in amplitude as a function of f_2/f_1 ratio," J. Acoust. Soc. Am. **85**, 220–229.

Heitmann, J., Waldmann, B., Schnitzler, H., Plinkert, P. K., and Zenner, H. (**1998**). "Suppression of distortion product otoacoustic emissions (DPOAE) near 2 $f1 - f2$ removes DP-gram fine structure—Evidence for a secondary generator," J. Acoust. Soc. Am. **103**, 1527–1531.

Kalluri, R., and Shera, C. (**2000**). "Are DPOAEs a mixture of emissions generated by different mechanisms?" Assoc. Res. Otorhinolaryngol. Abstracts **23**, 480.

Kemp, D. T. (**1978**). "Stimulated acoustic emissions from within the human auditory system," J. Acoust. Soc. Am. **64**, 1386–1391.

Kemp, D. T. (**1980**). "Toward a model for the origin of cochlear echoes," Hear. Res. **2**, 533–548.

Kemp, D. T. (**1986**). "Otoacoustic emissions, travelling waves and cochlear mechanisms," Hear. Res. **22**, 95–104.

Kemp, D. T. (**1987**). "Otoacoustic emission characteristics during moderate continuous stimulation-intermodulation," 12th International Congress of Acoustics B7-1.

Kemp, D. T. (**1998**). "Otoacoustic emissions: Distorted echoes of the cochlea's travelling wave," in *Otoacoustic Emissions Basic Science and Clinical Applications*, edited by C. I. Berlin (Singular Publishing Group, San Diego), Chap. 1, pp. 1–59, Fig. 1-12.

Kemp, D. T., and Brown, A. M. (**1983**). "An integrated view of cochlear mechanical nonlinearities observable from the ear canal," in *Cochlear Mechanics*, edited by E. DeBoer and M. A. Viergever (Delft University Press, Holland).

Kemp, D. T., and Knight, R. D. (**1999**). "Virtual DP reflector explains DPOAE wave and place fixed dichotomy," Association for Research in Otolaryngology Abstracts, 396.

Knight, R. D., and Kemp, D. T. (**1999**). "Relationships between DPOAE and TEOAE characteristics," J. Acoust. Soc. Am. **106**, 1420–1435.

Knight, R. D., and Kemp, D. T. (**2000a**). "Indications of different DPOAE mechanisms from a detailed $f1, f2$ area study," J. Acoust. Soc. Am. **107**, 457–473.

Knight, R. D., and Kemp, D. T. (**2000b**). "Separation of "wave" and "place" fixed $2f1-f2$ DPOAE," Assoc. Res. Otorhinolaryngol. Abstracts **23**, 987.

Kummer, P., Janssen, T., and Arnold, W. (**1995**). "Suppression tuning characteristics of the $2f1-f2$ distortion-product otoacoustic emission in humans," J. Acoust. Soc. Am. **98**, 197–210.

Lonsbury-Martin, B. L., Martin, G. K., Probst, R., and Coats, A. C. (**1988**). "Spontaneous otoacoustic emissions in a non-human primate. II. Cochlear anatomy," Hear. Res. **33**, 69–94.

Martin, G. K., Stagner, B. B., and Lonsbury-Martin, B. L. (**2000**). "Harmonic otoacoustic emissions in normal and noise-exposed rabbits," Assoc. Res. Otorhinolaryngol. Abstracts **23**, 231.

Martin, G. K., Jassir, D., Stagner, B. B., Whitehead, M. L., and Lonsbury-Martin, B. L. (**1998**). "Locus of generation for the $2f1-f2$ vs $2f2-f1$ distortion-product otoacoustic emissions in normal-hearing humans revealed by suppression tuning, onset latencies, and amplitude corelations," J. Acoust. Soc. Am. **103**, 1957–1971.

Martin, G. K., Lonsbury-Martin, B. L., Probst, R., Scheinin, S. A., and Coats, A. C. (**1987**). "Acoustic distortion products in rabbit ear canal. II. Sites of origin revealed by suppression contours and pure tone exposures," Hear. Res. **28**, 191–208.

Martin, G. K., Stagner, B. B., Jassir, D., Telischi, F. F., and Lonsbury-Martin, B. L. (**1999**). "Suppression and Enhancement of distortion-product otoacoustic emissions by interference tones above $f2$. I. Basic findings in rabbits," Hear. Res. **136**, 105–123.

Mauermann, M., Uppenkamp, S., van Hengel, P. W., and Kollmeier, B. (**1999a**). "Evidence for the distortion product frequency as a source of distortion product otoacoustic emission (DPOAE) fine structure in humans. I. Fine structure and higher-order DPOAE as a function of the frequency ratio $f2/f1$," J. Acoust. Soc. Am. **106**, 3473–3482.

Mauermann, M., Uppenkamp, S., van Hengel, P. W., and Kollmeier, B. (**1999b**). "Evidence for the distortion product frequency as a source of distortion product otoacoustic emission (DPOAE) fine structure in humans. II. Fine structure for different shapes of cochlear hearing loss," J. Acoust. Soc. Am. **106**, 3473–3482.

Moulin, A. (**2000**). "Influence of primary frequencies ratio on distortion product otoacoustic emissions amplitude. I. Intersubject variability and consequences on the DPOAE-gram," J. Acoust. Soc. Am. **107**, 1460–1470.

Neely, S. T., and Kim, D. O. (**1986**). "A model for active elements in cochlear biomechanics," J. Acoust. Soc. Am. **79**, 1472–1480.

Shera, C. A., and Guinan, J. J. (**1999**). "Evoked otoacoustic emissions arise by two fundamentally different mechanisms: A taxonomy for mammalian OAEs," J. Acoust. Soc. Am. **105**, 782–798.

Shera, C. A., and Zweig, G. (**1993**). "Noninvasive measurement of the cochlear traveling-wave ratio," J. Acoust. Soc. Am. **93**, 3333–3352.

Siegel, J., Borneman, A., and Dreisbach, L. (**2000**). "Suppressor conditions for optimal separation of distortion product otoacoustic emission sources," Assoc. Res. Otorhinolaryngol. Abstracts **23**, 983.

Stover, L. J., Neely, S. T., and Gorga, M. P. (**1996**). "Latency and multiple sources of distortion product otoacoustic emissions," J. Acoust. Soc. Am. **99**, 1016–1024.

Sun, X., Schmiedt, R. A., He, N., and Lam, C. F. (**1994**). "Modeling the fine structure of the $2f1-f2$ acoustic distortion product. I. Model development," J. Acoust. Soc. Am. **96**, 2166–2174.

Talmadge, C. L., Long, G. R., Tubis, A., and Dhar, S. (**1999**). "Experimental confirmation of the two-source interference model for the fine structure of distortion product otoacoustic emissions," J. Acoust. Soc. Am. **105**, 275–292.

Talmadge, C. L., Tubis, A., Long, G. R., and Tong, C. (**2000**). "Modeling the combined effects of basilar membrane nonlinearity and roughness on stimulus frequency otoacoustic emission fine structure," J. Acoust. Soc. Am. **108**, 2911–2932.

Tubis, A., Talmadge, C., Long, G. R., Dhar, S., and Tong, C. (**2000**). "Amplitude and group-delay fine structures of distortion product otoacoustic emissions as functions of primary levels and frequency ratios," Assoc. Res. Otorhinolaryngol. Abstracts **23**, 483.

Zweig, G., and Shera, C. A. (**1995**). "The origin of periodicity in the spectrum of evoked otoacoustic emissions," J. Acoust. Soc. Am. **98**, 2018–2047.